

11th

International Conference on the  
**Scientific and Clinical  
Applications of  
Magnetic Carriers**



**Wolfgang Schütt**  
Krems, Austria



**Maciej Zborowski**  
Cleveland, Ohio, U.S.A.



**Urs Häfeli**  
Vancouver, Canada

Vancouver, Canada | May 31-June 4, 2016

[www.magneticmicrosphere.com](http://www.magneticmicrosphere.com)



Coffee cup design by Cristina Rodriguez Rodriguez © 2016

## Welcome Message

It is our great pleasure to welcome you all to the now already 11<sup>th</sup> International Conference on the Scientific and Clinical Applications of Magnetic Carriers. We will again have lots of new and exciting presentations, concentrated on magnetic particles and their applications.

As in the past, we wish to cultivate discussions and a familiar atmosphere not only during the talks, but also during breaks, lunches and the boat trip. One of the main goals of this conference is to think about your research and that of your colleagues here, and get ready to start new collaborations. This will advance our field even more!

We wish you all a wonderful conference, with many new discoveries and oodles of new ways of working with magnetic particles.

Your organizers,

Urs Hafeli, University of British Columbia, Vancouver, Canada

Wolfgang Schuett, IMF Krems, Austria & Rostock, Germany

Maciej Zborowski, Cleveland Clinic Foundation, Cleveland, U.S.A.

**Front and Back Page Designs** by Veronika Schmitt @2014 (front page) and Cristina Rodriguez Rodriguez @ 2016 (back page)

# 11th International Conference on the Scientific and Clinical Applications of Magnetic Carriers

Vancouver, Canada | May 31-June 4, 2016 [www.magneticmicrosphere.com](http://www.magneticmicrosphere.com)

## 11th International Conference on the Scientific and Clinical Applications of Magnetic Carriers - Vancouver, BC, Canada

### Tuesday, May 31, 2016

18:00 Registration desk opens - at the Beaty Biodiversity Museum - 2212 Main Mall

18:30 Informal reception and welcome cocktail (Apero) at the Beaty Biodiversity Museum - generously sponsored by **Chemicell**; with a band sponsored by **Diagnostic Biosensors**

22:00 End of reception

### Wednesday, June 1, 2016

08:00 Registration desk opens - at the Nest - 6133 University Boulevard

#### Opening Session

09:00 Schütt / Zborowski Opening of the conference

09:10 Hafeli, Urs Short review of the last 2 years of magnetic carriers research Vancouver, Canada Talk 0

#### Coffee break

#### Session 1 Nanotechnology

Chair: Benjamin Shapiro

10:10 Mair, Lamar	Doing the Twist: Nanorods with Orthogonally Magnetized Segments Twist Their Way Through Viscoelastic Media	Bethesda, MD, USA	Talk 1
10:30 Tasci, Tonguc	Microwheels: Magnetic Bead Rolling Micro-Robots And Their Potential In The Non-Invasive Treatment Of Blood Clots	Golden, CO, USA	Talk 2
10:50 Simberg, Dmitri	Complement Activation and Immune Recognition of Superparamagnetic Iron Oxide (SPIO) Nanoworms	Aurora, CO, USA	Talk 3
11:10 Crawford, Thomas	Magnetic-field-directed self-assembly of programmable mesoscale shapes	Columbia, SC, USA	Talk 4
11:30 Huber, Dale	Measuring biodistribution of PEG coated PrecisionMRX nanoparticles with superparamagnetic relaxometry (SPMR)	Albuquerque, NM, USA	Talk 5
11:50 Nikitin, Maxim	Biocomputing nano- and microstructures as smart sensors and theranostic agents	Dolgoprudny, Russia	Talk 6
12:10 Lu, Si	Dual-Color Magnetic Barcodes with Ultra-High Encoding Capacity	Shanghai, China	Talk 7

#### Lunch

#### Session 2 Magnetic Drug Delivery / Magnetic Targeting

Chair: Urs Hafeli

13:50 Shapiro, Benjamin	Results and Challenges in Magnetically Targeting Therapy to Disease Targets	College Park, MD, USA	Invited Talk 1
14:40 Martel, Sylvain	Current challenges in the navigation of magnetic particles in the pig liver using an MRI scanner	Montreal, Canada	Talk 8
15:00 Shademanl, Ali	A Magnetic Sponge as an On-demand Drug Delivery Device	Vancouver, Canada	Talk 9
15:20 Zhang, Xingming	Development of a Real Time Image-Based Guidance System of Magnetic Nanoparticles for Targeted Drug Delivery	Jinju, Korea	Talk 10
15:40 Coffee break			

#### Session 3 Magnetic Drug Delivery / Magnetic Targeting

Chair: Thomas Crawford

16:20 Chen, Linjie	The target killing of <i>Staphylococcus aureus</i> by magnetotactic bacteria under a compound magnetic field in a microfluidic chip	Beijing, China	Talk 11
16:35 Hervault, Aziliz	Doxorubicin loaded dual pH- and thermo-sensitive magnetic nanosystem for combined hyperthermia and controlled drug delivery applications	London, UK	Talk 12
16:50 Sajjad, Umer	Advanced locomotion of microbeads on ferromagnetic surfaces	Kiel, Germany	Talk 13
17:05 Barnsley, Lester	Optimized shapes of magnetic arrays for drug targeting applications	Oxford, UK	Talk 14
17:20 Cao, Changqian	Biomimetic magnetoferritin nanoparticles for targeting and imaging of microscopic tumors	Beijing, China	Talk 15
17:35 Gabbasov, Raul	Exogenous Iron Redistribution Between Brain, Liver and Spleen After Administration of 57Fe3O4 Ferrofluid into the Brain Ventricles	Moscow, Russia	Talk 16

17:50 Poster session I (odd numbered posters) with Beer and Pretzels - generously sponsored by **micromod**

**Thursday, June 2, 2016**

08:00 **Registration desk opens** - at the Nest - 6133 University Boulevard

<b>Session 4 Magnetic Particle Synthesis</b>			<i>Chair: Maciej Zborowski</i>
09:00	Dietl, Tomasz	Nanospintronics Meets Magnetic Nanoparticles	Warsaw, Poland      Invited Talk 2
09:50	Rich, Megan	MRI visible polymer microcapsules for ultrasound induced targeted drug delivery	Birmingham, UK      Talk 17
10:05	Bahadur, Dhirendra	Magnetic nanohybrids for in vivo therapy of cancer	Mumbai, India      Talk 18
10:20	Chen, Ritchie	High-performance ferrite nanoparticles for magnetothermal deep brain stimulation	Cambridge, UK      Talk 19
10:35	<b>Coffee break</b>		
<b>Session 5 Magnetic Particle Synthesis</b>			<i>Chair: Thompson Mefford</i>
11:10	Schatte, Sarah	Magnetic Nanocubes in Self-Assembled Hydrogels	Berlin, Germany      Talk 20
11:25	Fratila, Raluca Maria	Nucleic and peptide nucleic acid-engineered iron oxide nanoparticles for magnetic hyperthermia-mediated drug delivery	Zaragoza, Spain      Talk 21
11:40	Dutz, Silvio	Biocompatible Magnetic Fluids of Modified Co-Ferrite Nanoparticles with Tunable Magnetic Heating Power	Ilmenau, Germany      Talk 22
11:55	Insin, Numpon	Photocatalytic and Bactericidal Activities of Colloidal Titania-Silica-Iron Oxides Nanocomposites	Bangkok, Thailand      Talk 23
12:10	Seino, Satoshi	Synthesis and characterization of hollow magnetic nanospheres modified with Au-nanoparticles for bio-encapsulation	Osaka, Japan      Talk 24
12:25	<b>Lunch</b>		
<b>Session 6 Biological Applications</b>			<i>Chair: Etelka Tombacz</i>
13:50	Dahan, Maxime	Magnetogenetic Control of Cell Signaling	Paris, France      Invited Talk 3
14:40	Devina, Jaiswal	Immunomagnetic Cancer Cell Capture and Release for Drug Response Study	Storrs, CT, USA      Talk 25
15:00	Graefe, Christine	Passage of SPIONs through Cell Layers	Jena, Germany      Talk 26
15:20	<b>Poster session II (even numbered posters) with coffee and cake</b>		
17:30	<b>Bus leaves to the boat</b>		
18:30	<b>Boat trip on the Magic Spirit from False Creek</b> - generously sponsored by <b>Stemcells</b> ; <b>Group picture in front of (or on) the boat</b>		

**Friday, June 3, 2016**

08:00	Registration desk opens - at the Nest - 6133 University Boulevard		
	<b>Session 7 Biological Applications</b>		<i>Chair: Gilbert Ryan</i>
09:00	Mohseni, Matin	In-vivo targeting and imaging of super-paramagnetic iron-oxide particles to subcutaneous tumour models	London, UK      Talk 28
09:20	Polyak, Boris	Magnetic cell delivery suppresses in-stent stenosis in injured arteries	Philadelphia, PA, USA      Talk 29
09:40	Tefft, Brandon	Magnetizable Stent-Grafts Enable Endothelial Cell Capture	Rochester, MN, USA      Talk 30
10:00	Prina-Mello, Adriele	Magnetic Nanoparticles Applied to Cancer Theranostics: a Translational Nanomedicine Perspective	Dublin, Ireland      Talk 31
10:20	<b>Coffee break</b>		
	<b>Session 8 Biological Applications</b>		<i>Chair: Kathy Saatchi</i>
11:00	Mair, Lamar	Biofilm Ablation: Rotating Nanorods Remove Microbes from Surfaces, Enhancing Antimicrobial Efficacy	Baltimore, MD, USA      Talk 32
11:15	Hanley, Thomas	Nanomaterial Phagocytosis and Cytotoxicity: Quantification by Magnetic Cytometry	Auburn, MA, USA      Talk 33
11:30	Aurich, Konstanze	Protein modified ferucarbotran particles for GMP conform production of magnetically labeled platelets from platelet concentrates	Greifswald, Germany      Talk 34
11:45	Ma, Yunn-Hwa	Characterization of Magnetic Nanoparticle Internalization by Glioma Cells: Effects of Poly-L-Lysine Coating	Taoyuan, Taiwan      Talk 35
12:00	Gilbert, Ryan	Combinatorial Biomaterial Approaches Using Iron Oxide Nanoparticles to Direct Axonal Regeneration Following Spinal Cord Injury	Troy, NY, USA      Invited Talk 4
12:50	<b>Greek Buffet Lunch - generously sponsored by Ferrotec</b>		
	<b>Session 9 Biosensors</b>		<i>Chair: Hakho Lee</i>
14:00	Zabow, Gary	Transforming magnetic microparticles into RF-addressable microsensors	Boulder, CO, USA      Talk 36
14:20	Nikitin, Petr	Highly sensitive magnetic nanoparticle quantification with 7-order linear range and its applications for multiplex biosensing	Moscow, Russia      Talk 37
14:40	Johansson, Christer	Sensitive magnetic biodetection using magnetic multi-core nanoparticles and RCA coils	Gothenburg, Sweden      Talk 38
15:00	<b>Coffee break</b>		
	<b>Session 10 Biosensors</b>		<i>Chair: Maxime Dahan</i>
15:30	Lee, Hakho	Magnetic Sensors for Clinical Diagnostics: from Nanoscale Vesicles to Cancer Cells	Boston, MA, USA      Invited Talk 5
16:20	Soheilian, Rasam	Smart assembly of magnetic microparticles utilizing 3D magnetic fields	Brookline, MA, USA      Talk 39
16:40	Metaxas, Peter	Towards frequency-based spintronic detection of magnetic nanoparticles	Crawley, Australia      Talk 40
17:00	Wang, Jian-Ping	Magnetic nanoparticle based biosensor for multiplex detection of disease	Minneapolis, MD, USA      Talk 41
17:20	Spassov, Simo	RADIOMAG – A COST networking project in experimental cancer treatment research, combining magnetic fluid hyperthermia and radiotherapy	Dourbes, Belgium      Talk 42
17:40	<b>Free evening</b>		

Saturday, June 4, 2016

08:00	<b>Registration desk opens - NOTE: NEW LOCATION</b> - Pharmaceutical Sciences Building, Auditorium 1101 - 2405 Wesbrook Mall	
	<b>Session 11 Magnetic Hyperthermia</b>	<i>Chair: Thanh Nguyen</i>
08:30	Sandre, Olivier Thermo-sensitive peptide coating onto SPIONs synthesized by the DEG-NMDEA route: in situ dynamic light backscattering during magnetic hyperthermia	Pessac, France Talk 43
08:45	Takemura, Yasushi Magnetic loss and constant magnetic rotation of magnetic nanoparticles in viscosity dependence evaluated by dynamic hysteresis measurement	Yokohama, Japan Talk 44
09:00	Dennis, Cindi Effect of Applied AC Magnetic Field on Response of Magnetic Nanoparticles	Gaithersburg, MD, USA Talk 45
09:15	Andreu, Irene Nano-objects to control Magnetic Hyperthermia performance	Burnaby, Canada Talk 46
09:30	Blanco-Andujar, Cristina How much does shape matter?	Strasbourg, France Talk 47
	Magnetically stimulated phase transformation of FeO/Fe3O4 nanocubes to single Fe3O4 phase: an alternative approach to prepare tumor hyperthermia agents	Genova, Italy Talk 48
09:45	Lak, Aidin Improving Nanoparticle Heating by prior Orientation of Particles in a static 3 T magnetic Field	Garching, Germany Talk 49
10:15	<b>Coffee break - sponsored by Perkin Elmer</b>	
	<b>Session 12 Magnetic Hyperthermia</b>	<i>Chair: Cindi Dennis</i>
10:45	Thanh, Nguyen Real-time tracking of delayed onset cellular apoptosis induced by intracellular magnetic hyperthermia	London, UK Talk 50
11:00	Southern, Paul Remote Monitoring of Magnetic Particle Temperature During Hyperthermia: the Ideal Dose-Response Metric?	London, UK Talk 51
11:15	Monnier, Christophe Lock-in thermography: Using heat as a marker for stability and distribution of magnetic nanoparticles in biological systems	Fribourg, Switzerland Talk 52
11:30	Millan, Angel Magnetic nanoplatform incorporating a molecular thermometer. A new tool for local hyperthermia	Zaragoza, Spain Talk 53
11:45	Lewis, Jerome Superparamagnetic Iron Oxides, from the Lab to Approval	Boston, MA, USA Invited Talk 6
12:30	<b>Lunch</b>	
	<b>Session 13 Magnetic Imaging / MPI / MRI</b>	<i>Chair: Silvio Dutz</i>
13:30	Bauer, Lisa Toward Magnetic Particle Imaging-Guided Hyperthermia (hMPI): Analysis of High-Performance Agents for MPI and Focused Hyperthermia	Cleveland, OH, USA Talk 54
13:45	Bagheri, Hoda A Novel Approach to Magnetic Particle Imaging	Burnaby, Canada Talk 55
14:00	Khandhar, Amit Pharmacokinetics of LS-008: a blood pool SPIO tracer for Magnetic Particle Imaging	Seattle, WA, USA Talk 56
14:15	Viereck, Thilo Approaches to Binding Detection in Magnetic Particle Imaging	Braunschweig, Germany Talk 57
14:30	Nacev, Aleksandar Ultra-Fast MRI for Magnetic Particle Manipulation and Imaging	Rockville, MD, USA Talk 58
14:45	Liebl, Maik Imaging the mobility of magnetic nanoparticles by magnetorelaxometry tomography	Berlin, Germany Talk 59
15:00	Quini, Caio Imaging Magnetic Nanoparticles in vivo by AC biosusceptometry	Botucatu, SP, Brazil Talk 60
15:15	Bao, Yuping Shape-dependent Cellular Uptake of two types of MRI T1 Contrast agents	Tuscaloosa, AL, USA Talk 61
15:30	Siegmund, Birte In vivo-Tracking of transplanted human adipose stromal cells using magnetic nanoparticles in MRI	Rostock, Germany Talk 62
15:45	<b>Closing Comments and Announcement of the NEXT MEETING: Urs Hafeli / Maciej Zborowski / Wolfgang Schuett</b>	
16:00	<b>Meeting ends</b>	

# Social Program

As always, we will not let science prevent us from learning new stuff, having fun together and enjoying Vancouver to the fullest.

## Tuesday, May 31

A welcome reception will be held at the [Beatty Biodiversity Museum](#) downstairs, **open to all participants of the conference**. It will start at 6:30 PM and go till 10 PM. Conference registration will be available at that location too from 6:00 PM till closure. This reception, with music, was made possible by our sponsors [Chemicell GmbH](#) and [Diagnostic Biosensors](#).



## Wednesday, June 1

During the day, we will have a **spouse tour** starting at 10 AM. This tour is complimentary and always fun!

After the talks, there will be a poster session with Beer and Pretzels, graciously sponsored by [micromod Partikeltechnology GmbH](#). The rest of the evening is free. Go and explore! In fact, you don't have to go very far, there is quite a few eateries and restaurants (especially in the village, One More Sushi, Burgoo, Chinese) available, and we also have a [few pubs](#) and [Biercraft](#) at UBC.

## Thursday, June 2

In the afternoon there will be a poster session with cake and coffee.



In the evening, we will have our traditional boat cruise (on the Magic Spirit) with sunset and dinner. This was made possible by our local sponsor [STEMCELL](#). Enjoy!

## Friday, June 3

Nothing planned for this night. Maybe you want to take a bus ride downtown? Or just check out the local pub on campus and some of the other places and discuss collaborations? Or walk down to the beach which is surrounding UBC and watch the sunset?



## Saturday, June 4

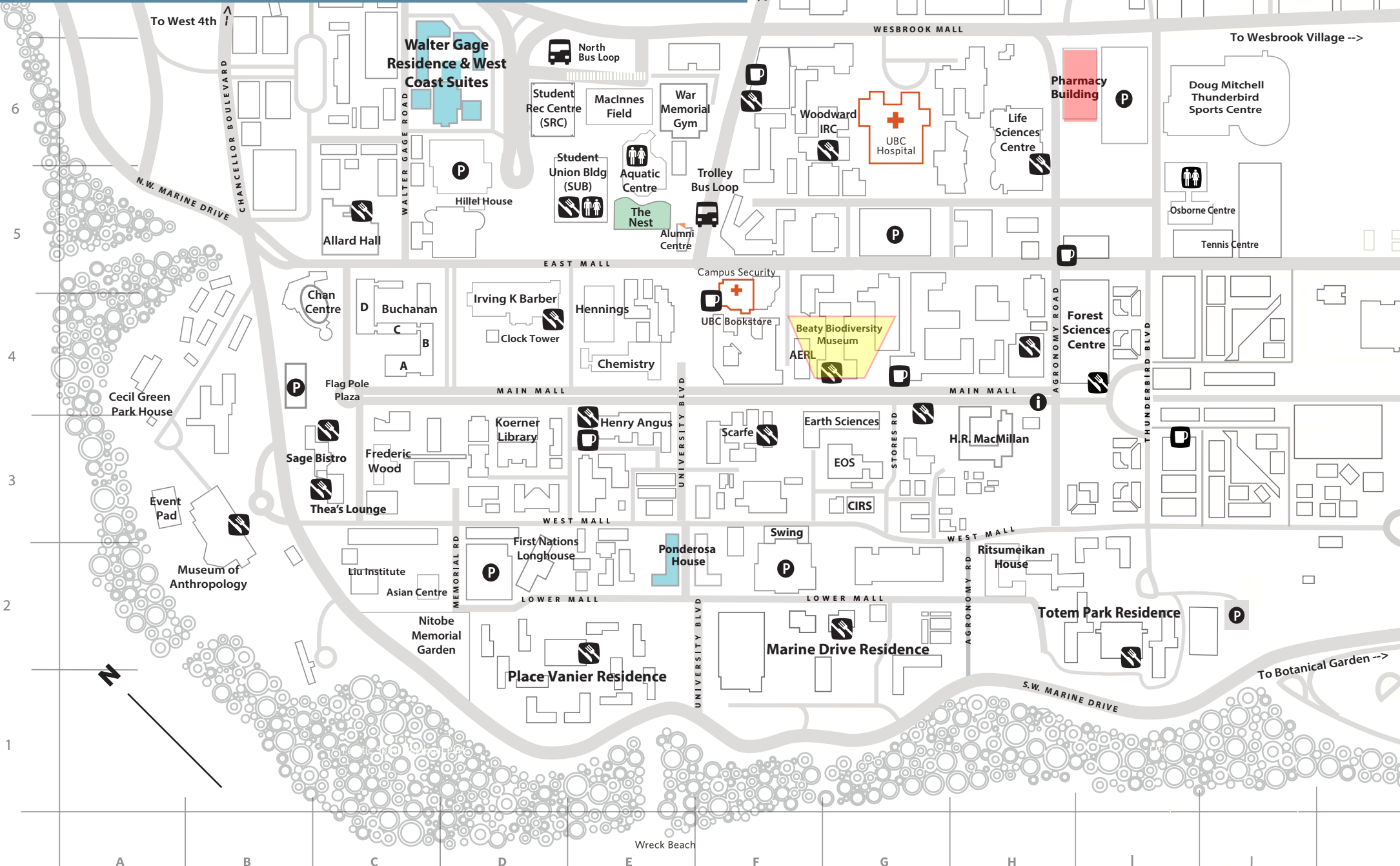
The meeting will end at 4 PM. Please take the opportunity and explore beautiful British Columbia on your own after the end of the conference! You might also be interested in a [whale watching tour](#), explore the wilderness surrounding the city, or even Vancouver Island, Whistler or the Rockies.



## 11th Scientific and Clinical Applications of Magnetic Carriers Conference 2016.

May 30 - June 6, 2016

University of British Columbia  
Vancouver BC



## Doing the Twist: Nanorods with Orthogonally Magnetized Segments Twist Their Way Through Viscoelastic Media

Lamar Main<sup>1</sup>, Alek Nacev<sup>1</sup>, Ryan Hilaman<sup>1</sup>, Pavel Stepanov<sup>1</sup>, Sagar Chowdhury<sup>2</sup>, Benjamin Shapiro<sup>2</sup>, Irving Weinberg<sup>1</sup>

<sup>1</sup>Weinberg Medical Physics J.L.C., Bethesda, Maryland, USA

<sup>2</sup>Fischell Department of Bioengineering, University of Maryland, College Park, Maryland, USA

Contact: Lamar.Mair@gmail.com

**Introduction:** As particles travel through viscoelastic media such as tissue, they encounter barriers that may significantly impede motion. We present nanorods capable of being simultaneously pulled and twisted using time-varying magnetic gradients and fields. We show that combining pulling and twisting increases translational velocities through collagen-rich matrix by factors of up to -2. Additionally, we show that combined pulling and twisting enables rods entrapped in dense regions of proteins to twist free and continue their journey. Thus, we conclude that twisting nanorods can enhance their ability to move through media to reach targets.

**Methods:** Rods have two distinct magnetic segments: one segment magnetized parallel to the long axis of the rod, and one segment magnetized orthogonally to the long axis of the rod (Fig. 1A, 1B). The magnetic actuation setup consists of a permanent magnet and two Helmholtz coils (Fig. 1C). To test motion, we place the rods in a collagen-rich biopolymer (Matrigel) and apply pulling forces, as well as combined pulling and twisting forces. The permanent magnet supplies a magnetic field and field gradient, while the Helmholtz coils supply a gradient-free rotating magnetic field.

**Results:** We synthesized rods with two magnet segments (nickel) separated by a nonmagnetic segment (gold) (Fig. 1A). In moving rods through viscoelastic biopolymer environments, we observe that particle speed pre-twisting (Fig. 1E, red data) is lower than particle speed with twisting (Fig. 1E, green data) or post-twisting (Fig. 1E, purple data). Combined magnetic pulling and twisting of the rods enhances transport through the media, versus pulling forces alone (Fig. 1E).

**Discussion:** Rods rotate due to the torque applied by the Helmholtz coils, which apply fields in the plane of the orthogonally magnetized rod segment (Fig. 1C). The rod twists around its long axis as opposed to tilting around its midpoint. Twisting occurs because the drag torque for twisting is significantly smaller than the drag torque for tilting. Twisting rotation generates a shear in the surrounding media, and this shear may reorganize the nearby proteins and protein corona. This reorganization of surrounding proteins may momentarily decrease the local effective viscosity, allowing the particle to move more easily through the matrix. Additionally, in some cases, the rotationally induced shear may induce lateral translation of the rod. Lateral translation may allow the rod to escape entrapment by particularly dense region of the matrix (Fig. 1D). We observe translational speeds ~4  $\mu\text{m/s}$  pre-twisting, versus translational speeds of ~6-8  $\mu\text{m/s}$  with twisting (Fig. 1E). We are currently working to elucidate the mechanisms which cause increases in speed post-twisting.

**Conclusion:** Data shows that rotation of rods improves particle motion through media. This is important for drug delivery because it may enable particles to be directed to targets more quickly and efficiently.

## Microwheels: Magnetic Bead Rolling Micro-Robots

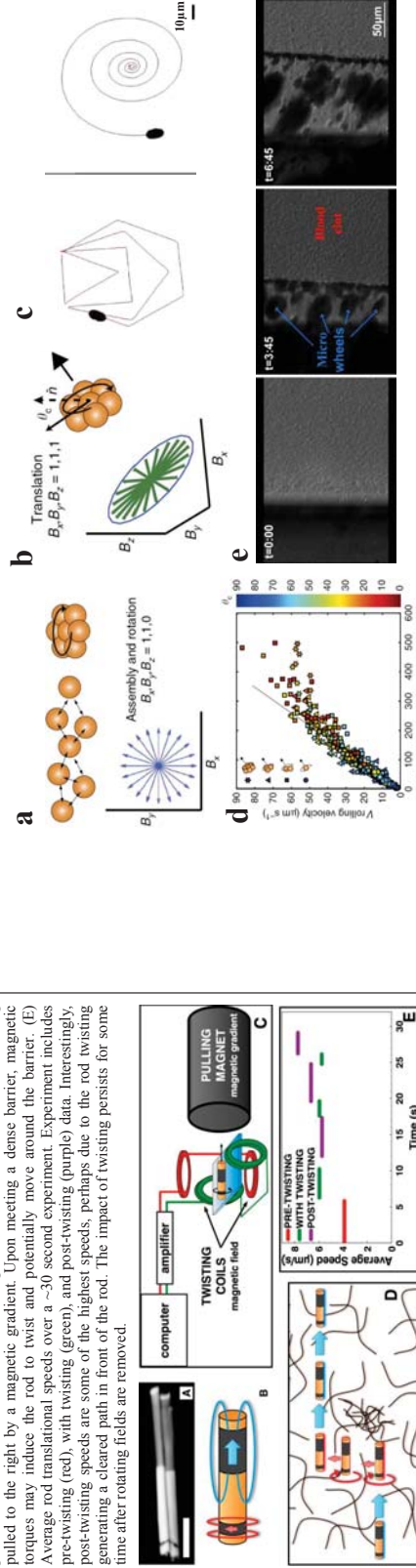
### And Their Potential In The Non-Invasive Treatment Of Blood Clots

T. O. Tasci<sup>\*</sup>, K. Rana<sup>†</sup>, K. B. Neeves<sup>†</sup>, D. W. M. Marr<sup>†</sup>

<sup>†</sup>Department of Chemical and Biological Engineering, Colorado School of Mines, Golden, CO  
email: tasci@mines.edu

Microrobots have great potential to revolutionize medicine by navigating through body fluids to achieve targeted therapy and diagnosis. Current microrobot technology requires complex microfabrication methods and resulting microrobots lack precise directional control and move at slower velocities.  
In this work, we have shown that by applying 3D rotating magnetic fields, magnetic micro particles can be assembled into wheel shaped structures (microwheels) that can roll and translate at high speeds (~100  $\mu\text{m/s}$ ) faster than other microrobot technologies<sup>1</sup>. The direction of the microwheels can be precisely programmed or controlled manually using joystick or keyboard control. One of the immediate medical applications of the microwheels is using them for the treatment of blood clots. By conducting *in vitro* experiments, we have demonstrated that the drug (t-PA) loaded microwheels can be effectively directed to a specific blood clot and break up them both mechanically and chemically. We have demonstrated that blood clot removal (fibrinolysis) rate with drug loaded microwheels is at least 5 times faster than the fibrinolysis rate via diffusion of the drug itself (current medical procedure).

With ease of assembly, high speed and precise directional-control, microwheels *in situ* has significant advantage over pre-fabricated devices as individual particles are injectable and small enough to pass through blood capillaries. Once the applied magnetic field is turned off, wheels disassemble into micron-sized particles removable via the body's natural defence mechanisms.



a) Microwheel assembly occurs by the application of a planar rotating field,  $B_x = B_0 * \sin(\omega t)$ ,  $B_y = B_0 * \sin(\omega t + \pi/2)$

b) By the addition of the  $B_z$  field, microwheel stands up at a camber angle  $\theta_0$ , and start to roll,  $B_z = B_0 * \sin(\omega t - \phi_b)$

c) Microwheel paths can be precisely preprogrammed or controlled via joystick. In these two experiments, microwheel is in 7mer configuration (composed of seven 4.5  $\mu\text{m}$  Dynabeads) and solid line shows the trajectory of the microwheel (rolling at 55  $\mu\text{m/s}$ )

d) A total of 368 experiments were conducted with monomer, dimer, trimer and 7mer microwheels at different magnetic field strengths and frequencies. Plot shows how microwheel rolling velocity changes with weighted angular frequency of the microwheel. Line indicates the slope (32  $\mu\text{m}^2/2\pi$ ), where  $m$  is the weight of the single particle and  $\eta$  is the dynamic viscosity.

e) Time lapse images showing the lysis of the blood clot. In this experiment, clot has a fibrinogen density of 10mg/ml. The individual magnetic beads forming the microwheels are 1  $\mu\text{m}$  in size and coated with tissue plasminogen activator (t-PA). Once the field is applied, 1  $\mu\text{m}$  beads form much bigger microwheels and attack the clot (via joystick control). As the field turned off, microwheels disassemble into individual 1  $\mu\text{m}$  particles. Clot is removed at an average rate of 20  $\mu\text{m}/\text{min}$ .

Reference: 1. Soft Mater., 7(18), 8169-8181

Talk #2

Talk #1

## Complement activation and immune recognition of superparamagnetic iron oxides (SPIO) in mice and humans

Guankui Wang<sup>1</sup>, Svetla Inturi<sup>1</sup>, Seyed Moein Moghimi<sup>2</sup>, Dmitri Simberg<sup>1</sup>

<sup>1</sup>The Skaggs School of Pharmacy and Pharmaceutical Sciences, University of Colorado Denver, Anschutz Medical Campus, 12850 E. Montview Blvd., Aurora, CO 80045

<sup>2</sup>Centre for Pharmaceutical Nanotechnology and Nanotoxicology, Department of Pharmacy, Faculty of Health and Medical Sciences, Universityparken 2, University of Copenhagen, DK-2100 Copenhagen, Denmark

There is an unmet need in efficient and safe contrast agents for magnetic resonance imaging (MRI) of various pathologies. Magnetic resonance imaging (MRI) agent superparamagnetic iron oxide (SPIO) is a core shell nanoparticle consisting of magnetic-magnhemite ( $\text{Fe}_3\text{O}_4$  and  $\gamma\text{-Fe}_2\text{O}_3$ ) core and biopolymer dextran shell (Gupta and Gupta 2005). SPIO nanoparticles are efficient contrast agents, but their clinical use is associated with significant immune reactions and propensity for clearance by liver and spleen (Gupta and Gupta 2005). Complement is the system of 30+ serum proteins that represents the first immune barrier to invading pathogens (Ricklin, Hajishengallis et al. 2010). Activation of complement cascade results in coating (opsonization) of nanoparticles with complement component C3 and release of extremely potent proinflammatory factors C3a and C5a. C3 binding leads to clearance by leukocytes and macrophages, while release of C5a results in the complement-induced pseudoallergy upon infusion of nanoparticulate delivery systems (Szobieni 2005). We will demonstrate the critical role of complement in immune recognition and clearance of SPIO in mice and humans. First we will show the data on the distinct mechanisms of complement activation in murine and human sera (Banda, Mehta et al. 2014) and (Chen et al., submitted). Second, we will demonstrate the active role of complement in the immune recognition of SPIO by blood leukocytes and macrophages (Inturi, Wang et al. 2015). Third, we will discuss some of the synthetic strategies and challenges to block complement activation in mice and human subjects (Wang, Inturi et al. 2014). Understanding the mechanisms of immune recognition and complement activation by SPIO can be very useful for rational design of improved imaging and drug delivery systems.

## References

- Banda, N. K., G. Mehta, Y. Chao, G. Wang, S. Inturi, L. Fossati-Jimack, M. Bottino, L. Wu, S. Moghimi and D. Simberg (2014). "Mechanisms of complement activation by dextran-coated superparamagnetic iron oxide (SPIO) nanoworms in mouse versus human serum." *Part Fibre Toxicol* **11**(1): e4.
- Gupta, A. K. and M. Gupta (2005). "Synthesis and surface engineering of iron oxide nanoparticles for biomedical applications." *Biomaterials* **26**(18): 3995-4021.
- Inturi, S., G. Wang, F. Chen, N. K. Banda, V. M. Holers, L. Wu, S. M. Moghimi and D. Simberg (2015). "Modulatory Role of Surface Coating of Superparamagnetic Iron Oxide Nanoworms in Complement Opsonization and Leukocyte Uptake." *ACS Nano* **9**(11): 10758-10768.
- Ricklin, D., G. Hajishengallis, K. Yang and J. D. Lambiris (2010). "Complement: a key system for immune surveillance and homeostasis." *Nat Immunol* **11**(9): 785-797.
- Szobieni, J. (2005). "Complement activation-related pseudoallergy: a new class of drug-induced acute immune toxicity." *Toxicology* **216**(2-3): 106-121.
- Wang, G., S. Inturi, N. J. Serkova, S. Merkulov, K. McCrae, S. E. Russek, N. K. Banda and D. Simberg (2014). "High-relaxivity superparamagnetic iron oxide nanoworms with decreased immune recognition and long-circulating properties." *ACS Nano* **8**(12): 12437-12449.

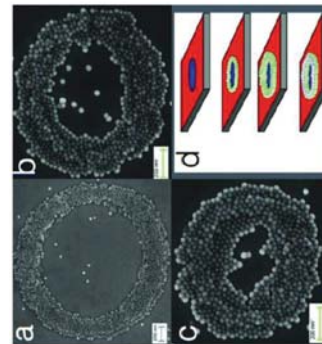
## Magnetic-field-directed self-assembly of programmable mesoscale shapes

L. Ye, T. Pearson, C. Dolbashian, P. Psatrak\*, A.R. Mohtasebzadeh, B. Fellows\*, O.T. Mefford\*, and T.M. Crawford\*

Smart State Center for Experimental Nanoscale Physics,

Dept. of Physics and Astronomy, University of South Carolina, Columbia, SC 29208

\*Materials Science and Engineering, Clemson University, Clemson, SC  
email: crawtm@mailbox.sc.edu



A key challenge in the self-assembly of magnetic nanoparticles is obtaining precise nanoscale control over the shapes created. A related challenge is extending this control to macroscopic dimensions, i.e. from nanometers to centimeters. Here, using magnetic field gradients at the surface of perpendicular magnetic recording media ( $\sim 10^7 \text{ T/m}$ ) that vary dramatically over the diameter of a single nanoparticle, we demonstrate assembly of 2D mesoscale shapes with feature sizes that range from 30 to 350 nm (Figure 1 a-c) [1] and can be templated over  $\text{cm}^2$  areas. Our 30 nm nanoparticles are synthesized by thermal decomposition and colloidal suspension in hexane [2]. The colloidal fluid is then dropped onto a piece of perpendicular media recorded with an array of custom shapes using a contact write/read tester [3]. After assembly, the excess hexane is removed and the resulting assembly imaged with Field-Emission Scanning Electron Microscopy (FE-SEM) to determine pattern fidelity and feature size.

The use of perpendicular recording media is critical because its out-of-plane magnetization allows isotropic 2D recording of user-defined template shapes [1-4]. The specific geometry of the magnetic fields and field gradients at transitions in perpendicular media produce forces that attract the nanoparticles both toward the surface and toward the transitions between adjacent, oppositely magnetized regions [4]. Importantly, at a height of 30 nm above the surface the lateral force extends up to 150 nm away from a transition and is directed toward the transition, allowing assembly of 30 nm nanoparticles into features as wide as 350 nm (Figure 1 a-c). Once a single layer is assembled, a second layer is observed to assemble on top of the first layer (Figure 1). By rinsing with hexane after assembly, we can make these features as narrow as a single 30 nm nanoparticle (Figure 2). We will discuss opportunities and challenges related to this technology for self-assembly, particularly the potential to improve control by optimizing recording media specifically for nanoparticle self-assembly.



Figure 2 – Parallel line features with 30 nm width (a single nanoparticle) obtained on perpendicular media by rinsing after assembly.

- References
- [1] L. Ye, T. Pearson, C. Dolbashian, P. Psatrak, A. R. Mohtasebzadeh, B. Fellows, O.T. Mefford, and T. M. Crawford, *Adv. Fct. Mat.* 10.1002/adfm.201504749 (2016).
  - [2] D. L. Huber, E. L. Venturi, J. E. martin, R. J. Provenco, J. Magn. Magn Mater. **278**, 311 (2004).
  - [3] T. D. Leonhardt, R. J. M. van der Heijden, T. W. Clinton, and T. M. Crawford, *IEEE Trans. Magn.* **37**, 1580 (2001).
  - [4] S. Yoshihurnura, G. Egawa, T. Miyazawa, Z. Li, H. Saito, J. Bai, and G. Li, *Phys. Conf. Ser.* **266**, 012065 (2011)

## Biocomputing nano- and microstructures as smart sensors and theranostic agents

### Measuring biodistribution of PEG coated PrecisionMRX™ nanoparticles with superparamagnetic relaxometry (SPMR)

Kayla E. Minser<sup>1</sup>, Caroline Weidon<sup>1</sup>, Andrew Gomez<sup>1</sup>, Todor Karaulanov<sup>1</sup>, Bill Anderson<sup>1</sup>, Dale L. Huber<sup>3</sup>, Helen J. Hathaway<sup>2</sup>, Edward R. Flynn<sup>1</sup>, Giulio F. Paciotto<sup>1</sup> and Erika C. Vreeland<sup>1\*</sup>

<sup>1</sup> University of New Mexico Health Sciences Center and University of New Mexico Comprehensive Cancer Center, Albuquerque, NM, USA

<sup>2</sup> Center for Integrated Nanotechnologies, Sandia National Laboratories, Albuquerque, NM, USA  
Email: Erika.Vreeland@seniorscientific.com

In this study, we demonstrate the use of Superparamagnetic Relaxometry (SPMR) for monitoring the biodistribution of superparamagnetic iron oxide ( $\text{Fe}_3\text{O}_4$ ) nanoparticles *in vivo*. SPMR uses superconducting quantum interference device (SQUID) sensors to measure the remnant magnetization of nanoparticles bound to cells following a brief magnetizing pulse. Unbound nanoparticles are not detected, making SPMR uniquely capable of discriminating between nanoparticles that are circulating freely in the bloodstream from those that have been immobilized in organs and tissues throughout the body.

To prolong their circulation time following injection, 25 nm PrecisionMRX™ nanoparticles were coated with methoxy-polyethylene glycol (PEG nps). PEG nps were suspended in 100  $\mu\text{L}$  of saline and injected intravenously via tail vein into three Balb/C mice at a dose of 5 mg/kg of body mass, while a control mouse was injected with 100  $\mu\text{L}$  of saline solution. Mice were measured individually on the MRX™ instrument at successive time points over the course of 24 hours. At the end of the time course, mice were euthanized and organs harvested for ex vivo MRX measurements. Histology was subsequently performed on excised organs.

MRX measurements of mice injected with PEG nps showed a magnetic signal in the location of the liver that slowly increased to a maximum over 24 hours (Fig. 1). Subsequent MRX measurements of excised organs confirmed that nanoparticles had been taken up primarily by the liver, with a smaller quantity detected in the spleen, lungs, and heart.

These experiments establish the utility of SPMR to monitor the accumulation of PEG coated PrecisionMRX nanoparticles in the liver following injection, an important parameter in determining their pharmacokinetics *in vivo* diagnostic and therapeutic use.

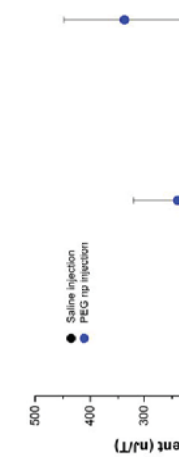


Figure 1. MRX measurements of injected mice over 24 hours. The measured moment in mice injected with PEG nps represents the accumulation of nanoparticles in the liver.

This work was performed, in part, at the Center for Integrated Nanotechnologies, an Office of Science User Facility operated for the U.S. Department of Energy (DOE) Office of Science. Sandia National Laboratories is a multi-program laboratory managed and operated by Sandia Corporation, a wholly owned subsidiary of Lockheed Martin Corporation, for the U.S. Department of Energy's National Nuclear Security Administration under contract DE-AC04-94AL85000.

<sup>1</sup>M.P.Nikitin<sup>1,2,3</sup>

<sup>1</sup>Moscow Institute of Physics and Technology (State University), Dolgoprudny, Russia

<sup>2</sup>General Physics Institute, Russian Academy of Sciences, Moscow, Russia

<sup>3</sup>Institute of Bioorganic Chemistry, Russian Academy of Sciences, Moscow, Russia

e-mail: max.nikitin@phystech.edu

Nanoparticles with biocomputing capabilities could potentially be used to create sophisticated robotic devices with a variety of biomedical applications such as intelligent sensors and theranostic agents. Recently, we have shown<sup>1</sup> that nano/microparticles can be transformed into autonomous biocomputing structures capable to implement a functionally complete set of Boolean logic gates (YES, NOT, AND and OR) and to bind with a target as result of computation. The logic gating functionality is incorporated into self-assembled particle/biomolecule interfaces, and the logic gating is achieved through the input-induced disassembly of the structures. In the experiments, the preference to magnetic nanoparticles is given because they can be manipulated with external magnetic fields, precisely quantified by their nonlinear magnetization and visualized with MRI.

The concept is indifferent to the nature of the interfaces used for assembly of the structures and input processing. In this work, to illustrate the capabilities of the approach we have used protein-assisted self-assembly of nanoparticles<sup>2,3</sup> for construction of the biocomputing structures. The employed antibody-based interfaces allow processing of many biomedically relevant inputs and are well suited for biosensing in a variety of complex media.

We demonstrate that the proposed biocomputing platform is compatible with many *in vitro* assay formats and result-detecting techniques such as lateral flow, ELISA, homogenous enzymatic and 3D-solid phase magnetic assays, etc. We also demonstrate feasibility of cell targeting based on logic-gated biochemical analysis of cell's microenvironment, which is especially appealing for development of the next-generation nanorobotic devices for theranostic applications.

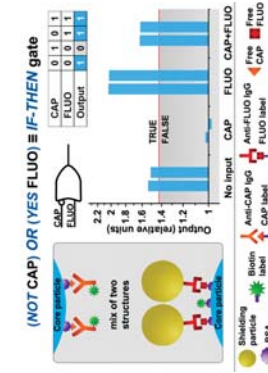


Fig.1. Example of the biocomputing structures that implement the IF-THEN logic gate with two inputs - chloramphenicol (CAP) and fluorescein (FLUO).

The research was supported by grants of Russian Science Foundation (#16-19-00131) and Russian Foundation of Basic Research (#15-33-21072).

[1]. Nikitin et al., Biocomputing based on particle disassembly, Nat Nanotechnol (2014).

[2]. Aghayeva, Nikitin et al., ACS Nano (2013).

[3]. Nikitin et al. Proc Natl Acad Sci USA (2010).

## Dual-Color Magnetic Barcodes with Ultra-High Encoding Capacity

Si Lu, Dingshengzhang, Shunlia Zhang, Hong Xu\*, Hongchen Gu

School of Biomedical Engineering, Shanghai Jiao Tong University, Shanghai 200030, P. R. China

\*E-mail: xuhong@sjtu.edu.cn

Quantum dot (QD) based optical encoded magnetic beads bear remarkable advantages in multiplexed bioassays. Though abundant research has been reported previously, the preparation of QD encoded barcodes with high encoding capacity and fluorescence stability still remains a challenge.

Here, a three dimensional encoding library of dual-color magnetic barcodes with ultra-high encoding capacity and fluorescence stability were achieved. Firstly, QD encoded magnetic host particles in different sizes and fluorescence intensity were prepared. QDs were immobilized onto the surface of different-sized magnetic core beads layer by layer via coordination interaction. Fluorescence intensity of the QD encoded beads was extremely uniform. Further encapsulation of silica and polyelectrolytes endowed the host particles with significant fluorescence stability. As-synthesized host particles were fluorescence stable in polar solvent of a wide pH range. Besides, their fluorescence intensity was almost unchanged over 100 days' storage. Secondly, dual-color magnetic barcodes were prepared through host-guest structure. FITC-doped carboxylated guest nanoparticles in three different fluorescence intensity levels were mixed at certain ratio and covalently conjugated onto the surface of QD encoded host particles. By a combinational use of size signal, QD fluorescence intensity and FITC fluorescence intensity, a three dimensional barcode library with an ultra-high encoding capacity of 100 barcodes was established successfully via flow cytometry system for the first time.

This work might pave a new way of synthesizing QD based encoded beads with ultra-high encoding capacity and fluorescence stability, which shows great potential in multiplexed bioassays of real physiological environment.

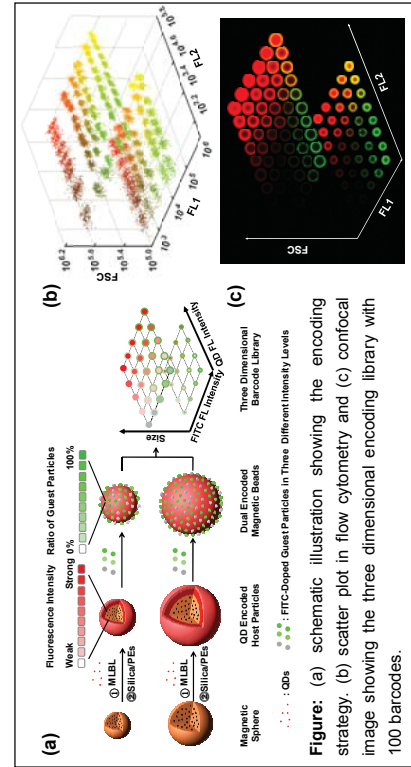


**Figure 1:** (a) schematic illustration showing the encoding strategy. (b) scatter plot in flow cytometry and (c) confocal image showing the three dimensional encoding library with 100 barcodes.

## INVITED TALK 1 RESULTS AND CHALLENGES IN MAGNETICALLY TARGETING THERAPY TO DISEASE TARGETS

Benjamin Shapiro

Professor  
Fischell Department of Bioengineering + The Institute for Systems Research  
University of Maryland, College Park, Maryland, USA [benshanp@umd.edu](mailto:benshanp@umd.edu)

Our group is developing magnet systems to direct and focus therapy to disease targets in the body. The goal is to design, construct, test and deliver to patients advanced magnet systems that can put the right drug or gene in the right place in the body. We will present results on how dynamic control of magnets and exploitation of nanoparticle physics can solve a key challenge in magnetic targeting: it can focus nanoparticles to deep targets between magnets. Magnet design can also enable 'magnetic injection' which enables topical (non-invasive) delivery to ear and eye targets. In addition to delivery and efficacy, results will be shown for safety. In particular, monitoring of live brain tissue for continued normal behavior during nanoparticle motion in the brain. Finally, clinical use of magnetic targeting would benefit from precision real-time imaging. Such imaging can be achieved by ultra-fast magnetic pulses that can enable real-time magnetic resonance imaging (MRI) with single cell spatial resolution. The talk will close with a summary of open questions, challenges and the opportunities for clinical use of magnetic targeting.

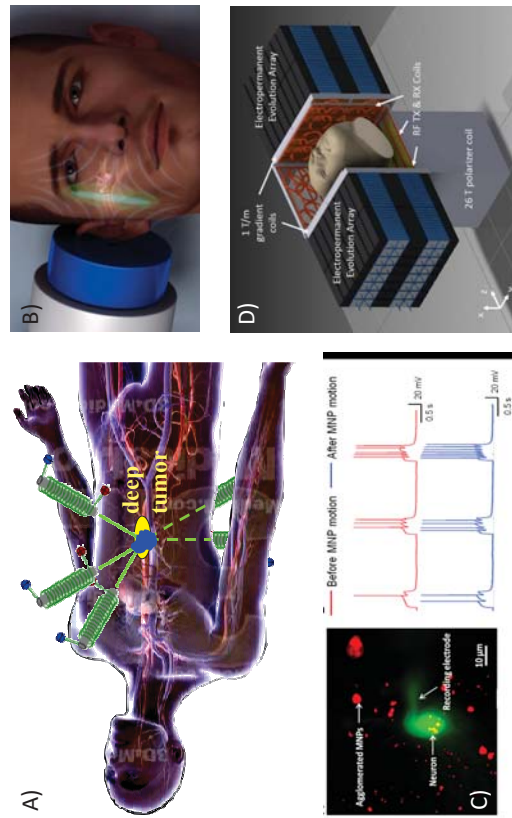


**Figure 1:** A) Focusing to deep tissue targets between magnets. B) Topical delivery to the cochlea. C) Magnetic motion safety studies in live brain tissue. D) Ultra-fast high resolution MRI (magnetic resonance imaging).

## Current challenges in the navigation of magnetic particles in the pig liver using an MRI scanner

Alexandre Bigot<sup>1\*</sup>, Ning Li<sup>2</sup>, Zeynab Nosrati<sup>3</sup>, Maxime Gérard<sup>4</sup>, François Michaud<sup>1</sup>, Samuel Kadoury<sup>5</sup>, Urs Häfeli<sup>3</sup>, Gilles Soulez<sup>1</sup>, Sylvain Martel<sup>2</sup>

<sup>1</sup>Clinical Image Processing Laboratory (LCT), Centre de Recherche du Centre Hospitalier de l'Université de Montréal (CRCHUM), Montréal, QC, CAN; <sup>2</sup>Nanorobots Laboratory, Department of Computer and Software Engineering and Institute of Biomedical Engineering, Polytechnique Montréal, Montréal, QC, CAN; <sup>3</sup>University of British Columbia, Faculty of Pharmaceutical Sciences, Vancouver, CAN; <sup>4</sup>Institute of Biomedical Engineering, Polytechnique Montréal, 2000 Edouard-Montpetit Blvd, Montréal, QC, CAN;  
\*Email: alexandre.bigot@umontreal.ca

Magnetic actuation is of tremendous interest for endovascular targeted therapies because it allows the control of untethered magnetic bodies without any harm to the patient. Our group decided to use a Magnetic Resonance Imaging (MRI) scanner as an actuator to steer therapeutic magnetic beads toward cancerous lesions in the body; this is referred to as Magnetic Resonance Navigation (MRN)<sup>1</sup>. We currently aim to achieve multi-bifurcation MRN (MB-MRN), i.e., navigation of beads along several consecutive vessels<sup>2</sup>, in a pig model with  $\text{Fe}_3\text{O}_4$  nanoparticles embedded in 250- $\mu\text{m}$ -diameter PLGA particles.

Current MRI gradient strengths (typically around 40 mT/m) combined with low saturation magnetization of  $\text{Fe}_3\text{O}_4$  magnetic carriers do not allow deep targeting because of the fast pulsatile blood flow which makes steering of carriers cumbersome. We currently investigate a balloon-occluded approach<sup>3</sup> in the pig which consists of using a balloon catheter to temporarily reduce the blood flow and eliminate the diastolic-systolic variation. In addition, as shown on the figure below, the liver is an intricate network of vessels and it is critical to gather geometric information (length, diameters) to compute the magnetic forces.

We conducted eight experiments on pigs (mean weight  $\pm$  SD =  $31.9 \pm 2.03$  kg) in order to collect flow information and geometric information about the liver for future MRN experiments. The balloon catheter allows reducing blood flow from 40.5 cm/s to 6.1 cm/s, a reduction of 85%. Furthermore, the pulsation is eliminated, simplifying both simulations and navigation.

We will give an overview of the most recent development of MRN as well as data from our *in vivo* experiments. In addition, results from magnetic particles synthesis and MR sequence development will be discussed. Balloon-occluded approach opens up the perspective of MB-MRN *in vivo* for deeper magnetic therapeutic targeting. This technology could have applications in brain cancer or liver cancer for better patient care.

## A Magnetic Sponge as an On-demand Drug Delivery Device

Ali Shademan<sup>1</sup>, Hongbin Zhang<sup>\*1</sup>, John K. Jackson<sup>2</sup>, Helen M. Burt<sup>2</sup>, Mu Chiao<sup>\*1</sup>  
<sup>1</sup>Department of Mechanical Engineering, University of British Columbia, Vancouver, BC, Canada.  
<sup>2</sup>Faculty of Pharmaceutical Sciences, University of British Columbia, Vancouver, BC, Canada.  
\*E-mail: [mchiao@omch.ubc.ca](mailto:mchiao@omch.ubc.ca), [dhb@vcs.ca](mailto:dhb@vcs.ca)

Magnetically regulated drug delivery is an approach for localized drug treatment. This method incorporates remote operation using a magnet without the need of internal power on the device.

We propose a drug delivery device using a magnetic sponge which can be squeezed under a magnetic field to release an exact dose of the payload drug. This sponge is made of polydimethylsiloxane (PDMS) incorporating with carbonyl iron (CI) microparticles which leads to magnetic PDMS. Furthermore, by utilizing a solvent casting and particulate leaching (SPL) technique, this magnetic PDMS becomes porous. The best w/w% ratio of CI to PDMS has been determined to be 100% from three different experimental ratios of 50%, 100%, and 150% to allow maximum deformation in various magnetic fields. Besides, a reservoir has been fabricated from PDMS, where drugs may be disposed. Subsequently, the magnetic sponge is placed inside the reservoir and sealed with a thin ( $\sim$ 10  $\mu\text{m}$  in thickness) PDMS membrane. An aperture ( $\sim$ 90  $\times$  90  $\mu\text{m}$ ) is later created at the centre of the membrane using laser ablation. The released drug dosage can be controlled by tuning the applied magnetic field. In this work, a drug delivery device of 7 mm in diameter with less than 2 mm thickness was fabricated. Drug release tests have been performed using methylene blue (MB) as a model drug. This device released exact doses of  $2.28 \pm 0.23$   $\mu\text{g}$  MB per actuation in a 120 mT magnetic field. However, more release can be achieved in stronger magnetic fields.

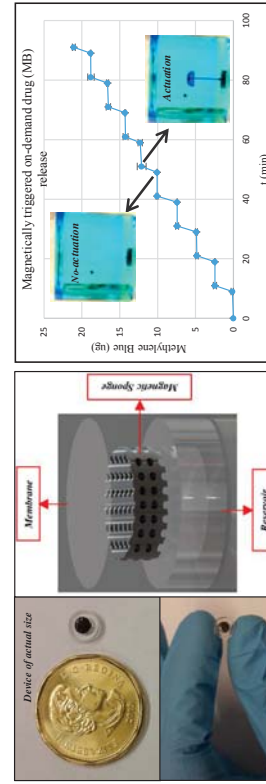


Figure 1 – (Left) 3D Segmentations of the hepatic arterial (red) and venous (blue) trees. (Right) Effect of a balloon catheter on the hepatic blood flow.  
1. Pouponneau, P. et al. *Biomaterials* **32**, 3481–3486 (2011);  
2. Bigot, A. et al. *IEEE Trans. Robot.* **30**, 719–727 (2014);  
3. Irie, T. et al. *Cardiovasc. Intervent. Radiol.* **36**, 706–713 (2013).

## Development of a Real Time Image-Based Guidance System of Magnetic Nanoparticles for Targeted Drug Delivery

Xingming Zhang<sup>1,2</sup>, Tian-Anh Le<sup>1</sup>, and Jungwon Yoon<sup>1\*</sup>

<sup>1</sup> School of Mechanical and Aerospace Engineering, Gyeongsang National University, Jinju 660-701, Republic of Korea.  
<sup>2</sup> School of Naval Architecture and Ocean Engineering, Harbin Institute of Technology at Weihai, Weihai, Shandong, China.  
\*Email: jw.yoon@gnu.ac.kr; Mobile: 82-10-2402-6904

Magnetic nanoparticles (MNPs) possess the ability to function at the cellular and molecular level of biological interactions, making them an attractive platform as contrast agents for Magnetic Particle Imaging (MPI) and as carriers for targeted drug delivery (TDD). TDD by using MNPs is an efficient technique to deliver drug molecules towards specific tissues in a human body.

The MNPs' guidance system is a combined electromagnetic actuation (EMA) and monitoring system, which can provide an accurate control scheme with MNP's localization for more precise targeting of the drug delivery. The localization of the MNPs is done on the basis of MPI with low amplitude excitation field. In this paper, we have developed a novel guidance system for MNPs position control, by alternately supply of different currents to coils set in time sequence, the coil set alternates functions between MPI and EMA simultaneously. Motion of MNPs is controlled by a gradient of magnetic field in EMA period, the distribution of MNPs is detected in MPI period and provides feedback to the EMA. The guidance system will provide simultaneous navigation and tracking for targeted drug delivery of MNPs in compact and efficient ways.

The experimental setup is shown in Figure (a). We apply a.c. current with d.c. offset in each differential current coils (DCCs) to achieve field free point (FFP) and scanning MNPs' distribution in workspace. The size of workspace is 3.5cm. The tube filled with MNP suspension was placed in workspace. MNPs aggregated into a cluster, which was moved by gradient field generated by DCCs during EMA periods. The distribution of MNPs was reconstructed as MPI image (Figure (b)). The core sizes of MNP used for guidance system are 60nm (Magne, 2.67Fe- $\mu$ g/ml) and 5mn (Resovit, 2.83 Fe- $\mu$ g/ml). The 1D MNPs guidance system has 0.3s MPI time and 0.2s EMA time, allowing a position control of MNPs. The movement of MNPs cluster could be observed from both camera and MPI image. The gradient field is 3 T/m for MPI. The experimental results show that the real time MPI-based guidance system could achieve MNPs position control with 2Hz MPI image update frequency, namely hybrid system frequency.

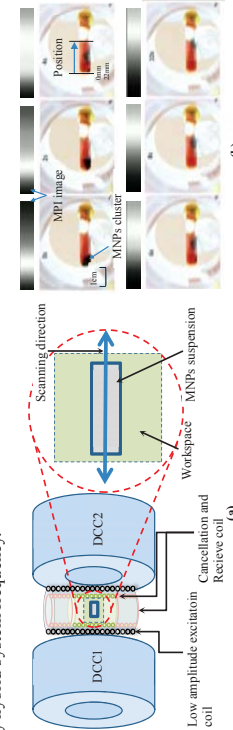


Figure: (a) 1-D Guidance system with 1 set of DCC1 and DCC2 and an excitation coil combined with a receive coil. The DCCs are used as actuation coils during EMA period and generated selection field during MPI period, and combination of excitation and receive coil is used to generate excitation field and collect MNPs signal. the MNPs suspension sample is filled in a glass tube, and placed in the workspace along the scanning direction. (b) MNPs are manipulated by guidance system. Magnetic force was to the right side, and during steering the particle cluster, MPI shown the position of cluster (90nm). The high concentration of MNPs is shown in white and low in black.

## The target killing of *Staphylococcus aureus* by magnetotactic bacteria under a compound magnetic field in a microfluidic chip

Linjie Chen<sup>1,2,3#</sup>, Changyou Chen<sup>1,3</sup>, Chuanfang Chen<sup>1,3</sup>, Pingping Wang<sup>1,3</sup>, Long-Fei Wu<sup>1,4</sup>, Tao Song<sup>1,2,3\*</sup>

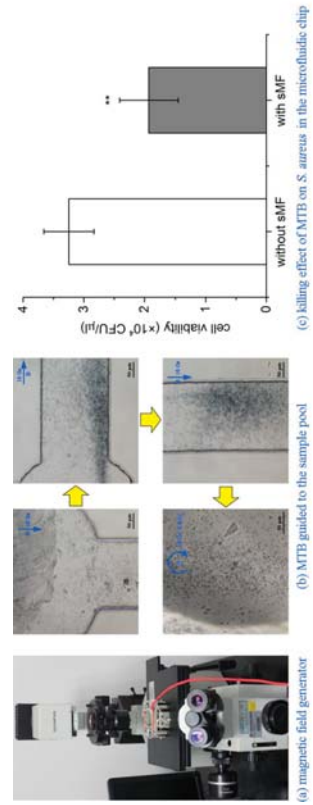
<sup>1</sup> Beijing Key Laboratory of Bioelectromagnetism, Institute of Electrical Engineering, Chinese Academy of Sciences, Beijing, 100190, P. R. China, <sup>2</sup> Graduate University of Chinese Academy of Sciences, Beijing, 100049, P. R. China, <sup>3</sup> France-China Bio-Mineralization and Nano-Structures Laboratory, Beijing, China, <sup>4</sup> Laboratoire de Chimie Bactérienne, UMR233, Aix-Marseille Université, Institut de Microbiologie de la Méditerranée, CNRS, Marseille, France.

#These authors contributed equally to this work. \*E-mail: songtao@mails.ecac.cn

Magnetotactic bacteria (MTB) which can orient along the magnetic field lines due to the endogenous magnetic particles, could be used to kill *Staphylococcus aureus* (*S. aureus*) in a microfluidic chip under the control of the applied magnetic field. In this work, we designed a compound magnetic field device set in a microscope to guide the MTB and kill *S. aureus* during all the process.

The device consisted of two pairs of common coils and controllable electrical sources. It could generate the guiding magnetic field (gMF) with the adjustable amplitude of  $\pm 1$  mT in arbitrary direction of the horizontal plane, the rotating-like magnetic field (rMF) and a swing magnetic field (sMF, 2Hz, 10mT) by controlling the currents in the common coils, all of which were utilized in the following operations. *S. aureus* was injected into a sample pool; the MTB, modified by its polyclonal antibody, was injected into the other pool in the microfluidic chip. Through applying a gMF, the MTB were guide to the sample pool, where a rMF was applied for the attachment of MTB to *S. aureus* and then the sMF was applied to kill *S. aureus*.

The study shows that the MTB could be navigated by the gMF to the sample pool. After exposure to sMF, 40.5% of *S. aureus* were killed. This result provides a new resolution for the targeted treatment of infectious diseases and cancers.



The compound magnetic field device and the results of target killing of *S. aureus*

## Doxorubicin loaded dual pH- and thermo-sensitive magnetic nanosystem for combined hyperthermia and controlled drug delivery applications

A. Hervault,<sup>a,c</sup> M. Lim,<sup>d</sup> C. Boyer,<sup>d</sup> A. E. Dunn,<sup>d</sup> K. Matsumura,<sup>c</sup> D. Mori,<sup>c</sup> S. Maenosono,<sup>\*c</sup> and N. T. K. Than<sup>\*ab</sup>

<sup>a</sup> Department of Physics & Astronomy, University College London, Gower Street, London, WC1E 6BT, UK. E-mail: [uh-louvain.ac.be](http://www.uh-louvain.ac.be), <http://www.uh-louvain.ac.be>

<sup>b</sup> UCL Healthcare Biomedical and Nanomaterials Laboratories, 21 Albermarle Street, London W1S 4BS, UK

<sup>c</sup> School of Materials Science, Japan Advanced Institute of Science and Technology, I-1 Asahidai, Nomi, Ishikawa 933-1292, Japan. E-mail: shinva@jaist.ac.jp

<sup>d</sup> School of Chemical Engineering, The University of New South Wales, Sydney, NSW2052, Australia

Magnetic nanocarriers have attracted increasing attention due to the possibility to deliver drugs and heat locally. Magnetic nanosystems that respond to both a change in pH and temperature can give spatial and temporal control over the release of the drug, by making use of the acidic pH found in tumor microenvironment and heat generated from the magnetic nanoparticles (MNPs) when exposed to an alternating magnetic field (AMF) as triggers for the drug release. Moreover, heat has been found to greatly enhance the intracellular drug uptake and the cytotoxic effect of many chemotherapeutic drugs, resulting in a synergistic effect.

In this work, we have developed a novel nanotherapeutic composed of an iron oxide core and a thermo-responsive polymer shell. The magnetic nanocomposite (MNC) allow for a triggered release of drugs as a consequence of hyperthermia and tumor acidic pH, through breakage of pH and heat labile Schiff base bonds that bind the drug molecules to the polymer. Iron oxide NPs synthesized by a microwave-assisted co-precipitation method were functionalized with the thermo-responsive polymer via a silanisation reaction. After fully characterizing the MNCs, their heating performances in an AMF were evaluated. Doxorubicin (dox) was loaded into the nanosystem via formation of imine bonds between the amine group of dox and the aldehyde group of the polymer, and the drug release kinetics were carefully studied as a function of the pH and the temperature.

The MNPs show a superparamagnetic behavior with a saturation magnetization around 70 emu/g. The LCST of the polymer was engineered around 39 - 40 °C and its successful grafting on the MNP surface was confirmed by FTIR and TGA analysis, yielding MNCs with a hydrodynamic diameter around 120 nm and good colloidal stability. Their potential as nanoheaters was confirmed with an ILP of 1.0  $\text{Nm}^2/\text{K}$ . As expected, faster and higher release of drug was obtained under hyperthermia conditions and tumour acidic pH, with 85.2 % of drug released after 48 h. Finally, MTT assay indicated that the MNCs show no cytotoxicity to cells even with concentrations up to 1 mg/ml.

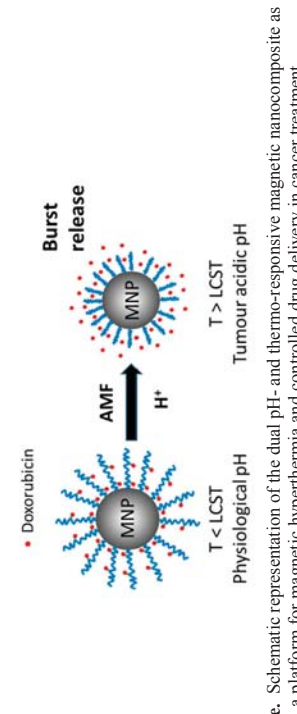


**Figure 1** Schematic representation of the dual pH- and thermo-responsive magnetic nanocomposite as a platform for magnetic hyperthermia and controlled drug delivery in cancer treatment.

## Advanced locomotion of microbeads on ferromagnetic surfaces

Umer Sajjad\*, Rasmus B. Holländer, Finn Klingbeil, Sugosh Deshpande, Qaisar Latif,

Jeffrey McCord

Nanoscale Magnetic Materials - Magnetic Domains, Institute for Materials Science  
Kiel University, Kaiserstraße 2, 24143 Kiel, Germany

\*Corresponding Author: [sajna@tf.uni-kiel.de](mailto:sajna@tf.uni-kiel.de)

The applications of magnetic micro- and nano particles have recently gained enormous interest in the field of diagnostics and nanomedicine due to their ability to attach, transport, sort and detach chemical and microbial species. Ferromagnetic surfaces for the lateral motion of functionalized superparamagnetic monodispersed microbeads (MB) are of great significance for the variable and flexible lateral transport of MBs.

We present a comprehensive experimental study that composes the lateral motion and dynamics of MBs with diameter from 2 to 8  $\mu\text{m}$ . On applying external magnetic fields, ferromagnetic structures patterned on a microfluidic Si-chip provide localized stray field gradients, by which a magneto-mechanical bonding between the parent magnetic structure and the magnetic particle forms. This enables the movement of particles with the application of rotating external magnetic fields. Numerical simulations fully predict our experimental findings.

We investigated the effect of MB size and susceptibility with its speed of motion on various magnetic model structures, i.e. a 30 nm thick  $\text{Ni}_{81}\text{Fe}_{19}$  disc with 30  $\mu\text{m}$  diameter [Fig. 1(a)] and determined the existence of a critical diameter of the MBs for a maximum attainable speed. The linear angular velocity of the MBs is found to be around half of the velocities around a circular ring and a disc with a two time bigger diameter [see MB trajectories in Fig. 1(a)-(c) for an equal time]. On the basis of the results structures were designed for the extended unidirectional motion of MBs under homogeneously rotating fields [Fig. 1(h)]. At a constant amplitude and frequency of the rotational field, zig-zag and curvilinear ferromagnetic wires serve for different velocities, owing to dissimilar regions of higher magnetic fields and thus field gradients. To disclose flexible directions of motion, MBs are transported on array structures. Here, the magnetic field is applied in square waveforms with specific field configurations to transport the MBs in various directions. For instance, an external field switching between 30° and -30°, respectively 30° and -90° leads to controlled vertical [Fig. 1(i), (j)] or diagonal MB motion. Transport velocities of more than 100  $\mu\text{m}/\text{s}$  are achieved.

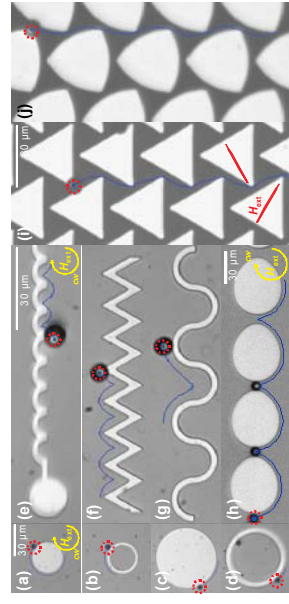


**Fig. 1** Tracked path (blue lines) of experimentally captured angular and directional motion of MBs with 4 (a-d) and 8  $\mu\text{m}$  (e-j) diameter.

We show that MBs with different diameters and effective volume susceptibilities are possible to be moved and sorted on various magnetic array structures with a repetitive field sequence. By choosing the appropriate shape, size and distance between neighbouring ferromagnetic structures and tuning external field sequences, ferromagnetic surface structures form a flexible basis for future Lab-on-Chip devices, where a reliable delivery of targeted species is realizable along with substantial speed.

## Optimized shapes of magnetic arrays for drug targeting applications

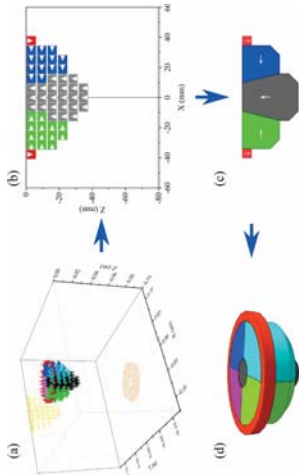
Lester C. Barnsley\*, Dario Carugo, Eleanor Stride

Institute of Biomedical Engineering, Department of Engineering Science, University of Oxford, Old Road Campus Research Building, Oxford OX3 7DQ, UK. \*E-Mail: [lester.barnsley@eng.ox.ac.uk](mailto:lester.barnsley@eng.ox.ac.uk)

Arrays of permanent magnet elements have been utilized as light-weight, inexpensive sources for applying external magnetic fields in magnetic drug targeting applications, but they are extremely limited in the range of depths over which they can apply useful magnetic forces.

In our previous study<sup>[1]</sup>, we developed an optimization routine to determine the configuration of an assembly of inexpensive, readily available cubic permanent magnet elements offering the maximum field gradient at a given distance from the array. The aim of the present study was to significantly expand this approach to the design of magnetic arrays consisting of elements of arbitrary shape. We show that the resultant arrays are capable of generating almost two to three times as much magnetic force as arrays constructed using cubic elements for the same volume of magnetic material, depending on the optimization distance.

A method for assembling arrays in practice is considered, quantifying the difficulty of assembly and suggesting a means for easing this difficulty without a significant compromise to the applied field or force. Finite element simulations of magnetic retention experiments were run to demonstrate the capability of a subset of arrays to retain magnetic microparticles against flow. The results suggest that, depending on the choice of array, a useful proportion of particles (more than 10%) could be retained at flow velocities up to 100 mm/s or to depths as far as 50 mm from the magnet. Finally, the optimization routine was used to generate a design for a Halbach array optimized to deliver magnetic force to a depth of 50 mm inside the brain.



An example of how an optimized magnetic array is converted into a design of cylindrically symmetrical permanent magnet segments.

1. L.C. Barnsley, D. Carugo, J. Owen, E. Stride, *Phys. Med. Biol.*, **60**, 8303 (2015)

## Biomimetic magnetoferritin nanoparticles for targeting and imaging of microscopic tumors

**Changqian Cao\***, Yao Cai, Tongwei Zhang, Caiyun Yang, Huangtao Xu, Rixiang Zhu, Yongxin Pan

Franco-Chinese Bio-Mineralization and Nano-Structures Laboratory, Key Laboratory of Earth and Planetary Physics, Institute of Geology and Geophysics, Chinese Academy of Sciences, Beijing, 100029, China.

Email: [changqiancao@mail.igcas.ac.cn](mailto:changqiancao@mail.igcas.ac.cn)

One of the major obstacles in clinical cancer intervention is the *in vivo* detection of tumors at pre-angiogenic stage, when the cancer is still confined to the site of origin and timely preventative treatment is possible. However, because pre-angiogenic tumors lack a direct connection to the blood stream, they are more difficult to target. Therefore, it is desirable to develop effective delivery of tumor cell-targeted diagnostic agents capable of crossing biological barriers. Recently, we biomimetically synthesized a novel magnetoferritin (M-HFn) nanoparticle with intrinsic multifunction by using genetically engineered recombinant human heavy-chain ferritin (HFn) as a biotemplate. It is demonstrated that without tumor targeted ligand modification, the HFn shell of M-HFn nanoparticles can be specifically targeted to transferin receptor 1 (TfR), which is widely overexpressed on a variety of cancer cells. The inner iron oxide core of M-HFn nanoparticles shows high transversal relaxivity and peroxidase-like activity. After intravenous injection, the M-HFn nanoparticles can intrinsically cross serial biological barriers (endothelium, epithelium and blood-brain barrier) and target to tumor cells overexpressed TfR1 *in vivo*. Combining these traits, the M-HFn nanoparticles are found a very promising contrast agent for the *in vivo* detection of microscopic (<1-2 mm) tumors by MRI and *in vitro* detection reagent of clinical tumor tissues with very high sensitivity and specificity.

### Acknowledgements

This work was supported by grants from National Natural Science Foundation of China (nos.: 41574062, 41204053, and 41330104, respectively), the CAS/SAFEA International Partnership Program for Creative Research Teams (KZCX2-YW-T10), the R&D of Key Instruments and Technologies for Deep Resources Prospecting (the National R&D Projects for Key Scientific Instruments, number ZDY/Z2012-1-01-02).

### References

- [1] Cai Y., Cao C., He X., Yang C., Tian L., Zhu R., Pan Y., Enhanced magnetic resonance imaging and staining of cancer cells using ferrimagnetic H-ferritin nanoparticles with increasing core size, *International Journal of Nanomedicine*, 2015; 10: 2619-2634.
- [2] Cao C., Wang X., Cai Y., Sun L., Tian L., Wu H., He X., Lei H., Liu W., Chen G., Zhu R., Pan Y. Targeted *in vivo* imaging of microscopic tumors with ferritin-based nanoprobes across biological barriers. *Advanced Materials* 2014;26(16):2566-71.
- [3] Fan K., Cao C., Pan Y., Lu D., Yang D., Feng J., Song J., Liang M., Yan X. Magnetoferritin nanoparticles for targeting and visualizing tumor tissues. *Nature Nanotechnology* 2012; 7(7): 459-64.
- [4] Cao C., Tian L., Liu Q., Liu W., Chen G., Pan Y. Magnetic characterization of non-interacting, randomly oriented, nanometer-scale ferrimagnetic particles. *Journal of Geophysical Research* 2010; 115(B07003), DOI: 10.1029/2009JB006855, 2010.

## Exogenous Iron Redistribution Between the Brain, the Liver and the Spleen After the Administration of the $^{57}\text{Fe}_3\text{O}_4$ Ferrofluid into the Ventricile of the Brain.

D.M. Polikarpov<sup>1</sup>, R.R. Gabbasov<sup>2</sup>, V.M. Cherepanov<sup>3</sup>, M.A. Chuev<sup>3</sup>, I.N. Mischenko<sup>3</sup>,

N.A. Loginova<sup>4</sup>, E.V. Loseva<sup>4</sup>, M.P. Nikitin<sup>5</sup> and V.Y. Panchenko<sup>3</sup>

<sup>1</sup>Department of Clinical Medicine, Faculty of Medicine and Health Science, Macquarie University, NSW, Australia

<sup>2</sup>National Research Center "Kurchatov Institute", Moscow, Russia

<sup>3</sup>Institute of Physics and Technology, Russian Academy of Sciences, Moscow, Russia

<sup>4</sup>Institute of Higher Nervous Activity and Neurophysiology, Russian Academy of Sciences, Moscow, Russia

<sup>5</sup>Moscow Institute of Physics and Technology, Dolgoprudny, Russia

(gabbasov\_r@mipt.ru; mrs@mipt.ru)

Drug delivery through the blood-brain barrier (BBB) is a challenge in the treatment of brain's disorders. Magnetic nanoparticles are considered to be one of the possible delivery systems for passing through the BBB. The delivery method is based on the concentration of a magnetic drug in the blood vessels of the brain by an external magnetic field followed by the transportation of the drug through the barrier by monocytes/macrophage. The possibility of such delivery of the magnetic drugs into the brain was confirmed experimentally by a number of researchers [1], therefore, the study of the biodegradation and/or clearance of the magnetic nanoparticles from the brain is the key task to support the safety of this medical technology. In our previous works, we developed an original method for an evaluation of the distribution, clearance and excretion of magnetic particles in the body, based on joint analysis of the Mössbauer and magnetization data in the framework of the single model of magnetic dynamic. It proved to be a useful tool for characterization of iron oxide nanoparticles, which continuously change their properties during the biodegradation. Using this technique we can clarify the biodegradation process by comparing the time evolutions of exogenous and endogenous iron concentrations in the body [2].

In [3] we studied a transportation of exogenous iron from the brain to the liver after the administration of  $^{57}\text{Fe}_3\text{O}_4$  ferrofluid into the ventricile of the rat brain. Initially, we assumed that the biodegradation processes in the liver and the spleen are similar due to the presence of a large amount of the same iron depositing protein, ferritin, in these organs. However, histological examination of the liver and spleen showed a fundamental difference in the mechanisms of processing of iron nanoparticles in these organs. Based on these data, in this report we present results of a more comprehensive study of simultaneous biodegradation processes of the magnetic nanoparticles in the spinal cord, liver and spleen after the administration of the ferrofluid into the brain.

The work was supported in part by the Russian Foundation for Basic Research under Grant 15-02-08171.

## References

- [1] Zainulabedin M, Saiyed, Nimisha H, Gandhi, Madhavan P.N, Nair. Magnetic nanoformulation of azidothymidine 5'-triphosphate for targeted delivery across the blood-brain barrier, Int J Nanomed. 5 (2010) 157–166.
- [2] I.Mischenko, M. Chuev, V.Cherepanov, M.Polikarpov, V.Panchenko. Biodegradation of magnetic nanoparticles evaluated from Mössbauer and magnetization measurements. Hyperfine Interact. (2013) 219:57–61.
- [3] D.Polikarpov, R.Gabbasov, V.Cherepanov, N.Loginova, E.Loseva, M.Nikitin, A.Yurenia, V.Panchenko. Mössbauer study of exogenous iron redistribution between the brain and the liver after administration of  $^{57}\text{Fe}_3\text{O}_4$  ferrofluid in the ventricile of the rat brain. Journal of Magnetism and Magnetic Materials. 380 (2015) 78–84.

## INVITED TALK 2

### NANOSPINTRONICS MEETS MAGNETIC NANOPARTICLES

Tomasz Dietl<sup>1</sup>

<sup>1</sup>Laboratory of Cryogenic and Spintronic Research, Institute of Physics, Polish Academy of Sciences, Warsaw, Poland;  
Institute of Theoretical Physics, University of Warsaw, Poland; Advanced Institute for Materials Research, Tohoku University, Sendai, Japan. \*e-mail: dietl@ipan.edu.pl

The minimum feature size of today's spintronic devices, obtained by top-down methods, reaches 11 nm [1]. At the same time, spinodal nanotechnology, a novel self-assembling method, allows one to obtain arrays of magnetic nanoparticles and nanocolumns embedded in functional semiconductors [2], as shown in Fig. 1.

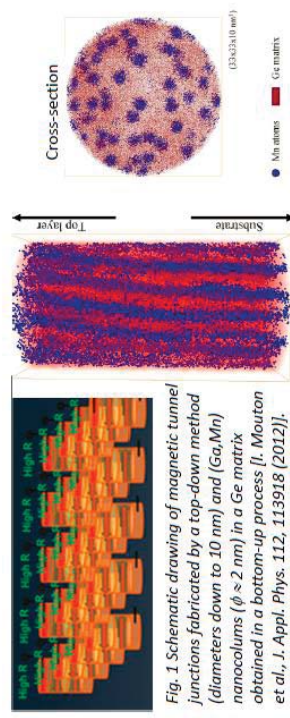


Fig. 1 Schematic drawing of magnetic tunnel junctions fabricated by a top-down method (diameters down to 10 nm) and (Ga/Mn) nanocolumns ( $\phi \approx 2$  nm) in a Ge matrix obtained in a bottom-up process [l. Mouton et al., J. Appl. Phys. 112, 113918 (2012)].

In the talk, the recent progress in semiconductor spintronics [3] as well as in random access and logic-in magnetic memories employing magnetic tunnel junctions [1,4] will be presented. Then the flow of ideas between nanospintronic and nanoparticle fields will be discussed, including the questions of surface/interfacial magnetism, magnetic cross-talking, thermal stability, magnetization reversal modes (nucleation vs. single-domain like [4,5]), and cross-over between semiclassical and quantum spin dynamics [6].

1. H. Sato, E.C. Enobio, M. Yamanouchi, S. Ikeda, S. Fukami, S. Kanai, F. Matsukura, and H. Ohno, "Properties of magnetic tunnel junctions with a MgO/CoFeB/Ta/CoFeB/MgO recording structure down to junction diameter of 1 nm", *Appl. Phys. Lett.* **105**, 062403 (2014).
2. T. Dietl, K. Sato, T. Fukushima, A. Bonanni, M. Janet, A. Barski, S. Kuroda, M. Tanaka, Phan Nam Hai, H. Kattayama-Yoshida, "Spinodal nanocomposition in semiconductors doped with transition metals", *Rev. Mod. Phys.* **87**, 1311 (2015).
3. T. Dietl, H. Ohno, "Dilute ferromagnetic semiconductors: Physics and spintronic structures", *Rev. Mod. Phys.* **86**, 187 (2014).
4. S. Kanai, F. Matsukura, S. Ikeda, H. Sato, S. Fukami, and H. Ohno, "Spintronics: from Basic Research to VLSI Application", *AAPPS Bulletin* **25**, 4 (Feb. 2015).
5. Y. Takeuchi, H. Sato, S. Fukami, F. Matsukura, and H. Ohno, "Temperature dependence of energy barrier in CoFeB-MgO magnetic tunnel junctions with perpendicular easy axis", *Appl. Phys. Lett.* **107**, 152405 (2015).
6. T. Dietl, "Spin dynamics of a confined electron interacting with magnetic or nuclear spins: A semiclassical approach", *Phys. Rev. B* **91**, 125204 (2015).

Invited Talk #2

Talk #16

## MRI visible polymer microcapsules for ultrasound induced targeted drug delivery

Megan Rich<sup>1</sup>, Aaron Alford<sup>2</sup>, Jun Chen<sup>3</sup>, Jennifer Sherwood<sup>3</sup>, Yuping Bao<sup>3</sup>, Eugenia Kharlamova<sup>2</sup>, Jason Warram<sup>1</sup>, Mark S. Boldig<sup>1</sup>

<sup>1</sup>Neurobiology Department, University of Alabama at Birmingham, Birmingham, AL, 35294 USA

<sup>2</sup>Department of Chemistry, University of Alabama at Birmingham, Birmingham, AL, 35294, USA

<sup>3</sup>Department of Chemical and Biological Engineering, University of Alabama at Tuscaloosa, Tuscaloosa, AL, 35487, USA

### Abstract

Often potential treatments and imaging contrast agents are kept from clinical or experimental use due to toxic effects or non-specific, off-target accumulation of drugs and imaging agents that can lead to unintended outcome and serious side effects. If materials carrying drugs and imaging contrast agents can be selectively deposited within target tissue, we can achieve specific imaging and highly effective treatment. Iron oxide ( $\text{Fe}_2\text{O}_3$ ) nanoparticle (NP) embedded microcapsules are engineered to provide MRI contrast (Fig. 1) and to release drugs only upon focal ultrasound administration. This system provides an encapsulation mechanism that is both biocompatible and stable and that can carry therapeutic concentrations of a variety of drugs; it allows the drugs to be cleared from the body without releasing a drug payload in non-target tissues. Capsules can become permeable upon ultrasound exposure providing non-invasive activation of drug release from capsules into target tissue.  $\text{Fe}_2\text{O}_3$  NPs embedded in the capsule wall enable visualization of capsules in circulation and NP displacement upon capsule activation with ultrasound exposure causes a change in MRI contrast confirming location and concentration of drug release to desired tissue.

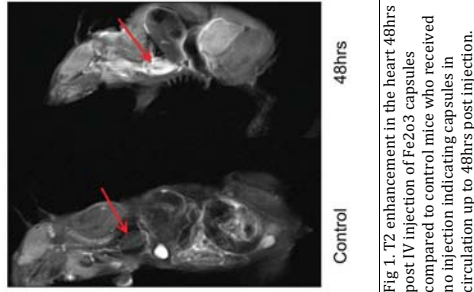


Fig 1. T2 enhancement in the heart 48hrs post IV injection of  $\text{Fe}_2\text{O}_3$  capsules compared to control mice who received no injection indicating capsules in circulation up to 48hrs post injection.

## Magnetic nanohybrids for in vivo therapy for cancer

**D. Bahadur, Saumya Nigam and Lina Pradhan**

Department of Metallurgical Engineering and Materials Science, Indian Institute of Technology, Mumbai-400076, E-mail: [dhiren@iitb.ac.in](mailto:dhiren@iitb.ac.in)

The deliberate design of nanohybrids for biological applications has been enabled by new advances in synthetic procedures through different soft chemistry routes. Such nanostructures when properly functionalized can be used as effective vehicles for biological entities *in vivo*. We discuss, here, pH and thermo sensitive dual drug delivery system in dual therapy mode(Hyperthermia + chemotherapy). Nano particulates (MNPs) with different shapes, composites, hybrids, core shell structure and magnetic fluids have been developed by various soft chemical methods. For efficient delivery of magnetic nano particulates with drug to the diseased site, magnetic fluid based release systems will be discussed with different possibilities of thermo sensitive and pH sensitive hydrogels, liposomes and dendrimers as carrier.

We will particularly emphasize some of our recent *in vitro* as well as *in vivo* results on lipid, dendrimer and hydrogel based nanohybrids with multifunctional capabilities. We have further investigated the synergistic effects of dual drug and dual therapy *in vivo* model in nude mice. The uptake of dual drug-lipid hybrid and regression of tumors were monitored through bioluminescence imaging post dual therapy combining hyperthermia with chemotherapy.

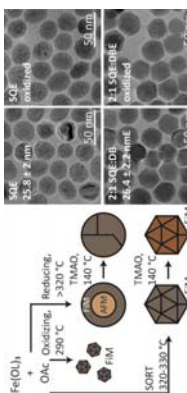
References:

1. S. Chandra, K.C. Banick, D. Bahadur, "Oxide and hybrid nanostructures for therapeutic applications", *Advance Drug Delivery Reviews*, 63, 1267-1281, 2011.

**High-performance Ferrite Nanoparticles for Wireless Magnetothermal Stimulation**  
 Ritchie Chen<sup>1,2</sup>, Gabriela Romero<sup>1,2</sup>, Michael G. Christiansen<sup>1,2</sup>, Polina Anikeeva<sup>1,2</sup>  
<sup>1</sup>Department of Materials Science and Engineering, <sup>2</sup>Research Laboratory of Electronics,  
 Massachusetts Institute of Technology, Cambridge, MA 02139. Email: rchen627@mit.edu

Wireless magnetothermal heat dissipation transduced by magnetic nanoparticles can be used for a variety of biomedical applications including cancer hyperthermia and deep brain stimulation. Thermal decomposition methods enable the synthesis of monodisperse ferrite nanoparticles yet variability in the reported magnetic properties are observed even when the syntheses are based on the same reactive components. We find that resulting defects and metastable phases can have detrimental impact on the hyperthermic performance of the nanoparticles in seemingly single-crystalline nanoparticles.

We recently identified that the electrochemical potential of the solvent environment influences the magnetic polymorph of the resulting ferrite nanoparticles. Reducing conditions produced metastable wüstite while oxidizing environments favored thermodynamically stable ferrite. Using a solvent optimized redox approach, we demonstrate the synthesis of nearly defect-free ferrite nanoparticles with some of the highest heating efficiencies, or specific loss powers, reported to date at the lowest magnetic field frequency and amplitude product relevant for clinical applications. We demonstrate that these optimized nanoparticles enable rapid modulation of membrane voltage for wireless cellular control as well as enhancement of T2 relaxivity for use as potent T2 magnetic resonance imaging contrast agents. Injection of optimized nanoparticles into the ventral tegmental area (VTA) of mice, a deep brain structure, enabled magnetothermal stimulation of heat-sensitized neurons in intact neural circuits.



Solvent-optimized redox tuning enables synthesis of nearly defect-free ferrite nanoparticles

## Magnetic Nanocubes in Self-Assembled Hydrogels

S. Schäffer<sup>1</sup>, J. Seigner<sup>1</sup>, S. Prévost<sup>1,2</sup>, M. Grädzel<sup>1</sup>

<sup>1</sup>Physikalische Chemie/Molekulare Materialwissenschaften, Institut für Chemie, Technische Universität Berlin, Straße des 17.

Juni 124, D-10623 Berlin

<sup>2</sup>Soft Matter Structure, ESRF – The European Synchrotron, 71 avenue des Martyrs, F-38000 Grenoble.

Thermoresponsive aqueous ferrogels with cubic magnetic nanoparticles (MNPs) incorporated into a self-assembled network are studied primarily by small angle scattering (SAS), rheology and electron microscopy. Comprehension of the interplay between network and MNPs enables manipulation of responses to mechanical stress, temperature and magnetic field.

Most ferrogels result from the addition of polymeric gelators to an existing ferrofluid.<sup>[1]</sup> The resulting ferrogels are composed of pockets of the original ferrofluid encapsulated by domains of polymer molecules at colloidal scale. Thus, such systems do not exhibit any significant synergistic response. A more elaborated ferrofluid, which can respond to stimuli, is thereby constructed by incorporation of monodisperse silica coated MNPs into a gel network, which interacts with them. Small angle scattering (SANS, SAS) is used to get a detailed picture of particle and gel fiber arrangement at nano-scale, while time-resolved SAS shows the kinetics of such systems (relaxation time and pathway of particles and network).

A new class of gels discovered within this project is based on combining fatty acids with basic amino acids. Such gels are eco-friendly, non-toxic, cheap and present attractive rheological and temperature-dependent properties. The viscosity changes reversibly over orders of magnitude by heating/cooling. By pH-variation, the system switches from a vesicle gel to a viscoelastic network formed by worm-like micelles, which is a very elegant way of tuning structure and properties. Highly monodisperse  $\text{Fe}_3\text{O}_4$ ,  $\text{CoFe}_2\text{O}_4$  (soft ferrite),  $\text{Mn}_x\text{Zn}_{1-x}\text{Fe}_2\text{O}_4$  (hard ferrite) nanocubes in a size range of 7 to 17 nm (edge length, corresponding to 10 to 30 nm space diagonal) were synthesized using a thermal decomposition route<sup>[2]</sup> resulting in a large scale reaction (2-3 gram). Such mono-disperse nanoparticles are required for detailed structural investigations (SAS). Commercial ferrogels are not suitable due to high polydispersity. In order to enhance colloidal stability and integrate these hydrophobic magnetic nanoparticles into a hydrogel network, they need to be surrounded by a protective shell, which subsequently can be modified chemically. A silica coating<sup>[3]</sup> has been obtained via reverse  $\mu$ -emulsion reactions. The particles are water dispersible with a homogeneous shell, whose thickness is tunable between 4 and 15 nm. The aim is to combine MNPs and gels to self-assembled ferrogels, whose properties cannot only be controlled by pH, temperature and composition, but also by a possible hydrophobic modification of the silica shell resulting in a versatile system of a responsive ferrogel.

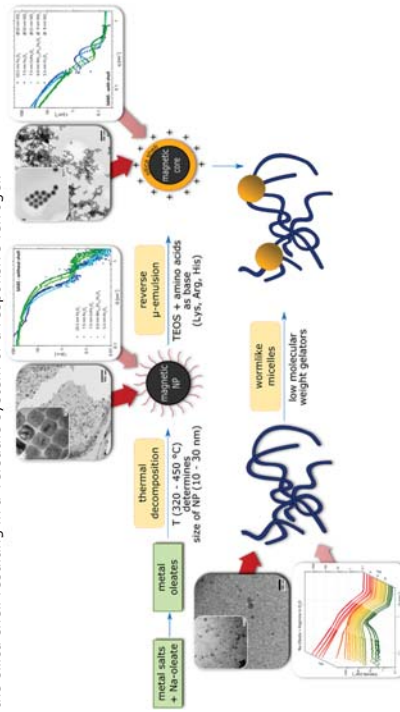


Fig. 1: Schematic outline of ferrogel synthesis including results by (cryo)-TEM, SAXS and SANS.

This work is supported by DFG PR1473/1 within the Priority Program SPP1681.

[1.] Krikhova, M. & Lattermann, G. J. Mater. Chem. **18**, 2842 (2008).

[2.] Park, J. et al., Nat. Mater. **3**, 891-895 (2004).

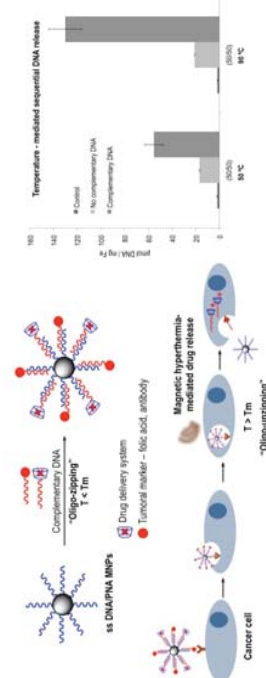
[3.] Ding, H. L. et al., Chem. Mater. **24**, 4572-4580 (2012).

## Nucleic and peptide nucleic acid-engineered iron oxide nanoparticles for magnetic hyperthermia-mediated drug delivery

Raluca Maria Fratila<sup>1</sup>, Vanessa Herrero García<sup>2</sup> and Jesús Martínez de la Fuente<sup>1,3</sup>

<sup>1</sup> Instituto de Ciencia de Materiales de Aragón (Universidad de Zaragoza - CSIC), Calle Pedro Cerbuna 12, 50009 Zaragoza, Spain. <sup>2</sup> Instituto de Nanociencia de Zaragoza, C/I Mariano Esquillor s/n, 50018 Zaragoza, Spain. <sup>3</sup> Institute of Nano Biomedicine and Engineering, Shanghai Jiao Tong University, Dongchuan Road 800, 200240, Shanghai, PR of China. E-mail: [fratila@unizar.es](mailto:fratila@unizar.es)

Nucleic acids play a key role in bionanotechnology due to their unique chemical, physical and biological properties, such as molecular recognition ability, programmed self-assembly properties and capacity to encode functional information. Peptide nucleic acids (PNA) are synthetic DNA analogues in which the negatively charged phosphate diester backbone is replaced by a neutral pseudo-peptide backbone, while retaining the four nucleobases of DNA.<sup>1</sup> Thus, PNA can hybridize with complementary DNA sequence obeying the Watson-Crick rules.<sup>2</sup> Moreover, PNA are more resistant to chemical and enzymatic degradation by proteases and nucleases than DNA. Despite these attractive features, PNA-nanoparticle conjugates have been only scarcely investigated when compared to their DNA counterparts. Herein, we report the use of nucleic and peptide acids (DNA and PNA) for the design of a multifunctional magnetic nanoparticle system for magnetic hyperthermia-mediated drug delivery. Hydrophobic 12 nm iron oxide magnetic nanoparticles were synthesized by thermal decomposition and transferred to water by coating with an amphiphilic polymer - poly(maleic anhydride-alt-1-octadecene), PMAO - . The carboxyl groups generated onto the surface of the MNPs upon hydrolysis of the maleic anhydride moieties were used for further bioconjugation using standard amide coupling chemistry. We have covalently attached single stranded DNA and PNA in different ratios (10/00, 75/25, 50/50, 25/75). These strands can be hybridized with complementary DNA strands functionalized with fluorescent labels, tumoral markers, antibodies or chemotherapeutic drugs (oligo-zipping). The functionalization efficiency was evaluated by fluorescence spectroscopy upon hybridization with fluorescent complementary DNA strand and the results indicate that the use of PNA increases the efficiency of the functionalization when compared to only DNA, with the 50/50 DNA/PNA ratio being the optimal one. Given the differences between the melting temperatures ( $T_m$ ) of the DNA-DNA and PNA-DNA double strands, a sequential release from the system can be achieved (oligo-unzipping). We are currently working on the reduction of the temperatures required for the sequential release for future *in vitro* applications of the multifunctional MNP system.



References: (1) Nielsen, P. E.; Egholm, M. *Curr. Issues Mol. Biol.* 1999, 1, 89-104. (2) Egholm, M.; Buchardt, O.; Christensen, L.; Behrens, C.; Freier, S. M.; Driver, D. A.; Berg, R. H.; Kim, S. K.; Norden, B.; Nielsen, P. E. *Nature* 1993, 365, 566-568. (3) Moros, M.; Pelaz, B.; Lopez-Larriba, P.; Garcia-Martin, M. L.; Grau, V.; de la Fuente, J. M., *Nanoscale*, 2010, 2, 1746.

## Biocompatible Magnetic Fluids of Modified Co-Ferrite Nanoparticles with Tunable Magnetic Heating Power

S. Dutz<sup>1</sup>, N. Buske<sup>2</sup>, J.H. Clement<sup>3</sup>, C. Gräfe<sup>3</sup>

<sup>1</sup> Institute of Biomedical Engineering and Informatics (BMTI), Technische Universität Ilmenau, Ilmenau, Germany

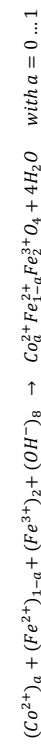
<sup>2</sup> MagneticFluids, Köpenicker Landstr. 203, 12437 Berlin, Germany

<sup>3</sup> Klinik für Innere Medizin II, Abteilung Hämatologie und Internistische Onkologie, Universitätsklinikum Jena, Jena, Germany

E-mail: [silvio.dutz@tu-ilmenau.de](mailto:silvio.dutz@tu-ilmenau.de), [n.buske@magnetfluids.de](mailto:n.buske@magnetfluids.de)

Scheme 1: Reaction equations for preparation of Co-doped inverse spinels.

Magnetic ( $\text{Fe}_2\text{O}_3$ ) particles with diameter around 10 nm have a very low coercivity ( $H_c$ ) and relative remanent magnetization ( $M_r/M_s$ ). Contrary, Co-ferrite ( $\text{CoO} \times \text{Fe}_2\text{O}_3$ ) particles of the same size have a very high  $H_c$  and  $M_r/M_s$ , which is magnetically too hard to obtain suitable specific heating power (SHP) in magnetic hyperthermia or good tracer performance in magnetic particle imaging (MPI). For optimization of the magnetic properties, the  $\text{Fe}^{2+}$  ions of magnetite were substituted by  $\text{Co}^{2+}$  step by step in our study which results in a Co doped inverse spinel with adjustable  $\text{Fe}^{2+}$  substitution degree. A Co-concentration of 0% ( $a = 0$ ) leads to the formation of pure iron oxide particles and a Co-concentration of 25% ( $a=1$ ) yields pure  $\text{CoFe}_2\text{O}_4$ .



Scheme 1: Reaction equations for preparation of Co-doped inverse spinels.

The particles were prepared from  $\text{Co}^{2+}$ ,  $\text{Fe}^{2+}$ , and  $\text{Fe}^{3+}$  chloride mixtures (0.02 molar) at different "a" values by co-precipitation with sodium hydroxide under stirring at 100°C for 90 minutes reaction time. The obtained particles were washed with distilled water using magnetic separation technique and stabilized in water with hydrochloric acid (intermediate) and with citric acid (negatively charged particles at pH=7). The structural properties of prepared particles were determined by means of transmission electron microscopy (TEM) and X-ray diffraction (XRD). For the magnetic characterization of the samples vibrating sample magnetometry (VSM) was used. Magnetic heating performance (SHP/SAR) was investigated in calorimetical measurements in alternating magnetic fields of different field strengths. The Co-content of the particles was determined by means of inductively coupled plasma optical emission spectrometry (ICP-OES). Biocompatibility was tested with the PrestoBlue Cell Viability Assay using human brain microvascular endothelial cells. For the ferrofluids containing the prepared particles, only a limited dependence of  $H_c$  and  $M_r/M_s$  on the Co content in the particles was found (Figure 1).

This confirms a stable dispersion of the particles within the ferrofluid. For dry particles, a strong correlation between Co content and  $H_c$  and  $M_r/M_s$  was found. For increasing Co concentrations from 0 to 8.6% (substitution rate "a" from 0 to 0.33) only a slight increase of  $H_c$  was found, but from 12 to 25% ("a" from 0.5 to 1) a strong linear increase results (Figure 1). Within this linear range of dependency, the magnetic properties of the particles, especially  $H_c$ , can be tuned easily by changing Co content of the particles. All particles have a size of around 10 nm and the obtained Co content correlates with the applied "a" during preparation. The prepared particles show no increased cytotoxicity compared to iron oxide particles up to a concentration of 25  $\mu\text{g}/\text{cm}^2$ . A specific correlation of heating power of gel-immobilized particles with the Co content will be presented and best samples show very good performance for application in hyperthermia.

Acknowledgements  
We thank Therakine GmbH, Berlin for generous support of this work as well as Moritz von der Luhe (University Jena) for TEM, Christa Schmidt (IPHT Jena) for XRD, and Ingo Appel (KIT Karlsruhe) for ICP-OES investigations.

## Photocatalytic and Bactericidal Activities of Colloidal Titania-Silica-Iron Oxides Nanocomposites

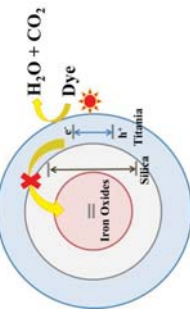
Padaraporn Chanhom,<sup>1</sup> Nisanart Charoenlap,<sup>2</sup> Numpon Insin<sup>1, \*</sup>

<sup>1</sup>Department of Chemistry, Faculty of Science, Chulalongkorn University, Bangkok, 10330, Thailand

<sup>2</sup>Laboratory of Biotechnology, Chulabhorn Research Institute, Bangkok, 10210, Thailand  
\*E-mail: Numpon.I@chula.ac.th

Superparamagnetic nanocomposites, multifunctional nanomaterials that are colloidal stable in absence of a magnetic field but response strongly when an external magnetic field was applied, have been utilized in various environmental and biomedical applications. However, an incorporation of photocatalytic activity into the nanocomposites using direct contacts of such photocatalysts as titania and iron oxides superparamagnetic nanoparticles leads to a decrease in photocatalytic activity due to electron transfer between the two materials. To solve the problem, materials with large bandgap were proposed to be used as an interlayer between the titania and iron oxides. For this work, we reported the preparation of new colloidal titania-silica-iron oxide nanocomposites (TSI) and photocatalytic and bactericidal activities of the nanocomposites.

The anatase titania, silica, and iron oxides nanocomposites (TSI) were synthesized using thermal decomposition method to obtain the iron oxides nanoparticle cores and reverse micro-emulsion method to prepare the silica and titania shells. X-ray diffraction (XRD) and transmission electron microscope (TEM) were used to characterize and confirm the structure of the nanocomposites. These nanocomposites showed high photocatalytic activity of above 97% degradation when used in the photodegradation of methylene blue. In order to study the effects of the thickness of silica interlayer, nanocomposites with different silica layer thicknesses were prepared. As a result, approximately 6 nm of silica interlayer is an enough thickness for inhibiting electron translocation between titania and iron oxide nanoparticles and maintaining the efficiency of photocatalytic activity of titania nanoparticles. These composites could effectively photo-degrade the dye (above 90% methylene blue degradation) for at least three cycles without regeneration. Moreover, the nanocomposites exhibited high antibacterial properties when tested against *Staphylococcus aureus*. From our study, the nanocomposites exhibited their potential in various applications including removal of organic pollutants and pathogenic bacteria in combination with convenient separation from the environments using an external magnetic field.



The proposed mechanism for the methylene blue photodegradation using colloidal titania-silica-iron oxide nanocomposites (TSI) as photocatalysis

Synthesis and characterization of hollow magnetic nanospheres modified with Au nanoparticles for bio-encapsulation

S. Seino\*, K. Suga, T. Nakagawa, T. A. Yamamoto

Department of Management of Industry and Technology, Graduate School of Engineering, Osaka University, Japan. \*E-mail : seino@mit.eng.osaka-u.ac.jp

Hollow magnetic nanospheres modified with Au nanoparticles were successfully synthesized. Au/SiO<sub>2</sub> nanospheres fabricated by a radiochemical process were used as templates for ferrite templating. After the ferrite plating process, Au/SiO<sub>2</sub> templates were fully coated with magnetite nanoparticles. Dissolution of the SiO<sub>2</sub> core lead to the formation of hollow magnetic nanospheres with Au nanoparticles inside. Figure 1 shows typical TEM and SEM images of the hollow magnetic nanoparticles modified with Au nanoparticles. The hollow magnetic nanospheres consisted of Fe<sub>3</sub>O<sub>4</sub> grains, with an average diameter of 60 nm, connected to form the sphere wall, inside which Au grains with an average diameter of 7 nm were encapsulated. Surface activity of Au grains against -SH groups were confirmed by the adsorption of cysteine. These hollow magnetic nanospheres are proposed as a new type of nanocarrier, as the Au grains could specifically immobilize biomolecules inside the hollow sphere.

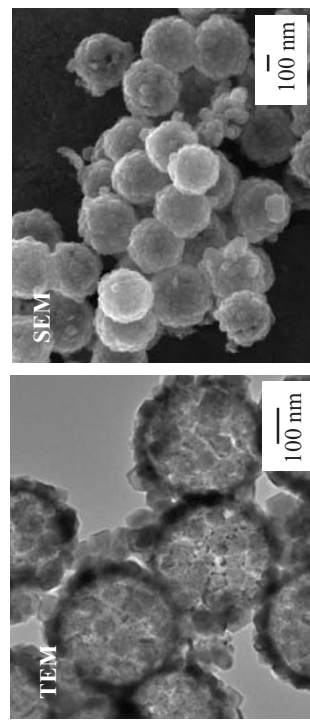


Fig. 1 Typical TEM and SEM images of hollow magnetic nanoparticles modified with Au nanoparticles.

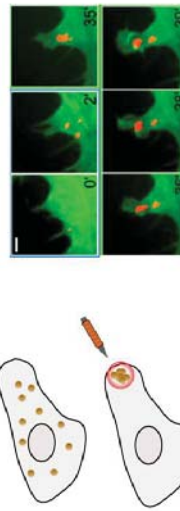
## INVITED TALK 3

### MAGNETIC MANIPULATION OF INTRACELLULAR SIGNALLING

Maxime Dahan<sup>1</sup>

<sup>1</sup> Institut Curie, Paris, France, \*e-mail: [maxime.dahan@curie.fr](mailto:maxime.dahan@curie.fr)

Investigating the dynamics of living cells requires not only imaging tools but also methods to perturb cellular activities with high spatio-temporal resolution. Here, we present an approach based on the use of functionalized magnetic nanoparticles (MNPs) inserted in the cytosol which can be displaced using magnetic forces at a subcellular level with magnetic fields. I will first discuss the key parameters underlying the dynamics of nanoparticles inside the cytosol, emphasizing the role of size and surface chemistry in the intracellular mobility. Next, I will show how MNPs can be used to activate Rac1/Cdc42 signaling pathways involved in cell migration, using sub-50 nm synthetic MNPs or engineered protein-based ferritin cages. Finally, I will describe our effort to target and manipulate organelle dynamics at the single cell level using magnetic actuation.



*Intracellular manipulation of magnetic nanoparticles (left) is used to locally accumulate functionalized nanoparticles and trigger signalling events. (Right: In this example, functionalized MNPs (in red) are brought to the membrane, leading to the formation of protrusion).*

#### References

1. F. Etoc, C. Vicario, D. Lisse, J. Piehler, J. M. Staude, M. Coppey, M. Dahan, "Magnogenetic control of protein gradients inside living cells with high spatial and temporal resolution", *Nanoletters* (2015) 15(5):3487-94.
2. Ou Chen, Lars Riedemann, Fred Etoc, Hendrik Hermann, Mathieu Coppey, Mariya Barch, Christian T. Farrat, Jing Zhao, Oliver Bruns, He Wei, Peng Guo, Jian Cui, Russ Jensen, Yue Chen, Daniel K. Harris, Jose M. Cordero, Zhongwu Wang, Alan Jasanioff, Dai Fukumura, Maxime Dahan, Rakesh K. Jain and Moungi G. Bawendi, "Magneto-Fluorescent Core-Shell Super nanoparticles", *Nature Communications* (2014) 5:5093.
3. F. Etoc, D. Lisse, Y. Bellalche, J. Piehler, M. Coppey, M. Dahan, « Subcellular control of Rac signalling by magnetogenetic manipulation in living cells», *Nature Nanotechnology* (2013) 8, 193–198.

magnetogenetic manipulation in living cells», *Nature Nanotechnology* (2013) 8, 193–198.

Invited Talk #3

## Immunomagnetic Cancer Cell Capture and Release for Drug Response Study

Devina Jaiswal<sup>1</sup>, Armin T. Radl<sup>1</sup>, Mu-Ping Neifi<sup>2</sup>, Kevin Claffey<sup>2</sup> and Kazunori Hoshino<sup>1,\*</sup>

<sup>1</sup>University of Connecticut Health Center, 260 Glenbrook Rd Unit 3247, Storrs, CT 06269-3247, USA  
<sup>2</sup>University of Connecticut Health Center, 263 Farmington Avenue, Farmington, CT 06030-3501, USA  
hoshino@engr.uconn.edu

**Introduction:** Real-time single cell analysis such as cell-cell or cell-nanoparticle interaction is important in understanding the biological system for applications such as immune response and drug delivery [1, 2]. Studies have been done for single cell analysis by trapping them in a microfluidic channel integrated with PDMS cell trapping array or microfiltration [3, 4]. Compared to other techniques, immunomagnetic immobilization of cells is a reversible process [5]. We demonstrate a technique where cancer cells can be dynamically captured and released utilizing micro-patterned magnets under a controlled external magnetic field for studying single cell interaction with nanoparticles.

**Material and Method:** Microfabrication technique was used to pattern thermally deposited nickel on a glass cover slip. An array of diamond shaped micromagnets (MMs) (60×60 × 0.200 μm) was aligned within the microfluidic channel made of PDMS (Polydimethylsiloxane) film (240 μm thick). A C-shaped solenoid was developed to generate and switch an external magnetic field of 0.04T. The solenoid was characterized using a Hall effect sensor and COMSOL. For cell study, MCF-7 cells (breast cancer cells) incubated with EpCAM (Epithelial cell adhesion molecule) functionalized magnetic beads (diameter: 3 μm) were flown over the MM pattern and captured in the channel. Pulsed nanoparticle input was introduced for 4 mins into the channel to interact with the immobilized cells to study cell-nanoparticle interaction as a model study for drug delivery application. The fluorescence intensity images were recorded real time and analyzed.

**Result:** Figure 1(A) shows a microfluidic channel placed between solenoid arms for cell capture. The magnetic field locally enhanced by MMs was 61.1% more than external uniform magnetic field (Fig. 1B). An average capture efficiency of 90.8±3.6% was achieved. Figure 1(C) panels show a cell (red arrow) travelling towards the MM with flow and getting trapped (middle panel) and released when magnetic field is removed. Cell-nanoparticle interaction was modeled to produce an association and dissociation coefficient of 0.778±0.11 and 0.0047±0.003, respectively (Figure 2).

**Conclusion:** In this study, an immunomagnetic cancer cell trapping microfluidic channel was designed and fabricated for real time cell-nanoparticle study as a model for drug delivery analysis. The magnetic field for solenoid and micromagnets was characterized. Cancer cells were captured at high capture efficiency of 90.8±3.6% and nanoparticle pulse input interaction with cells was studied on-chip.

#### References

1. Parrott, D.M., *Nature Reviews Cancer*, 2012, **12**, pp. 252-264.
2. Jin, H., et al. *ACS Nano*, 2009, **3**(1), pp. 149-158
3. Carlo, D.D., et al. *Lab Chip*, 2006, **6**, pp. 1445-1449
4. Zheng, S.Y., *Biomol. Microdevices*, 2011, **13**, pp. 203-213
5. Chen, P., et al. *Scientific Reports*, 2015, Article no. 8745, (inset).

**Figure 2: Nanoparticle interaction with cell**  
Figure 2: Nanoparticle interaction with cell was analyzed using data recorded in real time. Images of fluorescent cells were captured at different time points for analysis (inset).

Talk #25

## Passage of SPIONs through cell layers

**Christine Gräfe<sup>1</sup>, Ioana Slabu<sup>2</sup>, Robert Müller<sup>3</sup>, Andreas Hochhaus<sup>1</sup>, Ferdinand von Eggeling<sup>3,4,5</sup>, Frank Wiekhorst<sup>2</sup>, Joachim H. Clement<sup>1</sup>**

<sup>1</sup> Klinik für Innere Medizin II, Abteilung Hämatologie & Intern. Onkologie, Universitätsklinikum Jena, Germany

<sup>2</sup> Physikalisch-Technische Bundesanstalt, Berlin, Germany

<sup>3</sup> Leibniz-Institut für Photonische Technologien, Jena, Germany

<sup>4</sup> Klinik für Hals-, Nasen-, Ohrenheilkunde, Universitätsklinikum Jena, Germany

<sup>5</sup> Institut für Physikalische Chemie, Friedrich-Schiller-Universität Jena, Germany

Superparamagnetic iron oxide nanoparticles (SPIONs) are highly attractive candidates for numerous biomedical applications based on their unique characteristics including intrinsic biocompatibility and easy manufacturability. Although SPIONs have moved into focus of many studies, an fundamental knowledge of how SPIONs interact with biological environments is still missing but essential for their actual administration. In order to approach this issue a well-defined standardized test system is essential for generating comparative data. That is why aimed to establish a standardized *in vitro* test system to investigate and understand the passage of coated SPIONs through cell layers driven by magnetic forces.

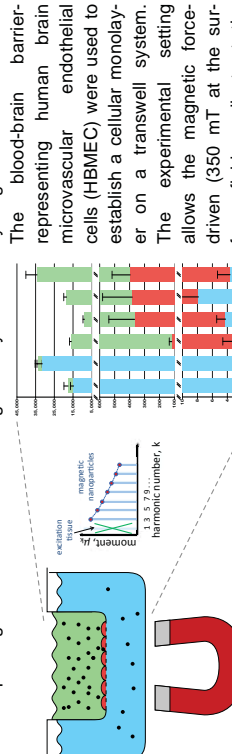


Figure 1: HBMEC-seeded transwell inserts were incubated with SPIONs and analyzed for SPION contents by means of MPS. By cell culture media adaption the cell layer's tightness could be optimized and evaluated by transendothelial electrical resistance (TEER) measurements, molecular permeability assays, and immune-staining of tight junction protein *zonula occludens-1* (ZO-1). Incubation of cell layers with polyethylenimine-coated fluidMAG-PEI/750/Q particles (chemicell GmbH, Berlin, Germany) compromises layer's integrity in a concentration-dependent manner indicating a layer-disrupting effect. In contrast, starch-coated fluidMAG-D SPIONs (chemicell GmbH, Berlin, Germany) did not affect tightness parameters significantly. Additionally, by means of magnetic particle spectroscopy (MPS) SPION-associated iron content within the different compartments was quantified specifically. Data show that fluidMAG-D particles easily traverse cell-free membranes whereas the presence of cells nearly completely prevents SPION crossing confirming high cell layer tightness. Notably, both MPS and atomic absorption spectroscopy reveal that fluidMAG-D are capable to overcome the BBB-representing layer in a time- and concentration dependent manner without diminishing cell layer integrity. The presented workflow seems appropriate for further precise SPION quantifications during nanoparticle-cell-interaction studies using the combination of the *in vitro* transwell system with magnetic particle spectroscopy quantification.

This work was supported by the DFG priority program 1681 (CL202/3-1, TR408/8-1, WI30/1-2, MU2382/4-1) and Clinical Research Group KFO213 (TR408/4-3).

## In-vivo targeting and imaging of super-paramagnetic iron-oxide particles to subcutaneous tumour models

Matin J. Monsani\*, J.J. Connell\*, P.S. Patrick, M. Zaw-Thin, T.L. Kalber, M.F. Lyngoe

One of the main challenges of the current clinical chemotherapy is the amount of off-target side effects caused by the non-selective nature of the therapeutics and drug delivery methods. This targeting inefficiency can be improved by delivery of a high concentration of the therapeutic to the target organ whilst reducing systemic dosing. Magnetic nanoparticles, in combination with applied magnetic fields, can non-invasively focus the delivery of small molecule drugs, antibodies and cells (1) to a specific site within the body to enhanced drug delivery efficacy. In addition, the particle behaviour within biological systems can be affected by physiological parameters such as the circulation time, extravasation rate, clearance time and blood vessel permeability. In order to assess the success of such a delivery system, it is important to be able to use various non-invasive imaging techniques not only to investigate the efficiency of particle delivery to the region of interest but also to assess the physiological parameters that impact the passage of nanoparticles. The assessment of physiological parameters will allows us to optimise the design of the combination of the nanoparticle and the external magnet system.

In this proof of principle study, LS147T human colorectal tumour cells were subcutaneously injected into nude CD-1 mice on each flank. After a period of 7 days, super-paramagnetic iron-oxide nanoparticles (Fluid Mag-CT particles (Chemicell), 100nm diameter with a magnetite core with carboxyl functional group) were intravenously injected into the mouse and a 1T neodymium magnet with positioned over the surface of one of the bilateral tumours for 20 minutes. T2 and T2\* weighted MR images were acquired before and after particle administration using respiratory-triggered spin-echo and gradient echo sequences respectively. In addition, dynamic contrast enhanced MR images (DCE, 2D gradient echo sequence with 1.5-second temporal resolution) and T1 maps (flow sensitive alternating inversion recovery with Look-Locker read out) were acquired to assess blood vessel permeability.

The reduction in T2\* across the magnetically targeted tumour after SPION injection was double that of the non-targeted tumour (as shown in Figure 1a & b) indicating successful magnetic targeting. The DCE analysis and T1 maps confirmed the abnormal wash-in and wash-out rates within the tumours, concurrent with the typical leaky vasculature of this tumour model.

The results presented here show that intravenously injected SPIONs accumulate in subcutaneous tumours to a greater extent when exposed to a magnetic field. Furthermore, quantitative MRI methods can be used to evaluate physiological parameters that impact the success of magnetic targeting. As tumours have a heterogeneous blood-tumour permeability (2), by using gadolinium-enhanced MRI, blood vessel permeability can be quantified such that magnetic targeting strategies can be refined to suit the individual tumour. Studies are ongoing on a range of tumour models, and employing radiolabelled SPIONs to enable quantification of iron oxide delivery to provide a new feedback loop to the optimization process leading towards targeting using gradient fields of MRI scanners.

(1) J Riegler et al., J. Phys. D (2011) (2) Lockman et al., J. Eng. MED (2010)

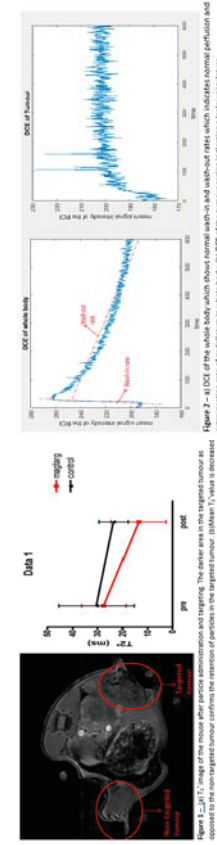


Figure 2 - a) DCE of the targeted tumor (red circles) and control tumor (black circles). b) T1 map of the enhancement rate of postmenopausal women in the targeted tumor (red) and control tumor (black).

## Magnetic cell delivery suppresses in-stent stenosis in injured arteries

Boris Polyakov<sup>1,2✉</sup>, Mikhail Medved<sup>1</sup>, Nina Lazareva<sup>1</sup>, Lindsay Steele<sup>1,3</sup>, Tirth Patel<sup>1</sup>, Menahem Y. Rotenberg<sup>4</sup>, Kimberly Wasko<sup>1</sup>, Andrew R. Kohut<sup>5</sup>, Richard Sensemig<sup>6</sup>, Gennady Friedman<sup>1,7</sup>  
<sup>✉</sup>bpolyakov@drexelmed.edu

<sup>1</sup>Department of Surgery, Drexel University College of Medicine, Philadelphia, PA 19102, USA; <sup>2</sup>Department of Pharmacology and Physiology, Drexel University College of Medicine, Philadelphia, PA 19102, USA; <sup>3</sup>Molecular Cell Biology and Genetics (MCBG) Program, Drexel University College of Medicine, Philadelphia, PA 19102, USA; <sup>4</sup>The Avram and Stella Goldstein-Goren Department of Biotechnology Engineering, Ben-Gurion University of the Negev, Beer-Sheva, 84105, Israel; <sup>5</sup>Department of Medicine, Division of Cardiology, Drexel University College of Medicine, Philadelphia, PA 19102, USA; <sup>6</sup>Department of Surgery, Perleman School of Medicine, University of Pennsylvania, Philadelphia, PA 19104, USA; <sup>7</sup>Department of Electrical and Computer Engineering, Drexel University, Philadelphia, PA 19104, USA

The advent of percutaneous transluminal angioplasty with stent implantation and the even more recent use of drug eluting stents have resulted in a paradigm shift in the care of obstructive vascular disease. However, deleterious sequelae of endovascular interventions are the result of unavoidable mechanical damage to the vessel wall. Disruption of the endothelial monolayer exposes the underlying media and induces a cascade of cellular and biological events, resulting in abnormal vascular wall function. Strategies that enhance the number of endothelial cells in the vessel wall following injury may limit complications such as thrombosis, vasospasm, and neointimal formation through reconstitution of a luminal barrier and cellular secretion of paracrine factors. The present study assessed the potential of magnetically-mediated delivery of endothelial cells (EC) to suppress in-stent stenosis induced by mechanical injury in a rat carotid artery stent angioplasty model. Syngeneic EC loaded (25pg magnetite/cell) with polylactide-based magnetic nanoparticles (MNP) and transduced with luciferase gene were delivered at the distal part of the stented artery under interrupted blood flow conditions using a brief exposure (12 min) to a uniform 1.4-kOe magnetic field. Bioluminescent imaging was used to demonstrate successful localization of the EC to the stented artery segment and assess viability of the delivered cells over two months. The therapeutic effect of the magnetic cell delivery was kinetically assessed by ultrasonic color Doppler imaging measuring morphological (lumen diameter) and hemodynamic changes (peak systolic velocity) in the targeted and non-targeted (control) animals. We found that after two months, magnetic localization of EC reduced in-stent stenosis at the distal part of the stented artery 1.8-fold, resulting in 12±1.2% and 21±2% decrease in lumen diameter in magnetically targeted and control animals respectively ( $p<0.05$ ). At the proximal part of the stented artery, there was no statistically significant difference between treated and control animals in the extent of lumen narrowing. Ratios of peak systolic velocities at the distal and proximal part of the stented artery indicated reduced stenosis (2.3-fold) in the animals of the treatment group ( $p<0.05$ ). The endpoint histological evaluation confirmed the protective effect of the targeted endothelium at the distal part of the stented artery (neointima/media ratios:  $2.01\pm0.36$  and  $3.26\pm0.61$  in treatment and control group respectively), which correlated with the detected traces of MNPs found only at the distal part of the stented artery. We conclude that magnetically-assisted delivery of EC is a promising experimental strategy for prevention of vessel lumen narrowing after stent angioplasty procedure.

**Acknowledgement:** This work was supported by the NIH award R01HL107771 to BP and Drexel University College of Medicine Clinical & Translational Research Institute (CTR) to BP.

## Magnetizable Stent-Grafts Enable Endothelial Cell Capture

B.J. Teff Ph.D.<sup>1</sup>, S. Uthamara<sup>2</sup>, J.J. Harburn Ph.D.<sup>3</sup>, O. Hlinomaz M.D. Ph.D.<sup>4</sup>, A. Lerman M.D.<sup>1</sup>, D. Dragomir-Daescu Ph.D.<sup>5</sup>, G.S. Sandhu M.D. Ph.D.<sup>1\*</sup>

<sup>1</sup>Department of Cardiovascular Diseases, <sup>2</sup>Division of Engineering,

<sup>3</sup>Department of Physiology and Biomedical Engineering

Mayo Clinic, 200 1st Street SW, Rochester, MN 55905, USA

Durham University, School of Medicine, Pharmacy and Health

<sup>4</sup>Department of Cardioangiology, Stockton-on-Tees, TS17 6BH, UK

ICRC, St. Anne's University Hospital, Pekarska 53, 666 91 Brno, Czech Republic

\*e-mail: sandhu.surgeon@mayo.edu

Emerging medical nanotechnology applications often utilize magnetic forces to guide the movement of superparamagnetic iron oxide nanoparticle (SPION)-labeled cells, drugs, and other agents in order to achieve a therapeutic effect. SPION-labeled endothelial cells have previously been captured on the surface of magnetizable 2205 duplex stainless steel stents in a porcine coronary implantation model. Recently, we have coated these stents with electrospun nanofibers of polyurethane to fabricate prototype stent-grafts. Facilitated endothelialization of stent-grafts may help improve the healing of arteries treated with stent-grafts, reduce the risk of thrombosis and restenosis, and enable small-diameter applications such as the coronary arteries.

Mechanical testing of prototype stent-grafts demonstrated they could withstand the crimping and balloon expansion necessary for vascular implantation without signs of fracture, tearing, nor delamination. When placed in an SPION-labeled cell suspension of  $1\times10^6$  cells/ml in the presence of an external magnetic field, magnetized stent-grafts successfully captured cells to the surface regions adjacent to the stent struts. Implantation within the coronary circulation (3-4 mm diameter) of a porcine model ( $n=13$ ) followed immediately by SPION-labeled autologous endothelial cell delivery resulted in widely patent devices with a thin, uniform neointima and no signs of thrombosis nor inflammation at 7 days (Fig 1). Furthermore, the magnetized stent-grafts successfully captured and retained SPION-labeled endothelial cells (Fig 2), whereas the non-magnetized control stent-grafts did not.

These data provide support to the observation that magnetization of stent-grafts enables the capture and retention of SPION-labeled endothelial cells following stent-graft placement. This, in turn, may lead to more rapid and complete healing of vascular stent-grafts with a concomitant improvement in long term device performance.

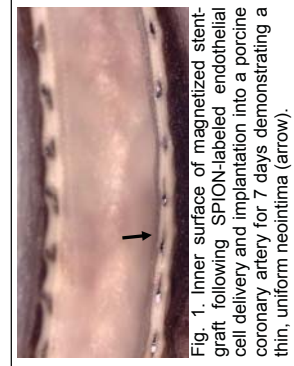


Fig. 1. Inner surface of magnetized stent-graft following SPION-labeled endothelial cell delivery and implantation into a porcine coronary artery for 7 days demonstrating a thin, uniform neointima (arrow).

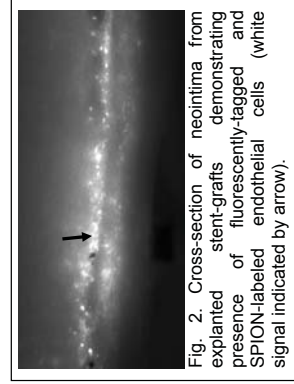


Fig. 2. Cross-section of neointima from explanted stent-grafts demonstrating presence of fluorescently-tagged and SPION-labeled endothelial cells (white signal indicated by arrow).

## Magnetic Nanoparticles Applied to Cancer Theranostics: a Translational Nanomedicine Perspective

Adrielle Prina-Mello<sup>1,3,\*</sup>, O. Gobbo<sup>2</sup>, Y. Volkov<sup>1,3</sup>

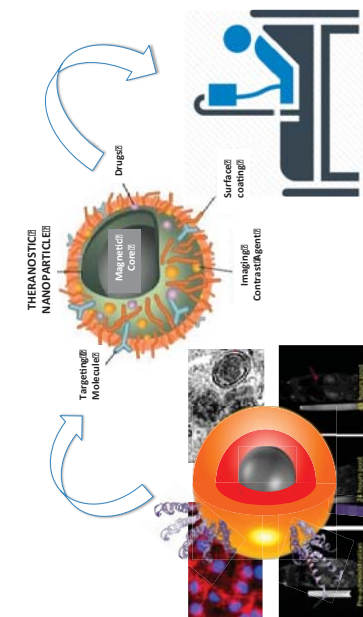
<sup>1</sup>School of Medicine and Trinity Translation Medicine Institute, Trinity College Dublin, Ireland; <sup>2</sup> School of Pharmacy and Pharmaceutical Sciences, Trinity College Dublin, Ireland; <sup>3</sup> Centre for Research on Adaptive Nanostructures and Nanodevices (CRANN), Trinity College Dublin, Ireland. \*E-mail: [prinam@tcd.ie](mailto:prinam@tcd.ie)

The rising global incidence of cancer is associated with high rates of mortality and morbidity worldwide. While new treatments are evolving, awaiting and reaching approval for different cancer types, the main prevention of cancer mortality is through early diagnosis, detection and treatment of this previously incurable disease.

Nanomedicine promises to develop innovative solutions of greater sensitivity, efficacy and less side effects than the standard existing diagnostics and treatment. In the last decades, the development of Theranostic approaches, as Two-in-One tools, are changing the way to treat cancer. The development of nano-tools for personalized medicine through fluorescent detection and magnetic resonance imaging has the potential to provide the diagnosis of cancer at much earlier stage compared to the currently available detection methods. Targeted properties of nanoparticles offer previously unachievable Theranostics potential allowing for simultaneous detection and treatment strategies.

In this paper, we not only overview some of the state-of-the-art nanotechnological applications for cancer therapy, but also highlight advances in the concept of personalized nanomedical theranostic therapies utilizing iron oxide magnetic nanoparticles in conjunction with MRI Imaging.

The main regulatory challenges towards the fast clinical translation of magnetic nanoparticles for personalised nanomedical theranostics involve extensive multi-disciplinary and international multicentre efforts, where the entire stakeholder's community has to be fully educated, duly informed and committed across the whole process from the bench to bedside.



Schematic of personalized nanomedical theranostics: from bench to bedside.

## Biofilm Ablation: Rotating Nanorods Remove Microbes from Surfaces, Enhancing Antimicrobial Efficacy

Lamar O. Mair<sup>1</sup>, Aleksander Nacev<sup>1</sup>, Ryan Hilman<sup>1</sup>, Pavel Stepanov<sup>1</sup>,

Jeffrey Haufield<sup>2</sup>, Amy Karlsson<sup>3</sup>, Benjamin Shapiro<sup>4</sup>, Irving N. Weinberg<sup>1</sup>

<sup>1</sup>School of Medicine and Health Sciences, George Washington University, Washington DC, USA  
<sup>2</sup>Weinberg Medical Physics LLC, Bethesda, Maryland, USA  
<sup>3</sup>Department of Chemical and Biomolecular Engineering, University of Maryland at College Park, USA  
<sup>4</sup>Fischell Department of Biengineering, University of Maryland at College Park, USA  
Contact: Lamar.Mair@gmail.com

**Introduction:** Fungal and bacterial biofilms cause a broad array of infections. New methods of combating these tenacious microbial havens are becoming increasingly important. One characteristic of biofilms that makes them particularly difficult to treat is their increased resistance to antimicrobial therapy. While free-floating microbes may be susceptible to a specific drug or therapy, biofilms of the same microbe often prove drug resistant due to a confluence of factors. The dense meshwork of polysaccharides that mechanically buttresses the biofilm, along with the evolution of persister cells capable of resisting antimicrobial attack, are but two of the many defenses biofilms may evoke. We attempted to determine whether biofilms could be disrupted mechanically (using rotating magnetic nanorods) and find out whether such disruption would affect fungal sensitivity to antimicrobials.

**Methods:** Cultures of the fungus *Aspergillus fumigatus* in saline were examined under four regimens (Figure 1, top row): A: no treatment (control), B: amphotericin B only, C: rotating nanorods only, and D: combined antimicrobials and rotating nanorods. Nanorods were nickel, with diameters ~0.25 μm and lengths ~8 μm. Rods were rotated using a cylindrical, diametrically magnetized permanent magnet attached to a motor. After treatment, fluid doses were extracted and compared visually. Extracted fluid doses were then cultured, and the method of counting colony-forming units (CFUs) was used to determine the effectiveness of treatment.

**Results:** Visual inspection of the extracted treatment fluids (Figure 1, middle row) showed that nanorod disruption treatments resulted in noticeably yellow/cloudy extracted treatment fluids (Groups C and D), corresponding to conversion of anchored microbes into freely-floating cells. Culturing the extracted treatment fluid from Groups A and B resulted in large quantities of viable colony-forming units in these groups. Moderate quantities of CFUs were seen in the group treated with nanorods alone. Low quantities of CFUs were observed in the group treated with both nanorods and amphotericin B. Overall, combined nanorod ablation and amphotericin B treatment demonstrated >90% kill rate, as compared with control, amphotericin B, or nanorods alone (Figure 1, bottom row).

**Discussion:** By rotating nanorods that are nearby or enmeshed in the biofilm, we believe we are able to mechanically remove populations of cells from the bulk of the film. These cells, once made planktonic, are significantly more susceptible to antifungal therapy and can thus be readily eliminated by coconcurrent medical therapy.

**Conclusion:** Nanorod rotation is capable of removing cells from their biofilm environs, making these cells more susceptible to elimination by commonly used antimicrobial therapies. By co-administering antimicrobial therapy with our biofilm ablation protocol, microbes were effectively eliminated.

Talk # 32

Talk # 31

## Protein modified ferucarbotran particles for GMP conform production of magnetically labeled platelets from platelet concentrates

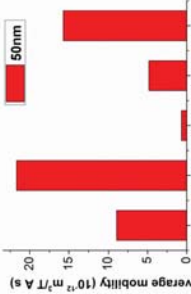
### Nanomaterial Phagocytosis and Cytotoxicity: Quantification by Magnetic Cytometry

C. Zhou<sup>1</sup>, Y. S. Choi<sup>1</sup>, T. R. Hanley<sup>1\*</sup>, A. E. David<sup>1</sup>, P. Todd<sup>2</sup>

<sup>1</sup>Department of Chemical Engineering, Auburn University, Auburn, AL 36849, USA  
<sup>2</sup>Techshot, Inc., 7200 Highway 150, Greenville, IN 47124, USA, \*E-Mail: hanley@auburn.edu

The phagocytosis of nanoparticles is of rising interest due to increased relevance to industrial toxicology, applications in medical diagnostics, therapeutics, gene therapy, theranostics, enhanced tumor targeting, and fundamental studies of subcellular behavior. For this reason the ingestion of nanoparticles by cells other than differentiated phagocytic cells such as macrophages, dendritic cells and astroglia, is of increasing interest in genetic control and mechanisms of phagocytosis, toxicity, drug delivery and gene therapy. This interest transcends applications of immune reagents, and the composition- and size-dependence of particle ingestion is an important issue.

The quantification of phagocytosis reveals its dependencies on cell type, time, particle composition, particle size and particle toxicity. By using paramagnetic nanobeads with adjustable surface chemistry we have been able to quantitatively characterize and determine the kinetics of phagocytosis as a function of particle size and surface chemistry. Magnetophoretic mobility and net magnetic susceptibility were measured by cell tracking velocimetry and used as quantitative indicators of number of particles ingested per cell. We found, for example, that cultured Chinese hamster ovary (CHO-K1) cells ingested animated (positively charged) 50-nm particles more effectively than naked starch-coated particles. The ingestion of PEG-coated particles increased with PEG molecular weight.



Data are reported that support the hypothesis that cytotoxicity of nanobeads is directly related to their incorporation into cells.

HSA conjugation onto ferucarbotran increased particle uptake into cells tenfold compared to bare ferucarbotran particle uptake (incubation iron concentration 0.5 mM; uptake: 0.0028±0.0022 pg vs.

0.023±0.007 pg iron/platelet, bare ferucarbotran vs. HSA-ferucarbotran respectively) as demonstrated by atomic absorption spectroscopy iron determination. Platelet imaging by fluorescent and electron microscopy showed uptake of the particles into the open canalicular compartment. A labeling rate of 82.6±14.6% platelets could be achieved. Platelet function testing by light transmission aggregometry and determination of the activation marker CD62p on cell surfaces revealed normal platelet function after incubation of PC platelets with ferucarbotran or HSA-ferucarbotran (0.5 mM iron concentration). Magnetic separation resulted in a yield of 55% of the HSA-ferucarbotran labeled platelets from spiked whole blood. Negative sterility tests according Ph. Eur. showed adequate aseptic manufacturing of HSA-ferucarbotran particles as well as of the magnetically labeled PC platelets. We demonstrate that magnetic labeling of platelets from PC can be improved by conjugation of human plasma proteins onto ferucarbotran nanoparticles. We succeeded in reisolation of magnetically labeled platelets from whole blood and we are able to produce protein coupled particles and magnetically labelled platelets from PC under EU GMP conditions.

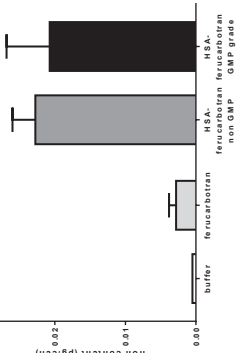


Fig.: Platelet iron content after incubation with buffer, ferucarbotran or HSA-ferucarbotran particles

## Characterization of Magnetic Nanoparticle Internalization by Glioma Cells: Effects of Poly-L-Lysine Coating

INVITED TALK 4

### COMBINATORIAL BIOMATERIAL APPROACHES USING IRON OXIDE NANOPARTICLES TO DIRECT AXONAL REGENERATION FOLLOWING SPINAL CORD INJURY

Yunn-Hwa Ma,<sup>1</sup> Yi-Ting Chang<sup>1</sup>, Yi-Ching Lu<sup>1</sup> and Daniel Horak<sup>2</sup>

<sup>1</sup>Department of Physiology and Pharmacology, Graduate Institute of Biomedical Sciences, College of Medicine, Chang Gung University, Taoyuan, Taiwan, ROC 33302;

<sup>2</sup>Institute of Macromolecular Chemistry, Academy of Sciences of the Czech Republic, 16200 Prague 6, Czech Republic

Magnetic nanoparticles (MNPs) have been tested in diagnosis/imaging and targeting therapy for treatment of solid tumors, which may require MNP internalization by tumor cells to achieve therapeutic objectives. Previous studies indicated that both magnetic force and poly-L-lysine (PLL) may enhance cellular uptake of MNPs. We hypothesized that PLL may modify surface characteristics of MNPs to enhance interaction of MNP and plasma membrane of tumor cells. Uptake of dextran-coated MNP (nanogag) with a zeta potential of  $-40.1 \pm 0.3$  mV by U87MG cells from human glioma was examined with transmission electron microscopy and quantitated by potassium thiocyanate method. Incubation of MNPs with the cell enhanced formation of microvilli-like structure with or without PLL, whereas PLL greatly increased MNPs on the surface of the cell membrane and numbers of the vesicles with MNPs in the cytoplasm. PLL at 0.3-1  $\mu\text{M}$  significantly increased cell-associated MNP ( $MNP_{cell}$ ) by approximately 8 to 10 fold. After pre-treatment of PLL for one h, removal of PLL from the medium prior to addition of MNPs completely blocked the enhancement effect of PLL on  $MNP_{cell}$  pre-mixing of PLL with dextran-coated MNPs for one h significantly enhanced  $MNP_{cell}$ . Therefore, a direct interaction of PLL with MNP may be required for the enhanced uptake of MNPs. Epigallocatechin gallate (EGCG), another uptake enhancer, induced augmented  $MNP_{cell}$  in a concentration- and time-dependent manner; however, the enhancement effects of PLL was greatly attenuated by addition of EGCG. It is likely that the negative charge of the carboxyl groups on EGCG may hinder the positive charge of amine of PLL required for the enhancement effect. PLL-coated MNPs, PLL-MNP<sub>n</sub> vs. PLL-MNP<sub>p</sub> were obtained by post-synthesis modification of the primary  $\gamma\text{-Fe}_2\text{O}_3$  colloid (obtained by coprecipitation and oxidation) with PLL, and the zeta potential of PLL-MNP<sub>n</sub> vs. PLL-MNP<sub>p</sub> measured  $-46.8 \pm 4$  vs.  $49.2 \pm 2$  mV, respectively. PLL coating consistently increased MNP<sub>cell</sub> compared with non-coated MNP<sub>n</sub> or MNP<sub>p</sub>; however, magnetic force did not enhance uptake of PLL-MNP<sub>n</sub> or PLL-MNP<sub>p</sub>. In addition, internalization of PLL-MNP<sub>n</sub> was about 3- and 5- fold of PLL-MNP<sub>p</sub> and dextran-coated MNP, respectively. The results suggested that surface characteristics of MNPs are pivotal in cellular uptake of MNPs. The enhancing effects of PLL coating may involve positive charge of the functional groups, but may be independent on the zeta potential.

Support of the Czech-Taiwanese project (Czech Science Foundation No. 16-01128J and MOST 105-2923-B-182-001-MY3) is acknowledged.

Spinal cord injury (SCI) affects approximately 12,000 Americans per year and leads to paralysis below the injury site. While several treatments are capable of restoring some function, there is no cure for SCI. One current challenge in achieving complete functional recovery is to develop approaches that encourage axonal regeneration through the lesion site. Axonal regeneration failure occurs due to the formation of an inhibitory glial scar and the lack of guidance cues.

One biomaterial fabrication process used to fabricate synthetic guidance cues is to produce fibers using electrospinning. Electrospinning produces polymeric fibers with nanoscale or microscale diameters. When these fibers are aligned, typically through the use of a spinning collection mandrel, the aligned fibers direct axonal regeneration within animal models of SCI. While axonal regeneration is robust using electrospun fiber guidance cues, developing biomaterials that also release neurotropic growth factors increases axonal regeneration.

In this study, we developed a novel nanoparticle consisting of poly-L-lactic acid (PLLA), iron oxide nanoparticles, and nerve growth factor (NGF). The purpose of this particle was to develop a drug-delivery vehicle that could be moved in the presence of a magnetic field to better assist the directional extension of regenerating axons. To determine the ability of the nanoparticles to direct neurite outgrowth, dorsal root ganglia (DRG) explants were cultured on a culture dish or aligned electrospun fibers. Cultures then received soluble NGF, particles without NGF, or particles containing NGF for a period of 2 days. Following staining of neurons, the length and direction of neurite outgrowth was assessed. Results show that NGF-releasing nanoparticles were better able to direct neurite extension than particles without NGF or soluble NGF treatment (Figure 1).

In summary, we have developed a novel approach utilizing magnetically mobile, drug-releasing nanoparticles to better direct neurite extension. We believe that electrospun fibers in combination with drug-releasing particles positioned precisely with a magnetic may be a powerful combinatorial approach for directing robust axonal regeneration following spinal cord injury.

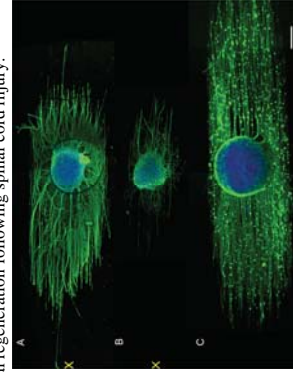


Figure 1: Aligned neurite extension from DRG cultured on PLLA microfibers is preferentially directed by NGF-nanoparticles. (A) Neurites extending from DRG cultured on aligned microfibers grew longer in the direction of the NGF-nanoparticles than away, while neurites extending from DRG cultured on aligned microfibers in the presence of (B) empty nanoparticles and (C) NGF containing medium. Scale bar = 500  $\mu\text{m}$ .

# Transforming Magnetic Microparticles into RF-addressable Microsensors

G. Zabow<sup>1,2\*</sup>, S. Dodd<sup>2</sup>, A. Koretsky<sup>2</sup>

<sup>1</sup>Applied Physics Division, National Institute of Standards and Technology (NIST), Boulder, CO, 80305, USA.  
<sup>2</sup>Laboratory of Functional and Molecular Imaging, National Institutes of Health (NIH), Bethesda, MD, 20892, USA.  
\*Email: [zabow@boulder.nist.gov](mailto:zabow@boulder.nist.gov)

From imaging, to drug delivery, to hyperthermia, to tissue engineering, magnetic nano- and microparticles are finding ever increasing use in an ever growing array of biomedical applications. What if those same magnetic particles could also simultaneously sense the local physiological conditions in their immediate surroundings? What if a magnetic particle could report back on the local pH, or temperature, or concentration of a particular analyte of interest as that particle moved through the body providing imaging contrast or delivering its cargo?

Here we present recent work on new, specially shaped, magnetic microparticles that incorporate 'smart' polymer gels that rapidly expand or contract in response to chosen environmental conditions<sup>1</sup>. As the stimuli-responsive polymers change shape, so too does the magnetic microstructure, causing a change in the magnetic field that the structure creates. In turn, the changing field results in a changing shift in the resonant magnetic precession frequency of nuclei in the particle's surroundings (such as, for example, water hydrogen protons), which can then be detected with regular nuclear magnetic resonance (NMR) equipment. In transducing the response of a smart polymer into an NMR frequency shift that can be detected remotely, the magnetic microparticles effectively act as radio-frequency (RF) analogs to optical fluorescent or plasmonic colorimetric nanosensors. Because smart polymers can be specifically targeted to multiple different variables, the same magnetic microparticle sensing platform should be adaptable to measure a variety of different physiological conditions or biomarkers of interest. Such magnetic particle sensors may therefore offer similarly broad application to that of optical colorimetric sensors except being probed in the RF, they may continue to function also in optically occluded locations, such as deep *in vivo*.

As a first example of such magnetic microparticle sensing, we demonstrate a pH sensor based on an acid-sensitized hydrogel sandwiched between a pair of magnetic disks (fig. 1), but we will also discuss more generally how such structures work and where else they may be applied.

## Reference:

1. G. Zabow, S.J. Dodd and A.P. Koretsky, *Nature* **520**, 73 (2015)

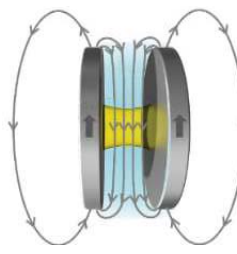


Fig 1: Schematic of shape-changing magnetic microparticle sensor. Expansion of a stimuli-responsive hydrogen (inner yellow post) shifts a pair of attached magnetic disks changing the local field, which shifts the NMR frequencies of nuclei in the surrounding medium.

# Highly sensitive magnetic nanoparticle quantification with 7-order linear range and its applications for multiplex biosensing

P.I. Nikitin<sup>1,2\*</sup>, A.V. Orlov<sup>1</sup>, V.R. Cherkasov<sup>3</sup>, S.L. Znayko<sup>1</sup>

<sup>1</sup>General Physics Institute, Russian Academy of Sciences, Moscow, Russia, <sup>2</sup>National Research Nuclear University MEPhI (Moscow Engineering Physics Institute), Russia, <sup>3</sup>Moscow Institute of Physics and Technology (State University), Dolgoprudny, Russia, \*E-mail: [nikitin@kapella.gpi.ru](mailto:nikitin@kapella.gpi.ru)

Magnetic nanoparticles (MP) attract a lot of attention as promising nanolabels for various analytical systems. However, on-site magnetic biosensors that have analytical characteristics comparable to those of laboratory methods are still to be developed. In this work, we developed multiplex Dry-Reagent ImmunoMagnetic (DRIM) analytical platform and demonstrated its performance for rapid high-precision quantitative *in vitro* diagnostics and food quality control. The platform combines the advantages of immunoassay chromatography with highly sensitive magnetic particle quantification (MPQ) from the entire volume of 3D structures by non-linear magnetization [1-3].

A new generation of multi-channel MPQ readers has been developed that offer the record limit of detection (LOD) of 0.4 ng or 60 zeptomoles of MP in 0.2 ml volume within extremely wide 7-order linear dynamic range (Fig. 1). These parameters to the best of our knowledge, currently have no analogs. The readers also provide the effective means for accurate MP mapping along all 3D components of the test strips for easy optimization of the assays as well as for metrology of MP for a variety of biochemical and medical applications.

The DRIM platform was optimized for multiplex quantitative detection of botulinum neurotoxin (BoNT) types A, B and E in complex matrices such as milk, apple and orange juices. The LODs were found to be 0.14, 0.11 and 0.30 ng/ml for BoNT-A, B and E, respectively. The LOD for detection of total prostate specific antigen in human serum was as good as 25 pg/ml. The DRIM platform permits measurements within the clinically relevant concentration range even when the most sensitive registration is required, e.g., PSA detection after radical prostatectomy. The method can be used for simple and sensitive quantitative *in vitro* diagnostics, food and safety control, etc.

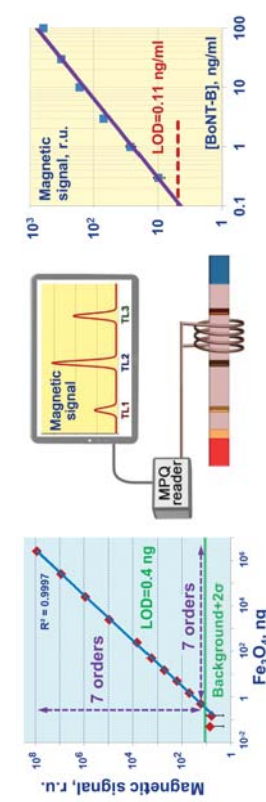


Fig. 1. Multi-channel MPQ reader calibration; readout setup; and BoNT-B dose-response curve. The research was supported by grants of Russian Science Foundation (# 16-12-10543, development of MPQ readers) and Russian Foundation of Basic Research (#14-29-07271), assay development.

- [1] P.I. Nikitin, P.M. Vetoshko. Patents RU2166751, RU2177611 (2000), EP1262766 (2001).
- [2] M.P. Nikitin V.O. Shipunova, S.M. Deyev, P.I. Nikitin. *Nature Nanotechnol* 9 (2014) 716–722.
- [3] A.V. Orlov, V.A. Bragina, M.P. Nikitin, P.I. Nikitin. *Biosens. Bioelectron.* 79 (2016) 423–429.

## Sensitive magnetic biodetection using magnetic multi-core nanoparticles and RCA coils

C. Johansson<sup>1\*</sup>, J. Blomgren<sup>1</sup>, A. Sarwar<sup>1</sup>, C. Jonasson<sup>1</sup>, F. Ahrentorp<sup>1</sup>, S. Sepahi<sup>2</sup>, E. Eriksson<sup>2</sup>, A. Kakhbukhov<sup>2</sup>, A. Jerska<sup>2</sup>, D. Winkler<sup>2</sup>, J. Schneidemar<sup>2</sup>, M. Nilsson<sup>3</sup>, J. Albert<sup>3</sup>, T. Zardan Gómez de la Torre<sup>3</sup>, M. Stromme<sup>6</sup>,  
<sup>1</sup> Acreo Swedish ICT AB, Arvid Hedvalls Backe 4, Göteborg, Sweden, <sup>2</sup> Chalmers, Göteborg, Sweden, <sup>3</sup> MedTech West and  
the University of Gothenburg, Göteborg, Sweden, <sup>4</sup> Stockholm University, Stockholm, Sweden, <sup>5</sup> Karolinska Institute,  
Stockholm, Sweden, <sup>6</sup> Uppsala University, Uppsala, Sweden. \*E-mail: christejohansson@acreo.se

Multi-core magnetic iron oxide based nanoparticles can be found in several biomedical applications such as in the areas of diagnostics, therapy, actuation and imaging. In this project we concentrate on using functionalized iron oxide based magnetic multi-core particles with a mean size of 100 nm (micromod Partikeltechnologie GmbH) sensing particles for the detection of influenza virus. Our aim is to develop a novel portable sensing platform for rapid detection of the influenza virus with sub-picomolar resolution. The detection principle relies on measurements of the changes in Brownian relaxation of suspended functionalized magnetic nanoparticles (MNPs) including volume amplification of the analysis using the padlock-probe-ligation technique and rolling chain amplification (RCA coils) [1-3]. The obtained RCA coils are in the size range of 1  $\mu\text{m}$ . For detection we use sensitive AC susceptibility (ACS) measured with an induction based technique (DynoMag) and high temperature superconducting quantum interference devices (HTS SQUID) [1, 4]. All steps of the bioassay in the final device will be performed on a disposable lab-on-a-chip system. The figures below show the HTS SQUID system, the DynoMag system and an example of the measurements (ACS vs frequency of a negative control sample and a sample containing 50 pM RCA coils formed from synthetic *Vibrio cholera* target DNA). During the incubation of the MNPs, the MNPs bind to the RCA coils resulting in changes in the Brownian relaxation frequency of the MNPs from ~0.5 Hz (free MNPs) to ~0.5 Hz (bound MNPs). The Brownian relaxation of bound MNPs are more or less disappearing from the measurement frequency window (above 1 Hz). Thus at about 100 Hz we detect the ACS signal from the remaining free MNPs that have not bound to the RCA coils. The reduction of the out-of-phase component of the AC susceptibility is our primary bio-detection technique.



**Figure 1** (left) HTS SQUID system, (middle) the DynoMag system and (right) out-of-phase component of ACS vs frequency for two measurements of a negative control (no binding) and a sample containing 50 pM RCA coils. For this mixing relation between MNPs and RCA coils most all of the MNPs bind to the RCA coils leaving only a small free MNP signal at about 100 Hz. For the HTS SQUID system the sample volume is 3  $\mu\text{l}$  and for the DynoMag system the sample volume is 80  $\mu\text{l}$ .

### References

- [1] Astalan, A. P. et al *Biosensors and Bioelectronics* **19**, 945 (2004).
- [2] Nilsson, M. et al. *Science* **265**, 2085 (1994).
- [3] Zardan Gómez de la Torre, T. et al, *Biosensors and Bioelectronics* **29**, 195 (2011).
- [4] Ösjöen, F. et al *Biosensors and Bioelectronics* **25** 1008 (2010).

**Acknowledgements:** The work is supported through Swedish Foundation for Strategic Research (SSF) grant “FLU-II” #SBEI3-0125, the Knut and Alice Wallenberg foundation, Swedish Infrastructure for Micro- and Nanofabrication – Myfab and by the European Commission Framework Programme 7 under the Nanomag project (grant agreement no: 604448).

### INVITED TALK 5

#### MAGNETIC SENSORS FOR CLINICAL DIAGNOSTICS: FROM NANOSCALE VESICLES TO CANCER CELLS

Cesar M. Castro<sup>1</sup>, Ralph Weissleder<sup>1</sup>, Hakho Lee<sup>1\*</sup>

<sup>1</sup>Center for Systems Biology, Massachusetts General Hospital, Boston, MA, USA

\*e-mail: hlee@mgh.harvard.edu

A major challenge in clinical medicine is the rapid and accurate measurement of biomarkers in diverse media. Biosensors based on magnetic detection are promising diagnostic platform for such medical diagnostics. Magnetic detection experiences little interference biological sample because of the inherently negligible magnetic background of biological objects; even optically turbid samples will often appear transparent to magnetic fields. With magnetic labeling, however, biomolecules or cells of interests can attain a high contrast against background. We have been developing different types of magnetic sensors optimized for specific biological targets. Our systems include a miniaturized NMR platform that is ideal for detecting nanoscale objects or molecules (e.g., exosomes, DNA, mRNA); a microHall chip to screen individual cells labeled with magnetic nanoparticles; and iii) a diamond-based magnetometer for ultra-sensitive magnetic imaging. This presentation will review each of these systems, with emphasis on its potential clinical applications. Common key components such as magnetic nanomaterials and labeling strategies will also be discussed.



**Fig. 1** Magnetic sensor technologies. From the left, Fe-based magnetic nanoparticles; a miniaturized NMR device for clinical applications; a microHall sensor chip for single cell detection; magnetically-labeled cells imaged by a diamond-based magnetometer.

## Smart assembly of magnetic microparticles utilizing 3D magnetic fields

<sup>1</sup>Department of Mechanical and Industrial Engineering, Northeastern University, Boston, MA 02115.  
 Email: [sheilani.t@husky.neu.edu](mailto:sheilani.t@husky.neu.edu)

**Abstract:** Directed assembly techniques of particle suspensions represent an exciting approach for the development of reconfigurable optical fluids that can bend, adsorb, or accentuate light. As two optical particles come together, they create local enhancement to the electromagnetic fields. Magnetic fields allow for the remote control of particle assembly in a massively parallel format in bulk fluid. However, linear magnetic fields offer very little tunability for the resultant assemblies. For example, a linear field will provide a time-dependent chain aggregation of magnetic particles. Instead, 2D rotating fields allow for enhanced tunability, creating planar assemblies. By expanding the applied magnetic field functions into the third dimension, a significantly large design space for particle assemblies can be realized.

Here, we have developed theoretical, numerical, and experimental investigations for three dimensional magnetic field functions capable of creating complex particle assemblies. These three dimensional sinusoidal field functions can generate suspensions full of particle dimers, trimers, and quadramers, for example, in bulk fluid away from substrates. These suspensions have long-term stability and can be quickly switched between states. In numerical simulations particles are considered as simple magnetic dipoles and effects of mutual polarization are neglected. Stokes equation has been implemented to capture the hydrodynamics and Forward Euler method was used to update the position of particles after each time step. In experiments, magnetic fields were applied using three 4 in. diameter iron-core solenoids that are placed in the x, y, and z direction. The solenoids are fed with current from three 20-5M bipolar operational amplifiers (Kepco) controlled with a LabView program. Magnetic fields generated were measured using 425 gaussmeter (Lake Shore Cryotronics Inc., OH, USA). Magnitudes of the applied magnetic fields are 8, 12, and 16 mT.

This material is based upon work supported by the National Science Foundation under Grant No. CNS-1329649.

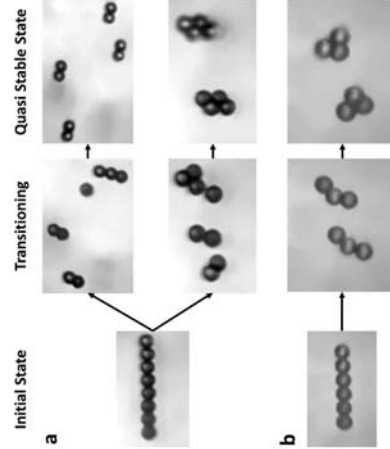


**Figure 1 – (a)** Formation of dimers and quadramers from a chain of 8 particles. **(b)** Formation of trimers from a chain of 6 particles.

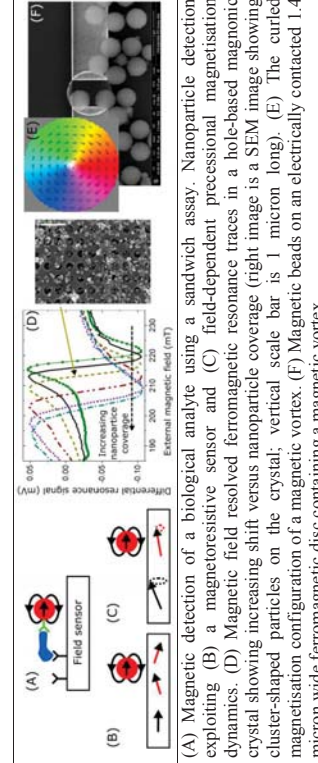
## Towards frequency-based spintronic detection of magnetic nanoparticles

Peter J. Metaxas<sup>1,\*</sup>, Manu Sushruth<sup>1</sup>, Jasper P. Fried<sup>1</sup>, Robert C. Woodward<sup>1</sup>, Mikhail Kosylev<sup>1</sup>, Stephane Xavier<sup>2</sup>, Cyril Deranbor<sup>3</sup>, Abdelladjid Anane<sup>3</sup>, Vincent Cros<sup>3</sup>, Jeremy Duzynski<sup>4</sup>, Rebecca O. Fuller<sup>4</sup>, Maximilian Albert<sup>5</sup>, Hans Fangohr<sup>5</sup>, Junjia Ding<sup>6</sup>, Xue Zhou<sup>6</sup> and Adekunle O. Adeyeye<sup>6</sup>

<sup>1</sup>School of Physics, University of Western Australia, Crawley, Australia; <sup>2</sup>Thales Research and Technology, Palaiseau, France; <sup>3</sup>Unité Mixte de Physique CNRS/Thales, Univ Paris-Sud & Univ. Paris-Saclay, Palaiseau, France; <sup>4</sup>School of Chemistry and Biochemistry, University of Western Australia, Crawley, Australia; <sup>5</sup>Faculty of Engineering and the Environment, University of Southampton, Southampton, UK; <sup>6</sup>Information Storage Materials Laboratory, Department of Electrical and Computer Engineering, National University of Singapore, Singapore \*peter.metaxas@uwa.edu.au

Magnetic biosensing exploits chemically functionalised magnetic nanoparticles for labelling and subsequent detection of analytes of interest in biological samples [Fig. A], opening routes to new technologies for point-of-care medical diagnostics [1]. Many solid state nanoparticle detection techniques are voltage-level based. For example, in conventional magnetoresistive sensors, the magnetic configuration within the device is modified by the nanoparticles' stray magnetic fields, generating a change in the device resistance (and thus the voltage across the device) [Fig. B]. In contrast, electrically probed, field-dependent magnetisation dynamics in magnetic nanostructures [Fig. C] offer a route towards intrinsically *frequency-based* sensing. This resonance-based approach potentially offers higher speed sensing with nano-scale devices [2] which can operate under very large magnetic field ranges. We demonstrate the potential of this approach first using large area, periodically nanostructured ferromagnets ("magnetic crystals") [3]. These systems enable us to probe ferromagnetic resonances confined to regions in the crystal with lateral dimensions on the order of 100 nm. Nanoparticles adsorbed near where the magnetisation dynamics are concentrated can induce resonance frequency shifts of -0.1 GHz with signs that depend predictably on the location of the resonant dynamics [Fig. D]. Secondly we look at nanoparticle sensing with the "gyrotropic" resonance of the ferromagnetic vortex state [Fig. E] in magnetic micro- and nano-disks. We show how the localized field of a nanoparticle can stiffen the vortex, leading to field sensitivities exceeding those conventionally measured in uniform fields [4]. We also experimentally demonstrate spintronic detection of superparamagnetic beads using electrically probed vortex resonance [Fig. F].

[1] Gaster et al., Nat. Med., 15, 1327 (2009). [2] Braganca et al., Nanotechnol., 21, 235202 (2010). [3] Metaxas et al., Appl. Phys. Lett. 106, 232406 (2015). [4] Fried and Metaxas, Phys. Rev. B, 93, 064422 (2016).



# Magnetic Nanoparticle Based Biosensor for Multiplex Detection of Disease

Kai Wu and Jian-Ping Wang<sup>a</sup>

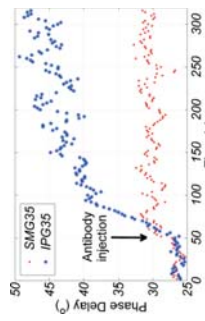
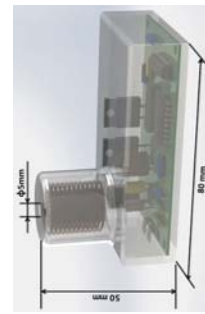
Department of Electrical Engineering, University of Minnesota, Minneapolis, MN 55455, USA  
Electronic mail: jpwang@umn.edu

Magnetic biosensors, compared to currently popular optical biosensors, have shown very environmentally safe and low cost to synthesis. The natural magnetic background noise is much less than optical method, which can push the detection limit further down. Herein, MNPs are used as probes to detect biomarkers (protein, DNA, etc.) by using a search coil based scheme for volume detection. The search coil based sensing scheme is one of the best candidates among them for future point-of-care (POC) devices and systems because of its unique integrated features: relatively high sensitivity at room temperature, dynamic volume detection, intrinsic superiority to measure ac magnetic field, functionality as an antenna for wireless information transmission, application driven properties such as low cost, portability and easy to use.

Due to the nonlinearity of magnetization curves of superparamagnetic nanoparticles, two alternating magnetic fields (one with high frequency  $f_1$  and the other with low frequency  $f_2$ ) that applied to MNP suspension will induce odd harmonics (the 3<sup>rd</sup> harmonic  $f_3=2f_1$ , the 5<sup>th</sup> harmonic  $f_5=4f_1, \dots$ ) in the detection coil. Relaxation time of MNPs will affect the phase and amplitude of harmonics we want to collect. For Brownian relaxation dominated MNPs, higher viscosity or binding with biomarkers will lead to longer relaxation time, thus larger phase lag and lower voltage will be collected.

We have successfully demonstrated the feasibility of using our search coil based magnetic sensor to test Human serum viscosity with an error rate of 0.3%<sup>2</sup>. Furthermore, MNPs can also be used for biomarker detection, and we reported real-time monitoring of binding kinetics of biomarkers<sup>1</sup>. Thus, it opens a new way for disease detection by simply using our search coil system and bio-functionalized MNPs. Furthermore, we theoretically investigated the feasibility of using the amplitude ratios of harmonic signals to estimate saturation magnetization of MNPs. Eight types of MNPs with average diameter of 30 nm and same concentration of 0.17 nmole/mL are compared. Finally, we theoretically and experimentally demonstrated that by utilizing the unique magnetic response cure of different types of MNPs, we are able to distinguish concentration of each type of MNPs in one homogeneous suspension<sup>3,4</sup>. Which indicates that it is possible to conduct the multiplex disease detection in our search coil system.

We have been developing a POC device capable of detecting a wide variety of diseases that will offer immediate results in a medical clinic or home with only a few drops of blood. This device that can be used anywhere will offer increased potential for disease control and improved human health.



Left: real-time monitoring of binding kinetics of biomarkers, with antibody injection at the 50th second<sup>1</sup>. Right: Schematic view of handheld device.

# RADIOMAG – A COST<sup>\*</sup> networking project in experimental cancer treatment research, combining magnetic fluid hyperthermia and radiotherapy.

Kai Wu<sup>a</sup>, Daniel Ortega<sup>2</sup>, Silvio Dutz<sup>3</sup>, Uwe Steinhoff<sup>4</sup>, Eva Natividad<sup>5</sup>, James Wells<sup>6</sup> & RADIOMAG-TEAM<sup>7</sup>

Simo Spassov<sup>1\*</sup>, Daniel Ortega<sup>2</sup>, Silvio Dutz<sup>3</sup>, Uwe Steinhoff<sup>4</sup>, Eva Natividad<sup>5</sup>, James Wells<sup>6</sup> & RADIOMAG-TEAM<sup>7</sup>

<sup>1</sup>Institut Royal Météorologique de Belgique, Dourbes, Belgium; <sup>2</sup>Madrid Institute for Advanced Studies in Nanoscience (IMDEA Nanociencia), Madrid, Spain; <sup>3</sup>Technische Universität Ilmenau, Ilmenau, Germany; <sup>4</sup>Physikalisch-Technische Bundesanstalt (PTB), Berlin, Germany; <sup>5</sup>ICMA (CSIC-Universidad de Zaragoza), Zaragoza, Spain; <sup>6</sup>National Physics Laboratory, Teddington, United Kingdom; <sup>7</sup>138 researchers from 24 countries (<http://www.cost-radiomag.eu>); \*e-mail: simo@meteo.be

Death rates attributed to cancer are the highest worldwide, even before cardiovascular diseases [1]. Therefore cancer research cannot wait, and new approaches are urgently required. RADIOMAG aims at teaming young and experienced scientists from different disciplines to enable current and to better coordinate new research concerning the efficiency of radiotherapy and its synergistic combination with magnetic fluid hyperthermia (MFH). The latter takes advantage of the heat generated by nanometre sized magnetic particles when subjected to alternating magnetic fields in order to kill or to damage cancer cells. Despite recent technological advances [2] and clinical trials, the MFH treatment is still far from becoming a standard practice.

The presentation will give an overview on the activities of this COST<sup>\*</sup> networking action and present first scientific results; demonstrating hereby the significance of EU support for better cooperation in science and technology and thus the optimisation of individual national research resources in order to put forward clear and well-grounded strategies for setting up a new anti-cancer therapy in future. Special emphasis will be given to a large double blind inter-laboratory ring test, during which twenty-one participants determined the specific absorption rate (SAR) and the intrinsic loss parameter (ILP) of two different ferrofluids. These first results show that a standardisation of the SAR/ILP determination is indispensable when testing the heat generation of newly developed ferrofluids for MFH application.

\* COST: European Cooperation in Science and Technology, ([www.cost.eu](http://www.cost.eu))  
**References**  
[1] Bernard, S.W. & C.P. Wild (eds.), WHO World Cancer Report, ISBN 978-92-832-0429-9, 2014.  
[2] Parizo, F., Emery, G., Sandre, O., Ortega, D., Garai, E., Plazaola, F. & F.J. Teran, Appl. Phys. Rev. 2, 041502, 2015.

1. L. Tu, Y. Jing, Y. Li and J.-P. Wang, Applied Physics Letters **98** (21), 213702 (2011).
2. K. Wu, J. Liu, Y. Wang, C. Ye, Y. Feng and J.-P. Wang, Applied Physics Letters **107** (5), 053701 (2015).
3. K. Wu, A. Barra, S. Iain, C. Ye, J. Liu and J.-P. Wang, Applied Physics Letters **107** (17), 173701 (2015).
4. L. Tu, K. Wu, T. Klein and J.-P. Wang, Journal of Physics D: Applied Physics **47** (15), 155001 (2014).

## Thermo-sensitive peptide coating onto iron oxide magnetic nanoparticles synthesized by the DEG-NMPDEA route: *in situ* dynamic light backscattering during magnetic hyperthermia

<sup>1</sup> Olivier Sandre<sup>1</sup>, Gaëtan Henrion<sup>1</sup>, Anthony Keyes<sup>1</sup>, Elisabeth Garanger<sup>1</sup>, Sébastien Lecommandoux<sup>1</sup>, Sarah MacEwan<sup>2</sup>, Ashutosh Chilkoti<sup>3</sup>, Yann Rodriguez<sup>3</sup>, Enrico Garai<sup>3</sup>, Juan-Man Collantes<sup>3</sup>, José Angel García<sup>3</sup>, Fernando Plaza<sup>3</sup>

<sup>1</sup> LCPO Univ., Bordeaux / CNRS / Bordeaux-INP, ENSCBP 16 Avenue Pey Berland, 33607 Pessac, France

<sup>2</sup> Department of Biomedical Engineering, Duke University, Campus Box 90281, Durham, North Carolina 27708, US

<sup>3</sup> Electritzaeta eta Elektronika Saita, Fisika Aplikatua II Saita, UPV/EHU, 644 48080 Bilbao, Spain

Magnetic hyperthermia (MH) is envisioned to become a well-recognized therapeutic method by oncologists to fight against incurable cancers such as glioblastoma [1]. On the other hand, several studies highlighted the possible high gap between the local temperature in the direct vicinity of nanoparticles (within nm) and the macroscopic bulk solvent temperature [2]. Cellular toxicity under a radiofrequency magnetic field was thus more likely ascribed to reactive oxygen species production, a phenomenon sometimes referred to as "cold" or "intravascular" hyperthermia [3]. In this presentation, we demonstrate that stationary gradients can indeed be maintained during several minutes at the vicinity of NPs and the bulk. The grafting of polymer chains at the surface of the NPs can aid in the comprehension of this phenomenon, by measuring a property of the NP suspension and comparing it to a calibration curve built up by macroscopic heating. Previous studies made such use of the nanoscale dimension of polymers with a thermo-degradable bond and a fluorescent probe to estimate the temperature reached locally in the near vicinity of the magnetic NPs under a radiofrequency magnetic field. Our approach consists in grafting onto iron oxide nanoparticles (NPs), a thermosensitive polymer brush, *i.e.* exhibiting a transition between swollen and dehydrated states. In a previous work we used synthetic commercial copolymers called Jeffamine™ to get thermosensitive contrast agents for magnetic resonance imaging (MRI) [4]. We combine this approach with a backscattered light intensity setup that enables following the hydrodynamic diameter variation of thermo-sensitive "magnetic" nanoparticles *in situ* while applying a radiofrequency AC magnetic field [5]; a fiber-based backscattering setup enabled positioning of the DLS remote-head (3) as close as possible to the coil (1) of a magnetic heating inductor to afford probing of the light backscattered by a sample placed in a thermalized water-jacket (2).

Magnetic iron oxide NPs were obtained following the forced hydrolysis pathway in polyol mixtures (DEG/DMDA) introduced by Canut et al [6, 7]. Reaction parameters (solvent, heating time, agitation,...) were varied leading to several sizes and morphologies: smooth spheres or "flower-like" multi-corones. The structure of the NPs was observed by transmission electron microscopy (TEM) and small angle neutron scattering (SANS). Their DC and AC magnetization curves, and their specific absorption rate (SAR) under alternating magnetic field were also reported at several radiofrequency and field strength values. Dynamic hysteresis curves were measured with the AC pick-up coil technique that enables much faster and precise SAR measurement than by calorimetry [8, 9]. In particular we found a threshold anisotropy field of the SAR vs. field strength curves in the 150–300 kHz range ascribed to collective dynamics of the cores as in a multidomain magnet, whereas they show individual superparamagnetic (quadratic) dependency in the higher frequency range 500–1000 kHz.

With the aim of applying this approach in cellular environments, we develop biocompatible and bio-nimicking coating matrix that exhibits thermosensitivity ( $\lambda$  being any amino acid but proline). We designed diblock ELP proteins with a hydrophobic block (sketched in dark blue) that undergoes deswelling transition at a critical temperature, and a hydrophilic block (light blue) driving steric repulsion. We showed previously that diblock ELPs form well defined micelles above their transition temperature, with a compaction of the core when temperature increases [10]. We report here their grafting onto iron oxide NPs resulting into core-shell NPs with high SAR, significant temperature-size response and good colloidal stability in biological buffers. Whereas the ELP brush thickness determined by *in situ* DLS under MH well correlates with fiber optic thermometry at long times (*i.e.* at thermal equilibrium), we were also able to detect a transient temperature drop in the range 10–50°C for several minutes between the surfaces of the NPs and the solvent, giving clues towards better understanding of MH by iron oxide NPs in intracellular compartments.

### References

- [1] E. Paricio, G. Henrion, O. Sandre, D. Ortega, E. Garaiola, F. Pazzolla, F. J. Teran, *Appl. Phys. Rev.* **2015**, 2, 041302
- [2] A. Riedinger, P. Giardia, A. Curcio, M. García, R. Cirigliani, I. Manza, T. Pellegrino, *Nano Lett.* **2013**, 13, 2399
- [3] V. Connord, P. Clerc, N. Haliati, D. El Hajji, D. Fourmy, V. Giguix, J. Carey, *Sensait* **2015**, 11, 2437
- [4] A. Hannequin, D. Stanic, L. Vander Elst, R. N. Muller, S. Lecommandoux, J. Thevenot, C. Boudelle, A. Trotter, P. Massot, S. Miroux, O. Sandre, S. Laurent, *Nanoscale* **2015**, 7, 3754
- [5] G. Henrion, E. Garanger, S. Lecommandoux, A. Wong, E. R. Gillies, B. Padron, T. Bayle, D. Jacob, O. Sandre, *J. Phys. D: Appl. Phys.* **2015**, 48, 494001
- [6] D. Caruntu, G. Caruntu, Y. Chen, C. J. O'Connor, G. Golovenda, V. L. Kolesnichenko, *Chem. Mater.* **2004**, 19, 1821
- [7] P. Huguenard, M. Levy, D. Allouey, L. Larigue, E. Pazzolla, V. Cabut, C. Ricoleau, S. Roux, C. Wilhelm, F. Gazeau, R. Bazzi, *J. Phys. Chem. C* **2012**, 116, 15702–15712
- [8] E. Garaiola, J.-M. Collantes, J.A. Garcia, F. Pazzolla, S. Moneti, F. Couillaud, C. Sandre, *J. Mag. Mag. Mat.* **2014**, 368, 432
- [9] E. Garaiola, O. Sandre, J.-M. Collantes, J.A. Garcia, S. Moneti, F. Pazzolla, *Nanotechnology* **2015**, 26, 015704
- [10] E. Garanger, S. R. MacEwan, O. Sandre, A. Chilkoti, S. Lecommandoux, *Macromol.* **2015**, 48, 6617

## Magnetic loss and constant magnetic rotation of magnetic nanoparticles in viscosity dependence evaluated by dynamic hysteresis measurement

Ryoji Takeda<sup>1</sup>, Ryochi Kitaguchi<sup>1</sup>, Satoshi Ota<sup>2</sup>, Tsutomu Yamada<sup>1</sup> and Yasushi Takemura<sup>1\*</sup>

<sup>1</sup> Department of Electrical and Computer Engineering, Yokohama National University, Yokohama, Japan

<sup>2</sup> Department of Electrical and Electronic Engineering, Shizuoka University, Hamamatsu, Japan

\*E-Mail: takemura@ynu.ac.jp

Theoretical description regarding Brownian process of magnetic nanoparticles (MNPs) indicates that the Brownian relaxation time depends on viscosity of a fluid. Here we report that specific loss power (SLP) depends on viscosity, but that the maximum degree of particle rotation is constant at the frequency of the local peaks of intrinsic loss power (ILP) corresponding to Brownian relaxation time as well as at the static excitation. It is found that the origin of viscosity dependence of SLP is change in phase delay of particle rotation. This result is significant for applications of hyperthermia as well as magnetic particle imaging.

A water based Fe<sub>3</sub>O<sub>4</sub> nanoparticle fluid was used in this study. Its primary and hydrodynamic diameters were 1.1±3 mm and 52±12 nm, respectively. The viscosity of sample was adjusted to 2.4, 4.7, 12 and 93 mPa·s by changing the weight ratio of MNPs, pure water, and glycerol. The concentration of these samples was constant at 90 mg·Fe/ml. ILP, which is defined as  $SLP/Hf^2$ , was quantified by area of dynamic hysteresis loop measured [1] for a wide frequency range from 10 Hz to 500 kHz.  $Hf$ : field intensity,  $f$ : frequency.

Figure 1 shows dynamic hysteresis loops of the samples at 10 kHz. With increasing the viscosity, both of magnetization and coercivity were reduced. It is owing to decrease in particle rotation at this fixed frequency. Figure 2 (a) shows dependency of ILP on frequency. The peak frequency due to Brownian relaxation was decreased with increasing viscosity. A larger ILP was obtained with lower viscosity samples, because coercivity due to delay of particle rotation was larger. Hysteresis loops at the peak frequency of each viscosity was shown in fig. 2 (b). It is notable that magnetization under  $H = 4$  kA/m was constant. It indicates that the degree of particle rotation was constant, and that the viscosity dependence of ILP was attributed to the viscosity dependence of ILP. We attribute to difference in phase delay of particle rotation. Thus, a particle in low viscosity is rotatable in similar degree with that in high viscosity despite large phase delay than that in high viscosity due to the shorter relaxation time in low viscosity. The Brownian relaxation time derived from peak frequency of Fig. 2 (a) is not proportional to viscosity, which does not agree with theory. The relaxation times for Brownian and Néel processes and further analysis are discussed in the presentation.

[1] Ota et al., *JAP* **117**, 170713 (2015).  
Acknowledgement: This work was partially supported by JSPS grant 15H05764 and 26289124.

Fig. 1 Hysteresis loops of Fe<sub>3</sub>O<sub>4</sub> nanoparticles with various viscosity at 10 kHz.

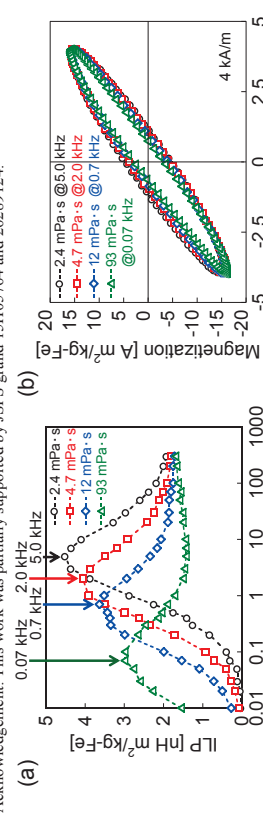


Fig. 2 (a) Frequency dependence of intrinsic loss power and (b) hysteresis loops at the peak frequency.

## Effect of Applied AC Magnetic Field on Response of Magnetic Nanoparticles

C.L. Dennis<sup>1</sup>, C. Glinka<sup>1</sup>, J.A. Borchers<sup>1</sup>, C. Grütter<sup>2</sup>, and R. Ivkov<sup>3</sup>

<sup>1</sup>National Institute of Standards and Technology, Gaithersburg, MD, USA

<sup>2</sup>Micromod Partikeltechnologie, GmbH, 18119 Rostock-Warnemünde, Germany

<sup>3</sup>Department of Radiation Oncology and Molecular Radiation Sciences, The Johns Hopkins University School of Medicine, Baltimore, MD, USA

Many applications have been developed for magnetic nanoparticles (MNPs) in recent decades, ranging from biomedical applications to electronics and data storage. However, most of these applications use AC magnetic fields, ranging from a few Hz (e.g. cell stimulation) to 100's of kHz (e.g. hyperthermia). Unfortunately, most of the magnetic characterization of MNPs has been done under DC magnetic fields. As the magnetic response of all magnetic materials is known to depend upon the timescale of the measurement, the DC magnetic response has only limited applicability to understanding the magnetic behavior under AC magnetic fields. Here, we begin examining the AC magnetic response of iron oxide MNPs suspended in water as a function of frequency, and correlate this with both the known DC and AC susceptibility measurements. Specifically, we directly measure the magnetic response using Time-Independent Small Angle Neutron Experiment (TISANE). Neutron scattering from a magnetic material has characteristic angular response. We can use the amplitude of this characteristic response as a function of the frequency and amplitude of the applied sinusoidal AC magnetic field to determine the magnetic behavior of the MNPs. In particular, we find that at low frequencies (10 Hz), the magnetization is able to track the AC magnetic field. However, at higher frequencies (1 kHz), the amplitude of the AC magnetic field is critical. At low fields (1 mT), the magnetization does not track the AC field at all, but remains fixed. At higher fields (10 mT), the magnetic anisotropy of the MNPs is overcome, and the magnetization tracks the AC magnetic field. This has significant implications for all applications, including imaging and magnetic nanoparticle hyperthermia.

## Nano-objects to control magnetic hyperthermia performance

Irene Andreu<sup>1,2</sup>, Eva Natividad<sup>1</sup>, Laura Solozábal<sup>1,3</sup>, Olivier Roubeau<sup>1</sup>

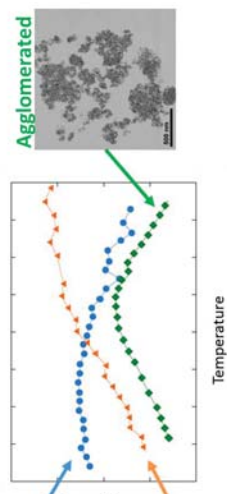
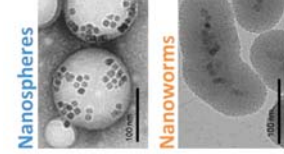
<sup>1</sup>Instituto de Ciencia de Materiales de Aragón (ICMA), CSIC-Universidad de Zaragoza, Campus Rio Ebro, María de Luna 3, 50018 Zaragoza, Spain; <sup>2</sup> Present address for I.A.: Department of Chemistry and 4D LABS, Simon Fraser University, 8888 University Dr., Burnaby, BC V5A 1S6, Canada and Department of Advanced Therapeutics, British Columbia Cancer Research Centre, 675 West 10th Avenue, Vancouver, BC V5Z 1L3, Canada;

<sup>3</sup>landreb@sfu.ca, <sup>3</sup>Present address for L.S.: Audi AG, Auto-Union-Strasse, 85057 Ingolstadt, Germany;

Magnetic hyperthermia is a cancer therapy that uses magnetic nanoparticles (MNPs) to increase the temperature of tumors under alternating magnetic fields. One current challenge is achieving therapeutic effects with a minimal amount of MNPs, for which high heating abilities are pursued. It has been shown that the same MNPs can generate significantly different amounts of heat, for example, when dispersed in different media [1] or after cell internalization [2], due to the different spatial arrangement of the MNPs, indicating that magnetic interactions must be taken into account when designing magnetic hyperthermia treatments.

In this work, we first show that the heating ability of the MNPs under study, initially measured when dispersed in a fluid, was reduced over 80% upon MNP agglomeration; a similar agglomeration occurs when MNPs are internalized by cells. The MNPs were then embedded in a polymer or silica matrix, forming injectable magnetic nano-objects with distinct fix arrangements. [3] The heating ability of closely-packed nano-objects remained high, contrarily to closely-packed MNPs, freely arranged after agglomeration. Their different magnetic response can be explained by the morphology of the obtained arrangements. Similar nano-objects are then proposed to provide high and reproducible heating powers for reliable magnetic hyperthermia treatments, thanks to their controlled magnetic interactions.

References: [1] I. Andreu et al. (2015) *J Magn Magn Mater* (380) 341-346; [2] Di Corato et al. (2014) *Biomaterials* (35) 6400-6411; [3] I. Andreu et al. (2015) *ACS Nano* (9) 2, 1408-1419



Centre: Heating ability as a function of temperature of the nano-objects. The side panels show Transmission Electron Microscopy of the nano-objects with distinct arrangements.

## How much does shape matter?

Cristina Blanco-Andujar, Geoffrey Cotin, Catalina Bordeianu, Florent Meyer, Delphine Felder-Flesch, Sylvie Bégin-Colin\*

Institut de Physique et de Chimie des Matériaux de Strasbourg (IPCMS, UMR CNRS-UoS 7504, 23 rue du Loess, BP 43, 67034 STRASBOURG cedex 2, France  
\*Corresponding author: sylvie.begin@ipcms.unistra.fr, Tel.: (33) 3 88 10 71 92

The use of magnetic hyperthermia (MH) as a stand-alone or an adjacent therapy for cancer is closer to be a reality in every hospital thanks to the positive results achieved by the clinical trials carried out by *Magforce™* (Germany) treating glioblastoma.<sup>1, 2</sup> Nonetheless, the need for direct intratumoral injection of large amounts of nanoparticles (NPs) to achieve a therapeutic effect only points out at the need of improving the available nanomaterials for MH.

Different parameters may be varied to increase the effective heat loss of a ferrofluid such as size, shape, anisotropy or composition, among others. Shape and aspect ratio may offer interesting possibilities as chain formation has been previously reported to increase heat loss.<sup>3</sup> However, this effect varies depending on media composition, which may affect heat loss in a cellular environment.

On that basis, plate-like, spherical and octopod shape NPs were prepared by thermal decomposition of iron stearate and functionalised with dendron ligands to achieve aqueous suspensions, which have been proven to be suitable for *in vivo* injection (Figure 1).<sup>4</sup> MH performance was found to be shape-dependent with octopod-shaped NPs exhibiting the highest SAR values of  $260 \text{ W g}^{-1}$ ,  $f = 579 \text{ kHz}$ ,  $8 \text{ kAm}^{-1}$ ,  $\text{ILP} = 7.1 \text{ nHm}^2 \text{ kg}^{-1}$  or  $960 \text{ W g}^{-1}$ ,  $f = 796 \text{ kHz}$ ,  $16 \text{ kAm}^{-1}$ ,  $\text{ILP} = 4.8 \text{ nHm}^2 \text{ kg}^{-1}$ . At the same time, their performance in MRI was investigated leading to relaxivity values of  $16.9$  and  $405.5 \text{ mM}^{-1} \text{ s}^{-1}$  for  $r_1$  and  $r_2$ , respectively, which was superior to that of commercial products like Resovist®. Finally, cell response was studied as a function of NP concentration and morphology, as well as under MH treatment.

The obtained results open the possibility of using this system as a theranostic platform thanks to the exhibited performance in MH and MRI at a cellular level. More importantly, this may enable tracking NPs prior/during MH treatment to assure particle accumulation in the target area.

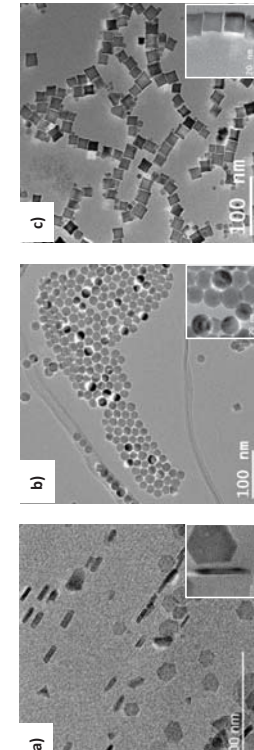


Figure 1. TEM images of a) plate-like, b) spherical and c) octopod shaped nanoparticles.

1. Maier-Hauff, K., et al. *Journal of Neuro-Oncology* 2007, 81, (1), 53-60.
2. Maier-Hauff, K., et al. *Journal of Neuro-Oncology* 2011, 103, (2), 317-324.
3. Martinez-Boubeta, C., et al. *Scientific Reports* 2013, 3.
4. Walter, A., et al. *Journal of Materials Chemistry B* 2015, 3, (8), 1484-1494.

## Magnetically stimulated phase transformation of FeO/Fe<sub>3</sub>O<sub>4</sub> nanocubes to single Fe<sub>3</sub>O<sub>4</sub> phase: an alternative approach to prepare tumor hyperthermia agents

Aidin Lak<sup>1</sup>, Dina Niculaes<sup>1</sup>, Giovanni Bertoni<sup>2</sup>, Markus J. Barthel<sup>1</sup>, George C. Anyfantis<sup>1</sup>, Simone Nitti<sup>1</sup>, Sergio Marras<sup>1</sup>, Athanassia Athanassiou<sup>1</sup>, Cinzia Giannini<sup>3</sup> and Teresa Pellegrino<sup>1</sup>

<sup>1</sup>Istituto Italiano di Tecnologia, Via Morego 30, 16163 Genova, Italy, <sup>2</sup> MEM-CNR, Parco Area delle Scienze 37/A, 43124 Parma, Italy, <sup>3</sup> Institute of Crystallography, National Research Council, via Amendola 122/O, Bari 70126 Italy, Email: teresa.pellegrino@iit.it and aidin.lak@iit.it

Structural and magnetic properties of nanoparticles strongly depend on the synthetic routes chosen for their preparation. The colloidal syntheses by non-hydrolytic methods have revealed several merits over conventional wet chemical hydrolytic processes mainly regarding controlled size distribution and good crystallinity. However, the non-hydrolytic methods result in hydrophobic particles merely soluble in organic solvents, yet the challenge is the concomitant water transfer and preservation of particle size and colloidal stability. The particle-particle interaction can compromise the success of the transfer process to a large extent particularly for particles having high magnetization. Indeed, to ultimately use magnetic nanoparticles in clinic as heat mediators or drug carriers for chemotherapeutic agents, it is vital to achieve their stability in physiological media and at the same time optimize their intrinsic magnetic features.

In this study, we demonstrate the novel use of magnetic hyperthermia (MH) set up to magnetically oxidize FeO/Fe<sub>3</sub>O<sub>4</sub> core-shell nanocubes to single Fe<sub>3</sub>O<sub>4</sub> phase. The core-shell nanocubes were first synthesized via decomposition of iron pentacarbonyl Fe(CO)<sub>5</sub>, resulting in non-interacting particles with moderate magnetization. They were readily transferred in water by PEG coating and then further exposed to MH treatment. We have found that after handful of MH treatments, the specific absorption rate (SAR) increases nearly three times while colloidal stability, size distribution and shape remain unaffected. The magnetically stimulated nanocubes showed a significantly higher saturation magnetization  $M_s$  than the initial core-shell ones, reflecting structural and compositional changes as confirmed by X-ray diffraction and HRTEM/STEM studies. Interestingly, on biotin-tagged nanocubes, the affinity of the biotin at the particle surface towards streptavidin ligands was preserved even after magnetic oxidation treatment. The here proposed method enables a mild transformation of nanocubes, resulting in more efficient heat mediators while concomitantly preserving their colloidal stability and molecular targeting. These are all crucial features for preparing optimal heat mediators for *in-vivo* hyperthermia.

REAL-TIME TRACKING OF DELAYED-ONSET CELLULAR APOPTOSIS INDUCED BY INTRACELLULAR MAGNETIC HYPERTERMIA

*Cristina Blanco-Andujar<sup>a,b\*</sup>, Daniel Ortega<sup>a,c\*</sup>, Paul Southern<sup>a\*</sup>, Stephen A. Nesbitt<sup>a</sup>, Nguyen Thi Kim Thanh<sup>a,c</sup> and Quentin A. Pankhurst<sup>a,c</sup>*

<sup>a</sup>Healthcare Biomagnetics Laboratory, UCL, 21 Albemarle Street, London, W1S 4BS, UK. <sup>b</sup>Institut de Physique et Chimie des Matériaux de Strasbourg (IPCMS) UMR-7504 CNRS-Université de Strasbourg, 23 rue du Loess, BP 34 67034 Strasbourg Cedex 2, France. <sup>c</sup>Instituto Madrileño de Estudios Avanzados en Nanociencia (IMDEA-Nanociencia), Cantoblanco 28049, Madrid, Spain. <sup>d</sup>Nanobiotecnología (IMDEA-Nanociencia), Unidad Asociada al Centro Nacional de Biotecnología (CSIC), Cantoblanco 28049, Madrid, Spain. <sup>e</sup>Biophysics Group, Department of Physics and Astronomy, University College London, Gower Street, London, WC1E 6BT, UK.

<sup>\*</sup>Email: [nth.thanh@ucl.ac.uk](mailto:nth.thanh@ucl.ac.uk) and [q.pankhurst@ucl.ac.uk](mailto:q.pankhurst@ucl.ac.uk); <http://www.nth-thanh.co.uk>

**Aim:** To assess cell death pathways in response to magnetic hyperthermia. **Materials & methods:** Human melanoma cells were loaded with citric-acid-coated iron-oxide nanoparticles, and subjected to a time-varying magnetic field. Pathways were monitored *in vitro* in suspensions and *in situ* in monolayers using fluorophores to report on early-stage apoptosis and late-stage apoptosis and/or necrosis. **Results:** Delayed-onset effects were observed, with a rate and extent proportional to the thermal-load-per-cell. At moderate loads, membranal internal-to-external lipid exchange preceded rupture and death by a few hours (the timeline varying cell-to-cell), without any measurable change in the local environment temperature. **Conclusion:** Our observations support the proposition that intracellular heating may be a viable, controllable, and non-aggressive *in vivo* treatment for human pathological conditions.

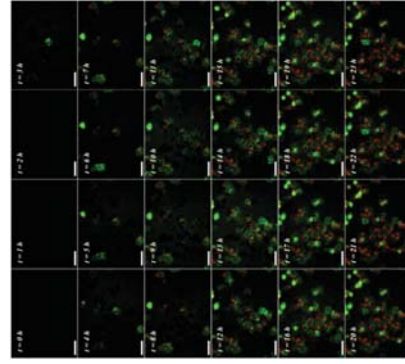


**Figure 1: Cell-by-cell real-time tracking of cell death pathways – fluorescence imaging.**  
Fluorescence microscopy images of CA-IONP-loaded DX3 cells during and after two hours of MFH treatment (from  $t = 0$  to 2 h) with a magnetic field delivering ca. 145 nW/cell of thermal energy. Cells were labelled with Annexin V-FITC (green) and DRAQ7 (far-red), and images were recorded hourly. Scale bar is 50  $\mu$ m in all images.

**Ref:** C. Blanco-Andujar, P. Southern, D. Ortega, S.A. Nesbitt, Q.A., Pankhurst and Thanh, N. T. K\*. (2016) Real-time tracking of delayed-onset cellular apoptosis induced by intracellular magnetic hyperthermia. *Nanomedicine*. **11:** 121-136.

## Improving Nanoparticle Heating by prior Orientation of Particles in a static three T magnetic Field

M.M. Beck<sup>1,\*</sup>, C. Lammel<sup>1</sup>, B. Gleich<sup>2</sup>

<sup>1</sup> Institute for Machine Tools and Industrial Management, Technical University of Munich, Boltzmannstr.15, 85748 Garching, Germany. <sup>2</sup> Institute of Medical Engineering, Technical University of Munich, Boltzmanstr. 11, 85748 Garching, Germany. \* Email: Mathias.Bech@tum.de

When nanoparticles are dispersed in a medium they are distributed and oriented randomly. If this medium is solid, heating by an alternating electromagnetic field cannot exploit the whole potential of these particles as the amount of energy transmission by Néel relaxation depends on the orientation of a particle within the applied field.

In an epoxy resin, magnetite nanoparticles ( $\text{Fe}_3\text{O}_4$ ) were dispersed (5 mass-% particles) which resulted in a size peak after dispersion of 33 nm in DLS (dynamic light scattering). The probe was then put in a homogeneous static magnetic field of a magnetic resonance imaging system (three Tesla MRI, GE 750MW). In the field, the resin solidified within 24 hours while a reference sample was cured outside the magnetic field. After immobilization of the particles, the sample was heated in an alternating electromagnetic field of 100 kHz with field strengths up to  $11.7 \text{ kA m}^{-1}$ . The probe was heated several times in different rotational angles to the magnetic field. The achieved heat input depended on the direction of the former static field to the applied alternating field.

The SAR (specific absorption rate) increased in average by a factor of 3.3, compared to the non directed reference, when the sample was oriented in the direction of the former applied static field (see Figure 1). Heating perpendicular to the curing field did only slightly affect the heating. This result shows that magnetite nanoparticles can be oriented in a static field and this orientation can be frozen in a cured matrix material. It indicates that the orientation of nanoparticles in one direction can increase the SAR and therefore lead to a faster heating process.

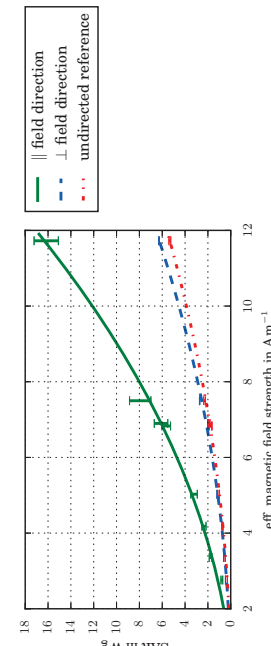


**Figure 1: The heating of 5 mass-% dispersed magnetite in cured epoxy resin depending on the orientation of the applied alternating electromagnetic field (100kHz) to the static field during solidification.**

# Remote Monitoring of Magnetic Particle Temperature During Hyperthermia: the Ideal Dose-Response Metric?

F.-Y. Lin<sup>1</sup>, P. Southern<sup>1,2</sup>, S. Hattersley<sup>2</sup>, Q. A. Pankhurst<sup>1</sup>

<sup>1</sup> UCL Healthcare Biomagnetics Laboratory, 21 Albemarle Street, London W1S 4BS, United Kingdom  
<sup>2</sup> Resonant Circuits Limited, 21 Albemarle Street, London W1S 4BS, United Kingdom  
 E-mail: fang-yu.lin.14@ucl.ac.uk

Magnetic hyperthermia has been proposed as a new modality for cancer chemotherapy. After injecting magnetic nanoparticles (MNPs) into a tumour, an alternative magnetic field (AMF) is applied which generates heat in the MNPs, and elevates the temperature of the tumour. Once this temperature reaches ca. 42 °C, the cancer cells become preferentially inhibited compared to healthy cells. Due to this selectivity and the inherent advantage of minimal invasiveness, magnetic hyperthermia has gathered great attention over the past decade. However, limitations exist. One major limitation is the difficulty of sensing the temperature in and around the tumour. The current gold standard is to directly insert a thermometer into the tumour, which is both invasive and necessarily a spot measurement only.

In this study we describe a new, non-invasive method to remotely monitor the global (i.e. averaged over the entire active volume) intra-tumoural temperature. The method is based on the resonant effect of an LC (inductance-capacitor) oscillator circuit, such as those used in some AMF generators (e.g. the MACH system made by Resonant Circuits Limited, London). In such a system, the resonant frequency  $= 1/2\pi\sqrt{LC}$ , where the inductive load  $L$  is sensitive in part to the magnetic induction of the injected MNPs. (In comparison, the capacitance  $C$  of the system is virtually unchanged by the MNPs.) Furthermore, the contribution to  $L$  of the MNPs is proportional to the magnetic susceptibility  $\chi$  of the MNPs, with  $L = L_0(1 + \alpha\chi)$ , where  $L_0$  is the inductance without any MNPs present, and  $\alpha$  is a volumetric factor corresponding broadly to the ratio of the volume of the injected material to the volume of the AMF-receiving region (albeit with appropriate corrections for the spatial variation of field strength within that region).

In practice, this means that when MNPs are injected into a patient, it is possible to measure an increase in the inductance  $L$  via a decrease in the oscillator resonant frequency  $f$  – as illustrated in Fig. 1 for a MNP sample comprising iron oxide nanoparticles particles. Its Fe concentration is 70 mgFe/mL, and the DLS Z-average and PDI are 127 nm and 0.209, respectively. Even more interesting, since the magnetic susceptibility of the MNPs is temperature dependent, it is possible to track the temperature rise at the target by monitoring the resonant frequency of the oscillator. This is also illustrated in Fig. 1.

In clinical applications of magnetic hyperthermia, a critical metric from the clinician's perspective is the 'dose-response' characteristic, which essentially asks: how much dose should be delivered to elicit a desired response? We propose that the method outlined here may be ideal way to provide this metric to users, as there is clearly a very strong correlation between the resonant frequency of the AMF generator – which is an easily measured quantity – and the temperature of the MNPs, and it is certainly translatable to a clinical setting.

## Lock-in thermography: Using heat as an indicator for stability and distribution of magnetic nanoparticles in biological systems

Christophe A. Monnier,<sup>1</sup> Thomas L. Moore,<sup>1</sup> David Burnand,<sup>2</sup> Laura Rodriguez-Lorenzo,<sup>1</sup> Curzio Rüegg,<sup>3</sup> Grégoire Bieler,<sup>3</sup> Barbara Rothen-Rutishauser,<sup>4</sup> Matthias Bonmarin<sup>4</sup> & Alke Petri-Fink<sup>1,2</sup>

<sup>1</sup> Adolphe Merkle Institute, University of Fribourg, Switzerland; <sup>2</sup> Chemistry Department, University of Fribourg, Switzerland; <sup>3</sup> Institute of Computational Physics, Zurich University of Applied Sciences, Switzerland  
<sup>4</sup> Department, University of Fribourg, Switzerland

Superparamagnetic iron oxide nanoparticles (SPIONs) and their ability to generate heat in an alternating magnetic field (AMF) are of great applicative value for treating complex diseases (*i.e., via hyperthermia*) or controlling drug release. Nonetheless, fulfilling these tasks requires that the SPIONs retain their heating capabilities in multicomponent biological environments. Assessing this parameter, both prior and after administration, is thus critical to promote the usage of these materials in the clinic and to further optimize them.

While current imaging or quantification modalities are capable of addressing these topics, most of them are invasive, destructive or limited in the amount of information they provide. To address these setbacks, we rely on a methodology based on lock-in thermography (LIT) to monitor the SPIONs and their respective thermophysical behavior in increasingly complex environments (*i.e., liquid, semi-solid and solid*). This is done by using the heat generated by the SPIONs as a tag, which in turn acts as an indicator to their state of dispersion, spatial location and concentration.

The proof of concept is given by using SPIONs with narrow size distributions and specific coating molecules (*i.e., PEG-catechol or citric acid*). Investigations are undertaken in different settings, starting from basic water dispersions up to local injections in mouse tissues. In all these situations, we can evaluate with LIT whether, how and when the heating capabilities are affected, and thus whether the SPIONs are still suitable for treatment.

In turn, this approach provides complementary abilities to evaluate overall SPION concentrations, their location and physical condition within a respective tissue. Moreover, it offers an insight into whether the thermal capabilities are retained *in situ*, thus offering the clinician the possibility to adapt AMF exposure times or concentrations after administration.

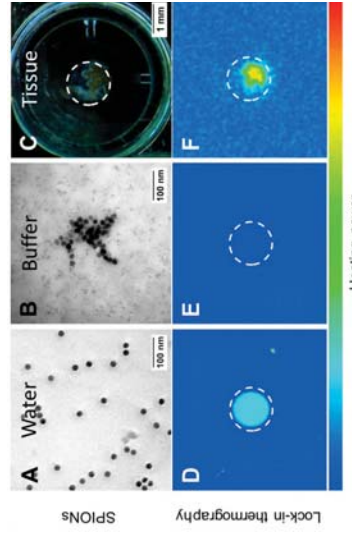


Figure 1: The thermal properties of SPIONs are guided by their surrounding environment. The state of dispersion of SPIONs may vary considerably in water (A), buffer (B) or tissues (C), depending on their surface functionalization or synthetic background. Using lock-in thermography (D-F) provides the necessary framework to investigate this parameter more in detail.

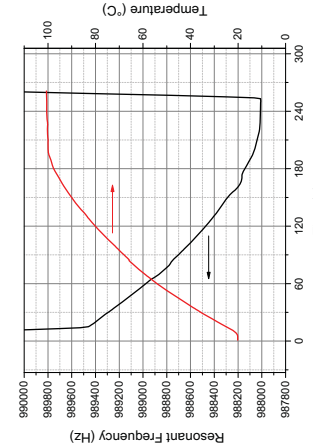


Fig 1: The correlation between resonant frequency of the LC oscillator and temperature of the MNPs.

## Magnetic nanoplatform incorporating a molecular thermometer. A new tool for local hyperthermia

Angel Millán,<sup>a</sup> Rafael Piñol,<sup>a</sup> Carlos D. S. Brites,<sup>b</sup> Rodney Bustamante,<sup>a</sup> Abelardo Martínez,<sup>c</sup> Nuno J. O. Silva,<sup>b</sup> José L. Muñoz,<sup>a</sup> Raquel Casas,<sup>a</sup> Julian Carey,<sup>d</sup> Carlos Esteve,<sup>a</sup> Cecilia Sosa,<sup>e</sup> Gustavo Lou,<sup>a</sup> Diego De Miguel Samaniego,<sup>f</sup> Lilianna Beola,<sup>g</sup> Amalia Ruiz,<sup>g</sup> Jesús M. de la Fuente,<sup>a</sup> Luis Martínez-Lostao,<sup>f</sup> Fernando Palacio,<sup>f</sup> Bellinda Sanchez,<sup>h</sup> Luis D. Carlos,<sup>i</sup>

<sup>a</sup> ICMA, CSIC–Universidad de Zaragoza, 50009 Zaragoza (Spain).

<sup>b</sup> Departamento de Física and CICECCO, Universidade de Aveiro, 3810-193 Aveiro (Portugal)

<sup>c</sup> Departamento de Electrónica de Potencia, 13A, Universidad de Zaragoza 50018 Zaragoza (Spain)

<sup>d</sup> Université de Toulouse, UPS, CNRS (UMR 5215), F-31077, Toulouse (France)

<sup>e</sup> Departamento de Toxicología, Universidad de Zaragoza, 50013 Zaragoza (Spain)

<sup>f</sup> Departamento de Bioquímica, Biología Molecular y Celular, Universidad de Zaragoza, Zaragoza, España

<sup>g</sup> Centro de Estudios Avanzados de Cuba, La Habana, Cuba

<sup>h</sup> Centro de Inmunología Molecular amillan@unizar.es

Magnetic hyperthermia has already been approved for therapy of cancer and other diseases. The treatment involves a direct injection of nanoparticles into the tumor and the application of an alternating magnetic field until the temperature at the borders of the tumor is reaching 43 °C. As the heating power of magnetic nanoparticles is moderate, the amount of nanoparticles to be injected for this purpose is very high and that means a long process until the nanoparticles are cleared from the body. On the other hand, experiments indicate that cell death can be produced without an increase of the cell temperature. This is suggesting that the development of local intracellular hyperthermia involving a smaller number of particles would be very possible. In order to make this strategy effective an adequate monitoring of the nanoheaters' local temperature will be required. In order to investigate this point we have developed a magnetic nanoplatform that incorporates a luminescent molecular thermometer. The thermometer is based on the luminescence emission of two lanthanide complexes with organic ligands that are located on the surface of the magnetic nucleus and in the interior of the hydrophobic part of an amphiphilic copolymer. One of the lanthanides emits with a constant intensity while the intensity of emission  $\lambda$  the other decreases with the temperature, thus the ratio of emission intensities gives the absolute temperature on the surface of the nanoparticle heater. The thermometer shows a fine sensitivity (5.8% K<sup>-1</sup> at 296 K), low uncertainty (0.5 K), high reproducibility (>99.5%), and fast time response (0.250 s). Time-resolved temperature measurements of the magnetic nucleus under an AC magnetic field reveal the existence of an important temperature gradient between nanoheaters and surrounding media. The existence of this gradient at intracellular level could be used to induce irreversible intracellular damage in tumor cells leading to cell death without having to increase the temperature of the whole tumor mass. A proof of concept of temperature mapping has been realized on cells that were incubated with the nanoparticles (Fig 1).

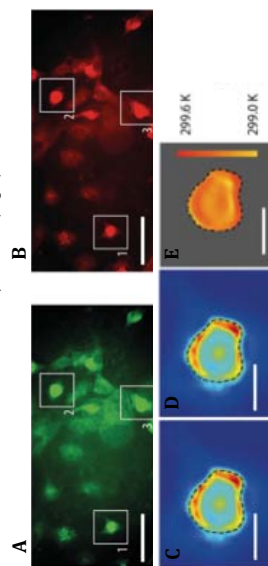


Figure 1. Imaging of Tb<sup>3+</sup> (A) and Eu<sup>3+</sup> (B) emissions from cell-internalized nanoparticles. Scale bars are 40  $\mu$ m. Pseudocolour maps of spot 1 in Fig A&B illustrating the co-localization of the Tb<sup>3+</sup> (C) and Eu<sup>3+</sup> (D) emissions. Temperature map (E) computed from this emissions at every pixel, and (F) histogram of the temperature distribution near the cell nucleus. Scale bars correspond to 10  $\mu$ m.

## INVITED TALK 6

### Superparamagnetic Iron Oxides, from the Lab to Approval

Jerome M. Lewis

Jlewis273@gmail.com

A few parenteral magnetic nanoparticles drugs have been successfully approved throughout the world or are currently in clinical trials. Examples include small molecules and biologics being attached to nanoparticles, as well as the nanoparticles being entrapped in liposomes. In general, the requirements for the approval of nanoparticles drugs are similar to other drugs, albeit with some minor distinctions in the exact requirements for each.

While the requirements for nanoparticles drug approvals are comparable to other drugs, nanoparticles present certain unique challenges and advantages during the drug approval process.

Careful planning for the nanoparticle drug's Chemistry, Manufacturing and Controls (CMC), Preclinical Trials, and Clinical Trials is necessary in order to successfully navigate the Drug Approval Process. For example, in Clinical Trial design there is the issue of what placebo to use in a Double Blind Placebo Controlled Trial, since nanoparticle drugs are black and no parental black placebos exist.

Absorption, Distribution, Metabolism, Excretion (ADME) preclinical animal trials demonstrate some advantages and disadvantages of nanoparticles. On one hand, the magnetic properties of the nanoparticle can be used to determine both concentration and distribution of the intact nanoparticles without radioactive labelling, but these properties will change as the drug is metabolized, and may require unusual study designs. However, the long tissue half-life of nanoparticles may require longer and more expensive animal studies.

CMC issues include, but are not limited to, size determination, sterility (both achieving and testing), heavy metals, stability indicating assays, color, particulates, visual inspection, stability, etc. CMC regulator reviewers are often organic chemists or biochemists with limited or no experience with magnetic nanoparticles, which requires the submitter to carefully address and explain magnetic nanoparticles' unique properties.

Invited Talk # 6

## Toward Magnetic Particle Imaging-Guided Hyperthermia (hMPI): Analysis of High-Performance Agents for MPI and Focused Hyperthermia

L.M. Bauer<sup>1,\*</sup>, S.F. Stu<sup>2</sup>, M.A. Griswold<sup>1,3</sup>, A.C.S. Samii<sup>2</sup>

<sup>1</sup>Department of Physics, Case Western Reserve University; Cleveland, OH USA

<sup>2</sup>Department of Chemistry, Case Western Reserve University; Cleveland, OH USA

<sup>3</sup>Department of Radiology, Case Western Reserve University and University Hospitals of Cleveland; Cleveland, OH USA

\*Email: lisabauer@case.edu

Tracer development is key to the growth of Magnetic Particle Imaging (MPI). Recent tracer development efforts have converged in the form of a spherical magnetic core with a diameter of 20-25nm. However, it is interesting to note that the tracers used in MPI are similar to those developed for therapeutic applications such as hyperthermia. There is a large body of work evaluating the effects of shape anisotropy and metal doping on hyperthermia efficiency, but no such studies exist for evaluating their effect on the MPI signal. In this work, we present the first systematic study of the effects of shape anisotropy and metal doping on the MPI signal, by analyzing the MPI performance of undoped magnetic spheres and cubes (SphCube) and zinc-doped magnetic spheres and cubes (Zn-SphCube). Further, we suggest that these agents may be useful for Magnetic Particle Imaging-guided hyperthermia.

To analyze the MPI performance of all tracers, we used magnetic particle relaxometry, which measures the one-dimensional point-spread function (PSF) of a tracer. Relaxometry is a powerful tool for predicting MPI image resolution and SNR, as the MPI image is essentially a convolution of the PSF with the spatial distribution of tracers. Relaxometry experiments were carried out using Case Western Reserve University's custom x-space magnetic particle relaxometer, with operating frequency  $f_{\text{ex}}=16.8\text{kHz}$  and excitation field strength  $B_{\text{ext}}=20\text{mT}$ . Hyperthermia performance was evaluated using a machine from MSI Automation ( $\text{f}_{\text{hyp}}=380\text{kHz}$ ,  $H=16\text{kA/m}$ ,  $t=3\text{s}$ ). To demonstrate focused heating, hyperthermia experiments were carried out with and without the presence of an external magnetic field gradient ( $G=0.4\text{T}/\text{m}$ ), using samples containing zinc-doped cubic nanoparticles.

The results from these experiments suggest that zinc-doping enhances MPI performance, as seen in Figure 1a, in the 2-fold increase in PSF peak of zinc-doped particles compared to their undoped magnetite counterparts. Further, though the zinc-doped cubes have a suboptimal SNR and asymmetric PSF (Figure 1a), they outperform a commercially available sample in relaxometry experiments and have outstanding hyperthermia performance (not shown). The ability to focus hyperthermia (Figure 1b,c) using magnetic gradients similar to those used for MPI suggests that it may be possible to achieve MPI-guided hyperthermia using these agents. While there is unlikely to be a single agent optimized for both purposes, it is likely that there is a middle ground that enables high quality imaging with efficient, focused heating.

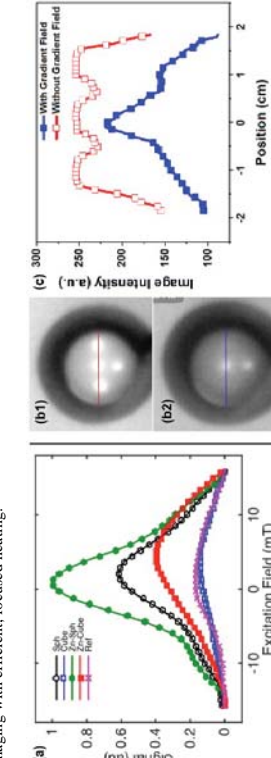


**Figure 1.** Magnetic particle relaxometry and focused hyperthermia results. (a) Measured PSFs from all samples, including a commercially available reference sample. (b) Thermal camera images obtained during hyperthermia experiments, showing the ability to focus heating to a small region near where  $B=0$ . Figure b1 was obtained in the absence of an external magnetic field gradient, while Figure b2 was obtained in the presence of a  $0.4\text{T}/\text{m}$  gradient with a zero value near the center. The image intensity profiles in (c) correspond to the lines drawn in Figures b1 and b2.

## A Novel Approach to Magnetic Particle Imaging

H. Bagheri\* and M.E. Hayden

Department of Physics, Simon Fraser University, Burnaby BC CANADA. \*email: hbagheri@sfu.ca

Magnetic Particle Imaging (MPI) is an imaging modality in which the acquired signal is derived from the nonlinear response of superparamagnetic nanoparticles (SPNs) to applied magnetic fields. Intense magnetic field gradients are applied to ensure that the SPN magnetization is saturated everywhere except in the vicinity of a Field Free Point (FFP). This ‘selection field’ is then modified or distorted in such a way that the FFP can be positioned at any desired location within the Field of View (FOV). Typically, manipulation of the FFP is accomplished by running currents through a system of ‘drive coils’. Harmonics of the characteristic drive frequency are then generated by the SPNs in the vicinity of the FFP as the local magnetization attempts to follow changes in the applied field. These harmonics are then detected inductively, and comprise the signal from which images are derived. High frequency operation and intense magnetic fields (and field gradients) are desirable from the perspective of enhancing resolution and signal-to-noise ratio (SNR). But, ultimately they are limited by Health Safety considerations such as the induced Specific Absorption Rate (SAR) and peripheral nerve stimulation. Conventional MPI systems operate at frequencies of order 25 kHz.

We have adopted a novel approach to MPI in which the functions of SPN excitation (harmonic generation) and FFP manipulation are decoupled from one another. SPN excitation is accomplished by applying a uniform oscillating magnetic field at frequencies that are typically in the range 40 to 400 kHz or higher. This increase in frequency relative to conventional systems is accompanied by a substantial increase in SNR. At the same time, FFP manipulation is accomplished via mechanical rotation of permanent magnet arrays at frequencies that are much lower than those employed in conventional systems. This reduction in frequency in turn promises a corresponding reduction in SAR when human-scale imagers are considered.

In addition to its potential for scalability, the decoupling of SPN excitation from FFP manipulation in our approach to MPI facilitates experiments that provide new insight into issues such as image resolution. An example of data from one such experiment is shown in the figure below. Images of a phantom acquired at progressively higher harmonics of the fundamental (drive) frequency yield progressively higher resolution, albeit at the expense of SNR. The design and operation of our prototype imager will be described, and experiments probing limits of its performance, such as the study of resolution pictured below, will be presented.

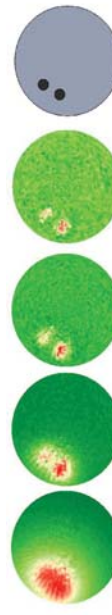


**Figure 1.** Left-to-right: Images of a phantom acquired at the 3<sup>rd</sup>, 5<sup>th</sup>, 7<sup>th</sup>, and 9<sup>th</sup> harmonics of an 80 kHz drive field. The phantom (grey, rightmost panel) consists of two squat cylindrical SPN-filled voids separated by 1.8 mm. The diameters of the FOVs and the phantom are 9 mm.

## Pharmacokinetics of LS-008: a blood pool SPIO tracer for Magnetic Particle Imaging

Amit P Khandhar<sup>a</sup>, Paul Keselman<sup>b</sup>, Scott J Kemp<sup>b</sup>, R Matthew Ferguson<sup>b</sup>, Bo Zheng<sup>b</sup>, Patrick W Goodwill<sup>b</sup>, Steven M Connolly<sup>b</sup> and Kannan M Krishnan<sup>ad</sup>

<sup>a</sup>LockSpin Labs, PO Box 95632, Seattle WA; <sup>b</sup>University of California, Department of Bioengineering, Berkeley CA; <sup>c</sup>Magnetic Insight Inc., Newark CA; <sup>d</sup>University of Washington, Department of Materials Science & Engineering, Seattle WA.

<sup>d</sup>Corresponding author: email: amit@lockspin.com

Magnetic Particle Imaging (MPI) [1] promises to combine the safety of MRI, the speed of CT, and the sensitivity of PET. Superparamagnetic iron oxide (SPIO) nanoparticles are the only source of signal in MPI, thus MPI is a tracer imaging modality that provides exceptional depth-independent contrast. Knowledge of SPIO pharmacokinetics (PK) is critical to understanding their capabilities for *in vivo* MPI. For applications requiring intravenous administration (e.g. cardiovascular, stroke and molecular imaging), SPIO clearance from systemic circulation must be well characterized. For MPI, it is also important to evaluate the loss in signal, which correlates directly to imaging capability and may or may not match SPIO clearance profile. In this study, we evaluated the blood half-life of LS-008 – a long-circulating high resolution SPIO tracer – in mice using both, *ex vivo* magnetic particle spectroscopy (MPS) measurements and *in vivo* imaging in a MPI scanner.

LS-008 is the first MPI-optimized tracer consisting of PEGylated, monodisperse, and single-coated SPIO nanoparticle cores [2]. Physical properties of LS-008 are provided in Table 1. Core diameter ( $d_c$ ) was determined from TEM, hydrodynamic diameter ( $d_h$ ) and zeta potential ( $\zeta$ ) from DLS, and MPI scanner-independent signal intensity ( $\chi_{\text{sig}}$ ) and full width at half maximum ( $\chi_{\text{sig}}^{\text{FWHM}}$ ) of the differential susceptibility ( $\chi_d$ ) were measured in a Magnetic Particle Spectrometer (MPS; 25 kHz, 20 mT  $\text{m}^{-1}$ ). CD-1 female mice were used for all blood half-life experiments. LS-008 in PBS was injected as a bolus in the tail vein at 5 mgFe/kg dose. For half-life evaluation with MPS, we used 3 mice (6–8 weeks old) per time point. Blood collected retro-orbitally was analyzed in our MPS. For half-life evaluation using imaging, a total of 3 mice (12–15 weeks old) were used. Mice were imaged with respiratory gating in a 3.5 T/m  $\times$  3.5 T/m  $\times$  7 T/m image with 20mT/40 drive field in  $z$  and a 3.5cm  $\times$  3.5cm  $\times$  3.5cm FOV. Scans were done at 30 minute intervals with the longest time point at 6 hours after injection. We selected the neck region for signal analysis due to the presence of major blood vessels and its relative isolation from perfused tissues in the abdomen and head regions.

MPS signal from blood was converted to SPIO concentration ( $\mu\text{gFe}/\text{ml}$ ) using LS-008's known signal per unit mass (Figure 1a). Since MPS measures a scanner-independent signal from the tracer, it provides a crucial snapshot of the physicochemical state of SPIO in blood. The  $\chi_{\text{d,FWHM}}$  at different time points was compared with the native response in water to ensure tracer performance was preserved during circulation. SPIO clearance followed first-order elimination ( $R^2 = 0.99$ ) and blood half-life ( $t_{1/2}$ ) was  $105 \pm 8$  minutes. In the *in vivo* MPI imaging experiment,  $t_{1/2}$  was averaged from 3 mice. There are several advantages to this method: first, each mouse provides the entire profile, *removing subject-to-subject variability within a curve but highlighting variability between subjects*. Secondly, no blood is collected, thus SPIO clearance is uninterrupted due to changes in blood volume. Figure 1b shows SPIO elimination curves ( $\mu\text{gFe}/\text{ml}$ ) from imaging 3 mice; Figure 1c shows mouse 1 imaged at  $t = 15$  and 362 minutes. The average  $t_{1/2}$  was  $103 \pm 46$  minutes from imaging, which agrees well with the MPS method but there is high variability between mice. Thus, more animals would be needed to achieve good statistical significance from the imaging experiment.

We evaluated the blood half-life of LS-008, a long circulating PEGylated MPI tracer, using *ex vivo* MPS and *in vivo* MPI imaging. Both methods are complementary and help correlate tracer behavior with imaging capability. LS-008, injected intravenously, showed  $t_{1/2}$  of over 100 minutes in mice.

[1] B. Gleich and J. Weizenecker, *Nature*, vol. 435, no. 7046, pp. 1214–1217, 2005.

[2] R. M. Ferguson *et al.*, *IEEE Trans. Med. Imag.*, **99**, 1 - 9 (2014).

## Approaches to Binding Detection in Magnetic Particle Imaging

T. Viereck<sup>a</sup>, C. Kuhmann<sup>a</sup>, S. Draack<sup>a</sup>, M. Schilling<sup>a</sup>, F. Ludwig<sup>a</sup>

<sup>a</sup>Institut fuer Elektrische Messtechnik und Grundlagen der Elektrotechnik, TU Braunschweig, Braunschweig, Germany, \*E-Mail: [T.viereck@tu-bs.de](mailto:T.viereck@tu-bs.de)

Magnetic Particle Imaging (MPI) is an emerging medical imaging modality based on the non-linear response of magnetic nanoparticles to an exciting magnetic field. MPI has been recognized as a fast imaging technique with high spatial resolution in the mm range.

Magnetic nanoparticles with a core diameter around 25 nm, which are favorable for MPI, can relax both via the Néel mechanism and the Brownian rotational motion, which makes it possible to discriminate the particle binding state or the viscosity of the medium. With that, MPI is promoted to a functional imaging method, where functionalized nanoparticles can be selectively imaged. We have demonstrated that we are able to provide the spatial distribution of the particle in the imaging plane and at the same time estimate the particle mobility, equivalent to the Brownian time constant depending on hydrodynamic diameter and/or viscosity of the medium.

Most MPI scanners work with sinusoidal excitation fields in the frequency range around 25 kHz. As such, MPI is not particularly sensitive to characteristic Brownian frequencies in the lowest kHz range, typically found in physiological media. Therefore, the imaging sequence of the scanner has to be modified and adjusted for maximized sensitivity towards binding detection.

In this contribution, we compare different approaches to achieve sensitive binding detection in MPI. For that, a standard MPI imaging protocol at 25 kHz, a dual-frequency approach at 25 kHz and 10 kHz, which takes advantage of the frequency-dependence of the particle's magnetization response, and a newly developed imaging sequence for MPI, that utilizes the field-dependence of the time constants, are used to separate immobilized particles from the particle suspension.



**Figure 1:** Phantom with two adjacent lines, one filled with a FeraSpin™ XL suspension and the other with the same particles immobilized in a Mannitol:D matrix; a) reconstruction of the phantom in a 1D field-of-view at 1 T/m imaging gradient showing a good separation of the mobile and immobile parts. b) false color overlay of both contributions in the same image (blue=immobile, yellow=mobile).

Financial support by the German Research Foundation DFG (LU 800/5-1) and via SPP1681 (SCHI 383/2-1) is acknowledged.

## Ultra-Fast MRI for Magnetic Particle Manipulation and Imaging

A. Nacev<sup>1</sup>, R. Hilfaman<sup>1</sup>, L.O. Mai<sup>1</sup>, P. Stepanov<sup>1</sup>, J. M. Weinberg<sup>1</sup>, S.T. Fricke<sup>2</sup>, J.M. Algaire<sup>3</sup>, B. Shapiro<sup>4</sup>  
<sup>1</sup>Wenberg Medical Physics, LLC, <sup>2</sup>Children's National Medical Center, <sup>3</sup>Institute for Research in Electronics and Applied Physics (IREAP),  
University of Maryland at College Park, <sup>4</sup>Fischell Department of Biengineering and the Institute for Systems Research, University of  
Maryland at College Park. \*Corresponding author: alek.nacev@wennbergmedicalphysics.com

**Purpose.** Diagnostic confidence in molecular imaging probes is increased when they can be overlaid onto anatomic images. Magnetic particle imaging (MPI) has been overlaid with x-ray CT [1]. We wanted to explore the possibility of developing a system capable of MRI, magnetic particle MRI (MP-MRI), and eventually MPI on one platform.

**Methods.** Sections of a head scanner (Figure 1) have been built that are capable of ultra-fast magnetic gradients, and whose static field can be adjusted from 0 to 0.3 Tesla, and augmented by a pre-polarizing field of up to 10 Tesla. Published clinical trials have shown that such fast gradients do not cause unwanted peripheral nerve stimulation [2]. Studies of spatial resolution and image quality (signal-to-noise ratio, or SNR) were conducted. Fast pulse sequences were implemented from magnetic T2-decay, in order to achieve positive contrast from magnetic particles. The gradient coils can be used for imaging and manipulation of magnetic particles.

**Results.** With ultra-fast pulses, it was possible to collect about 100 times more repetitions than a comparable conventional MRI sequence, demonstrating SNR of 134 with the static field of 0.3 T, comparable to literature reports about image quality obtained in compatible times from a 7 T conventional MRI scanner [3]. The device achieved a spatial resolution of 30 microns (Figure 2), comparable in size to single cells. A pulse sequence which highlighted sections with rapid T2-decay (MP-MRI) was able to overlay images of magnetic particles onto an anatomic MRI of brain tissue (Figure 3), without the loss of MRI signal at particle locations.

**Conclusions.** Ultra-fast MRI systems that employ magnetic gradient pulses with slew rates 1000 times higher than conventional MRI enable cell-sized spatial resolution and real-time image guidance. This new combined MRI/MP-MRI system provides the capability of combining imaging with magnetic manipulation to precisely deliver magnetic therapy to disease locations.

### References

- [1] B. Zheng, M. P. von See, E. Yu, B. Gunel, K. Lu, T. Vazin, D. V. Schaffter, P. W. Goodwill, and S. M. Conolly, "Quantitative Magnetic Particle Imaging Monitors the Transplantation, Biodistribution, and Clearance of Stem Cells In Vivo," *Theranostics*, vol. 6, no. 3, pp. 291-301, Jan. 2016.
- [2] I.N. Weinberg, P. Y. Stepanov, S. T. Fricke, R. Probst, M. Urdaneta, D. Warmov, H. Sanders, S. C. Glidden, A. McMillan, P. M. Starewicz, and J. P. Reilly, "Increasing the oscillation frequency of strong magnetic fields above 101 kHz significantly raises peripheral nerve excitation thresholds," *Med. Phys.*, vol. 39, no. 5, pp. 2578-83, May 2012.
- [3] V. Juras, G. H. Welsch, I. M. Noebauer-Huhmann, K. M. Friedrich, C. Kronnerwetter, P. Baer, L. Valkovic, and S. Trattnig, "Comparison of the Performance of MRI Clinical Sequences for Ankle Imaging at 3T vs 7T," in *European Society of Radiology*, 2011.

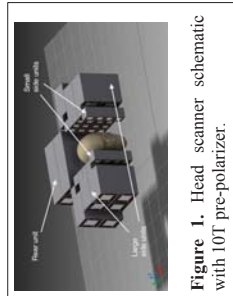


**Figure 1.** Head scanner schematic with 10T pre-polarizer.

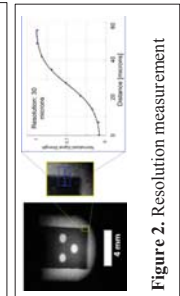


**Figure 2.** Resolution measurement

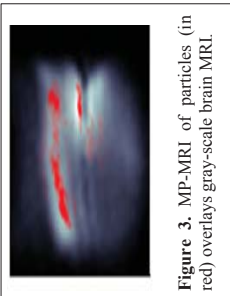


**Figure 3.** MP-MRI of particles (in red) overlays gray-scale brain MRI.

## Imaging the mobility of magnetic nanoparticles by magnetorelaxometry tomography

Mark Liebl<sup>1</sup>, Uwe Steinhoff<sup>1</sup>, Daniel Baumgarten<sup>2</sup> and Frank Weikhorst<sup>1</sup>

<sup>1</sup>Physikalisch-Technische Bundesanstalt, Berlin, Germany,

<sup>2</sup>Institute of Biomedical Engineering and Informatics, Technische Universität Ilmenau, Germany  
mark.liebl@ptb.de

Due to their unique magnetic properties magnetic nanoparticles (MNPs) have great potential in cancer treatment approaches, in magnetic drug targeting they are transported by magnetic fields through the vascular system to accumulate a therapeutic drug to a target, in magnetic hyperthermia they produce heat to kill cancer cells when exposed to a strong alternating magnetic field. To monitor and to assess the success of these applications a quantitative imaging of the MNP distribution inside a body is essential. Furthermore, since the MNPs are acting on a cellular level, an imaging taking into account the mobility of the MNP within the biological matrix would be extremely advantageous.

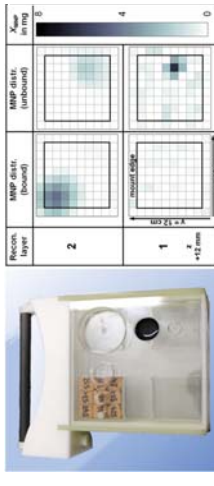


**Fig. 1.** Mobility-specific MRX tomography. left: Phantom support containing an MNP distribution of unbound (1m) MNP suspension with 12mg Fe) and bound (9 MNP loaded epoxy cubes with 6 mg Fe/cube) MNPs; right: estimated MNP distributions for unbound and bound MNPs. The chosen voxel size exceeds the dimension of the mount as indicated by the black square to compensate for possible edge effects in the reconstructions. Physical non-plausible negative MNP content is not shown in the reconstructions.

Magnetorelaxometry (MRX) tomography is a technique ideally suited for quantitative imaging of a MNP distribution in biological tissue. MRX is based on the magnetic moment relaxation of MNP after switching off an external magnetic field (used to align the magnetic moments first to obtain a net magnetic moment). Thereby, the mobility of the MNP partly determines the relaxation. The image of a MNP distribution is reconstructed from sequential MR X measurements using spatially varying magnetic field patterns for spatially encoded relaxation signals [1]. The MRX tomography imaging can be further extended by including information about the influence of the MNP mobility on the relaxation into the reconstruction [2].

As a proof of concept, we used two different mobility states of MNP, fluid (Brownian and Néel) relaxation and immobilized (merely Néel relaxation) [3]. For the measurements we assembled in the top layer (1) of a mount (10x10x6cm<sup>3</sup>) a suspension of fluid MNPs (Berlin Heart GmbH, Germany) and in the lower layer (2) 9 MNP loaded cubes (edge length of 12mm) of MNP immobilized in epoxy as depicted in fig. 1 (left). Magnetic field patterns were sequentially generated for 1s from 30 planar excitation coils (d=36mm) and relaxation signals were detected by 304 SQUID magnetometers. Applying the extended MRX tomography approach, we could reconstruct the MNP distributions  $\mathbf{X}_{\text{un}}$  for bound and  $\mathbf{X}_{\text{in}}$  for unbound MNPs with a resolution in the milligram per cm<sup>3</sup> range and a total deviation of MNP amount of less than 10%. Both estimated MNP distributions are illustrated in fig. 1 (right). The field of view covered about 240 cm<sup>3</sup>. The total measurement time was 15 min allowing for 10 averages to improve the signal to noise ratio. We conclude that MRX tomography provides a quantitative imaging of the spatial distribution and mobility of MNP over a volume larger than 100 cm<sup>3</sup>. Thus, MRX tomography might become a valuable tool in MNP-assisted cancer therapies.

Acknowledgements: This research was supported by German Research Foundation (priority program 1681, grant WI 4230/1-2, and research group FOR917) and the German Federal Ministry of Education and Research (BMBF) as part of the Improfile Transfer project MAMUD (Grant 031P1605X).

[1] M. Liebl, U. Steinhoff, F. Weikhorst, J. Haeschen and L. Trahms: Quantitative imaging of magnetic nanoparticles by magnetorelaxometry with multiple

[2] F. Weikhorst, U. Steinhoff, D. Eberbeck, L. Trahms: Magnetorelaxometry assisting biomedical applications of magnetic nanoparticles. *Pharm. Res.* 29, 1189-1202, 2012.

[3] M. Liebl, F. Weikhorst, D. Eberbeck, P. Radon, D. Gadelh, D. Baumgarten, U. Steinhoff, and L. Trahms: Magnetorelaxometry procedures for quantitative imaging and characterization of magnetic nanoparticles in biomedical applications. *Biomed. Tech.*, 60(5), 427-433, 2015.

## IMAGING MAGNETIC NANOPARTICLES IN VIVO BY AC BIOSUSCEPTOMETRY

Cáio C. Quini<sup>1</sup>, Ronaldo V. R. Matos<sup>1</sup>, André G. Próspero<sup>1</sup>, Paulo R. Fonseca<sup>2</sup>, Guilherme A. Soares<sup>1</sup>, Leonardo Antônio Pinto<sup>1</sup>, Nicholas Zaffelato<sup>3</sup>, Andris F. Bakutis<sup>3</sup>, José R. A. Miranda<sup>1</sup>

<sup>1</sup>Laboratório de Biomagnetismo, Bioscience Institute of Botucatu, Unesp, SP - Brazil

<sup>2</sup>Universidade Federal do Mato Grosso, Campus Barra do Garça, MS - Brazil

<sup>3</sup>Instituto de Física, Universidade Federal de Goiás, Goiânia, GO - Brazil

Nanoparticles present an extraordinary potential for both diagnostic and therapeutic applications. *In vivo* detection and monitoring of nanocarriers, however, remains a challenge. Although several techniques claim to achieve satisfactory results, there are still room for improvements, specially regarding temporal resolution. The AC Biosusceptometry (ACB) system is a research tool, extensively employed on monitoring gastrointestinal tract physiological properties and has been recently applied to monitor magnetic nanoparticles (MNPs) in animal models. As a detection probe, when compared to other similar techniques, the ACB method presents considerably higher temporal resolution, mainly due to its physical working principle. Our technique is based upon a magnetic flux transformer, which allow us to detect and quantify magnetic samples based on the variation in magnetic inductance from an excitation pickup coil to a detection one. Here we describe the first *in vivo* application of the ACB system as an imaging probe for magnetic nanoparticles. In this preliminary study, we tested two different systems aiming for better spatial resolution and higher temporal resolution. The objective of this association between different systems was to perform a more reliable signal acquisition, using a multichannel ACB system to monitor the nanoparticles injection in real time and its accumulation into organs of interest, followed by a static image performed by a single sensor scan to achieve higher spatial resolution. After the *in vivo* monitoring, we sacrificed all animals and imaged all organs of interest. For this experiment, we employed a citrate coated, manganese ferrite nanoparticle due to its good magnetic susceptibility. Five male Wistar rats, properly anesthetized by urethane, were submitted to MNP intravenous injection while monitored by the multichannel ACB system. After 30 minutes of acquisition, we sacrificed all animals and collected heart, lungs, liver, spleen and kidneys. We employed the ACB scanner to image the organs and obtain *ex vivo* results. Figure 1 illustrates one frame acquired by the multichannel system (1A) and the *ex vivo* image on regards to particles distribution within the liver (1B), respectively. These aspects together will allow us to perform complete pharmacokinetic analysis, associated with real time accumulation, simultaneously, in different organs of interest, followed by accumulation patterns within organs and sequential quantitative information over MNPs biodistribution.

**Index Terms**— AC Biosusceptometry, Magnetic Nanoparticles, *in vivo* imaging

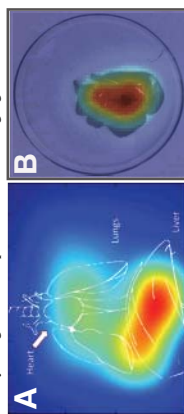


Figure 1: 1A illustrates the MNP distribution acquired *in vivo* and in real time, while 1B shows an *ex vivo* image of the liver, both acquired using the ACB system.

## Shape-dependent Cellular Uptake of two types of MRI T<sub>1</sub> Contrast agents

Jennifer Sherwood,<sup>1</sup> Lindsey Maher,<sup>1</sup> Mark Bolding,<sup>2</sup> Yiping Bao<sup>1\*</sup>

<sup>1</sup>Chemical and Biological Engineering, <sup>3</sup>Alabama Innovation and Mentoring of Entrepreneurs,

The University of Alabama, Tuscaloosa, AL 35487

<sup>2</sup>Department of Radiology, The University of Alabama at Birmingham, Birmingham, AL 35233

Iron oxide nanoparticles have been explored as contrast agents for magnetic resonance imaging (MRI) for decades. However, previously FDA-approved iron oxide-based MRI contrast agents were taken off market primarily due to the lack of clinical uses. FDA-approved iron oxide nanoparticles were primarily used as negative ( $T_2$ ) contrast agents, which have low resolution and background interference caused by body fluids and voids. However, iron oxide nanoparticles are still in clinical use for iron deficiency treatments, indicating their great biocompatibility and biodegradability. Recent research efforts have been focusing on exploring iron oxide nanoparticles as positive ( $T_1$ ) contrast agents, serving as a safer alternative to clinically used gadolinium complexes. Two types of iron oxide nanoparticle-based  $T_1$  contrast agents are reported with robust  $T_1$  contrast *in vivo*, such as ultrasmall ( $< 4$  nm) nanospheres [1] and ultrathin nanowires ( $2 \times 20$  nm) [2]. However, these two types of contrast agents have distinctly morphological differences. In this study, we systematically investigated the shape-dependent cellular uptake behaviors of these two contrast agents and further evaluated their effectiveness for cellular MRI. Figure 1 shows represented cellular uptake images of human liver cells (HepG2) treated with these two types of nanoparticles for 24 hours. Our studies suggested these two types of  $T_1$  MRI contrast agents may have distinct blood circulation and localization behaviors *in vivo*.

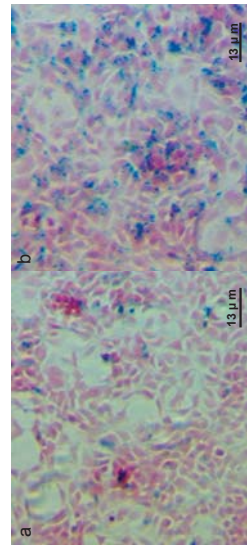


Figure 1. Cellular uptake behaviors of iron oxide ultrathin nanowires (a) and ultrasmall nanospheres (b)

1. B. H. Kim, et al., "Large-Scale Synthesis of Uniform and Extremely Small-Sized Iron Oxide Nanoparticles for High-Resolution  $T_1$ -Magnetic Resonance Imaging Contrast Agents," *J Am. Chem. Soc.* 133, 12624–2011.
2. T. Maher, et al., "Ultrathin Iron Oxide Nanowhiskers as Positive Contrast Agents for Magnetic Resonance Imaging," *Adv. Funct. Mater.* 25, 490, 2015.

## In vivo-Tracking of transplanted human adipose stromal cells using Magnetic Nanoparticles in Magnetic Resonance Imaging

B. J. Siegmund<sup>1\*</sup>, A. Kasten<sup>1</sup>, J.-P. Külln<sup>2</sup>, K. Winter<sup>3</sup>, C. Grüttner<sup>4</sup>, B. Frierich<sup>1</sup>

<sup>1</sup>Institute of Maxillofacial and Facial Plastic Surgery, University Medicine Rostock, Germany

<sup>2</sup>Institute of Diagnostic Radiology and Neuroradiology, Ernst-Moritz-Arndt-University, Greifswald, Germany

<sup>3</sup>Translational Centre for Regenerative Medicine, University of Leipzig, Germany

<sup>4</sup>Micromod Partikeltechnologie GmbH, Rostock, Germany

\* E-Mail: bire.siegmund@med.uni-rostock.de

**Introduction:** Adipose tissue engineering using autologous stem cells has been advocated for treatment of soft tissue defects. With a view to strategies improving the efficacy of stem cell transplantation, cell tracking might be useful. Here we report the *in vivo* tracking of adipose stem cells (ASC) in a SCID-mouse model of adipose tissue engineering by means of nanoparticle labeling and magnetic resonance imaging (MRI).

**Methods:** ASC were isolated from human adipose tissue and labeled with two types of magnetic nanoparticles (MNP), BNF starch (10 µg Fe/ml) and nanomag®-D-sPIO (25 µg Fe/ml). Previous *in vitro* studies had shown, that internalized MNP in the used concentration had no effect on cell metabolism nor on cell differentiation. The labeled cells were seeded on collagen scaffolds and implanted subcutaneously at the back of SCID mice (n=69). Cell seeded scaffolds without MNP were implanted as a control. MRI scans were performed 24 hours, 4, 12 and 28 days and 4 months after implantation (Bruker Clin. Scan 7T MRI). The iron content and the volume stability of the transplants was measured over the time using Osirix software. After sacrifice the constructs were processed for histomorphometric quantification, including berlin blue stain for detection of MNP.

**Results:** ASC seeded constructs were successfully visualized *in vivo*. Labeled cells showed high contrast (T2\*-weighted sequence) in comparison to the controls. However, quantification of the cells by using the T2\* weighted sequence was not possible because of partially high iron concentrations inside the implants, which leaded to immeasurable high values. As expected, a shrinkage and loss of volume of the cell-septa was observed over time due to partial loss of cells in the center of the constructs. Correlation between MRI and histomorphometry concerning construct size measurement was high with a significance of  $p < 0.001$  in the labeled groups and  $p = 0.005$  in the control group. Cells were successfully visualized in MRI in tissue sections. In contrast to *in vitro* studies, berlin blue stain was not exclusively specific for MNP-labeled cells.

**Conclusions:** MNPs are, depending on the concentration and distribution, suitable *in vitro* and *in vivo* cell visualization in MRI. The tracking of mesenchymal stem cells labeled by MNP in MRI is a sensitive and non-invasive method for evaluation of the fate of transplanted stem cells.



**Figure 1:** MRI scans (T2\*-sequence, coronal view) twelve days after implantation. a) Control group showed high contrast on the collagenous scaffolds. b) BNF starch labeled and c) nanomag®-D-sPIO labeled cells showed high contrast on the collagenous scaffolds.

# 11th International Conference on the Scientific and Clinical Applications of Magnetic Carriers

Vancouver, Canada | May 31-June 4, 2016 [www.magneticmicrosphere.com](http://www.magneticmicrosphere.com)

11th International Conference on the Scientific and Clinical Applications of Magnetic Carriers - Vancouver, BC, Canada

## Posters

#	First Author	Title	Location
1	Andreu, Irene	Gadolinium-doped Magnetite Nanoparticles using a Single Source Precursor Synthesis Route	Burnaby, Canada
2	Angelova, Ralitsa	Magnetically modified sheaths of Leptothrix sp. as an adsorbent for Amido black 10 B removal	Ceske Budejovice, Czech Republic
3	Anker, Jeffrey	Towards monitoring drug release in situ with multimodal radioluminescent, photoluminescent, and MRI Contrast Agents	Clemson, SC, USA
4	Baldikova, Eva	PMMA-stabilized ferrofluid/chitosan/yeast composite for bioapplications	Ceske Budejovice, Czech Republic
5	Banuazizi, Seyed Amir Hossein	Ultrarapid detector of flowing labeled magnetic nanoparticles based on spin torque oscillator	Stockholm, Sweden
6	Beck, Mathias	Influence of Material and Concentration on Nanoparticle Heating	Garching, Germany
7	Beg, Muhammad Shahbaz	Porous Anisotropic Fe <sub>3</sub> O <sub>4</sub> -SiO <sub>2</sub> Nanocapsules for Theranostic Applications	Mumbai, India
8	Bender, Philipp	Numerical inversion methods to analyze magnetization data	Santander, Spain
9	Bhattacharya, Mangolika	Inclusion of Dipolar Interactions in the Mathematical Modelling of Magnetic Hyperthermia through the Landau-Lifshitz-Gilbert equation	Waterford, Ireland
10	Begin-Colin, Sylvie	Magnetic carbon nanotubes combining MRI and therapy as nanoprobes to explore biological processes	Strasbourg, France
11	Bogart, Lara	Assessment of synthesis-dependent oxidative aging of iron oxide nanoparticles as determined using room temperature Mössbauer spectroscopy	London, UK
12	Bonvin, Debora	Small and biocompatible coatings of iron oxide nanoparticles for improved detection and treatment of metastases	Lausanne, Switzerland
13	Brusentsov, Nikolay	Combined magneto-thermo-chemotherapy of solid tumors controlled by MRI and electronic sensor	Moscow, Russia
14	Cabrera, David	Harnessing viscosity effects to tailor the dynamical magnetic response of magnetic nanoparticles	Madrid, Spain
15	Chandra, Sudeshna	Fabrication of Bio-Magnetic Sensors based on Macromolecules Functionalized Iron Oxide Nanoparticles	Mumbai, India
16	Chiriac, Horia	Mechanically-induced necrosis of human malignant cells by sharp magnetite nanoparticles	Iasi, Romania
17	Chiriac, Horia	Preparation and characterization of a low Curie temperature Fe-Cr-Nb-B ferrofluid	Iasi, Romania
18	Chun-Rong, Lin	Synthesis and magneto-optical behaviors of Fe <sub>3</sub> O <sub>4</sub> /Ag nanocomposite spheres	Pingtung, Taiwan
19	Crippa, Federica	Influence of ligand exchange on crystallography, magnetic and thermal behavior of iron oxide nanoparticles for hyperthermia treatment	Fribourg, Switzerland
20	de la Presa, Patricia	Effect of the aggregation degree on the heating efficiencies of Mn, Fe and Co oxides nanoparticles	Madrid, Spain
21	De-Leon-Prado, Laura Elena	Synthesis and characterization of nanosized Mg <sub>x</sub> Mn <sub>1-x</sub> Fe <sub>2</sub> O <sub>4</sub> ferrites by both sol-gel and thermal decomposition methods	Saltillo, Coahuila, Mexico
22	Dey, Chaitali	Improvement of Drug Delivery by Hyperthermia Treatment using Magnetic Cubic Cobalt Ferrite Nanoparticle	Kolkata, India
23	Dey, Tania	Magnetite Nanoparticles: comparison of different synthetic methods	Limerick, Ireland
24	Engelmann, Ulrich	Feasibility of Hyperthermia Induced Apoptosis of Pancreatic Tumor Cells with Internalized Magnetoliposomes	Aachen, Germany
25	Famiani, Simone	Synthesis and characterization of plasmonic highly-magnetic nanoparticles	London, UK
26	Feoktystov, Artem	Small-Angle Neutron Scattering Contrast Variation as a tool for magnetic nanoparticle characterization	Garching, Germany
27	Fratila, Raluca Maria	Magnetic nanoparticles for bioorthogonal click chemistry	Zaragoza, Spain
28	Friedrich, Ralf	Covalent versus adsorptive binding of thrombolytics to SPIONs for directed targeting of fibrin-based matrices	Erlangen, Germany
29	Gazova, Zuzana	Inhibition of amyloid aggregation of lysozyme by application of magnetic nanoparticles coated with different types of dextran	Kosice, Slovakia
30	Geers, Christoph	An abstract approach to quantify the heating power of magnetic nanoparticles	Fribourg, Switzerland

31	Ghavami Nejad, Amin	Novel Route to immobilization of Magnetic Nanoparticles on polymeric Nanofibers for Hyperthermic Chemotherapy	Jeonju, Korea
32	Goetzfried, Marisa	Functionalization of DNA Nanostructures with Au-plated Superparamagnetic Iron Oxide Particles	Garching, Germany
33	Graefe, Christine	Serum Concentration Affects Protein Corona Mass, Surface Charge, and Nanoparticle-Cell Interaction	Jena, Germany
34	Heidsieck, Alexandra	Optical Measurement of the Magnetic Moment of Magnetically Labeled Objects	Garching, Germany
35	Hirota, Noriyuki	In-situ observation of particles deposition process on a ferromagnetic filter during high-gradient magnetic separation process	Tsukuba, Japan
36	Hoemann, Peter	Uncertainty Impacts on Quantitative Magnetic Nanoparticle Imaging using Magnetorelaxometry	Ilmenau, Germany
37	Horak, Daniel	TAT- and RGDS-modified Luminescent and PEG&#amp;SiO <sub>2</sub> -coated Magnetic Nanoparticles for Tumor Targeting and Diagnosis	Prague, Czech Republic
38	Hsu, Hao-Lung	Preparation of Thermosensitive Magnetic Liposome Encapsulated Recombinant Tissue Plasminogen Activator for Targeted Thrombolysis	Taoyuan, Taiwan
39	Hsu, Hao-Lung	Self-Assembled Magnetic Nanoparticles Based On Folic Acid-Oleoyl Chitosan for Targeted Delivery of Doxorubicin	Taoyuan, Taiwan
40	Huang, Wei	Immobilization of laccase on magnetic nanoparticles for enhancing biocatalysis	Beijing, China
41	Iacovita, Cristian	Polyethylene glycol mediated synthesis of magnetic nanoparticles as potential magnetic hyperthermia agents	Cluj-Napoca, Romania
42	Insin, Numpon	Size-dependent Cytotoxicity and Inflammatory Responses of PEGylated Silica-Iron Oxide Nanocomposite Size Series	Bangkok, Thailand
43	Jasso-Teran, Rosario Argentina	Synthesis, characterization and hemolysis studies of Zn(1-x)Ca <sub>x</sub> Fe <sub>2</sub> O <sub>4</sub> ferrite synthesized by sol for hypertermia treatment applications	Saltillo, Coahuila, Mexico
44	Jirak, Zdenek	Titania-coated manganite nanoparticles for theranostic applications	Prague, Czech Republic
45	Joos, Alexander	Size-dependent MR relaxivities of magnetic nanoparticles	Garching, Germany
46	Kafash Hoshiar, Ali	Effective Parameters in Aggregation of Nano Particles during Magnetic Guided Drug Delivery in Mice Brain	Yoon, Korea
47	Kaibi, Amel	Microstructure Evolution and Magnetic Properties of Nanocrystalline (Ni <sub>75</sub> Fe <sub>25</sub> ) <sub>95.6</sub> Si <sub>3.5</sub> Thin Films	Tebessa, Algeria
48	Kaibi, Amel	Microstructure Evolution and Magnetic Properties of Nanocrystalline Ni <sub>75</sub> Fe <sub>25</sub> Thin Films: Effects of Substrate and Thickness.	Tebessa, Algeria
49	Kaman, Ondrej	Preparation of Mn-Zn ferrite nanoparticles and their silica-coated clusters as contrast agents for MRI	Praha, Czech Republic
50	Komissarova, Lubov	Developing the Massart Method for Obtaining Biocompatible Magnetite Nanoparticles of Given Sizes	Moscow, Russia
51	Koneracka, Martina	Preparation of Ploy-L-Lysine Functionalized Magnetic Nanoparticle and Influence on Cancer Cells Viability	Kosice, Slovakia
52	Kopcansky, Peter	Radiation-enhanced decomposition of protein amyloid fibrils by magnetic nanoparticles	Kosice, Slovakia
53	Krafcik, Andrej	Disparity of native, reconstructed ferritin and magneto-ferritin in low-field and high-field MRI	Bratislava, Slovakia
54	Kubovcikova, Martina	STRUCTURE AND STABILITY OF MAGNETIC FLUIDS AT INTERFACE WITH SILICON BY NEUTRON REFLECTOMETRY	Kosice, Slovakia
55	McCoey, Julia	Non-invasive High Resolution Magnetic Field and Temperature Imaging	Melbourne, Australia
56	Lee, Jung-Rok	The Transduction Mechanism and Applications of Giant Magnetoresistive Biosensors	Stanford, CA, USA
57	Lim, Byeonghwa	Magnetophoretic transport system for digital control of single particle and cells	Daegu, Korea
58	Liu, Chunzhao	Synthesis of Functional Magnetic Nanoparticles for Microalgal Cell Separation	Beijing, China
59	Loewa, Norbert	Magnetic Nanoparticles in different biological environments as seen by Magnetic Particle Spectroscopy	Berlin, Germany
60	Ludwig, Frank	Standardization of the analysis of single-core magnetic nanoparticles	Braunschweig, Germany
61	Mandal Goswami, Madhuri	Biocompatibility of DNA Engineered Cobalt-ferrite Nanoparticles for Cancer Cell Imaging and Hyperthermia Therapy	Kolkata, India
62	Manisekaran, Ravichandran	Au@CoFe <sub>2</sub> O <sub>4</sub> yolk-shell nanoparticles: An efficient MRI contrast agent, Magneto-Hyperthermal and drug-delivery armada for cancer Theranostics	Mexico City, Mexico
63	Mattern, Anne	Magnetic Nanoparticle-Gel Materials for Development of Magnetic Particle Imaging Phantoms	Ilmenau, Germany
64	Modak, Nipu	Separation of magnetic beads in a Hybrid continuous flow microfluidic device	Kolkata, India
65	Morales, Irene	Permeability of Matrigel to magnetic nanoparticles	Madrid, Spain
66	Musikhin, Sergei	Magnetic and Fluorescent Nanoparticle Conjugates for Targeting of Hsp70-positive Malignant Brain Tumors	St. Petersburg, Russia
67	Nacev, Aleksandar	Focusing Magnetic Particles to Central Targets between External Electromagnets	Rockville, MD, USA
68	Nguyen, Thanh	SYNERGETIC EFFECT OF MULTI-DRUG LOADED MAGNETIC LIPOSOME IN CHEMO-THERMOTHERAPY	London, UK
69	Nigam, Saumya	Peptide Dendrimer-Fe <sub>3</sub> O <sub>4</sub> Nanoparticles as contrast agents in non-invasive magnetic resonance imaging	Mumbai, India
70	Nosrati, Zeynab	Production of Magnetic Microspheres by a Micro Co-Flowing Device as a Potential Approach for Magnetic Resonance Navigation Technology	Vancouver, Canada
71	Nowak, Johannes	A capillary viscometer designed to measure the magnetoviscous effect of biocompatible ferrofluids diluted in sheep blood	Dresden, Germany
72	Ota, Satoshi	Magnetization dynamics of magnetic nanoparticle associated with magnetic relaxation characterized by alternating current hysteresis measurement	Hamamatsu, Japan

73	Palanisamy, Selvamani	Layer-by-layer Assembled Prednisolone Magnetic Microcapsules (PMC) Assisted Controlled and Targeted Drug Release at Rheumatoid Arthritic Joints	Trichy, India
74	Pandey, Sudip	Optimizing magnetic properties for self-controlled hyperthermia applications	Carbondale, IL, USA
75	Papaefthymiou, Georgia	Magnetic-Relaxation and Heat-Dissipation Characteristics of Iron-Oxide Ferrofluids Prepared by Surfactant-Assisted Ball-Milling	Villanova, PA, USA
76	Pham, Binh	In vivo biodistribution of sterically stabilised superparamagnetic iron oxide nanoparticles via intraperitoneum injection	Camperdown, Australia
77	Pham, Nguyen	Stable and non-toxic superparamagnetic iron oxide nanoparticles as multimodal (PET/SPECT-MRI) imaging probes	Camperdown, Australia
78	Phranot, Ajkidkarn	Synthesis, Characterization, Drug Release and Transdental Delivery Studies of Magnetic Nanocubes coated with Biodegradable Poly(2-(dimethyl amino)ethyl methacrylate)	Bangkok, Thailand
79	Polikarpov, Mikhail	3D Imaging of Magnetic Particles Using the 7-Channel Magnetoencephalography Device Without Pre-Magnetization or Displacement of the Sample	Moscow, Russia
80	Quini, Caio	Evaluating magnetic nanoparticle distribution through ACB tomography	Botucatu, SP, Brazil
81	Radon, Patricia	Design and Characterization of a device to quantify the Magnetic Drug Targeting Efficiency of Magnetic Nanoparticles in a Tube Flow Phantom	Berlin, Germany
82	Radon, Patricia	Investigation of Magnetic Targeting Properties of FluidMAG-D	Berlin, Germany
83	Rahn, Helene	Long-term calibration phantom for MRI, MRX-CT and X-ray-CT imaging of body tissues enriched with magnetic nanocomposites	Dresden, Germany
84	Rajan Unnithan, Afeesh	An Implantable Smart Magnetic Nanofiber Device for Endoscopic Hyperthermia Treatment and Tumor-Triggered Controlled Drug Release	Jeonju, Korea
85	Ramachandra Kurup Sasikala, Arath	Multifunctional Nanocarriers for Cancer Theranostics: Remotely Controlled Graphene Nanoheaters for Thermo-Chemosensitisation and MRI	Jeonju, Korea
86	Ramaswamy, Bharath	Magnetic drug delivery to the cochlea to prevent cisplatin induced hearing loss	College Park, MD, USA
87	Ramaswamy, Bharath	On the safety of magnetic nanoparticle (MNP) motion in live brain tissue	College Park, MD, USA
88	Raval, Yash	Glycoconjugate-Functionalized Magnetic Nanoparticles for Bacteria Specific Targeting and Inactivation via MagMED	Clemson, SC, USA
89	Remmer, Hilke	Dynamics of magnetic nanoparticles in viscoelastic media	Braunschweig, Germany
90	Reyes-Rdz, Pamela Yajaira	Structural and magnetic properties of Mg <sub>1-x</sub> Zn <sub>x</sub> Fe <sub>2</sub> O <sub>4</sub> magnetic nanoparticles prepared sol-gel method	Saltillo, Coahuila, Mexico
91	Rizal, Conrad	Magnetic Alloys and Nanoparticle-based Bio-nanomagnetic Materials and Devices	La Jolla, CA, USA
92	Rizal, Conrad	Magnetoplasmonic Nanosensors for Biosensing	La Jolla, CA, USA
93	Royer, David	Using Injection molding for fabrication of a continuous-flow magnetic cell sorter	Lyon, France
94	Ruemennapp, Christine	Comparison of Magnetic Nanoparticles with different Functional Groups for the Detection of Molecules using Magnetic Resonance	Garching, Germany
95	Saengruengrit, Chalathan	Synthesis of Magnetic Nanocomposites for Application in Protein Delivery to Immune Cell	Bangkok, Thailand
96	Samarikhala, Melisa	pH/NIR light-Controlled Multi-Drug Release via a Mussel-Inspired Nanocomposite Hydrogel for Chemo-Photothermal Cancer Therapy	Jeonju, Korea
97	Sanchez, Javier	Synthesis of Mn <sub>x</sub> Ga <sub>1-x</sub> Fe <sub>2</sub> O <sub>4</sub> magnetic nanoparticles by thermal decomposition method for medical diagnosis applications	Saltillo, Coahuila, Mexico
98	Schmidt, Ann-Kathrin	Ni nanorods interact with human cells and induce changes in intracellular signalling and gene expression	Jena, Germany
99	Schroeder, Christian	Numerical Investigation of the Magneto-Dynamics of Self-Organizing Nanoparticle Ensembles: a Hybrid Molecular and Spin Dynamics Approach	Bielefeld, Germany
100	Shih, Kun-Yauh	Microwave synthesis and antibacterial properties of silver/magnetite/graphene composite	Pingtung, Taiwan
101	Shih, Kun-Yauh	Synthesis and characterization of Iron oxide/Reduced graphene oxide composites	Pingtung, Taiwan
102	Soukup, Dalibor	Protein Corona Nanoparticles Increase Cancer Cell Proliferation	Stoke-on-Trent, UK
103	Soukup, Dalibor	The Effect of Inter-Particle Interactions on SAR values and Magnetic Response of Biogenic Zn-doped Nanoparticles	Stoke-on-Trent, UK
104	Soukup, Dalibor	The Effect of Protein Coated In-Situ Formed Aggregates of Iron Oxide Nanoparticles on Cell-Nanoparticle Interactions	Stoke-on-Trent, UK
105	Southern, Paul	Temperature and AC Field Dependence of Magnetic Susceptibility and its use in Magnetic Hyperthermia	London, UK
106	Stange, Robert	Acceleration of superparamagnetic particles due to an optimized magnetic field to improve Biomagnetic Separation	Dresden, Germany
107	Steinhoff, Uwe	Interpreting static and dynamic magnetization behavior of magnetic nanoparticles in terms of magnetic moment and energies	Berlin, Germany
108	Stiuflci, Rares	Magnetoliposomes nanocarriers for drug delivery applications: synthesis and characterization	Cluj-Napoca, Romania
109	Subbiah, Latha	Gemcitabine Loaded Magnetic Nanoparticles for Magnetically Triggered Thermo-Chemo Therapy	Tiruchirappalli, India
110	Sun, Jiajia	The Force Analysis for Superparamagnetic Nanoparticles-based Gene Delivery in an Oscillating Magnetic Field	Xi'an, China
111	Szekeres, Marta	The effect of polycarboxylate shell of magnetite nanoparticles on protein corona formation in blood plasma	Szeged, Hungary
112	Takeda, Ryoji	Neel relaxation and its anisotropic behavior in superparamagnetic nanoparticle evaluated by dynamic hysteresis measurement	Yokohama, Japan
113	Teruyoshi, Sasayama	Three-Dimensional Magnetic Nanoparticle Imaging Using a Small Gradient Field and Multiple Pickup Coils	Fukuoka, Japan
114	Thanh, Nguyen	Protein A conjugated iron oxide nanoparticles for separation of Vibrio cholerae from water samples	London, UK

115 Thanh, Nguyen	Synthesis of magnetic cobalt ferrite nanoparticles with controlled morphology, monodispersity and composition: the influence of solvent, surfactant, reductant and synthetic condition	London, UK
116 Thorat, Nanaaheb	Multimodal graphene@Fe <sub>3</sub> O <sub>4</sub> SPIOs with unusually enhanced specific absorption rate for synergistic cancer therapeutics and MRI	Limerick, UK
117 Tippkoetter, Nils	Aqueous droplets with a superparamagnetic and -hydrophobic particle shell for lab-in-a-drop bioprocesses	Kaiserslautern, Germany
118 Tombacz, Etelka	Possibilities and limitations of carboxylated/PEGylated SPIONs for theranostics	Szeged, Hungary
119 Toth, Ildiko	Clustering of carboxylated magnetite nanoparticles with polyethylenimine via electrostatic or chemical interactions	Szeged, Hungary
120 Veintemillas-Vergaguer, Sabino	Tunning the magnetic properties of ferrihydrite by dextran coating	Madrid, Spain
121 Visscher, Martijn	Simulation of essential probe characteristics for intra-operative handheld detection of magnetic tracers	Enschede, The Netherlands
122 Cotin, Geoffrey	Magnetism engineered nanoparticles towards innovative biocolloids combining MRI and magnetic hyperthermia properties	Strasbourg, France
123 Wang, Pingping	The interaction of bacterial magnetosomes and human liver cancer cells in vitro	Beijing, China
124 Weidner, Andreas	Intentional Formation of a Protein Corona on Magnetic Nanoparticles	Ilmenau, Germany
125 Witte, Kerstin	Particle size- and concentration-dependent separation of magnetic nanoparticles	Rostock, Germany
126 Yang, Liangrong	Effect of immobilized amine density on cadmium(II) adsorption capacities for ethanediamine-modified magnetic poly-(glycidyl methacrylate) microspheres	Beijing, China
127 Yang, Ming Da	Hyperthermia enhancement of iron oxide nanoparticle in bacterial biofilms	Hsinchu,Taiwan
128 Yang, Ming Da	Special magnetic structure for cell sorting by novel 3D printing	Hsinchu,Taiwan
129 Yang, Pei-Ching	Immobilization of Recombinant Tissue Plasminogen Activator on Magnetic Graphene Oxide for Targeted Delivery of Thrombolytic Agents	Taoyuan, Taiwan
130 Yang, Pei-Ching	Magnetic Graphene Oxide as a Carrier for Dual Targeted Delivery of Chemotherapy Drugs in Cancer Therapy	Taoyuan, Taiwan
131 Yang, Pei-Ching	Poly(lactide-co-glycolide) Magnetic Nanoparticles for Delivery of Plasminogen Activators	Taoyuan, Taiwan
132 Yeh, Barry	Utilizing magnetic and hydrodynamic properties to improve the homogeneity of superparamagnetic nanoparticles	Auburn, CO, USA
133 Yohannes, Yonas	A highly Efficient and Cost Effective Bioactivated Superpara-Magnetic beads and its Immuno-diagnostic (Clinical Diagnosis) applications	Spring Valley, CA, USA
134 Yoshida, Takashi	Effect of Alignment of Easy Axes on Dynamic Magnetization of Immobilized Magnetic Nanoparticles	Fukuoka, Japan
135 Yurenja, Anton	Effect of magnetic field on the ability of magnetite nanoparticles to penetrate into live cells	Moscow, Russia
136 Zavisova, Vlasta	Influence of magnetic fluid with betulinic acid on cancer cells viability	Kosice, Slovakia
137 Zborowski, Maciej	Tessellated permanent magnets for flow-through, open gradient separations of weakly magnetic materials	Cleveland, OH, USA
138 Zaloga Jan	Pharmaceutical Formulation of HSA hybrid coated Iron Oxide Nanoparticles for Magnetic Drug Targeting	Erlangen, Germany
139 Gao, Jie	MALDI-TOF MS Combined With Magnetic Beads For Quantification of Serum Protein Biomarkers	Bergen, Norway
140 Calabresi, Marcos	AC biosusceptometry to assess colonic contractility in rats with ulcerative colitis	Botucatu, SP, Brazil
141		
142		

## Magnetically modified sheaths of *Lepothrix* sp. as an adsorbent for Amido black 10 B removal

### Gadolinium-doped Magnetite Nanoparticles using a Single Source Precursor Synthesis Route

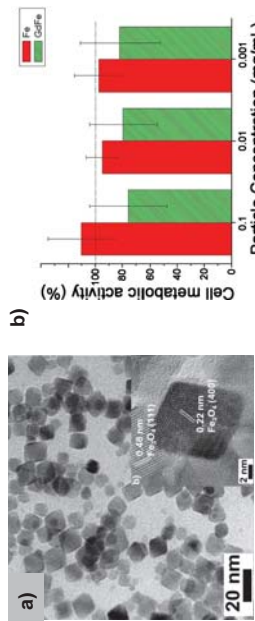
I. Andreu<sup>1,2,\*</sup>, F. Douglass<sup>3</sup>, D. A. MacLaren<sup>4</sup>, C. Berry<sup>5</sup>, M. Murrie<sup>5</sup>, M. Castro<sup>1</sup>

<sup>1</sup> ICMA- Dept. Ciencia y Tecnología de Materiales y Fluidos, CSIC-Univ. de Zaragoza, Zaragoza, Spain; <sup>2</sup> Simon Fraser University, Dept. of Chemistry, Burnaby, BC, Canada; <sup>3</sup> WestCHEM School of Chemistry, University of Glasgow, Glasgow, UK; <sup>4</sup> School of Physics and Astronomy, University of Glasgow, UK; <sup>5</sup> Institute of Molecular Cell and Systems Biology, University of Glasgow, UK. \*E-Mail : i.andreu@sfu.ca

New therapeutic agents based on superparamagnetic iron oxide based nanoparticles (NPs) combining diagnosis (imaging) and therapy (Drug Delivery and Magnetic Hyperthermia) are still in development. Among the different strategies to reach this multifunctionality, ion doping has been scarcely explored although promising results have been obtained, for example, on magnetite,  $\text{Fe}_3\text{O}_4$ , doped with Gadolinium [1]. However, these previous studies showed low heating ability and poor magnetic properties, while the synthetic procedure combines the use of two different precursors.

A new single source precursor route, using a bimetallic Fe/Gd precursor (tentative formula of  $[\text{Fe}_{1-x}\text{Gd}_{x}\text{O}(\text{O}_2\text{CPh})_x\text{H}_2\text{O}]_3$ ) to synthesize Gd-doped  $\text{Fe}_3\text{O}_4$  ( $\text{Gd:Fe}_3\text{O}_4$ ) NPs is presented. NPs are prepared via the high temperature decomposition of the precursor in a mixture of benzyl ether, oleic acid and oleylamine.

TEM characterization shows octahedral NPs (average size of  $12 \text{ nm} \pm 2.6 \text{ nm}$ ) with  $\text{Fe}_3\text{O}_4$  crystalline structure. EDX and EELS measurements confirm the presence of Gd in the NPs with a concentration around 2.5 mol%. SQUID measurements revealed that the presence of  $\text{Gd}^{3+}$  ions in the NPs are responsible for a decrease in saturation magnetisation, presumably as a result of the decrease in crystalline symmetry upon uptake of large  $\text{Gd}^{3+}$  ions into the  $\text{Fe}_3\text{O}_4$  lattice. This decrease in crystalline symmetry will have an associated increase in magnetocrystalline anisotropy. Preliminary studies show that human fibroblast cells exposed to  $\text{Gd:Fe}_3\text{O}_4$  NPs do not show critical toxicity, and specific absorption rate (SAR) measurements give SAR value of  $3.7 \pm 0.6 \text{ W/g}_{\text{Fe}}$ , slightly higher than the previously reported values.



a) TEM images of Gd:Fe<sub>3</sub>O<sub>4</sub> NPs and b) Cell metabolic activity with MTT assay of Fe<sub>3</sub>O<sub>4</sub> and Gd:Fe<sub>3</sub>O<sub>4</sub> NPs.

[1] P.S. Jiang et al., J. Nanosci. Nanotechnol., 12 (2012) 5076-5081.

## Magnetically modified sheaths of *Lepothrix* sp. as an adsorbent for Amido black 10 B

Ralitsa Angelova<sup>1,2,3</sup>, Eva Baldíková<sup>4,5</sup>, Kristyna Pospišková<sup>6</sup>, Mirka Safaríková<sup>1,4</sup>, Ivo Safárik<sup>1,4,6,\*</sup>

<sup>1</sup> Department of Nanobiotechnology, Biology Centre, ICB, CAS, Na Sadkach 7, 370 05 Ceske Budejovice, Czech Republic

<sup>2</sup> Department of General and Industrial Microbiology, Faculty of Biology, Sofia University “St. Kliment Ohridski”, 8 Dragan Tsankov Blvd, 164 Sofia, Bulgaria

<sup>3</sup> Laboratory Microwave Magnetics, Institute of Electronics, Bulgarian Academy of Sciences, 72 Tzarigradsko Chaussee Blvd, 1784 Sofia, Bulgaria

<sup>4</sup> Global Change Research Institute, CAS, Na Sadkach 7, 370 05 Ceske Budejovice, Czech Republic

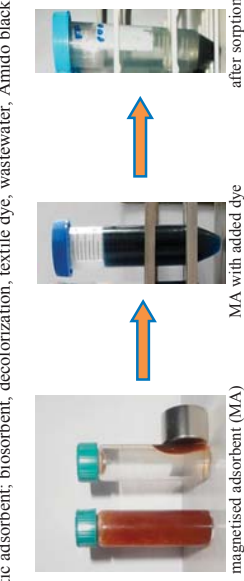
<sup>5</sup> Department of Applied Chemistry, Faculty of Agriculture, University of South Bohemia, Branisovska 1457, 370 05 Ceske Budejovice, Czech Republic

<sup>6</sup> Regional Centre of Advanced Technologies and Materials, Palacky University, Slechtitelu 27, 783 71 Olomouc, Czech Republic

The goal of this study was to assess the biosorption of Amido black 10 B dye from aqueous solutions on magnetically modified sheaths of *Lepothrix* sp. in a batch system. The magnetic modification of the sheaths was performed using both microwave-synthesized iron oxide nano- and microparticles and perchloric acid stabilized ferrofluid. The native sheaths and both magnetically modified materials were characterized by SEM and FTIR. The effect of various parameters was studied using the adsorbent magnetized by both methods.

The observed maximum adsorption capacities of both types of magnetized material at room temperature were found to be 339.2 and 286.1 mg of dye per 1 g of ferrofluid modified and microwave-particles modified adsorbent, respectively. The dye removal efficiency decreased with increasing the initial dye concentration. Thermodynamic study of dye adsorption indicates a spontaneous (negative value of Gibbs energy) and endothermic (positive value of enthalpy) process in the temperature range between 279.15 – 313.15 K. Positive value of entropy indicates an increase in randomness of adsorbed species. Maximum adsorption capacity was obtained at pH 2 value. The data were fitted to various equilibrium and kinetic models. Experimental data matched well with the pseudo-second order kinetics and Langmuir and Freundlich isotherm models.

It can be concluded that the *Lepothrix* sheaths have excellent efficacy for dye adsorption. This material can be used as an effective, low-cost adsorbent.



**Keywords:** *Lepothrix* sp.; sheaths; magnetic fluid; microwave synthesis; magnetic iron oxides; magnetic adsorbent; biosorbent; decolorization, textile dye, wastewater, Amido black 10 B

A demonstration of the excellent adsorption capacity of magnetized *Lepothrix* sheaths

Towards monitoring drug release *in situ* with multimodal radioluminescent, photoluminescent, and MRI Contrast Agents

Jeffrey N. Anker<sup>1,2\*</sup>, Gretchen Shober<sup>1</sup>, Hongyu Chen<sup>1</sup>, Thomas Moore<sup>2</sup>, Dan C. Colvin<sup>3</sup>, John C. Gore<sup>3</sup>, Frank Alexic<sup>2</sup>.

<sup>1</sup> Chemistry Department, Center for Optical Materials Science and Engineering Technology (COMSET), and SC BIOCAST, Clemson University

<sup>2</sup> Bioengineering Department, Clemson University

<sup>3</sup> Vanderbilt University Institute of Imaging Science (VUllS), Department of Radiology and Radiological Science, Vanderbilt.

\*Email: janker@clemson.edu

We synthesized gadolinium oxy sulfide phosphors for multimodal optical X-ray, and MRI imaging. The particles are photostable and emit light with narrow spectral peaks when excited by blue light, X-rays, or alpha/beta radiation. The particles can also be coated with polymers for targeting and/or controlled drug release. If the drug is labelled with a radionuclide (e.g., <sup>3</sup>H), radioactive decays will generate luminescence only when the drug is in close proximity to the phosphor. The drug release rate can therefore be monitored *in situ* by measuring the luminescence intensity, provided that the nanoparticle concentration/tissue extinction effects can be estimated with other techniques (e.g., external X-ray beam excitation). We discuss the requirements for such *in vivo* measurements and show preliminary results for several of features (X-ray imaging, MRI, photoluminescence and radioluminescence), and nanoparticle delivery to mouse brain tumor xenografts (Figure 1).

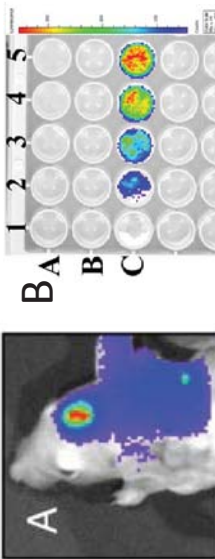


Figure 1. **A)** Non-invasive imaging of radioluminescent PEG-PLA-Gd<sub>2</sub>O<sub>3</sub>:S:Eu nanoparticles in intracranial glioblastoma tumor in BALB/C mouse. **B)** Radioluminescence from Gd<sub>2</sub>O<sub>3</sub>:Eu particles exposed to varying concentrations of alpha-emitting <sup>227</sup>Rn. Row A contains only Th(NO<sub>3</sub>)<sub>4</sub>, row B contains empty wells, and row C contains Gd<sub>2</sub>O<sub>3</sub>:Eu<sup>3+</sup> with linearly increasing Th(NO<sub>3</sub>)<sub>4</sub> concentrations (0, 7, 14, 21, 28 mg). Color bar represents raw luminescence photon counts.

## PMAA-stabilized ferrofluid/chitosan/yeast composite for bioapplications

E. Baládková<sup>1\*</sup>, M. Stepanek<sup>2</sup>, M. Uchman<sup>2</sup>, M. Slouš<sup>3</sup>, L. Nydlova<sup>1</sup>, K. Pospisikova<sup>4</sup>, M. Safarikova<sup>1,5</sup>, I. Safarik<sup>1,4,5</sup>

<sup>1</sup> Global Change Research Institute CAS, České Budějovice, Czech Republic (CR); <sup>2</sup> Department of Physical and Macromolecular Chemistry, Faculty of Science, Charles University, Prague, CR; <sup>3</sup> Institute of Macromolecular Chemistry, CAS, Prague, CR; <sup>4</sup> Regional Centre of Advanced Technologies and Materials, Palacky University, Olomouc, CR;

<sup>5</sup> Department of Nanobiotechnology, Biology Centre, Institute of Scientific and Technical Information of the Czech Academy of Sciences, České Budějovice, CR; \*email address: baludko@email.cz

A simple procedure for synthesis of magnetic fluid stabilized by poly(methacrylic acid) was developed. This ferrofluid was used to prepare magnetically responsive chitosan composite material. Both ferrofluid and PMAA/chitosan microparticles were characterized in detail using optical microscopy, scanning electron microscopy, transmission electron microscopy, static and dynamic light scattering, small-angle neutron scattering, energy dispersive X-ray spectroscopy and Fourier transform infrared spectroscopy.

Magnetic PMAA/chitosan microparticles were employed as a magnetic carrier for immobilization of baker's yeast, *Saccharomyces cerevisiae* cells were successfully incorporated into chitosan during its preparation. PMAA/chitosan/yeast biocomposite was then tested as an adsorbent of selected organic dyes. The experimental data followed well the Langmuir adsorption isotherm model, and the maximum adsorption capacities were found to be 116.6 mg/g and 104.3 mg/g for crystal violet and safranin O, respectively. This biocompatible material was also utilized for sucrose hydrolysis; enzyme activity of one-day and one-month old biocatalyst remained unaltered.

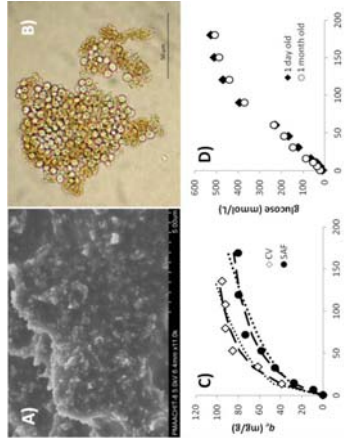


Fig.1: **A)** SEM image of the surface of PMAA-chitosan microparticles showing aggregates of iron oxide nanoparticles from the ferrofluid; **B)** optical microscopy of PMAA/chitosan/yeast composite; **C)** Langmuir (- - -) and Freundlich (---) adsorption isotherms on PMAA-chitosan/yeast composite; **D)** time dependence of sucrose hydrolysis using PMAA/chitosan/yeast biocatalyst

**Acknowledgements:** This research was supported by the Czech Science Foundation (Grant No. 14-11516S, Technology Agency of the CR (T101026118) and by Ministry of Education, Youth and Sports of the CR (LO1305 and POLYMAT LO1507, Program NPU).

# Ultrarapid detector of flowing labeled magnetic nanoparticles based on spin torque oscillator

Seyed Amir Hossein Banaziz<sup>1</sup>, Sohrab R. Sani<sup>1,2</sup>, Fatjon Qejvanaj<sup>1,3</sup>, S. Majid Mohseni<sup>4</sup> and Johan Åkerblom<sup>1,3,5</sup>

<sup>1</sup>) Department of Material and Nano Physics, School of Information and Communication Technology, KTH-Royal Institute of Technology, Electrum 229, 164 40 Kista, Sweden.

<sup>2</sup>) Department of Physics, New York University, New York, NY 10003, USA.

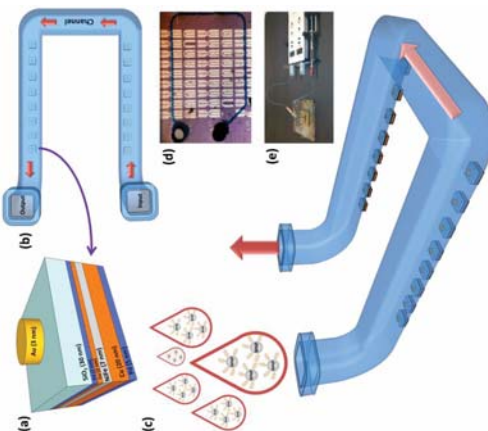
<sup>3</sup>) Nanosc AB, Electron 205, 164 40 Kista, Sweden.

<sup>4</sup>) Department of Physics, Shahid Beheshti University, 19839 Tehran, Iran.

<sup>5</sup>) Department of Physics, University of Gothenburg, 412 96 Gothenburg, Sweden.

Developing magnetic biosensors has become an important area of research with recent advances in nanomaterials and nanofabrications and these sensors have emerged as a powerful platform of diagnostic and monitoring tools. Among the developed spintronic devices, the Nano-Contact Spin Torque Oscillator (NC-STO) is a nano-scale electrical device which has a capability of generating microwave signals over a wide range of GHz frequencies and with a wide, and rapid, current and field tenability owing to spin momentum transfer. [1,2] The NC-STO is highly promising for applications in both ultra-fast and ultra-sensitive biosensors. The significant part of studies on magnetic sensing has been focused on GMR trilayers. While recently, in a novel type of STOs, its driven microwave signals from about 250 MHz to above 3 GHz based on a single ferromagnetic layer (Single-layer STOs) underneath a nano-contact, have been observed under zero applied field. [3]

In this study, we investigate using a series of the single layer STOs as a platform for a new type of magnetic biosensors. When this series of nano-scale devices are introduced into biological systems, their small size, ultra-sensitivity and operation in zero applied field enable them to operate as probes suitable as candidates for the next generation of diagnostic and therapeutic techniques. This sensor not only can be used for biological experiments as a rapid and accurate analyzer, but also provides an excellent potential to be placed in specific organs in our body to have a real time monitoring of drug delivery rate and performance, as well as diagnose different type of cancers using magnetic nanoparticles (MNP)s labeled by biomarkers and also to control therapies or to continuously monitor the relapse of cancer after the initial remission.



Schematic representation of (a) a single layer NC-STO, (b) a 2x8 array of NC-STOs (top view) with a microfluidic channel on top of them, (c) for the flowing liquid sample and (c) a sample including labeled MNP's which are entering the microfluidic channel. (d) The sensing area which has a 2x8 array of single layer NC-STOs. The blue line indicates the location of microfluidic channel fabricated using PDMS with a width of 100  $\mu\text{m}$ , and a length of 5 mm. (e) Implemented sensor test using a flow rate controller to inject the sample to the channel input and then extract it from the output.

## Influence of Material and Concentration on Nanoparticle Heating

M.M. Beck<sup>1,\*</sup>, C. Lammler<sup>1</sup>, B. Gleich<sup>2</sup>

<sup>1</sup> Institute for Machine Tools and Industrial Management, Technical University of Munich, Boltzmannstr. 15, 85748 Garching, Germany. <sup>2</sup> Institute of Medical Engineering, Technical University of Munich, Boltzmannstr. 11, 85748 Garching, Germany. \* Email: Mathias.Beck@tum.de

Choosing the material and amount of nanoparticles is one of the first steps in planning a process of electromagnetic heating of non-conductive materials. Except for custom synthesized particles, there is neither a general overview of different materials for nanoparticles nor a dependence of the heating rate on the filler degree if they are dispersed in a solid material.

The tested materials were several iron oxide alloys including rare earth compounds that may be paramagnetic on nanometer level (BaFeO, CoFeO, CoO, DyFeO, Fe<sub>2</sub>O<sub>3</sub>, Fe<sub>3</sub>Q<sub>4</sub>, MnFeO, NiZnFeO, SrFeO, YFeO and ZnFeO). These were dispersed using ultrasound in an epoxy resin which was then cured and therefore the particle immobilized. These probes were heated in an alternating electromagnetic field and compared regarding their SAR (specific absorption rate) over a range of field strength at 100 kHz. The tested magnetite (Fe<sub>3</sub>O<sub>4</sub>) showed the highest SAR, followed by NiZnFeO and maghemite (Fe<sub>2</sub>O<sub>3</sub>) (see Figure 1). The rare earth alloys showed only a small energy absorption.

Regarding the concentration, we tested magnetite and YFeO with 1 mass-%, 5 mass-% and 10 mass-% in a cured epoxy resin. As can be seen in Figure 2, the iron oxide showed a linear dependence of heating rate to concentration in the range up to 10 mass percent. This result can be used for process planning of nanoparticle heated systems.

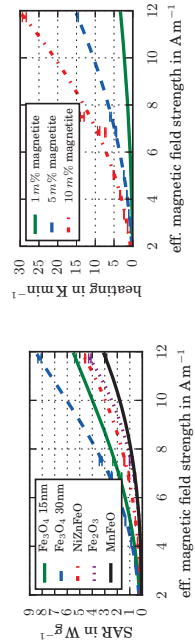


Figure 1: The two tested magnetits had the highest energy absorption. The different alloys did not show a higher SAR. Figure 2: The heating rate increased linearly with the amount of magnetic nanoparticles in the examined range from 1 to 10 mass percent.

- References:  
[1] J. Słoneczewski, J. Magn. Magn. Mater. **159**, L1 (1996).  
[2] L. Berger, Phys. Rev. B **54**, 9353 (1996).  
[3] S. R. Sani, et al., IEEE Trans. Magn. **49**, 4331 (2013).

## Numerical inversion methods to analyze magnetization data

P. Bender<sup>1</sup>, D. González-Alonso<sup>1</sup>, L. Fernández Barquín<sup>1</sup>, R. Costo<sup>2</sup>, M. P. Morales<sup>2</sup>, L. K. Bogart<sup>3</sup>, P. Southern<sup>3</sup>, Q. A. Pankhurst<sup>3</sup>, O. Posth<sup>4</sup>, U. Steinhoff<sup>4</sup>, C. Johansson<sup>5</sup>

<sup>1</sup>Departamento CITIMAC, Faculty of Science, University of Cantabria, 39005 Santander, Spain

<sup>2</sup>UCL Healthcare Biomagnetics Laboratory, 21 Albemarle Street, W1S 4BS London, UK

<sup>3</sup>Physikalisch-Technische Bundesanstalt, 10587 Berlin, Germany

<sup>5</sup>Acero Swedish ICT AB, 40014 Göteborg, Sweden

Email: benderpf@unican.es

<sup>1</sup>Department of Metallurgical Engineering and Materials Science, <sup>2</sup>Centre for Research in Nanotechnology and Science (CRNTS), Indian Institute of Technology Bombay, Powai, Mumbai-400076, India

<sup>3</sup>Department of MRI, Dr. Balabhai Nanavati Hospital and Research Center, Mumbai, India – 400056

\*To whom correspondence should be addressed. dhiren@iitb.ac.in (D. Bhaduri), +91-22-2576 7632. <sup>‡</sup> These authors contributed equally to this work.

Porous anisotropic  $\text{Fe}_3\text{O}_4@\text{SiO}_2$  nanocapsules of average length  $\sim$ 520 nm and diameter  $\sim$ 180 nm is prepared by annealing of  $\text{FeOOH}@\text{SiO}_2$  NRs at 300 °C under the continuous flow of forming gas ( $\text{H}_2$  7% + Ar 93%). The magnetic nanocapsules possess ferrimagnetic nature with magnetization of  $\sim$ 20 emu/g at 20 kOe and coercivity,  $H_c \sim$ 50 Oe. The aqueous suspension of the porous  $\text{Fe}_3\text{O}_4@\text{SiO}_2$  nanocapsules is stable over a time frame of one month and also exhibits a very high  $R_2$  relaxativity value of  $192 \text{ mM}^{-1} \text{ s}^{-1}$ . The enhanced  $R_2$  value is due to the anisotropic rod shape of nanocapsules which induce a strong magnetic field gradient and hence a fast dephasing of water protons. Further,  $R_2$  relaxivity of  $\text{Fe}_3\text{O}_4@\text{SiO}_2$  nanocapsules were analysed on HeLa cells for MRI contrast. As compared to untreated cells, a concentration dependent  $R_2$  darkening effect is observed in HeLa cells incubated with  $\text{Fe}_3\text{O}_4@\text{SiO}_2$  nanocapsules. The porous nanocapsules show high loading efficiency of 65 % of doxorubicin (DOX) in 2 mg of  $\text{Fe}_3\text{O}_4@\text{SiO}_2$  NRs and hence is an excellent drug carrier vessel. The drug release study shows a pH-dependent behavior with  $\sim$ 58% release at pH 7.4 and  $\sim$ 17% release at pH 7.4 over a period of 72 h. The induction heating studies of the NRs at different alternating magnetic fields (293, 335, 377 and 419 Oe) were carried out, which exhibit a sharp increasing trend of SAR value with the increase of magnetic field. These anisotropic nanocapsules seem to possess excellent theranostic properties.

## Porous Anisotropic $\text{Fe}_3\text{O}_4\text{-SiO}_2$ Nanocapsules for Theranostic Applications

Muhammad Shabbaz Beg,<sup>1,‡</sup> Jeetkanta Mohapatra,<sup>2,‡</sup> Lina Pradhan,<sup>2,‡</sup> D. Bhaduri,<sup>1</sup> Department of Metallurgical Engineering and Materials Science, <sup>2</sup>Centre for Research in Nanotechnology and Science (CRNTS), Indian Institute of Technology Bombay, Powai, Mumbai-400076, India

There is an urgent need for the standardization of the physical properties of magnetic nanoparticles, particularly for clinical applications of magnetic nanoparticles [1]-[4]. The aim of the EU FP7 project NanoMag is to improve, redefine and ultimately standardize existing analysis methods [5]. One of the main objectives within this project is to identify distinct correlations between the macroscopically measurable quantities of particle ensembles to the physical properties of individual particles on the nanoscale. Of vital importance is the analysis of DC and AC magnetization measurements to extract, for example, the core magnetic moment and relaxation time distributions of the particle ensembles. These distributions determine the macroscopic properties of the samples and are decisive for the particle performance with respect to the intended application. For example in magnetic hyperthermia, the optimization of the magnetic relaxation behaviour, leading to a maximum in energy absorption at a given driving frequency, is of utmost interest.

The usual approach to extract the core moment or relaxation time distribution from DC and AC magnetization measurements is by fitting the experimental data on the basis of an assumed shape of the distribution function (e.g. log-normal [6]). In the case of more complex magnetization behavior of such ensembles (e.g. core-shell types or multimodal distributions), *a priori* assumptions of the distribution can result in misleading results, as briefly discussed in [7]. With this in mind, Rijssel et al. [7] amongst others, opted for a numerical inversion of the  $M(H)$  data to extract the discrete core moment distribution  $P(\mu)$ . In recent years several other inversion methods were introduced for the analysis of DC magnetization data [8,9].

In the present study we apply these methods to analyze  $M(H)$  curves of typical iron oxide nanoparticle ensembles (Figure 1). Additionally, we test whether these methods are suitable to extract the relaxation time distribution from AC susceptibility measurements to obtain more detailed information about their quite complex relaxation behavior in colloidal dispersion. This work is supported by EU FP7 project NanoMag (grant no. 604448).

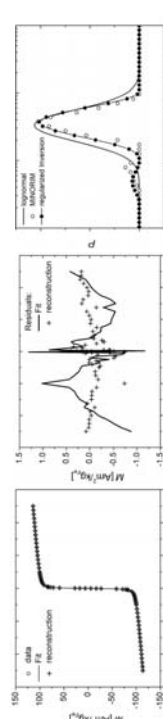


Figure 1. **Left:** Isothermal magnetization measurement of a colloidal dispersion of IONPs ( $d = 11 \text{ nm}$ ) at  $T = 300 \text{ K}$ , the lognormal fit and the reconstructed  $M(H)$  curve for  $P(\mu)$  determined by numerical inversion using MINORIM [7]. **Middle:** Residuals of the reconstructed curve are close to zero, whereas for the lognormal fit systematic deviations are observed. This strongly indicates that the  $P(\mu)$  determined by numerical inversion is a close approximation of the "real" distribution. **Right:** Extracted moment distributions by fitting  $M(H)$  under assumption of a lognormal distribution, by numerical inversion using MINORIM [7] and by a regularized inversion comparable to Berkov et al. [8].

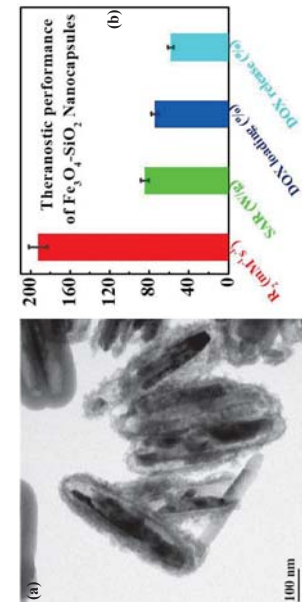


Figure 2: (a) TEM image of Porous  $\text{Fe}_3\text{O}_4\text{-SiO}_2$  Nanocapsules and their (b) theranostic performance.

- [1] Q. Pankhurst et al. *J. Phys. D Appl. Phys.* **36** (2003) R167-R171. [2] O. Posth et al., In *IMEKO XXI World Congress* (pp. 1362-1367) [3] S. Bogren et al., *Int. J. Mol. Sci.* **16** (2015) 20308-20325. [4] F. Ludwig et al., *Magnetics, IEEE Trans. Mag.* **50** (2014) 5300204-1-51 NanoMag-Project. Available online: [www.nanomag-project.eu](http://www.nanomag-project.eu). [5] R. W. Chantrell et al., *IEEE Trans. Mag.* **14** (1978) 975-977. [6] J. van Rijssel et al., *JMM* **353** (2014) 110-115. [7] D. V. Berkov et al., *J. Phys. D: Appl. Phys.* **33** (2000) 1-7. [8] T. Weser et al., *Z. Phys. B Condens. Matter* **59** (1985) 253-256.

## Inclusion of Dipolar Interactions in the Mathematical Modelling of Magnetic Hyperthermia through the Landau-Lifshitz-Gilbert equation

Materials Characterisation and Processing Group, Waterford Institute of Technology, Waterford, Ireland.

[pjcregg@wit.ie](mailto:pjcregg@wit.ie), [kmarfey@wut.ie](mailto:kmarfey@wut.ie), [mangalka@gmail.com](mailto:mangalka@gmail.com)

Magnetic hyperthermia is the heating of magnetic nanoparticles (MNPs) via a varying magnetic field. This heating can directly kill cancer cells, so by locating particles in a tumour, magnetic hyperthermia treatment (MHT) can be effected. Furthermore in combination with radiotherapy and/or chemotherapy lower levels of heating can be effective. Better design of MHT can be achieved through a greater understanding of the complexities of the heating mechanisms. The role of interparticle interactions has been acknowledged as being significant in modelling MHT[1][2]. Furthermore, there are typically two mechanisms which lead to heating, Delye and Néel relaxation. Recently, the Néel relaxation has received increased attention [3][4]. This study models the Néel mechanism of heating through the Landau-Lifshitz-Gilbert equation and incorporates interparticle interactions that can occur when the particles are closely spaced. This model should allow for greater understanding of the experimental measurement of the heating where the strength and frequency of the field are varied and so allow for better control of the heating to optimise the therapeutic effects of Magnetic Hyperthermia. Results show significant dependence of the average heating on interparticle positions and distance. The Néel model in the limit of high damping can be readily adapted for Debye relaxation by appropriate rescaling of parameters.



Figure 1: Damped precession of magnetic moments of MNPs in random positions and orientations due to an external magnetic field,  $H$ .

## References

- [1] Luis C. Brancutino et al. Effect of magnetic dipolar interactions on nanoparticle heating efficiency: Implications for cancer hyperthermia. *Sci. Rep.*, 3:2887, 2015.
- [2] J. Carrey et al. Simple models for dynamic hysteresis loop calculations of magnetic single-domain nanoparticles: Application to magnetic hyperthermia optimization. *J. Appl. Phys.*, 109(8), 2011.
- [3] R. Regmi et al. Temperature dependent dissipation in magnetic nanoparticles. *J. Appl. Phys.*, 115(17), 2014.
- [4] P. F. de Châtel et al. Magnetic particle hyperthermia: Néel relaxation in magnetic nanoparticles under circularly polarized field. *J. Phys.: Condens. Matter*, 21:124202(8pp), 2009.

**Magnetic carbon nanotubes combining MRI and therapy as nanoprobes to explore biological processes.**

**D. Begin<sup>1</sup>, D. Mertz<sup>2</sup>, A. Bianco<sup>3</sup>, F. Gazeau<sup>4</sup>, S. Begin-Colin<sup>2</sup>**

1- Institut de Chimie et Procédés pour l'Energie, l'Environnement et la Santé (ICPEES) UMR-7515 CNRS-Université de Strasbourg, 25 rue Becquerel, 67087 Strasbourg cedex 2 France

2-Institut de Physique et de Chimie de Strasbourg (IPCMS) UMR 7504 CNRS-Université de Strasbourg, 23 rue du Loess, BP 34 67034 Strasbourg cedex 2, France

4- CNRS, Institut de Biologie Moléculaire et Cellulaire, Laboratoire d'Immunopathologie et Chimie Thérapeutique, UPR 3572, 67000 Strasbourg, France

4- Laboratoire Matière et Systèmes Complexes (MSC), UMR 7057 CNRS/Université Paris-Diderot, PRES Sorbonne Paris Cité, 75205 Paris cedex 13, France

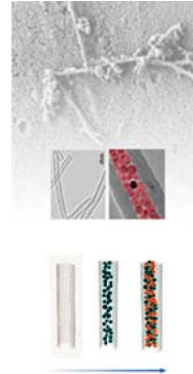
In the field of the synthesis and functionalization of magnetic nanoparticles (NPs) for biomedical applications, most researches aim at developing multifunctional theranostic NPs which can both identify disease states and deliver therapy and allow thus following the effect of therapy by imaging. The main challenges are the design of NPs which will allow, in one nano-object, combining imaging and efficient therapy, the design of an organic coating for colloidal stability and their *in vitro* and *in vivo* validation.

In that context, we have developed magnetic carbon nanotubes combining both diagnostic and therapeutic properties. Carbon nanotubes (CNTs) were filled with a very high loading with ferrite NPs to develop their magnetic manipulation and theranostic applications. The originality of the filling process was the use of CNTs as nanoreactors and which provide also stable containment of nanomagnets.

Cellular studies showed very promising results in terms of magnetic handling and hyperthermia at the subcellular level. The magnetic CNTs thus prepared are adjustable within the cell by an external magnetic field. By rotating them such a nano-drilling on the cells, they increase their uptake by tumor cells and potentiate the cytotoxic effect of light irradiation. They are capable of absorbing and efficiently converting NIR light into heat to generate thermoabative temperatures and cell lysis. They can be used as T2 agents for MR image-guided photothermal therapy.

These multifunctional magnetic CNTs visible by MRI, activated by light and manipulated magnetically are good candidates for local activation and control of biological processes in the body.

**References :** *Chem. Mater.* 2012, 24, 1549–1551, *Nanoscale* 2013, 5, 4412–4421, *J. Mater. Chem. A*, 2013, 1, 13853–13861, *Chemistry – An Asian Journal*, 2015, 10, 160–165, *ACS Nano* 2014, 8, 11290–11304



## Assessment of synthesis-dependent oxidative aging of iron oxide nanoparticles as determined using room temperature Mössbauer spectroscopy

L.K. Bogart<sup>1\*</sup>, C. Blanco-Andujar<sup>2</sup> and Q. A. Pankhurst<sup>1</sup>

\*email: l.bogart@uci.ac.uk

<sup>1</sup> Healthcare and Biomagnetics Laboratory, University College London,  
21 Albemarle Street, London, W1S 4BS, UK

<sup>2</sup> Institut de Physique et de Chimie des Matériaux de Strasbourg (IPCMS), UMR CNRS-UdS 7504, 23 rue du Loess, BP 43, 67034 Strasbourg cedex 2, France

The potential use of iron oxide nanoparticles (IONPs) in biomedical applications is well known [1]. In many cases, magnetite has been preferred over maghemite because of its higher saturation magnetisation moment; however, the ferrous iron in magnetite can have toxic consequences *in vivo* due to the Fenton reaction [2]. With this in mind, any IONP system intended for *in vivo* use requires quantification of its ferrous iron content, using a suitable method such as that recently reported using  $^{57}\text{Fe}$  Mössbauer spectroscopy [3, 4]. In this work we highlight that an additional aspect that must be taken into account is the oxidative aging characteristic of the IONPs, and that this may vary significantly from one synthesis route to another.

In this study, we compare the oxidative aging of IONPs synthesised using standard co-precipitation and novel microwave-assisted routes. Both samples have identical mean core size and initial mean magnetite content (50% w/w magnetite/maghemite), and were stored under ambient conditions for two years. Evolution of the mean magnetic content was assessed using Mössbauer spectroscopy (Figure 1), which can be used to accurately distinguish between magnetic and maghemite with  $\pm 5\%$  uncertainty [3, 4]. We observe that the magnetic content of co-precipitation samples dropped to ca. 25% in 10 days, whilst the microwave samples took ca. 100 days to reach the equivalent point. In both samples, we observed a rate of oxygen diffusion that is two orders of magnitude faster than that expected in bulk magnetite at 300 K [5, 6], which we consider most likely to be related to the nanoparticulate state.

It is notable that both preparative routes result in materials that show significant oxidative aging for an entire year after synthesis. This result may be an important consideration for researchers in the field, given that commonly measured *in vitro* cell line parameters such as cytotoxicity might prove to be dependent on how recently the IONPs in question were synthesised.

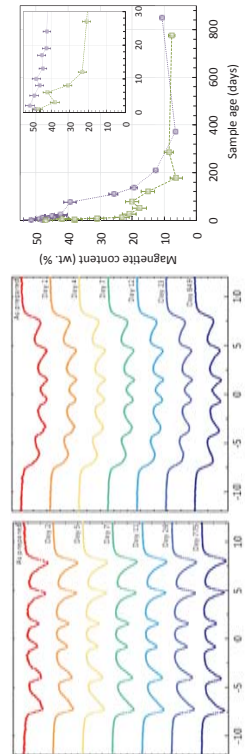


Figure 1. Normalised room temperature Mössbauer spectra for IONPs synthesised using (left) co-precipitation, CP, and (middle) microwave synthesis, MS, techniques. Right panel: temporal evolution of the mean magnetite content (w/w % magnetite/maghemite+maghemite) for the CP (circles) and MS (triangles) samples.

## Small and biocompatible coatings of iron oxide nanoparticles for improved detection and treatment of metastases

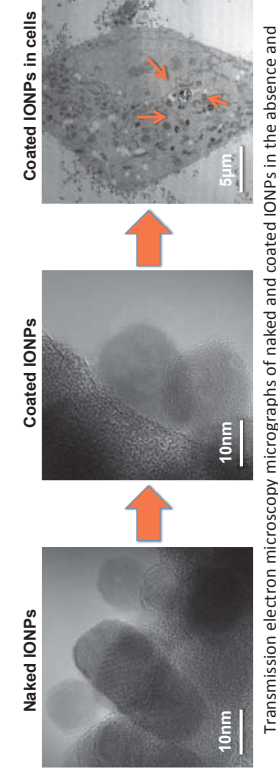
D. Bonvin<sup>a\*</sup>, D. T.L. Alexander<sup>b</sup>, H. Hofmann<sup>a</sup>, and M. Mionic Ebersold<sup>a,c,d</sup>

<sup>a</sup>Powder Technology Laboratory, Ecole polytechnique fédérale de Lausanne (EPFL), Lausanne, Switzerland  
<sup>b</sup>Interdisciplinary Centre for Electron Microscopy (ICME), Ecole polytechnique fédérale de Lausanne (EPFL), Lausanne, Switzerland

<sup>c</sup>Center for Biomedical Imaging (CIBM), Lausanne, Switzerland

<sup>d</sup>Department of Radiology, University Hospital (CHUV) and University of Lausanne (UNIL), Lausanne, Switzerland  
<sup>\*</sup>EPFL STI IMX LTP, MXD 333, Station 12, 1015-Lausanne, Switzerland, debora.bonvin@epfl.ch

Lately, iron oxide nanoparticles (IONPs) have been the focus of intense clinical research. One very promising application is their use in theranostics where IONPs act both as contrast agents for magnetic resonance imaging (MRI) and as heating sources for tumor elimination. As their *in vivo* performance strongly depends on their stability in aqueous solutions, we developed biocompatible coatings to prevent their aggregation in unbuffered water. Current coatings are made of large molecules such as sugars (e.g. dextran) or polymers, which are known to accumulate in the liver and spleen, diminishing the IONPs' access to the tumor and exerting toxic effects. Here, we report the results of *in vitro* screening of 11 biocompatible coating strategies based on small molecules. Small coating sizes increase the number of IONPs which can be located inside small volumes, for instance metastases in lymph nodes (< 3mm), and thus improve the efficiency of hyperthermia treatment as well as increase the MR signal. In order to target this particular type of tumors, we chose coating molecules with at least one functional chemical group for further coupling with targeting ligands (e.g. antibodies). This specific and exclusive location of IONPs inside tumors not only removes false negatives in MR images (tumors which appear as healthy spots), but also avoids serious secondary damage of healthy body tissues during the hyperthermia treatment. The 11 coated-IONPs were fully characterized, revealing the presence of the coating molecules arranged in 2 to 3 layers longitudinally to the IONPs. As the biological environment responds very differently in contact with IONPs of different sizes and surface charges, the hydrodynamic diameters and zeta potentials of coated-IONPs were determined by dynamic light scattering (DLS) to predict their *in vivo* behavior. In addition, qualitative and quantitative analysis of the chemical groups available for further functionalization of the IONPs with targeting ligands was done by X-ray photoelectron spectroscopy (XPS). Besides the physico-chemical characterization of the coated-IONPs, we investigated their *in vitro* behavior in the presence of different cell lines and showed very low toxicities and coating-dependent cellular uptake.



Transmission electron microscopy micrographs of naked and coated IONPs in the absence and presence of lymph node metastases cells.

- [1] Q.A. Pankhurst *et al.* *J. Phys. D Appl. Phys.* **36** (2003) R167-R181 [2] Brillat, E.; Sires, I.; Oltraz, M. *A. Chemistry. Chem. Rev.* (2009) **109**, 6570-6631; [3] da Costa, G., *et al.* *J. Phys. Chem. B* (2014), **118**, 11738-11746; [4] Salazar, J. S., *et al.*, *Chem. Mater.* (2011) **23**, 1379-1386; [5] Gallagher, K. J., *Nature* (1968) **217** 1118-1121; [5] Sidhu, P. S., *et al.*, *J. Inorg. Nucl. Chem.* (1977) **39**, 1953-1958.

## Combined magneto-thermo-chemotherapy of solid tumors controlled by MRI and electronic sensor

N.A. Brusentsov<sup>a</sup>, I.S. Golubeva<sup>a</sup>, Yu.A. Pirogov<sup>b</sup>, N.V. Anisimov<sup>b</sup>, M.V. Gulyaev<sup>b</sup>,

V.A. Polianskiy<sup>c</sup>, A.V. Zhukov<sup>c</sup>, V.D. Kuznetsov<sup>d</sup>, O.A. Bocharova<sup>a</sup>

<sup>a</sup>Blokhin Russian Cancer Research Center, RAS, 115478 Moscow, Russia; <sup>b</sup>Lomonosov Moscow State University, Moscow 119992, Russia; Institute of Mechanics, MSU, Moscow 117192; <sup>c</sup>Mendeleev University of Chemical Technology of Russia, 125047 Moscow, Russia. E-mail: brusensov2005@yandex.ru

Magnetically controlled Dextran-ferrite nanoparticles (DF) have been successfully tested as a negative MRI contrast agent for imaging centers early malignant proliferation of solid tumors in mice 3 - 4 days after tumor inoculation. Method of early contrast magnetic resonance imaging (MRI) has been developed on the basis of successive intravenous injections of DF and Magnevist® (MVI). Fig. 1 (a, b, c, d). To reduce toxicity of arsenic on normal tissue and the limitations of traditional thermotherapy, improve activity of Fe<sub>3</sub>O<sub>4</sub> were doped by As<sub>2</sub>O<sub>3</sub> and coated by dextran (DF-As<sub>2</sub>O<sub>3</sub>). Contents: Fe<sub>3</sub>O<sub>4</sub> of 26 to 27%; As<sub>2</sub>O<sub>3</sub> of 0.2 to 0.3%; H<sub>2</sub>O from 1.7 to 1.9%; dextran 71-72% [1, 2]. Quantitative determination DF in mice performed on the basis of their nonlinear magnetization by an electronic sensor with inductive coils [3]. By scanning of animal body with primary and infiltrative tumors on the electron-sensor defined quantity of DF and therapy view. DF-As<sub>2</sub>O<sub>3</sub> content was evaluated in mice liver and tumor: when the ratio of tumor / liver exceed ten carried multi-layered capsule surrounding MPC (between white arrows); (c) MRI image of vessels feeding malignant proliferation centers (MPC) (between black arrows); (d) multi-layered capsule surrounding MPC, 4-5 days after inoculation (MTHT) tumors in controlled conditions. The first set 48 mice with adenocarcinoma Ca 755 (Ca 755), the second set 48 mice with a solid form of Ehrlich carcinoma (EC)

(EC) images showing the development of Ehrlich carcinoma (EC). (a) Early contrast MRI images start malignant inflammation within 1-2 days after inoculation 10<sup>6</sup> axillary viable EC cells (ECV); (b) swelling, malignancy, focal tissue proliferation and angiogenesis in 3-4 days after the inoculation of ECC (large black arrow), ectema and vascular malignancy (small black arrows); (c) MRI image of vessels feeding malignant proliferation centers (MPC) (between white arrows); (d) multi-layered capsule surrounding MPC, 4-5 days after inoculation (MTHT) tumors in controlled conditions. The first set 48 mice with adenocarcinoma Ca 755 (Ca 755), the second set 48 mice with a solid form of Ehrlich carcinoma (EC) were divided into 3 groups each (1, 1' groups of 12 mice; 2, 2' mice and 3, 3' mice). Tumor volume was 3 - 4 mm<sup>3</sup> in the first- and second sets (groups 1-3) and 5 - 10 mm<sup>3</sup> in 1'-3' groups. By scanning of animal body with primary and infiltrative tumors on the electron-sensor scanner defined quantity of DF-As<sub>2</sub>O<sub>3</sub> and therapy view.

In each six mice from 2, 2' groups we treated by MTCT. Into the tumor a composition of DF sol (0.2 ml 40%) was injected together with mixture of chemo drugs: Mitoxantrone (MX) - 0.5 mg/kg, Dacarbazine (DC) - 5.0 mg/kg and Doceataxel (DT) - 2.5 mg/kg. In each six mice from 3, 3' groups we treated by MTHT: into the tumor a composition of DF-As<sub>2</sub>O<sub>3</sub> sol (0.2 ml of 40%) was injected together with mixture of MX 0.5 mg/kg, DC 5 mg/kg and DT 2.5 mg/kg. Within 35 minutes of mice maintained in RF magnetic field at 0.88 MHz produced by localized high-Q resonator fed with 0.15 kW power. Was assessed the artifactor characteristics of this complex DF-As<sub>2</sub>O<sub>3</sub>-MX-DC-DT. In control: each 12 mice from 1, 2 sets, 1, 1' groups-only the buffer (0.9% NaCl) was injected and MTHT 6 x 35 min was done in a 3 days after tumor inoculation. For Ca 755 (group 1), all animals died within 36 days; (Group 1') all animals died within 27 days. In experiment: MTCT 6 x 35 min was done in a 3 days after tumor inoculation, using combinations of DF 0.2 ml 40% sol with MX 0.5 MR / kg DT 2.5 MR / kg increased life span of mice with Ca 755 in group 2 to 190%, in group 2' to 180%, and in EC, group 2 to 70%, and in EC, group 2' to 50%; MTCT 6 x 35 min was done in 3 days after tumor inoculation, using combinations of DF-As<sub>2</sub>O<sub>3</sub> 0.2 ml 40% sol with MX 0.5 MR / kg, DC 5.0 MR / kg DT 2.5 MR / kg in group 3 increased life span of mice with Ca 755 to 210%, in group 3' to 170% for EC Group 3 to 200%, in group 3' up to 140%.

Different aspects of the work were supported by RFBR grants: N 16-01-00157; 14-29-07271; 14-02-00840; 15-02-07791; 15-04-09372; 15-04-09499; 15-33-21072.

References:  
[1] N.A. Brusentsov, J. Gen. Chem. Ru. 83 (2013) 2548-2558. doi:10.1134/S1070363213120530.

## Harnessing viscosity effects to tailor the dynamical magnetic response of magnetic nanoparticles

David Cabrera<sup>1</sup>, María Elena Matera<sup>2</sup>, Aidin Lak<sup>2</sup>, Daniel Ortega<sup>1,3</sup>, Pablo Guardia<sup>2</sup>, Ayyappan Sathya<sup>2</sup>, Frank Ludwig<sup>4</sup>, Teresa Pellegrino<sup>2</sup> and Francisco J. Teran<sup>1,3</sup>

1) IMdea Nanociencia, Campus Universitario de Cantoblanco, 28049 Madrid, Spain.  
2) Istituto Italiano di Tecnologia, via Morego 30, 16163 Genova, Italy.  
3) Nanobiotechnolog (IMdea Nanociencia), Unidad Asociada al Centro Nacional de Biotecnología (CSIC), 28049 Madrid, Spain.

4) Institut für Elektrische Messtechnik und Grundlagen der Elektrotechnik, TU Braunschweig, D-38106 Braunschweig, Germany

The potential of magnetic heating mediated by magnetic nanoparticles (MNP) to remove tumors has boosted the research on magnetic hyperthermia. The precise control of MNP heat release is crucial for clinics and requires that heating efficiency remains invariant under distinct environmental conditions. In superparamagnetic MNP, the interplay between Néel and Brownian relaxation processes governs the MNP heating efficiency under different viscosity conditions. In order to better understand the parameters that render the magnetic hyperthermia response sensitive to viscosity, we have studied the AC magnetic response from different magnetic nanoparticles dispersed in distinct viscous media. We observed that SAR values from 21 nm cobalt ferrite MNP dispersed in water undergo a 99% decrease upon increasing viscosity 60 times. Besides, 19 nm magnetic nanocubes show a 80% SAR decrease but just 16% for 14 nm nanocubes. The SAR reduction with viscosity is clearly visualised by studying the shape changes of the corresponding AC hysteresis loops. Such variations are different for cobalt ferrite (where remanence and coercivity diminish) and iron oxide (where remanence diminishes and coercitivity is maintained constant) MNP. AC susceptibility measurements reveal that such viscosity effects are related to magnetic anisotropy. Thus, Brownian/Néel magnetic relaxation process dominates for MNP with large/small anisotropy energy barrier, respectively. Even in the case of MNP where Néel relaxation dominates, we have found that the AC magnetic response is sensitive to viscosity under given alternating field conditions. Low field intensities render AC hysteresis loops remarkably sensitive to viscosity, opposed to the case of large field intensities, independently of frequency values. These results contribute a more precise identification of the best MNP candidates and field conditions for the clinical applications of magnetic hyperthermia.

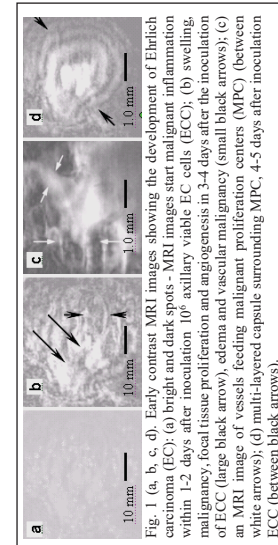


Fig. 1 (a, b, c, d). Early contrast MRI images showing the development of Ehrlich carcinoma (EC). (a) Bright and dark spots; (b) MRI images start malignant inflammation within 1-2 days after inoculation 10<sup>6</sup> axillary viable EC cells (ECV); (c) malignancy, focal tissue proliferation and angiogenesis in 3-4 days after the inoculation of ECC (large black arrow), ectema and vascular malignancy (small black arrows); (d) MRI image of vessels feeding malignant proliferation centers (MPC) (between white arrows); (e) multi-layered capsule surrounding MPC, 4-5 days after inoculation (MTHT) tumors in controlled conditions.

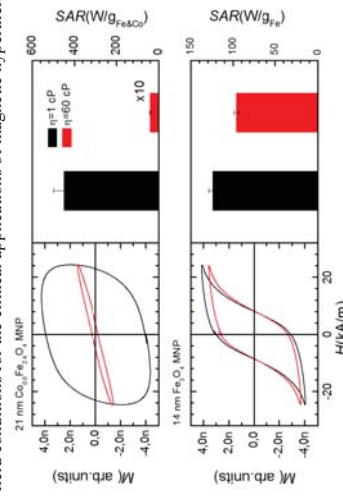


Figure: AC hysteresis loops and SAR values obtained from MNP dispersed in different viscosity media at 100 kHz and 24 kA/m.

## Fabrication of Bio-Magnetic Sensors based on Macromolecules Functionalized Iron Oxide Nanoparticles

Sudeshna Chandra<sup>1,2</sup>, Mayank Gupta<sup>1</sup>, Dhirendra Bahadur<sup>1</sup>

<sup>1</sup>Department of Metallurgical Engg. & Materials Science, Indian Institute of Technology Bombay  
Powai, Mumbai-400076, India

<sup>2</sup>Department of Chemistry, Sunandan Divatia School of Science, NMIMS University  
Vile Parle (West) Mumbai-400056, India Email: [sudeshna.chandra@nmims.edu](mailto:sudeshna.chandra@nmims.edu)

Functionalized iron oxide (magnetic) nanoparticles are a very promising candidate for detection and sensing of target molecule as they can be manipulated and detected by magnetic interactions. The biological recognition moiety of the functionalized coating results in binding of the target analyte which causes a change in the interaction of the nanoparticles under the influence of an external magnetic field. This forms the basis of the fabrication of a bio-magnetic sensor. The present study reports the use of three different macromolecules *viz.* glycol chitosan (GC), poly ethylene glycol methyl ether (PEGME) and poly sodium stereo-4 sulphate (PSSNa) to functionalize and cap the magnetic nanoparticles. The magnetic nanoparticles were characterized using FTIR, XRD, TEM and TGA to evaluate their structural and surface properties. TEM shows spherical shaped nanoparticles with mean size of ~11, 12 and 13 nm for GC, PEGME and PSSNa-MNPs respectively. TGA evaluates the weight loss of the modified MNPs and confirms the coating on the surface of the MNPs. Bovine serum albumin (BSA) was immobilized on the functionalized MNPs and detection studies were carried out using AC susceptibility studies on a physical property measurement system. Detection of BSA immobilized functionalized MNPs was exhibited at 300 K by the measurement of the imaginary part of the magnetic susceptibility over a frequency range and is based on the changes of dynamic magnetic properties of the magnetic nanoparticles which makes use of the Brownian relaxation of magnetization (Figure 1).

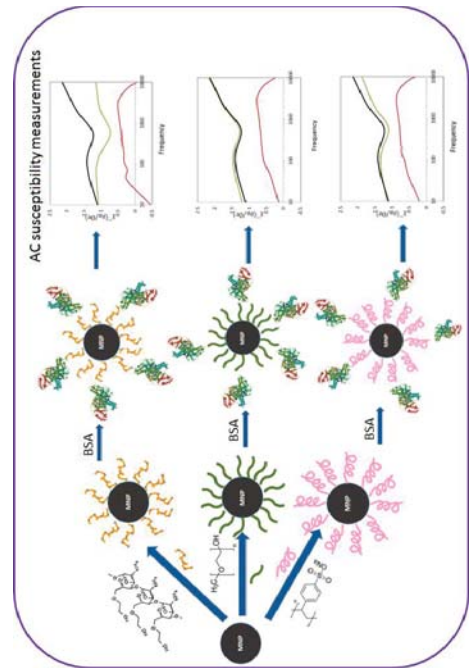


Figure 1: Schematic representation of the proposed bio-magnetic sensor based on functionalized magnetic nanoparticles

## Mechanically-induced necrosis of human malignant cells by sharp magnetic nanoparticles

Horia Chiriac, Dumitru-Daniel Herlea, Ecaterina Radu, Nicoleta Lupu

National Institute of Research and Development for Technical Physics, 700050 Iasi, Romania

The incidence of cancerous disease is expected to increase worldwide by more than 75% by the year 2030. Consequently, much effort is focused on finding novel efficient therapies to cure cancer or reduce the side effects of current treatments. Therefore, apart from the conventional medical methods based on molecular or radio-therapy, other approaches focusing on magnetic materials as platforms for inducing physical destruction of the cancerous cells are also considered. Accordingly, it was very recently showed that disk-shaped permalloy microparticles with magnetic anisotropy, placed in rotating magnetic fields, can affect irreversibly the fate of a cancerous cell through mechanical disruption of the cell membrane [1,2]. Here, we present our latest results regarding the effect of biocompatible magnetite nanoparticles with shape anisotropy and sharp edges on the viability of human osteosarcoma cancerous cells. The magnetic particles were synthesized by chemical precipitation starting from  $\text{FeCl}_2$ , glycerin and NaOH. The nanoparticles were generally in octahedral, pyramidal or prismatic shape (Fig. 1).

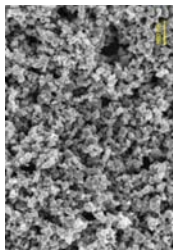


Figure 1. SEM image of the sharp magnetic nanoparticles.

After incubation with cancerous cells for 24 h, the particles were subjected to vibrating magnetic fields (0.3 T and frequency of 3 Hz) for 3 min. The nanoparticles, aligned in chains, followed the lines of the dynamic magnetic fields and induced necrosis of the cells through strong mechanical interactions. After magnetic treatment, the viability of the cells was evaluated by using a conventional MTT colorimetric assay versus controls. The results showed that the cytotoxic effect is related to the concentration of magnetic nanoparticles. Accordingly, for 0.5 mg/mL concentration, the viability decreased with 12%, whereas for 5 mg/mL the decrease was about 40%. We assume that the cell necrosis has resulted from the mechanical disruption of the cells network, cell membrane or/and the inner organelles. The influence of the magnetic field intensity and dimensions of the magnetic nanoparticles on the cell viability will be also presented. In a comparative experiment, we have tested the magnetic hyperthermia effect induced on the cancerous cells by the magnetic nanoparticles when subjected to alternating magnetic fields (30 mT). The results showed a decrease of cell viability of about 45% for a concentration of nanoparticles of 5 mg/mL. This study showed that sharp magnetic nanoparticles can be good candidates for the newly developed approach for cancer treatment. By conjugation with anticancer drugs and coupled with magnetic hyperthermia processes, these anisotropic nanoparticles could greatly improve the necrosis rate and therefore the success of the anti-cancer treatment.

The research for this paper was financially supported by the ANCSI through Nucleu Program, Contract No. 28N/2016 (PN 16 37 01 03).

[1] Yu Cheng et al., *Rotating magnetic field induced oscillation of magnetic particles for in vivo mechanical destruction of malignant glioma*, Journal of Controlled Release **223** (2016) 75–84.

[2] [http://www.ieemagnetics.org/index.php?option=com\\_content&view=article&id=236&Russell\\_Cowburn&catid=78:2015-distinguished-lecturers-&Itemid=165](http://www.ieemagnetics.org/index.php?option=com_content&view=article&id=236&Russell_Cowburn&catid=78:2015-distinguished-lecturers-&Itemid=165).

## Preparation and characterization of a low Curie temperature Fe-Cr-Nb-B ferrofluid

Horia CHIRIAC, Ecaterina RADU, Camelia DANCEANU, George STOIAN, Nicoleta LUPU  
National Institute of Research and Development for Technical Physics, 700050 Iasi, Romania

Ferrofluids are colloidal suspensions of magnetic particles (NPs) that have been lately investigated for different biomedical applications such as contrast agents for MRI, magnetic cell separation, magnetically guided embolization and magnetic hyperthermia. Recently, we have developed a new type of ferrromagnetic nanoparticles with Curie temperature ranging from 16 to 50°C based on glassy Fe<sub>79-x</sub>Cr<sub>x</sub>Nb<sub>0.3</sub>B<sub>20</sub> alloys ( $\alpha = 11.5\text{-}13\text{ at.\%}$ ) [1]. A content of 12.5% Cr leads to a Curie temperature around 47°C. These particles appear to be suitable for self-regulated hyperthermia and are also biocompatible, as shown in our previous studies [2]. The purpose of this work was to prepare a ferrofluid based on low Curie Fe<sub>67.2</sub>Cr<sub>1.2</sub>Nb<sub>0.3</sub>B<sub>20</sub> particles, to have a suspension of particles with good stability and to avoid their agglomeration, aspects that are important in biomedical applications. To this aim, NPs with sizes under 100 nm were dispersed by sonication for 30 min. at 80°C in an aqueous solution containing calcium gluconate, then the mixture was allowed to settle for 12 h. The suspension was separated in two phases: an excess of gluconate solution on top and a black ferrofluid, which could be manipulated with a magnet, on the bottom. The upper part was removed and the resulting ferrofluid was subjected to further analysis. The obtained saturation magnetization for the ferrofluid was 1.5 emu/cm<sup>3</sup>. The heating power of the ferrofluid was investigated by using a magnetic induction hyperthermia unit. The SAR value for calcium gluconate-Fe<sub>67.2</sub>Cr<sub>1.2</sub>Nb<sub>0.3</sub>B<sub>20</sub>-ferrofluid is 8.72 W/g for a frequency of 185 kHz and a value of 41 mT of the alternating magnetic field applied. When the ferrofluid is introduced in the AC magnetic field, its heating curve starts to saturate after 12 min. of continuous heating, when temperature reaches 47°C, and increases afterwards with only 0.6°C during the next 20 min. The viscosity of the ferrofluid was also assessed, being equal to 3.56 mPa\*s, similar to blood viscosity at 37°C. Cytotoxicity tests performed on osteosarcoma cells showed that the cellular viability was not significantly reduced, the calcium gluconate-ferrofluid presenting a good biocompatibility. Moreover, a very uniform distribution of the particles in the cell culture was observed in the case of ferrofluid as compared to bare magnetic particles, as can be seen in Figure 1. This represents an advantage for hyperthermia as well as for drug delivery applications, because it will provide a homogenous distribution of the heat and of the bioactive material in the targeted tissue, respectively.

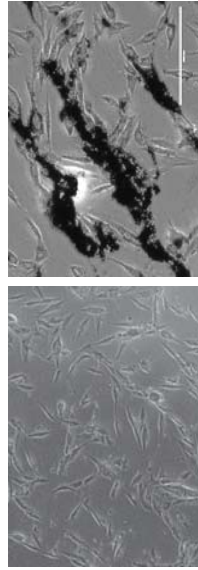


Figure 1. Distribution of ferrofluid (left) and bare magnetic particles (right) in cell culture.

### Acknowledgement

This work was supported by a grant of the Romanian National Authority for Scientific Research, CNDRUEFISCDI, project number 148/2012 (HYPERTHERMIA).

- [1] H. Chiriac, N. Lupu, M. Lostan, G. Ababei, M. Grigoras, C. Danceanu, "Low  $T_c$  Fe-Cr-Nb-B glassy sub-micron powders for hyperthermia applications", *J. Appl. Phys.* **115** (2014) 17B520.
- [2] H. Chiriac, T. Petres, E. Carasevici, L. Labusca, D.-D. Heraea, C. Danceanu, N. Lupu, "In vitro cytotoxicity of Fe-Cr-Nb-B magnetic nanoparticles under high frequency electromagnetic field", *J. Magn. Magn. Mater.* **380** (2015) 13-19.

## Synthesis and magneto-optical behaviors of Fe<sub>3</sub>O<sub>4</sub>/Ag nanocomposite spheres

Chun-Rong Lin<sup>1\*</sup>, Cheng-Tai Tsao<sup>1</sup>, Kun-Yauh Shih<sup>2</sup>, Yaw-Teng Tseng<sup>1</sup>, Jian-Shing Lee<sup>1</sup>, Hua-Shu Hsu<sup>1</sup>

<sup>1</sup>Department of Applied Physics, National Pingtung University, Pingtung 90003, Taiwan

<sup>2</sup>Department of Applied Chemistry, National Pingtung University, Pingtung County 90003, Taiwan

The synthesis of the Fe<sub>3</sub>O<sub>4</sub>/Ag nanocomposites has been the target of recent efforts because these materials are extensively used in antibacterial and medical products, electronics, catalysts, and biosensors. We presented a cost-effective and one-step method for synthesizing Fe<sub>3</sub>O<sub>4</sub>/Ag (FA) nanocomposite spheres (NCSS). The NCSSs were synthesized via thermal decomposition of iron nitrate (Fe(NO<sub>3</sub>)<sub>3</sub>·9H<sub>2</sub>O) and silver nitrate (AgNO<sub>3</sub>) in the mixture containing paraffin liquid, oleyamine and oleic acid. The molar ratios Ag/Fe of AgNO<sub>3</sub> to Fe(NO<sub>3</sub>)<sub>3</sub>·9H<sub>2</sub>O were set to be 0.12 (AF1), 0.24 (AF2), and 0.48 (AF3). The transmission electron microscope (TEM), X-ray diffraction (XRD), vibrating sample magnetometer, and magnetic circular dichroism (MCD) were used for the sample characterization. The NCSS size ranged from 200 to 400 nm, which was estimated by TEM images. X-ray diffraction (XRD) patterns show that the characteristic peaks of NCSSs are composed of the cubic spinel phase of Fe<sub>3</sub>O<sub>4</sub> nanoparticles (NPs) and the FCC phase of Ag NPs. The mean crystalline sizes of NPs in NCSSs, as calculated using Scherrer's formula, were 9.9 nm and 6.0 nm for Fe<sub>3</sub>O<sub>4</sub> NPs and Ag NPs, respectively. Magnetic measurements indicate that Fe<sub>3</sub>O<sub>4</sub> NPs are superparamagnetic at room temperature and show a ferromagnetic character at 78 K. The MCD spectra of Fe<sub>3</sub>O<sub>4</sub>/Ag nanocomposite spheres (NCSS) strongly depend on silver concentration. To clarify the origin of the Fe<sub>3</sub>O<sub>4</sub>/Ag NCSS MCD data, we have carried out the MCD spectra decomposition to several Gauss-shaped components and identified the component energies with the transitions between the Fe<sub>3</sub>O<sub>4</sub> energy states.

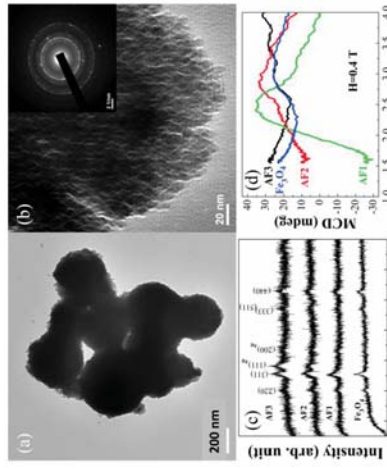


Fig. 1. (a) Fe<sub>3</sub>O<sub>4</sub>/Ag NCSSs (AF1); (b) Higher magnification images of NCSSs (AF1); (c) XRD patterns of Fe<sub>3</sub>O<sub>4</sub>/Ag NCSSs prepared using various AgNO<sub>3</sub> concentration; (d) MCD spectra of Fe<sub>3</sub>O<sub>4</sub>/Ag NCSSs prepared using various AgNO<sub>3</sub> concentration.

## Influence of ligand exchange on crystallography, magnetic and thermal behavior of iron oxide nanoparticles for hyperthermia treatment

F. Crippa<sup>1</sup>, D. Burmann<sup>2</sup>, B. Gori<sup>2</sup>, S. Bals<sup>2</sup>, A.M. Hirz<sup>3</sup>, M. Lattuada<sup>1</sup>, L. Haeni<sup>1</sup>, B. Rothen-Rutishauser<sup>1</sup> and A. Peuri-Fink<sup>4</sup>.

<sup>1</sup> Adolphe Merkle Institute, University of Fribourg, Switzerland, <sup>2</sup> EMAT, University of Antwerp, Belgium, <sup>3</sup> Institute of Geophysics, ETH Zurich, Switzerland, <sup>4</sup> Chemistry Department, University of Fribourg, Switzerland

The thermal decomposition of iron oleate complexes in organic solvent is a robust and popular route to synthesize highly monodisperse superparamagnetic iron oxide nanoparticles (SPIONs). However, the resulting oleic acid coated nanoparticles are not stable in polar solvents and therefore unsuitable for biomedical applications. To overcome this limitation, these synthesized SPIONs are commonly subjected to a phase transfer step prior to any subsequent surface functionalization or application. Here, we investigate how ligand exchange procedures may affect the magnetic and thermal properties of SPIONs, subsequently making them attractive candidates for magnetic hyperthermia.

Large-scale synthesis of oleic acid coated SPIONs (core diameter = 20 nm) is achieved by thermal decomposition of the iron oleate complex in an automated reactor that controls crucial reaction parameters. High Resolution Scanning Transmission Electron Microscopy and X-Ray Diffraction studies of oleic acid coated SPIONs show a wustite ( $\text{FeO}$ )/magnetic ( $\text{Fe}_3\text{O}_4$ ) core/shell structure (Figure 1). This observation is in agreement with magnetic measurements and hyperthermia tests that highlight weak superparamagnetism and poor thermal properties. However, when the particles are transferred to water with a high temperature ligand exchange procedure, the wustite core is oxidized to a single crystal of magnetite. In particular, we observe that the magneto-thermal properties of functionalized SPIONs are significantly enhanced by the thermal annealing process that occurs during ligand exchange. The nanoparticles show a pronounced superparamagnetic behavior, and their thermal signature is increased by more than ten times.

The possibility for large-scale synthesis is given by thermal decomposition and post-processing treatments. Consequently, the altering of the crystalline structure renders the SPIONs more efficient for magnetic hyperthermia.

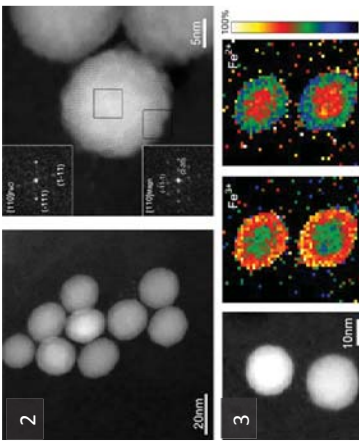


Figure 1: TEM size distribution (1), high-angle annular dark field-STEM (2) and STEM-electron energy loss spectroscopy (3) measurements of 20 nm oleic acid coated SPIONs revealing a core/shell crystalline structure.

## Effect of the aggregation degree on the heating efficiencies of Mn, Fe and Co oxides nanoparticles

P de la Presa, M Espinosa, I Morales, A Hernando

*Instituto de Magnetismo Aplicado (UCM-ADIF-CSIC), P.O. Box 155, Las Rozas, Madrid 28230, Spain.*  
*Dpto Física de Materiales, Fac. CC Fisicas, Univ. Complutense de Madrid.*

The heating efficiency of magnetic nanoparticle (NPs) is nowadays intensively investigated because the applications to magnetic cancer therapy. Recently, a proof of concept on the application to heterogeneous catalysis has been reported. These new concepts consist in taking advantage of the heating efficiency of the NPs to produce in-situ catalysis. This opens a new and wide range of possibilities in the area of NPs heating efficiency since these new applications are not limited by biocompatibility of the materials or limitations on the frequency or amplitude of the applied field. In this work, the effect of the magnetic interactions on the specific absorption rates (SAR) is studied for aqueous and organic colloids of uniform Mn, Fe and Co oxides NPs. Hyperthermia and magnetic characterizations are performed in the liquid phase of colloids consisting of 12 nm uniform NPs dispersed in water or hexane with concentrations below 20 mg/ml. The aqueous colloids form aggregates with high polydispersity degree, whereas in the hexane colloid the NPs are disaggregated with hydrodynamic sizes determined by the particle size plus the organic chain, allowing to unravel the effect of the magnetic interactions to the NPs heating efficiencies.

The magnetic properties show that, at room temperature, Mn and Fe oxide NPs are at the limit from superparamagnetic to ferromagnetic behavior, whereas the cobalt ferrites are blocked. By applying an alternating magnetic field of 110 kHz and 200 Oe, the disaggregated NPs show a higher SAR in all the cases. This effect is primarily a consequence of the release of the Brownian relaxation; however, there exist other mechanisms, like cancellation of dipolar interactions or the formation of particle chains, which can contribute significantly to the enhancement of the particle heating efficiency. In the case of Fe oxide NPs, a decrease of SAR with increasing concentration is observed, whereas for aqueous colloids, SAR is almost independent of concentration. These results suggest that the magnetic interactions tend to decrease the effective field acting on a particle.

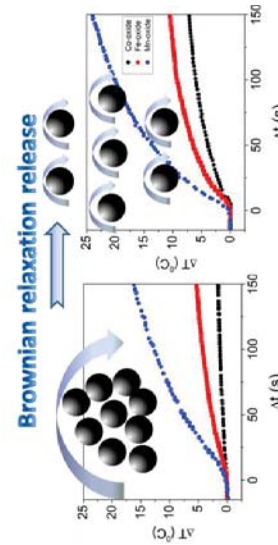


Figure 2: Temperature increase as a function of time for agglomerated (left) and disagglomerated nanoparticles (right) for an applied field of 200 Oe at 110 kHz.

# Improvement of Drug Delivery by Hyperthermia Treatment using Magnetic Cubic Cobalt Ferrite Nanoparticle

## Synthesis and characterization of nanosized $Mg_xMn_{1-x}Fe_2O_4$ ferrites by both sol-gel and thermal decomposition methods

L. E. De-León-Prado<sup>1\*</sup>, D. A. Cortés-Hernández<sup>1</sup>, J. M. Almanza-Robles<sup>1</sup>, J. Sánchez<sup>1</sup>, P. Y. Reyes-Rdz<sup>2</sup>, R. A. Jasso-Terán<sup>1</sup>, G. F. Hurtado López<sup>2</sup>.

<sup>1</sup> Cinvestav-Unidad Saltillo, Av. Industria Metalúrgica #1062, Parque Industrial Saltillo-Ramos Arizpe, CP 25900, Ramos Arizpe, Coah., México. <sup>2</sup> Centro de Investigación en Química Aplicada, Blvd. Enrique Reyna Hermosillo #140, CP 25294, Saltillo, Coah., México. \*E-Mail : laura.elena.prado@gmail.com

Ferrites are metal oxides which allow the manipulation of their magnetic properties depending on physical and chemical parameters such as composition, structure and size, as well as synthesis parameters. For this reason they are considered as potential materials for biomedical applications such as magnetic hyperthermia or contrast agents for magnetic resonance imaging (MRI). This paper reports the synthesis of  $Mg_xMn_{1-x}Fe_2O_4$  ( $x = 0-1$ ) nanoparticles by both sol-gel and thermal decomposition methods. In order to determine the effect of synthesis conditions on the crystal structure and magnetic properties of the ferrites, the synthesis was carried out for each method varying some parameters, including composition. The materials obtained were characterized by X-ray diffraction (XRD), vibrating sample magnetometry (VSM) and transmission electron microscopy (TEM). By both methods it was possible to obtain ferrites having a single crystalline phase with a cubic spinel structure and a behavior near to that of superparamagnetic materials (high values of saturation magnetization and low values of remanence magnetization and coercivity). Saturation magnetization values were higher for materials synthesized by sol-gel, while by thermal decomposition, particles showed a functionalized surface by means of an oleic acid coating obtained in a single step. Furthermore, in both cases, particles have a spherical-like morphology and nanometric sizes (11-15 nm). Therefore, these materials can be considered as potential candidates for their use in biomedical areas.

**Chaitali Dey<sup>1\*</sup>, Madhuri Mandal<sup>2</sup>, Arghya Adhikary<sup>1</sup> and Ajay Ghosh<sup>1</sup>**

<sup>1</sup>Centre for Research in Nano science & Nano technology, Block-JD-2, Sector-II, Salt

Lake, Kolkata-700098

<sup>2</sup>S.N. Bose National Centre for Basic Science, Block-JD, Sector-III, Salt Lake, Kolkata-700098

\*Corresponding author E-mail: chaitalidey29@gmail.com

Recently Magnetic nanoparticles (MNPs) have drawn enormous attention as promising drug carrier in the field of therapeutic treatment as its magnetic property can be tuned by changing many parameters. Here we report a novel synthesis method, characterization and application of a new class of ferromagnetic cubic cobalt ferrite MNP (having size approximately 12-15 nm) for hyperthermia treatment. The MNPs are characterized by XRD, TEM, FESEM, AC magnetic hysteresis and VSM. These MNPs are very much pH and temperature sensitive. These were loaded with DOX and a drug release study was done at different pH and temperatures and found that the amount of released drug was greater in case of elevated temperature and lower pH. So, here we have developed a temperature and pH sensitive drug delivery system to minimize the intracellular toxicity of the released drug as the particles are biocompatible and added advantage of use of this kind of magnetic particles is that, it can be controlled by external magnetic field.

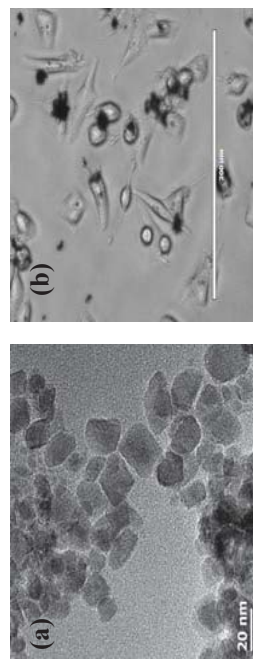
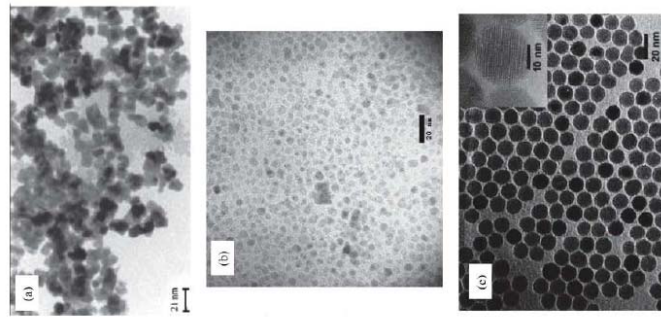


**Fig. 1.** (a)TEM image of  $CoFe_2O_4$  MNP. (b) In - vitro cellular attachment of  $CoFe_2O_4$  MNP.

## Feasibility of Hyperthermia Induced Apoptosis of Pancreatic Tumor Cells with Internalized Magnetoliposomes

**Iron Oxide Nanoparticles: comparison of different synthetic methods**  
Tania Dey  
Mechanical Engineering Department, Limerick Institute of Technology, Moylish Park  
Campus, Limerick, Ireland  
E-mail: taniadey@hotmail.com

**Abstract**  
Magnetite ( $\text{Fe}_3\text{O}_4$ ) and maghemite ( $\text{Fe}_2\text{O}_3$ ) nanoparticles can be synthesized by various methods, such as: (a) Solution method (b) Co-precipitation (c) Microemulsion (d) Polyol process (e) High temperature decomposition of precursor (f) Spray pyrolysis and (g) laser pyrolysis. This review-style talk is based on numerous literature reports, where these synthetic methods will be compared in terms of particle size, size distribution, morphology, magnetic properties and biomedical applicability. Factors affecting the variation will be critically analyzed and guidelines will be provided.

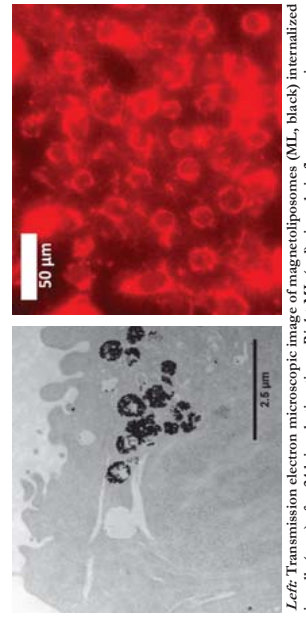


Hyperthermia with the use of magnetic nanoparticles (MNP) is a challenging but most promising approach for cancer therapy. After being magnetically trapped at the tumor site, MNP are heated in alternating magnetic fields (AMF) to approx. 43 °C, which causes tumor cell apoptosis. For an effective and controllable hyperthermia application, two parameters are most important: the amount of internalized MNP in tumor cells and their heating characteristics in AMF. In this study, we evaluated if a sufficient temperature could be achieved by cell internalized MNP heated up in AMF and if cell death could be induced in this way.

The heating of pancreatic tumor cell lines MiaPaCa-2 and BxPC-3 loaded with different amounts of self-synthesized magnetoliposomes nanoparticles (MLs) was measured with a custom-built setup. The MLs consisted of a fluorescent bi-layer of phospholipids and multiple magnetite ( $\text{Fe}_3\text{O}_4$ ) cores with a diameter of  $(10.0 \pm 0.5)$  nm each. The hydrodynamic diameter of the MLs was  $(90 \pm 5)$  nm. Cell loading was performed by incubation of tumor cells for up to 24 h at 37 °C in a DMEM cell medium with MLs, which had an iron concentration of 150 µg/ml. Transmission electron microscopy and fluorescence microscopy were used to depict the uptake of MLs into the tumor cells (see Figure). The internalized iron-content per cell was determined with a magnetic particle spectrometer (MPS). After application of AMF for approx. 30 min, cell viability was assessed by clonogenic assay.

The cellular uptake of MLs was time-dependent, cell line-specific and saturated: For both MiaPaCa-2 and BxPC-3 cell lines, the MLs cell internalization followed an exponential growth function which saturated after about 24 h cell incubation time at an iron load of  $(110 \pm 6)$  pg/cell and  $(30 \pm 2)$  pg/cell, respectively. The time constants of the exponential growth were  $(7.2 \pm 1.4)$  h and  $(4.0 \pm 0.6)$  h, respectively. In AMF, cells with the saturated MLs loading reached temperatures of approx. 44 °C and 43.5 °C, which caused the cell survival fraction to drop to approx. one third compared to untreated tumor cells for both MiaPaCa-2 and BxPC-3 cell lines.

These results demonstrate the feasibility of hyperthermia in pancreatic cancer treatment by confirming cell death of pancreatic tumor cells at temperatures of approx. 43 °C. Further investigations are planned, which aim for the optimization of MNP dosage in targeting experiments as well as the assessment of incubation times and AMF parameters needed for a successful hyperthermic therapy.



*Left:* Transmission electron microscopic image of magnetoliposomes (ML, black) internalized in cells (grey) after 24 h incubation time. *Right:* ML (red) viewed via fluorescence microscopy.

## Synthesis and characterization of plasmonic highly-magnetic nanoparticles

<sup>1</sup> Department of Physics and Astronomy, University College London, Healthcare Biomagnetic and Nanomaterials Laboratories 21 Albenmarle Street, London W1S 4BS.

Emails: [simone.famiani.15@ucl.ac.uk](mailto:simone.famiani.15@ucl.ac.uk); [nkt.thanh@ucl.ac.uk](mailto:nkt.thanh@ucl.ac.uk)

Magnetic nanoparticles are currently receiving a great deal of attention due to their vast potential for biomedical applications such as hyperthermia therapy, drug delivery and diagnostic agents.

So far, the most widely studied magnetic materials are the oxidized forms of iron. Indeed these demonstrate attractive features such as superparamagnetism at room temperature and suitable size, and have been approved by the Food and Drugs Administration Agency leading to their experimentation in *in vivo* studies. However, for most of the above applications, iron oxide nanoparticles are far from ideal since the highest magnetic moment that can be reached is 92 emu/g for magnetite.

Conversely, pure metallic iron shows a higher magnetic moment (217 emu/g), still retains superparamagnetic behaviour at suitable size and has low toxicity, which would improve their performance in biomedical applications. However, the use of Fe nanoparticles is limited due to their quick oxidation once exposed to air and/or biological environments. Therefore, coating the iron core is essential to expand the use of these nanoparticles in biomedical applications.

Amongst the most promising materials that are currently under study, is gold, particularly in core@shell form, which would not only provide more stability but would also add therapeutic properties to the single particle<sup>1</sup>. In this study we aim to synthesize core@shell nanoparticles with a crystalline bcc-Fe core embedded in a thin gold shell. A “bridge” layer between the two materials would be essential in order to achieve the formation of the system without damaging the sensitive iron core. The spacer used here, a silica layer, could provide the support for depositing a gold nanoshell via its easy functionalisation. Moreover, the size of the silica spacer can be tuned over a wide range, yet still retaining a compact size<sup>2</sup>, which plays a crucial role in tuning the final plasmonic properties too.

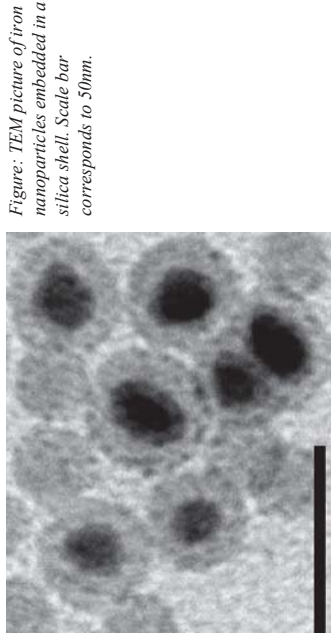


Figure: TEM picture of iron nanoparticles embedded in a silica shell. Scale bar corresponds to 50nm.

## Small-Angle Neutron Scattering Contrast Variation as a tool for magnetic nanoparticle characterization

A.V. Feoktystov<sup>1\*</sup>, M.V. Avdeev<sup>2</sup>, L. Vekas<sup>3</sup>, P. Kopcansky<sup>4</sup>, R. Perzynski<sup>5</sup>,

V.M. Garamus<sup>6</sup>, A. Ioffe<sup>1</sup>, Th. Brückel<sup>7</sup>,

<sup>1</sup>Jülich Centre for Neutron Science (JCNS) at Heinz Maier-Leibnitz Zentrum (MLZ), Forschungszentrum Jülich GmbH, Garching, Germany

<sup>2</sup>Frank Laboratory of Neutron Physics, Joint Institute for Nuclear Research, Dubna, Moscow reg., Russia

<sup>3</sup>Center for Fundamental and Advanced Technical Research,

Romanian Academy – Timisoara Branch, Timisoara, Romania

<sup>4</sup>Institute of Experimental Physics, SAS, Kosice, Slovakia

<sup>5</sup>Sorbonne Université, UPMC Univ Paris 06, UMR 8234, PHENiX, Paris, France

<sup>6</sup>Heinrich Heine Universität Düsseldorf, Institut für Material- und Coastal Research, Geesthacht, Germany

<sup>7</sup>Jülich Centre for Neutron Science (JCNS-2) and Peter Grünberg Institute (PGI-4), JARA-FIT, Forschungszentrum Jülich GmbH, Jülich, Germany

\*E-Mail: [a.feoktystov@fz-juelich.de](mailto:a.feoktystov@fz-juelich.de)

Small-angle neutron scattering (SANS) is a powerful non-destructive technique applied for structure determination in many fields of science such as soft condensed matter, particularly for structure research on magnetic nanoparticles in ferrofluids. Because neutrons possess magnetic moment, their scattering on magnetic nanoparticles gives information about nuclear as well as magnetic structure of the matter simultaneously.

Additional important SANS feature in condensed matter studies is the contrast variation. It is based on the fact that the scattering length of hydrogen (H) and deuterium (D) atoms differ significantly and thus by varying the H/D ratio in the sample or solvent one can enhance or weaken the scattering contribution of one or other component of the multicomponent system. Core-shell magnetic nanoparticles are the ideal system for the SANS contrast variation.

Several examples of the SANS contrast variation on magnetic fluids as well as the developed approach of the basic functions are presented. Classical organic magnetic fluids with the single-layer stabilization (Fig. 1a) by oleic or myristic acid are studied and the size-regulation effect of the stabilized magnetic nanoparticles is found. The SANS contrast variation on biocompatible water-based ferrofluids with the double-layer stabilization (Fig. 1b) by myristic or lauric acid revealed their complex structural organization with a large initial aggregation. Addition of polyethylene glycol (PEG) to the biocompatible water-based magnetic fluid with the sodium oleate stabilization has been shown to lead to the reorganization of the aggregation in the system. SANS of polarized neutrons together with the contrast variation revealed a significant difference in nuclear and magnetic correlation length for water-based ferrofluid with charge stabilization (Fig. 1c). For biomedical applications of magnetic fluids the aggregation is one of the limiting factors and the SANS can give information about its character and structure.

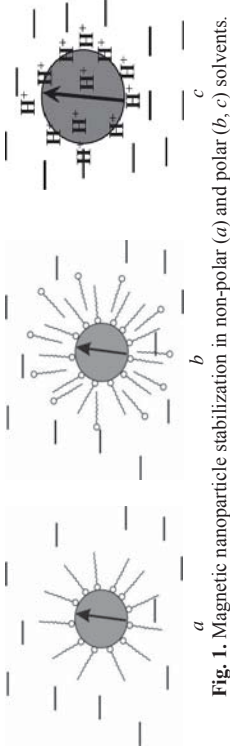


Fig. 1. Magnetic nanoparticle stabilization in non-polar (a) and polar (b, c) solvents.

### References:

- [1] Barathan, R., et al. (2011). "Theranostic Nanoshells: From Probe Design to Imaging and Treatment of Cancer." *Accounts of Chemical Research* 44(10): 936-946

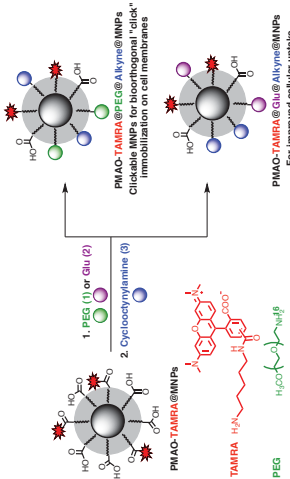
- [2] Karan, N. S., et al. (2015). "Plasmonic giant quantum dots: hybrid nanostructures for truly simultaneous optical imaging, photothermal effect and thermometry." *Chemical Science* 6(4): 2224-2236

## Magnetic nanoparticles for bioorthogonal "click" chemistry

Raluca Maria Fratila<sup>1</sup>, Marcos Navascuez<sup>1</sup>, Javier Idiago<sup>1</sup>, Maite Eceiza<sup>2</sup>, Jesus Maria Alzpira<sup>2</sup> and Jesus Martinez de la Fuente<sup>1,3,4</sup>

1. Instituto de Ciencia de Materiales de Aragón (Universidad de Zaragoza – CSIC). Calle Pedro Cerutina 12, 50009, Zaragoza, Spain. 2. Universidad del País Vasco, Centro Joxe Mari Korta, Avda. Tolosa 72, 20018, San Sebastián, Spain. 3. Institute of Nano Biomedicine and Engineering, Shanghai Jiao Tong University, Dongchuan Road 800, 200240, Shanghai, PR of China. E-mail: jfratila@unizar.es

Bioorthogonal strain-promoted "click" [3 + 2] azide-alkyne cycloaddition (SPAAC) reaction uses the ring strain to activate the alkyne, thus avoiding the use of the cytotoxic Cu(I) catalyst typically employed for "click" azide-alkyne cycloadditions (CuAAC).<sup>1</sup> We are currently investigating its use as a tool to immobilize magnetic nanoparticles (MNPs) on cell surfaces for magnetic hyperthermia studies. Our aim is to compare how the subcellular localization (on the plasma membrane or inside the cells) of MNPs affects their healing behaviour when compared to MNPs in solution. In this work, we present our preliminary results concerning the functionalization of MNPs with strained alkynes. Hydrophobic 12 nm iron oxide MNPs were synthesized following a seed-mediated thermal decomposition methodology and transferred to water by coating with a fluorescent amphiphilic polymer (poly(maleic anhydride-alt-1-octadecene), PMAO-TAMRA).<sup>2</sup> The MNPs were further functionalized stepwise with poly(ethylene glycol) (PEG 1 to increase colloidal stability) or a glucopyranose derivative (Glu 2 to enhance cellular uptake) and with a strained alkyne (3, <sup>3</sup>-Gel electrophoresis, HRMAS NMR studies and z-potential measurements of the resulting MNPs confirmed the successful functionalization. We are currently investigating the bioorthogonal "click" attachment of the MNPs on cell membranes and their internalization profile, respectively.



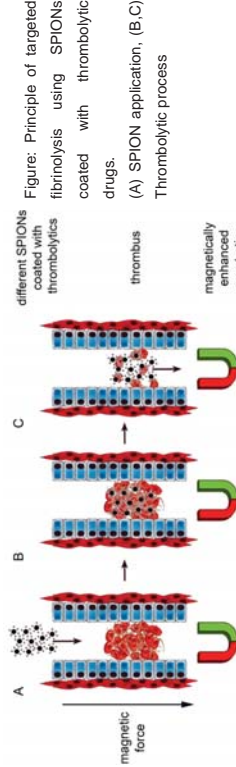
R. M. F. acknowledges financial support from Universidad de Zaragoza (JUZ-2014-CIE-03) and European Union (Marie Skłodowska-Curie grant agreement No. 657215). References: (1) J. C. Jewel, C. R. Berrozi, Chem. Soc. Rev., 2010, 39, 1272. (2) M. Moros, B. Pelaz, P. Lopez-Larubia, M. L. Garcia-Martin, V. Grau, J. M. de la Fuente, Nanoscale, 2010, 2, 1746. (3) The cyclooctynyl amine derivative 3 was prepared in three steps and 56 % overall yield starting from 8,8-dibromocyclo[5.1.0]octane and following a chromatographic purification-free method adapted from the literature: A. Bernardin, A. Cazet, L. Guyon, P. Delamnoy, F. Vinel, D. Bonnaffons, J. Texier, Biconjugate Chem. 2010, 21, 583.

## Covalent versus adsorptive binding of thrombolytics to SPIONs for directed targeting of fibrin-based matrices

R. P. Friedrich<sup>1&\*</sup>, J. Zaloga<sup>1&\*</sup>, E. Schreiber<sup>1</sup>, I. Y. Tóth<sup>2</sup>, E. Tombácz<sup>2</sup>, J. Nowak<sup>3</sup>, S. Odenthal<sup>3</sup>, C. Alexiou<sup>1</sup>

<sup>1</sup> Department of Otorhinolaryngology, Section for Experimental Oncology and Nano-medicine (SEON), Else Kröner Fresenius-Stiftung-Professorship, University Erlangen, Germany; <sup>2</sup> Department of Physical Chemistry and Materials Science, University of Szeged, Hungary; & These authors contributed equally to this work; <sup>3</sup> Technische Universität Dresden, Chair of Magnetofluidynamics, Measuring and Automation Technology, Dresden; \* E-Mail: ralf.friedrich@uk-erlangen.de; jan.zaloga@uk-erlangen.de

Functionalized superparamagnetic iron oxide nanoparticles are frequently used to develop vehicles for photodynamic therapy, hyperthermia, imaging and drug delivery. In this study we directly compared the covalent and non-covalent binding of tissue plasminogen activator (tPA), a protein commonly used for the treatment of specific diseases of the circulatory system (e.g. stroke, cardiac infarction), the most important cause of premature death in Europe. tPA is the main emergency drug for ischemic stroke and catalyses the conversion of plasminogen to plasmin and thereby dissolves fibrin-based clots. This protein suffers from very low bioavailability and therefore has to be administered in relatively high doses, which can cause potentially serious side effects like internal bleedings. Coupling of the protein to iron oxide nanoparticles for Magnetic Drug Targeting (MDT) to blood clots could provide higher bioavailability and could help to overcome the drawbacks caused by this high dosage. Here, we first purified a clinically available preparation of tissue plasminogen activator (tPA, Actilyse®) by tangential flow filtration and then coupled the protein to polyacrylic acid-co-maleic acid (PAM) coated SPIONs using a covalent and non-covalent approach to investigate different advantages and disadvantages for drug release and activity. Using dynamic light scattering (DLS), pH-dependent electrophoretic mobility measurements and different tPA activity assays, we showed that the properties of the SPIONs significantly differs depending on the binding strategy. Covalent linkage significantly improves the reactivity and long term stability of the conjugated SPION-tPA system compared to simple adsorption. Investigation of covalent and non-covalent functionalized SPIONs revealed diverging attributes, which should be taken into account when developing nanoparticles for different applications.



Acknowledgment: The authors would like to thank the German Research Foundation (SPP1681 (AL552/5)) for their financial support.

## Inhibition of amyloid aggregation of lysozyme by application of magnetic nanoparticles coated with different types of dextran

Z. Gazova<sup>1</sup>, Z. Bednarkova<sup>1,2</sup>, E. Demjent<sup>1</sup>, S. Dutz<sup>3</sup>, P. Kopcarovsky<sup>1</sup>, K. Ulicna<sup>1,5</sup>

<sup>1</sup> Department of Biophysics, Institute of Experimental Physics, Slovak Academy of Sciences, Kosice, Slovakia

<sup>2</sup> Department of Biochemistry, Faculty of Sciences, Safarik University, Kosice, Slovakia

<sup>3</sup> Institute of Biomedical Engineering and Informatics (BMTI), Technische Universität Ilmenau, Ilmenau, Germany

<sup>4</sup> Department of Biophysics, "Carol Davila" University of Medicine and Pharmacy, Bucharest, Romania

<sup>5</sup> Institute of Biology and Ecology, Faculty of Science, Safarik University, Kosice, Slovakia  
e-mail: gazova@saske.sk

For several diseases, including Alzheimer's and Parkinson's diseases or diabetes mellitus, the conversion of normally soluble protein into fibrillar aggregates is of central importance. Since hen egg-white lysozyme (HEWL) is one of the best known proteins with well-characterized molecular structure and physico-chemical properties it serves as model protein for study of protein amyloid aggregation *in vitro* very often. HEWL is homologous (40%) to human lysozyme and its mutant variants form massive amyloid deposits in the liver and kidneys of individuals affected by systemic lysozyme amyloidosis. Until now, several therapeutic approaches have been suggested to deal with amyloidogenic diseases. In recent years the attention has been devoted to nanoparticles that inhibit amyloid fibril formation by disturbing their self-assembly processes.

In our study we investigated the effect of magnetic nanoparticles (MNP) on amyloid aggregation of HEWL by means of ThT assay, FTIR spectroscopy and AFM technique. For these experiments we used superparamagnetic iron oxide ( $\text{Fe}_2\text{O}_3$ ) cores of about 10 nm coated with carboxymethylxanthan (CMD), dextran (DEX) or diethylaminoethoxydextran (DEAE), respectively.

We found that the interference of nanoparticles with HEWL led to a decrease of ThT fluorescence intensities with an increasing nanoparticle concentration and the  $\text{IC}_{50}$  values were determined to be in the  $\mu\text{g}/\text{ml}$  range. The most effective inhibitory effect was obtained for negatively charged CMD and neutral dextran nanoparticles (DEX). AFM confirmed the found MNP inhibition effect on HEWL fibrilization (in Fig. 1 shown for CMD MNPs). The kinetic profiles for HEWL fibrilization in presence of the different MNP have shown that CMD and DEX nanoparticles prolong lag phase and decrease values for plateau phase. A w/w ratio HEWL/CMD MNPs = 1:1. Concentration of lysozyme was 10  $\mu\text{M}$  (equivalent to 147  $\mu\text{g}/\text{ml}$ ). The bars represent 1  $\mu\text{m}$ .

nanoparticles no significant changes in viability relative to control at concentrations close to  $\text{IC}_{50}$  values were found.

Our results indicate that all three types of MNP are able to prevent the amyloid self-assembling of lysozyme and the extent of the inhibition depends on their physico-chemical properties. The investigated particles possess no cytotoxicity, which is promising for further investigation of these nanoparticles as candidates for therapy of amyloid-related diseases.

### Acknowledgement

This work was supported by the research grant from the Slovak Grant Agency Vega 2/181/13 and 2/0175/14.

## An abstract approach to quantify the heating power of magnetic nanoparticles

C. Geers<sup>1\*</sup>, C. Monnier<sup>1</sup>, F. Crippa<sup>1</sup>, D. Burnand<sup>3</sup>, M. Lattuada<sup>1</sup>, M. Bonmarin<sup>2</sup>, A. Petri-Fink<sup>1,3</sup>

<sup>1</sup>Adolphe Merkle Institute, University of Fribourg, Chemin des Verdiers 4, 1700 Fribourg, Switzerland

<sup>2</sup>Institute of Computational Physics, Zurich University of Applied Sciences, Technikumstrasse 9, 8400 Winterthur,  
<sup>3</sup>Chemistry Department, University of Fribourg, Chemin du Musée 9, 1700 Fribourg, Switzerland \*E-Mail:  
christoph.geers@unifrib.ch

Magnetic nanoparticles (NPs) and their ability to convert magnetic energy into heat are currently explored around the globe for various kinds of biomedical applications, with a particular emphasis on hyperthermia treatment. The heating power of these materials is dictated by a myriad of internal (e.g. NP size, polydispersity or crystallinity) and external (e.g. magnetic field strength or frequency) phenomena. However, experimentally conveying the effective heating power is not always straightforward, reproducible or easily feasible with conventional methods (e.g. fiberoptic cables, thermocouples or standard IR imaging). Variations among synthetic batches are not promotive either, as this requires every individual sample to be investigated and validated before administration.

Our group is thus dedicated to developing more reliable and precise experimental methods to evaluate the heating power of the respective magnetic NPs. In this context, we present an abstract approach based on lock-in thermography to screen the thermal signatures, and consequently their effective therapeutic value, at unprecedented thermal resolutions. Superparamagnetic iron oxide nanoparticles (SPIONS) exposed to an alternating magnetic field (AMF) were used as model NPs to validate the setup, and their thermal properties were investigated in different states of matter. This included NPs in liquid, semi-solid and aggregated state.

Compared to conventional techniques, this approach is fast, sensitive, non-invasive alternative and capable of probing multiple and dilute specimens simultaneously. In turn, this would contribute in speeding up screening procedures or comparative studies.



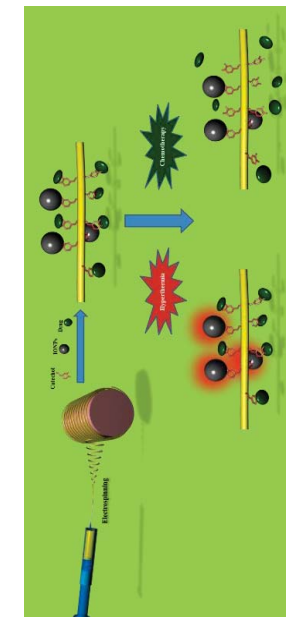
## Novel Route to immobilization of Magnetic Nanoparticles on polymeric Nanofibers for Hyperthermic Chemotherapy

Amin GhavamiNejad, Afesh Rajan Unithan, Chan Hee Park and Cheol Sang Kim

<sup>1</sup> Department of Bionanosystem Engineering Graduate School, Chonbuk National University, Jeonju City, Republic of Korea.

For the first time in literature, we report a method for the versatile synthesis of novel, mussel-inspired, electrospun nanofibers with catechol moieties. These mussel-inspired nanofibers are used to bind iron oxide nanoparticles (IONPs) and the borate-containing anticancer drug Bortezomib (BTZ) through a catechol metal binding mechanism adapted from nature. These smart nanofibers exhibit a unique conjugation of Bortezomib to their 1, 2-benzenediol (catechol) moieties for enabling a pH-dependent drug delivery towards the cancer cells and the IONPs via strong coordination bonds for exploiting the repeated application of hyperthermia. Thus these smart magnetic nanofibers can be used as a potential platform for the synergistic anticancer treatment combining both hyperthermia and chemotherapy.

**Keywords:** hyperthermia, chemotherapy, magnetic nanoparticles, mussel-inspired nanofiber, electrospinning.



## Functionalization of DNA Nanostructures with Au-plated Superparamagnetic Iron Oxide Particles

Marisa A. Goetzfried<sup>\*\*</sup>, Kilian Vogele<sup>\*</sup>, Christine Rümenapp<sup>†</sup>, Bernhard Gleich<sup>‡</sup>, Friedrich C. Simmel<sup>\*</sup>, Tobias Pirzer<sup>\*</sup>

<sup>\*</sup>Physics Department and ZNN/WSI, TU München, Garching, Germany

<sup>†</sup>Zentralinstitut für Medizintechnik (IMETUM), TU München, Garching Germany

<sup>‡</sup>Email: mgoetzfried@mytum.de

The recent technological development created a demand for novel tools such as hybrid materials. We functionalized DNA-nanostructures with superparamagnetic iron oxide particles (SPIOs) to combine their inorganic and organic properties. SPIOs are produced by coprecipitation of  $\text{FeCl}_2$  and  $\text{FeCl}_3$  and plated with gold by reduction of  $\text{HAuCl}_4$  on the surface in acidic solution.<sup>1,2</sup> The attachment of thiol-modified DNA oligonucleotides to the gold coating enables the functionalization of DNA nanostructures such as DNA origami tiles.<sup>3,4</sup> The functionalization quality of the DNA structures was determined by atomic force microscopy (AFM).

The next steps will be the usage of different types of nanostructures and magnetic nanoparticles (MNP) of various sizes and metals. The application of a controlled magnetic field might be the first step towards the construction of molecular devices based on DNA and MNP.

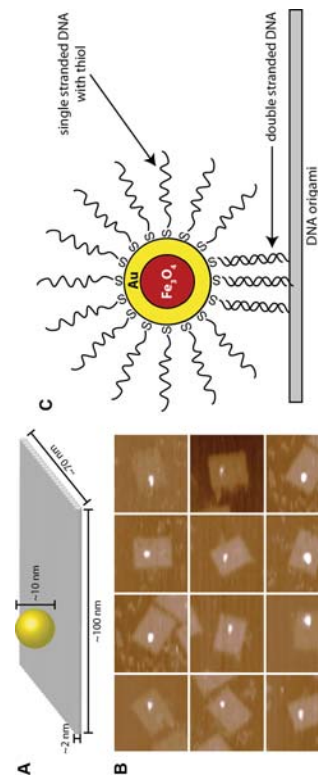


Figure: A) Illustration of a gold-coated iron oxide particle binding to a rectangular DNA origami. B) AFM-images of gold-coated MNP bound to the DNA rectangle. C) Illustration of the binding principle and the composition of the used nanoparticles.

### References:

1. Rümenapp, C., Gleich, B., Mannherz, H. G. & Haase, A. Detection of molecules and cells using nuclear magnetic resonance with magnetic nanoparticles. *380*, 271–275 (2015).
2. Abdelfattah-Jacquin, C., Dichtl, M., Jakobsmeier, L., Hiller, W. & Sackmann, E. Gold Plating and Biofunctionalization of Ferrimagnetic Magnetic Tweezers: Application for Local Studies of Soft Surface-Grafted Polymer Films. *Langmuir* **17**, 2129–2136 (2001).
3. Kuzyk, A. et al. DNA-based self-assembly of chiral plasmonic nanostructures with tailored optical response. *Nature* **483**, 311–314 (2012).
4. Rothemund, P. W. K. Folding DNA to create nanoscale shapes and patterns. *Nature* **440**, 297–302 (2006).

## Serum concentration affects protein corona mass, surface charge, and nanoparticle-cell interaction

**Christine Gräfe<sup>\*1</sup>, Andreas Weidner<sup>\*2</sup>, Moritz v.d. Lühe<sup>3,4</sup>, Christian Bergemann<sup>5</sup>,**

**Felix H. Schacher<sup>3,4</sup>, Silvio Dutz<sup>2</sup>, Joachim H. Clement<sup>1,4</sup>**

<sup>1</sup>Department of Hematology and Oncology, Jena University Hospital, Jena, Germany  
<sup>2</sup>Institute of Biomedical Engineering and Informatics (BMTI), Technische Universität Ilmenau, Ilmenau, Germany  
<sup>3</sup>Institute of Organic Chemistry and Macromolecular Chemistry (OMC), Friedrich-Schiller-Universität Jena, Jena, Germany

<sup>4</sup>Jena Center for Soft Matter (JCSM), Friedrich-Schiller-University Jena, Jena, Germany  
<sup>5</sup>Chemieell GmbH, Berlin, Germany

\* The authors contributed equally to this work.

Due to their large surface-to-volume ratio magnetic nanoparticles (MNPs) show a pronounced reactivity towards their environment leading to the adsorption of surrounding components. Especially the adsorption of proteins on the particles' surface leads to the formation of the so-called protein corona which is immediately formed upon contact between nanoparticles and biological systems. It provides the nanoparticles with a new biological identity and thus, plays an essential role for the biological impact including the cellular uptake and cytotoxicity. A particularly less investigated issue is whether the absolute amount of proteins bound to the particle surface affects interactions of distinct particles with cells and, eventually, cellular uptake. In this study we describe a strategy to control the amount of corona proteins binding to the particle surface and the impact of such a protein corona on particle-cell interactions.

For corona formation, polyethyleneimine (PEI) coated MNP were incubated in RPMI cell culture medium supplied with fetal calf serum (FCS) of varying amounts between 0% and 100%. Sodium dodecyl sulfate polyacrylamide gel electrophoresis (SDS-PAGE) and silver staining were used in order to estimate the protein corona mass and the size distribution of the participating proteins. Additionally, the zeta potential of incubated particles was measured. Human brain microvascular endothelial cells (HBMEC) representing the blood-brain barrier were used for *in vitro* incubation experiments. Flow cytometry was applied to investigate the consequences of the FCS dependent protein corona formation on the interaction of MNP with the cells. Furthermore, nuclei and actin cytoskeleton of incubated cells were stained fluorescently and laser scanning microscopy was used for analysing the cellular uptake of MNPs.

Figure 1: Mass-dependent separation of protein corona by SDS-PAGE and silver stain. Zeta potential as well as SDS-PAGE clearly reveal a gain of corona proteins on MNP with increasing amount of FCS in incubation medium. For MNP incubated with lower FCS concentrations especially medium-sized proteins of molecular weights between 30 kDa and 100 kDa could be found within the protein corona. For MNP incubated within higher FCS concentrations the fraction of corona proteins of 30 kDa and less increased. Flow cytometry as well as laser scanning microscopy reveal that the presence of the protein corona reduces both, the interaction and the uptake of PEI-coated MNP by HBMEC within a 30 min-incubation. The results indicate that not only the composition of the nanoparticle shell but also the composition of the incubation environment are a tool to navigate the corona formation, composition and fate, which is of major importance for medical applications on nanoparticles.

This work was supported by the DFG priority program 1681 (CL2023/1, DU1233/4-1, SCHIA1640/7-1).

## Optical Measurement of the Magnetic Moment of Magnetically Labeled Objects

Alexandra Heidsieck<sup>1,2</sup>, Sarah Rudigkeit<sup>1</sup>, Christine Rümenapp<sup>1</sup>, and Bernhard Gleich<sup>1,3</sup>

<sup>1</sup>Zentralinstitut für Medizintechnik, Technische Universität München, Garching, Germany  
<sup>2</sup>Email: aleheid@tum.de, 3 Email: gleich@tum.de

The magnetic moment of magnetically labeled cells, microbubbles or microspheres is an important optimization parameter for many targeting, delivery or separation applications. The quantification of this property is often difficult, since it depends not only on the type of incorporated nanoparticle, but also on the intake capabilities, surface properties and internal distribution.

We describe a method to determine the magnetic moment of those carriers using a microscopic setup and an image processing algorithm. In contrast to other works, we measure the diversion of superparamagnetic nanoparticles in a static fluid. The set-up is optimized to achieve a homogeneous movement of the magnetic carriers inside the magnetic field. The evaluation is automated with a customized algorithm, utilizing a set of basic algorithms, including blob recognition, feature-based shape recognition and a graph algorithm.

We present example measurements for the characteristic properties of different types of carriers in combination with different types of nanoparticles. Those properties include velocity in the magnetic field as well as the magnetic moment. The investigated carriers are adherent and suspension cells, while the used nanoparticles have different sizes and coatings to obtain varying behavior of the carriers.



Magnetic set-up(a), overlay of microscopic images including reconstructed trajectories (b) and evaluated magnetic moment (c)

## In-situ observation of particles deposition process on a ferromagnetic filter during high-gradient magnetic separation process

Noriyuki Hirota<sup>1</sup>, Tatsuharu Ando<sup>2</sup>, Tadamitsu Takano<sup>2</sup>, Hidehiko Okada<sup>1</sup>

<sup>1</sup> Fine Particle Engineering Group, National Institute for Materials Science, 3-13 Sakura Tsukuba, Japan

<sup>2</sup> Department of Mechanical Engineering, Nihon University, 1-2-1 Iwanicho, Narashino, 275-8375, Japan

e-mail: hirota.noriyuki@nims.go.jp

In High Gradient Magnetic Separation (HGMS), magnetic particles suspended in a fluid are separated based on the strong magnetic force due to the steep magnetic field gradient formed by the magnetization of ferromagnetic fielder wires. Particles can be collected even the opening of the filter is much larger than the particle size, therefore, loss of pressure is small enough. It realizes the efficient process. Furthermore, filter can be reused easily because collected particles detached from the filter when the magnetic field removed. To optimize the condition for the magnetic separation process, simulations are often carried out; however, the volume of deposited particles is often ignored and the effect of deposited particles on the flow is not considered properly in such cases.

Information about the way of particles deposition on the filter wire seems to contribute for the optimization of separation condition in practical processes. In this study, therefore, *in-situ* observations of particles deposition process on the filter in HGMS were carried out in superconducting magnet bore.

The magnet used in this study was cryocooler operated type of superconducting magnet that can generate up to 13 T. The housing of the filter was made of acryl. It enables us to observe inside of separation cell. A CCD camera, model UN43H of ELMO Co. Ltd., was used for *in-situ* observation. It can be utilized even under the high magnetic field in the superconducting magnet bore. The filter used here was made of SUS430 whose whole diameter and wire diameter were 2.5 mm and 0.22 mm, respectively (30 mesh). Zirconia ferrite particles were suspended in distilled water and was used for the experiment. Sample suspension was flowed from the above of the magnet and the behavior of particles near the filter set at the magnetic field center was observed. A series of experiments were carried out with changing the applied magnetic field and flow rates.

Figure shows the observed deposition of particles under 10 T. It was observed that the spike-like structure was formed toward the upper stream direction. As a result, the length of the spike structure tends to be long with higher applied magnetic field and lower flow velocity. These observations were qualitatively understood with considering the effects of flow and of the magnetization of wires to the spatial magnetic field distribution. Details of these observations will be reported in this presentation.

## Uncertainty Impacts on Quantitative Magnetic Nanoparticle Imaging using Magnetorelaxometry

Peter Hönninen<sup>1,2</sup>, Maik Liebf<sup>2</sup>, Daniel Baumgarten<sup>1,3\*</sup>

<sup>1</sup> Institute of Biomedical Engineering and Informatics, Technische Universität Ilmenau, Ilmenau, Germany;

<sup>2</sup> Physikalisch-Technische Bundesanstalt, Berlin, Germany; <sup>3</sup> Institute of Electrical and Biomedical Engineering, University of Health Sciences, Medical Informatics and Technology, Hall in Tyrol, Austria

\* Email: daniel.baumgarten@tu-ilmenau.de

Novel approaches of quantitative magnetic nanoparticle (MNP) imaging using magnetorelaxometry (MRX), where parts of an MNP distribution are subsequently activated by multiple excitation coils underneath a sensor system, require accurate knowledge of reconstruction deviations due to measurement uncertainties. We investigated sources of uncertainties within an experimental MRX setup and estimated their impact on the deviation in MNP quantification. The results provide suggestions for improvements of the method. The MRX setup comprises a system of regularly positioned excitation coils mounted to a rabbit-sized MNP phantom, both located underneath a 304 SQUID-vectormagnetometer device [1]. Within this setup, MRX noise data were recorded and the coil localization uncertainty was estimated. Additionally, manufacturer defined uncertainties on coils and phantom were taken into account. The impact of the obtained uncertainties on MNP quantification was estimated in numerical simulations using a simplified model consisting of sensor system, one excitation coil and two point-like MNP-sample of clinically tolerable doses in the milligram range, positioned in distances of 1 cm and 3.8 cm to the upper coil level, respectively.

For the near source, displacements of the excitation coil within the uncertainty range yielded the largest deviation of the total MNP amount. Uncertainties in the shifting of the sensor array relative to MNP-sample and excitation coil contribute slightly lower quantification deviations. Measurement noise impacts appeared small. In contrast to that, the far source demonstrates a much higher noise impact due to a lower SNR. Since the impact of the other uncertainty sources decreases, noise dominates the reconstruction quality for this source.

Our results show that uncertainties in quantitative magnetorelaxometry imaging of magnetic nanoparticles are generally small. The largest potential for a further reduction of measurement uncertainties lies in the precision of mounting the excitation coil system. Besides, an improvement could be gained by reducing uncertainties in the localization of the coil system. However, these are difficult to obtain with respect to restrictions of the measurement setup.



Figure: a) MRX measurement setup; b) Response metrics of uncertainties for source 1 cm (left) and 3.8 cm below upper coil level (right).

Figure *In-situ* observation of deposition of magnetic particles on the ferromagnetic filter under 10 T

## TAT- and RGDS-modified Luminescent and PEG&SiO<sub>2</sub>-coated Magnetic Nanoparticles for Tumor Targeting and Diagnosis

D. Horák<sup>1\*</sup>, U. Kostiv<sup>1</sup>, V. Patlska<sup>1</sup>, V. Proks<sup>1</sup>, H. Engstová<sup>2</sup>, P. Ježek<sup>2</sup>

<sup>1</sup> Institute of Macromolecular Chemistry AS CR, <sup>2</sup> Institute of Physiology AS CR, Prague, Czech Republic

\* E-mail address: horak@jimc.cz

Specific targeting and *in vivo* visualization of cancer cells is of crucial importance for early detection and treatment of cancer. We have developed novel 28 nm monodisperse poly(ethylene glycol) (PEG)-modified SiO<sub>2</sub>-coated Fe<sub>3</sub>O<sub>4</sub> superparamagnetic nanoparticles and 36 nm monodisperse NaYF<sub>4</sub>:Yb<sup>3+</sup>/Er<sup>3+</sup> upconversion nanoparticles (Figure 1 a) synthesized by oleic acid-stabilized thermal decomposition of Fe(III) oleate and lanthanide chlorides in the presence of NaF, respectively. Modification of the particle surface (Figure 1 b) was achieved by hydrolysis/condensation of tetramethyl orthosilicate/(3-aminopropyl)triethoxysilane using a water-in-oil (w/o) reverse microemulsion and reaction with methoxy PEG succinimidyl ester. Physicochemical properties of the nanoparticles were determined by scanning and transmission electron microscopy, atomic absorption and FTIR spectroscopy, magnetic resonance imaging and/or confocal inverted fluorescence microscopy. In biological experiments, neural stem cell viability and labeling efficiency of PEG&SiO<sub>2</sub>-modified nanoparticles were evaluated. While SiO<sub>2</sub>-coated nanoparticles exhibited a highly efficient concentration-dependent labeling efficiency, PEG&SiO<sub>2</sub>-particles had excellent biocompatibility.

To specifically target the human epithelial cervix carcinoma (HeLa) cells, upconversion lanthanide nanoparticles were conjugated with the cell-adhesive RGDS and cell-penetrating TAT peptides. The TAT&SiO<sub>2</sub>-NaYF<sub>4</sub>:Yb<sup>3+</sup>/Er<sup>3+</sup> particles were localized predominantly in the cell cytoplasm. In contrast, the RGDS&SiO<sub>2</sub>-NaYF<sub>4</sub>:Yb<sup>3+</sup>/Er<sup>3+</sup> particles adhered to the cell surface. Excellent visibility and facile monitoring of the RGDS- and TAT-conjugated NaYF<sub>4</sub>:Yb<sup>3+</sup>/Er<sup>3+</sup> nanoparticles in the living cells (Figure 1 c, d) is very promising for perspective use of the drug-conjugated upconversion nanoparticles in theranostic applications.

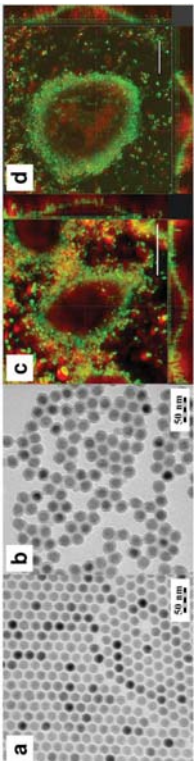


Figure 1. TEM micrographs of (a) NaYF<sub>4</sub>:Yb<sup>3+</sup>/Er<sup>3+</sup> and (b) SiO<sub>2</sub>-NaYF<sub>4</sub>:Yb<sup>3+</sup>/Er<sup>3+</sup> nanoparticles. Luminescence image of HeLa cells (green, excitation 480 nm) after incubation with (c) RGDS&SiO<sub>2</sub>-NaYF<sub>4</sub>:Yb<sup>3+</sup>/Er<sup>3+</sup> and (d) TAT&SiO<sub>2</sub>-NaYF<sub>4</sub>:Yb<sup>3+</sup>/Er<sup>3+</sup> (red, excitation 970 nm, detection 500-700 nm). Scale bar 20 μm.

Acknowledgement. Support of Czech Science Foundation (No. 15-0118975) is acknowledged.

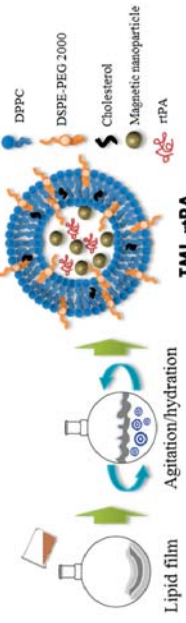
## Preparation of Thermosensitive Magnetic Liposome Encapsulated Recombinant Tissue Plasminogen Activator for Targeted Thrombolysis

Hao-Lung Hsu and Jyh-Ping Chen\*

Department of Chemical and Materials Engineering, Chang Gung University, Kwei-San  
Taoyuan 333, Taiwan, ROC, \*E-mail: jpcchen@mail.cgu.edu.tw

Thromolytic drugs play a critical role in the treatment of various cardiovascular diseases including acute myocardial infarction, pulmonary embolism, deep vein thrombosis, arterial thrombosis and peripheral vascular thromboembolism. However, thromolytic agents, such as tissue plasminogen activator, tend to dissolve both pathological thrombi and fibrin deposit at sites of vascular injury, resulting in hemorrhagic toxicity at therapeutic doses. Plasminogen activators also have short half-life and are immunogenic because of their foreign nature. By encapsulating proteins within novel carrier systems, an increased half-life and decreased immunogenicity might be obtained. Further, targeted delivery of thrombolytic agents followed by controlled drug release may reduce the risks of haemorrhage and toxicity associated with systemic administration, thus offering a promising, minimally invasive approach that could control and treat thrombosis.

We propose a more efficient thromolytic drug delivery system using PEGylated thermosensitive magnetic liposome (TML) for magnetic targeted delivery of recombinant tissue plasminogen activator (rtPA) to the site of thrombus followed by temperature-triggered controlled drug release. We examine the preparation of rtPA-loaded TML from 1,2-dipalmitoyl-sn-glycero-3-phosphocholine (DPPC), distearoylphosphatidyl ethanolamine-N-poly(ethylene glycol) 2000 (DSPE-PEG 2000) and cholesterol by solvent evaporation/sonication and freeze-thaw cycles method. The objective was to optimize the formulation of TML-rtPA using response surface methodology (RSM). The experimental parameters or variables considered were the molar percentages of DPPC, DSPE-PEG and cholesterol, and the molar ratio of lipid/magnetic nanoparticle. The results of the experiments are rtPA encapsulation efficiency and rtPA release percentages at 37 °C and 43 °C. The effects were investigated within the context of RSM that incorporates design of experiments and non-linear regression. All formulations were characterized for physicochemical properties by nanoparticle tracking analysis (NTA), transmission electron microscopy (TEM), and X-ray diffraction (XRD). The distribution of the mean diameter of TML-rtPA was 90–120 nm in size and with spherical shape. The drug release depends mainly on the composition of DSPE-PEG 2000. Magnetic targeting effect and thermosensitive release of rtPA could be confirmed from *in vitro* thrombolysis experiments. The prepared TML-rtPA will be useful for magnetically guided target thrombolysis, followed by an alternating magnetic field for controlled release of rtPA by hyperthermic effects for treating thrombosis in a clinical setting.



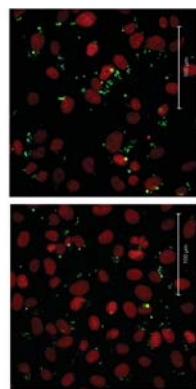
## Self-Assembled Magnetic Nanoparticles Based On Folic Acid-Oleoyl Chitosan for Targeted Delivery of Doxorubicin

Hao-Lung Hsu<sup>1</sup>, Yi-Cian Lai<sup>1</sup>, Yu-Jen Lu<sup>2</sup>, Jyh-Ping Chen<sup>1\*</sup>

<sup>1</sup>Department of Chemical and Materials Engineering, Chang Gung University,  
<sup>2</sup>Department of Neurosurgery, Chang Gung Memorial Hospital, Kwei-San, Taoyuan

Targeted delivery of therapeutic agents to the brain has enormous potential for the treatment of brain tumor. However, the blood-brain barrier (BBB) significantly impedes the entry of drug molecules into the brain from the bloodstream. Drug-loaded magnetic particles represent a promising alternative strategy in overcoming the BBB. Oleyl-chitosan (OCS) could self-assemble into core-shell structures in aqueous solution and provide the effective core compartment for loading iron oxide nanoparticles and doxorubicin (DOX). We prepared magnetic oleoyl-chitosan nanoparticles (MOCNP) as an efficient magnetic targeted drug delivery system for brain tumor treatment. Folic acid (FA)-conjugated OCS could be synthesized and incorporated into MOCNP to further enhance the targeting efficiency by targeting cancer cells overexpressing folate receptors on cell surface. MOCNP and FA-MOCNP were 200~250 nm in size and with a spherical shape. The drug encapsulation (EE) efficiency was up to 95% with drug loading efficiency (LE) at 25%. After modification with FA, EE and LE were not significantly different. Drug release studies showed pH-dependent release with rapid release at pH 5.5, whereas at pH 7.4 there was a sustained release after a burst release. The physicochemical properties of MOCNP and FA-MOCNP were fully characterized.

The anti-tumor and targeting efficiency of MOCNP and FA-MOCNP were examined using human glioblastoma cells (U87) *in vitro*. The IC<sub>50</sub> value is dependent on the molar ratio of FA in FA-MOCNP, which are 131, 93 and 17 µg/ml for FA-MOCNP synthesized with 0, 10 and 50% FA-OCS. This is consistent with the fluorescence imaging results using fluorescently labelled nanoparticles, which indicated enhanced endocytosis of FA-MOCNP by U87 cells followed by controlled release of DOX into the cell nucleus. These results suggested that FA-MOCNP may be a promising dual targeting carrier for DOX by efficiently delivering the chemotherapy drug to folate receptor-targeted tumor tissues under magnetic guidance.



Cellular uptakes of FITC-labelled (green) MOCNP (left) and FA-MOCNP (right).

## Immobilization of laccase on magnetic nanoparticles for enhancing biocatalysis

Beijing Research Institute for Nutritional Resources, Beijing 100069, P.R. China  
Email: beijimnhw@126.com

Large-pore magnetic mesoporous silica nanoparticles (MMSNPs) with wormhole framework structures were synthesized by using tetraethyl orthosilicate as the silica source and amine-terminated Jeffamine surfactants as template. Immobiolaccate was attached on these MMSNPs through a silane-coupling agent and chelated with Cu<sup>2+</sup>.

The Cu<sup>2+</sup>-chelated MMSNPs (MMSNPs-CP TS-IDA-Cu<sup>2+</sup>) showed higher adsorption capacity of 98.1 mg g<sup>-1</sup>-particles and activity recovery of 92.5% for laccase via metal affinity adsorption in comparison with MMSNPs via physical adsorption. Storage stability and temperature endurance of the adsorbed laccase on MMSNPs-CP TS-IDA-Cu<sup>2+</sup> increased significantly, and the adsorbed laccase retained 86.6 % of its initial activity after 10 successive batch reactions operated with magnetic separation. The immobilized laccase on the magnetic mesoporous silica nanoparticles has been developed for efficient phenol degradation. The degradation rate of phenol by the immobilized laccase was 2-fold higher than that of the free laccase, and the immobilized laccase retained 71.3 % of its initial degradation ability after 10 successive batch treatments of coking wastewater. The phenol degradation in the coking wastewater was enhanced in a continuous treatment process by the immobilized laccase in a magnetically stabilized fluidized bed (MSFB) because of good mixing and mass transfer. The magnetic laccase catalyst with the MSFB provides a promising avenue for the continuous enzymatic degradation of phenolic compounds in industrial wastewater.

## Polyethylene glycol mediated synthesis of magnetic nanoparticles as potential magnetic hyperthermia agents

Cristian Iacovita<sup>1</sup>, Rares Stiufluc<sup>1</sup>, Gabriela Stiufluc<sup>2</sup>, Adrian Florea<sup>3</sup>, Romulus Tetean<sup>2</sup> and Mihai C. Lucaci<sup>1</sup>

<sup>1</sup> Department of Pharmaceutical Physics-Biophysics, Faculty of Pharmacy, "Iuliu Hatieganu" University of Medicine and Pharmacy, Pasteur 6, RO-40039 Cluj-Napoca, Romania

<sup>2</sup> Department of Condensed Matter Physics and Advanced Technologies, Faculty of Physics, "Babes Bolyai" University, Kogălniceanu 1, RO-400084 Cluj-Napoca, Romania

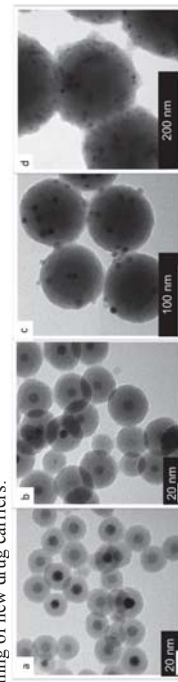
<sup>3</sup> Department of Cell and Molecular Biology, Faculty of Medicine, "Iuliu Hatieganu" University of Medicine and Pharmacy, Pasteur 6, RO-400349 Cluj-Napoca, Romania

E-mail: cristian.iacovita@univcluj.ro or crissiac@yahoo.com

One current challenge of magnetic hyperthermia is achieving therapeutic effect with a minimal amount of magnetic nanoparticles (MNPs). This implies the development of MNPs with enhanced magnetic properties and efficient heat induction. We report an approach based on thermal decomposition of FeCl<sub>3</sub> in the presence of polyethylene glycol of molecular weight of 200 (PEG200) and sodium acetate, in a solvothermal system. This approach allows the synthesis of poly-dispersed cubic and polyhedral MNPs displaying high crystallinity and broad sizes, which can be tuned between 30 and 230 nm by varying the reaction time and the PEG200 amount. The presence of physisorbed PEG200 on the MNPs surface is faintly detected through FT-IR Spectroscopy. The surface of MNPs undergoes oxidation into magnetite as proven by RAMAN spectroscopy. The magnetic characterization performed at room temperature on powder reveal that iOMNPs are ferromagnetic with a coercive field of 160–170 Oe. The evolution of magnetization with the temperature in FC curves below the blocking temperature (300 K) indicates the occurrence of strong magnetic dipole-dipole interactions between MNPs, which vary with both shape and size. Consequently, the specific absorption rate (SAR) values of MNPs, obtained in magnetic fields from 10 kA/m to 60 kA/m at both 195 kHz and 355 kHz frequencies, depend on the concentration of MNPs in water. The SAR values of iOMNPs significantly increase for applied magnetic field exceeding the coercive field, since larger hysteresis loops are covered. From the fitting of SAR values as a function of applied magnetic field with a sigmoidal function, it has been found that SAR values reach saturation when the amplitude of the applied magnetic field is twice the coercive field. By dispersing the MNPs in PG600 (liquid) and PG1000 (solid), it was found that the SAR values decrease by 50 or 75 %, indicating that the Brownian friction within the solvent was the main contributor to the heating power of MNPs. The method has been successfully applied to synthesis ferrites of cobalt, manganese, nickel and zinc. Their hyperthermia properties have been assessed and compared with those reported for iron oxide MNPs. The biocompatibility of all MNPs with human umbilical vein endothelial cells (HUVEC) has been evaluated using MTT assay. The results show that both nickel and zinc ferrites exhibits toxicity while the rest of ferrites present cell viability.

### Acknowledgements:

This research was supported by the Romanian National Authority for Scientific Research, CNCSIS-UEFISCDI, projects nos. PN-III-ID-PCE-2012-4-0531 and PN-II-RU-TE-2014-4-177.



TEM images of the size series of PE Gyated silica-iron oxide nanocomposites with the diameter of (a) 24.86±4.38, (b) 45.24±5.00, (c) 98.10±8.88 and (d) 202.22±6.70 nm

## Synthesis, characterization and hemolysis studies of $Zn_{(1-x)}Ca_xFe_2O_4$ ferrite synthesized by sol for hypertermia treatment applications

R.A. Jasso-Terán<sup>1\*</sup>, P.Y. Reyes-Rodríguez<sup>1</sup>, D.A. Cortés-Hernández<sup>1</sup>, H.J. Sánchez-Fuentes<sup>1</sup>, L.E. de León-Prado<sup>1</sup>

<sup>1</sup> CINVESTAV IPN-Unidad Saltillo, Industria Metalúrgica 1062 Parque Industrial Saltillo Ramos Arizpe, C.P. 25900, Ramos Arizpe, Coahuila, México, E-mail: arg.jasso@gmail.com

Nanoparticles have potential applications in biomedicine in areas such as magnetic resonance imaging (MRI), drug delivery and magnetic hyperthermia. In this work, the synthesis of  $Zn_{(1-x)}Ca_xFe_2O_4$  ferrite,  $x = 0, 0.25, 0.50, 0.75$  and 1.0, was performed by sol-gel method followed by a heat treatment at 400 °C for 30 min.

Samples were analyzed by X-ray diffraction (XRD) and vibrating sample magnetometry (VSM). The  $Zn_{0.5}Ca_{0.5}Fe_2O_4$ ,  $Zn_{0.25}Ca_{0.75}Fe_2O_4$  and  $CaFe_2O_4$  ferrites showed more appropriate magnetic properties. Saturation magnetization of  $Zn_{0.5}Ca_{0.5}Fe_2O_4$ ,  $Zn_{0.25}Ca_{0.75}Fe_2O_4$  and  $CaFe_2O_4$  were 31.31, 38.30 and 40.02 emu/g, respectively. These samples were analyzed by transmission electron microscopy (TEM) and the average particle size was about 14 nm for  $Zn_{0.5}Ca_{0.5}Fe_2O_4$ , 12 nm for  $Zn_{0.25}Ca_{0.75}Fe_2O_4$  and 13 nm for  $CaFe_2O_4$ . The heating capacity of nanoparticles was evaluated under an appropriate magnetic field using a solid state induction heating equipment and the results showed that  $Zn_{0.5}Ca_{0.5}Fe_2O_4$  and  $CaFe_2O_4$  ferrites have an appropriate heating ability for hyperthermia applications. Hemolysis testing showed that  $Zn_{0.5}Ca_{0.5}Fe_2O_4$  and  $CaFe_2O_4$  nanoparticles are not cytotoxic when using suspensions within the range of 0.5 and 5 mg of ferrite/ml of water. According to the results obtained, these ferrites are potential materials for cancer treatment by magnetic hyperthermia therapy.

## Titania-coated manganese nanoparticles for theranostic applications

Z. Jirák<sup>1\*</sup>, J. Kulíčková<sup>1</sup>, V. Herynek<sup>2</sup>, A. Gálisová<sup>2</sup>, J. Koktan<sup>1,3</sup>, and O. Kaman<sup>1</sup>

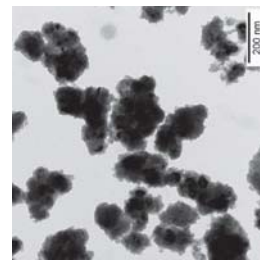
<sup>1</sup> Institute of Physics, AS CR, Cukrovarnická 10, 162 00 Praha 6, Czech Republic

<sup>2</sup> Institute for Clinical and Experimental Medicine, Videnská 1958/9, 140 21 Praha 4, Czech Republic

<sup>3</sup> University of Chemistry and Technology, Prague, Technická 5, 166 28 Praha 6, Czech Republic

\*E-mail: jirak@fzu.cz

Nanostructured titanium dioxide is attractive material for biomedical applications that employ photocatalytic and redox properties of these novel systems, including generation of reactive oxygen species. As the application of titania for nanoparticle coatings is concerned, the preparation is not so facile as the deposition of silica. The present study describes a new procedure whereby nanoparticles of  $La_{1-x}Sr_xMnO$ , known as efficient negative contrast agents in MRI, are successfully covered with a continuous shell of titania.



Single-phase magnetic particles of  $La_{0.55}Sr_{0.35}MnO$  (LSMO) with the mean size of crystallites of 25 nm were prepared by a sol-gel process, followed by thermal treatment and mechanical processing. So-obtained magnetic cores were stabilized by cetyltrimethylammonium bromide. The subsequent encapsulation into titania was carried out by continuous addition of titanium(IV) butoxide. Further, silica-coated particles, containing the same LSMO cores, were prepared as a comparative sample. Importantly, TEM analysis of the titania-coated product showed a well-developed shell around all magnetic cores with the thickness of 10–20 nm and only minor admixtures of free titania (Fig. 1).

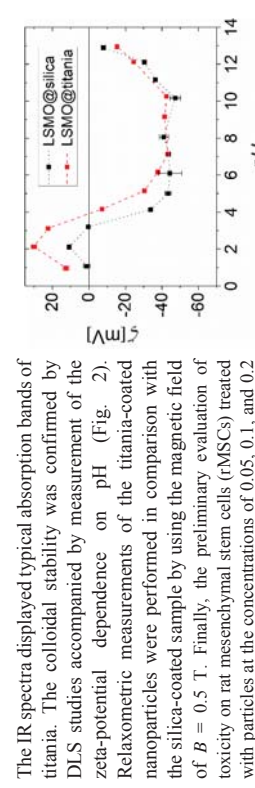


Fig. 1 Titania-coated LSMO

The IR spectra displayed typical absorption bands of titania. The colloidal stability was confirmed by DLS studies accompanied by measurement of the zeta-potential dependence on pH (Fig. 2). Relaxometric measurements of the titania-coated nanoparticles were performed in comparison with the silica-coated sample by using the magnetic field of  $B = 0.5$  T. Finally, the preliminary evaluation of toxicity on rat mesendymal stem cells (rMSCs) treated with particles at the concentrations of 0.05, 0.1, and 0.2 mmol(Mn) $^{-1}$  for 24 h indicated cell viability comparable with a control, whereas measurements of labelled rMSCs at different fields ( $B = 0.5$ , 1, and 4.7) evidenced strong contrast effect of the titania-coated particles in MRI.

Fig. 2 Zeta-potential as function of pH for titania- and silica-coated LSMO

## Size-dependent MR relaxivities of magnetic nanoparticles

A. Joos<sup>1,2</sup>, N. Löwa<sup>2</sup>, S. Düwell<sup>3,4</sup>, C. Hundshammer<sup>3,4</sup>, F. Wiekhorst<sup>2</sup>, B. Gleich<sup>1</sup>, A. Haase<sup>1</sup>

<sup>1</sup> Zentrainstitut für Medizintechnik, Technische Universität München, Garching, Germany

<sup>2</sup> Physikalisch-Technische Bundesanstalt, Berlin, Germany

<sup>3</sup> Department of Nuclear Medicine, Klinikum rechts der Isar, Technische Universität München, München, Germany

<sup>4</sup> Department of Chemistry, Technische Universität München, Garching, Germany

E-mail: ajos@tum.de

Magnetic nanoparticles (MNPs) can be used as remotely controlled carriers for magnetic drug targeting and as contrast agents in magnetic resonance imaging (MRI). For these applications it is crucial to quantitatively determine the spatial distribution of the MNP concentration and the MNPs aggregation state, both of which can be approached by MR relaxometry. Theoretical considerations and experiments have shown that  $R_2^*$  relaxation rates are sensitive to aggregation state and size of the aggregates, whereas  $R_2^*$  is independent of aggregation state and therefore suited for MNP quantification if the condition of static dephasing is met [1]. Our goal is to verify the theoretical predictions for the size dependence of relaxivities with standard MNPs and check whether these meet the static dephasing condition.

In order to obtain MNPs with different well-defined hydrodynamic sizes  $d_{hyd}$ , Ferucarbotran (FER) particles were fractionated using an asymmetric flow field-flow system [2]. The hydrodynamic diameter  $d_{hyd}$  and the diameter of the core material  $d_c$  of the fractions were obtained by dynamic light scattering and multi-angle laser light scattering, respectively. The iron concentration of each fraction was determined using inductively coupled plasma mass spectrometry. The relaxation rates  $R_2$  and  $R_2^*$  were measured in aqueous medium with a 1 Tesla NMR spectrometer and extracted by mono-exponential curve fitting to the MR relaxation curves.

The hydrodynamic and core diameter both linearly increased with fraction number. To be able to compare the relaxation properties of the different size fractions, which had different iron content, the relaxivities are shown here instead of the relaxation rates (Figure 1). The results show a strong dependence of the relaxivities on the MNP size. For smaller MNPs,  $r_2^*$  and  $r_2$  are very similar and increase with increasing particle size, which is in accordance with the motional averaging regime or outer sphere theory [1]. For larger MNPs,  $r_2^*$  is considerably smaller than  $r_2$ , which can be explained by the refocusing pulses becoming effective echo time ( $20 \mu\text{s}$ ) and eventually saturates. For the largest MNPs,  $d_{hyd} > 100 \text{ nm}$ ,  $r_2$  seems to decrease again, which could be explained by the partial refocusing model [1]. The  $r_2^*$  trend for these MNPs is not so obvious because of the stronger scattering of the measured values. However, it can be safely stated that MNPs up to a hydrodynamic diameter of 65 nm do not fulfill the condition of static dephasing because of the drastic increase of  $r_2^*$  relaxivities. With respect to iron content, these particles represent by far the largest portion in the unfractionated sample.

The combination of hydrodynamic fractionation and MR relaxometry is ideally suited to characterize MNP systems with regard to quantitative MRI. Our experiments confirm the outer sphere relaxation theory for small MNPs. We have shown that the majority of FER particles do not meet the condition for static dephasing which is a precondition for reliable quantification based on MRI relaxometry. Thus, FER should not be used for quantitative MRI, since potential size alteration strongly affects MNP relaxivity.

[1] Roch et al., Superparamagnetic colloid suspensions: Water magnetic relaxation and clustering, J Magn Magn Mater 2005; 293: 532-539  
[2] Löwa et al., Hyphenation of Field-Flow Fractionation and Magnetic Particle Spectroscopy, Chromatography 2015; 2: 655-668

## Effective Parameters in Aggregation of Nano Particles during Magnetic Guided Drug Delivery in Mice Brain

Ali Kafash Hoshiar, Tuan Anh Le, Jungwon Yoon

School of Mechanical Engineering, Gyeongsang National University, Jinju, Republic of Korea

E-mail: jwyoon@gnu.ac.kr

The Magnetic-guided nanorobotic systems have emerged as the ultimate tool for steering the magnetic nanoparticles in the vascular system. The primary goal in the Targeted Drug Delivery (TDD) is to guide a drug to a desired position and provide an optimal concentration of the drug in the location of interest.

We have developed a novel system for TDD based on magnetic actuators. In this system, using the computational platform, first, a Modified Field Function (MFF) for steering nanoparticles is developed. Then the magnetic actuators apply the MFF on the test subject, and the magnetic nanoparticles are steered in the mice brain. The mice brain samples show a trace of the clustered nanoparticles which is a clear evidence of the aggregation.

Computational simulations have been used to model this aggregated particles and to study the influential parameters. The effects of the environment, process and particle properties have been investigated to control and eliminate unwanted aggregation. The knowledge gained through detailed computational, and experimental studies helped us to clarify the most influential parameters and impose more control over the process.

Based on our results the most critical parameters which play the major role in this phenomenon are particle size and adhesive energy, velocity and viscosity of the environment and magnetic force intensity. Understanding the influence of these parameters helped us to increase the target efficacy over the nanoparticles and lead in more accurate TDD.

### A- Experimental Setup

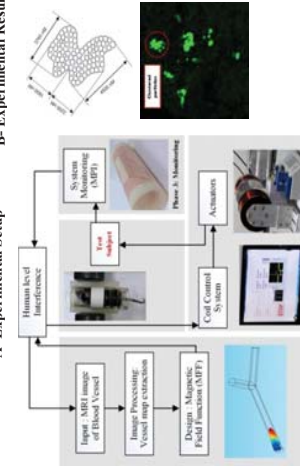


Figure 1: Experimental Setup  
Photo 1: Magnet focusing Beads  
Photo 2: Actuators  
Schematic of the magnetically guided drug delivery system, the evidence of the aggregation and simulation of influential forces

### B- Experimental Results

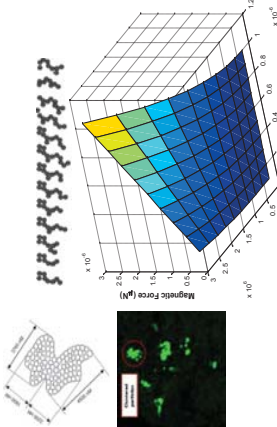


Figure 2: Experimental Results  
magnetic force (mN)  
magnetic intensity (A/m²)  
particle diameter (nm)  
Schematic of the magnetically guided drug delivery system, the evidence of the aggregation and simulation of influential forces

### C- Computational Simulation

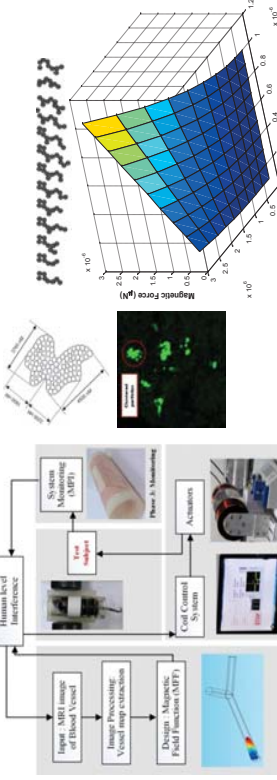


Figure 3: Computational Simulation  
magnetic force (mN)  
magnetic intensity (A/m²)  
particle diameter (nm)  
Schematic of the magnetically guided drug delivery system, the evidence of the aggregation and simulation of influential forces

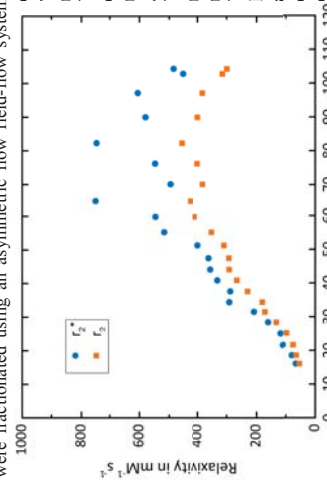


Figure 1: Relaxivities of size fractionated FER particles. The error bars of the mono-exponential fits are smaller than the symbols. This is in accordance with the motional averaging regime or outer sphere theory [1]. For larger MNPs,  $r_2^*$  is considerably smaller than  $r_2$ , which can be explained by the refocusing pulses becoming effective echo time:  $20 \mu\text{s}$ ) and eventually saturates. For the largest MNPs,  $d_{hyd} > 100 \text{ nm}$ ,  $r_2$  seems to decrease again, which could be explained by the partial refocusing model [1]. The  $r_2^*$  trend for these MNPs is not so obvious because of the stronger scattering of the measured values. However, it can be safely stated that MNPs up to a hydrodynamic diameter of 65 nm do not fulfill the condition of static dephasing because of the drastic increase of  $r_2^*$  relaxivities. With respect to iron content, these particles represent by far the largest portion in the unfractionated sample.

The combination of hydrodynamic fractionation and MR relaxometry is ideally suited to characterize MNP systems with regard to quantitative MRI. Our experiments confirm the outer sphere relaxation theory for small MNPs. We have shown that the majority of FER particles do not meet the condition for static dephasing which is a precondition for reliable quantification based on MRI relaxometry. Thus, FER should not be used for quantitative MRI, since potential size alteration strongly affects MNP relaxivity.

## Microstructure Evolution and Magnetic Properties of Nanocrystalline $(\text{Ni}_{75}\text{Fe}_{25})_{95.6}\text{Si}_{3.5}$ Thin Films

A. Kaibi<sup>\*1</sup>, A. Guittoum<sup>2</sup>, R. M. Öksüzoglu<sup>3</sup>, C. Yavru<sup>3</sup>, S. Özgün<sup>3</sup>, M. Boudissa<sup>4</sup>, M. Kechouane<sup>1</sup>

<sup>1</sup> University Larbi TEBESSI, Sciences of Materials Department, Faculty of physics, Tebessa, Algeria.

<sup>2</sup> Nuclear Research Centre of Algiers, Algiers, 02 Bd Frantz Fanon, BP 399, Algeria.

<sup>3</sup> University of Anadolu, Faculty of Engineering, Department of Materials Sciences and Engineering, Eskişehir İkinci Eylül Campus, 26555, Turkey.

<sup>4</sup> ENMC Laboratory, Physics Department, University of Sétif, 19000, Algeria.

\*E-mail: kaibi\_amel@yahoo.fr

We report on the structural, microstructural and magnetic properties of  $(\text{Ni}_{75}\text{Fe}_{25})_{95.6}\text{Si}_{3.5}$  thin films with different thicknesses were deposited by vacuum evaporation from nanocrystalline powder onto Si (1 1 1) substrate. The thickness varies from 19 nm to 110 nm. The as deposited films were characterized by Grazing incidence X-ray diffraction (GIXRD), Scanning Electron Microscopy (SEM), Atomic Force Microscopy (AFM) and vibrating sample magnetometry (VSM). From GIXRD spectra, we have shown that the grazing X-ray diffraction patterns (GIXRD), we have shown the presence of a strong <200> texture for the lowest thicknesses 19 nm and 25nm. For the 59 nm, a strong <111> preferred orientation is developed. However, for higher thicknesses, a polycrystalline structure is present. From the Scanning Electron Microscopy observations (SEM), we have shown that the surface seems to be very dense with many fine grains. The analysis of EDX spectra revealed that the sample composition is close to the starting Ni75Fe25 powder. A more accurate investigation of the morphology was performed with the atomic force microscopy (AFM). We have shown the existence of nanosized grains with a uniform distribution. The mean diameter of the grains increases from 23 nm to 30 nm when the thickness increases. From magnetic measurements, we have shown the existence of a

## Microstructure Evolution and Magnetic Properties of Nanocrystalline $\text{Ni}_{75}\text{Fe}_{25}$ Thin Films: Effects of Substrate and Thickness.

A. Kaibi<sup>\*1</sup>, A. Guittoum<sup>2</sup>, R. M. Öksüzoglu<sup>3</sup>, C. Yavru<sup>3</sup>, S. Özgün<sup>3</sup>, M. Boudissa<sup>4</sup>, M. Kechouane<sup>1</sup>

<sup>1</sup> University Larbi TEBESSI, Sciences of Materials Department, Faculty of physics, Tebessa, Algeria.

<sup>2</sup> Nuclear Research Centre of Algiers, Algiers, 02 Bd Frantz Fanon, BP 399, Algeria.

<sup>3</sup> University of Anadolu, Faculty of Engineering, Department of Materials Sciences and Engineering, Eskişehir İkinci Eylül Campus, 26555, Turkey.

<sup>4</sup> ENMC Laboratory, Physics Department, University of Sétif, 19000, Algeria.

\*E-mail: kaibi\_amel@yahoo.fr

Permalloy (Py) thin films were evaporated from nanocrystalline soft Ni75Fe25 powder onto glass and Al2O3 substrates [1]. The thicknesses of these films range from 16 nm to 250 nm. The as deposited films were characterized by Grazing incidence X-ray diffraction (GIXRD), Scanning Electron Microscopy (SEM), Atomic Force Microscopy (AFM) and vibrating sample magnetometry (VSM). From GIXRD spectra, we have shown that the films are amorphous for the thinner films. However, for the thicker films, a polycrystalline fcc structure is present. For the intermediate thicknesses, the nature of substrate determines the texture of the films. The SEM micrographs indicate that the nature of substrate influences on the morphology and grains size of Py films. From AFM observations, the nanocrystalline nature of the grains is evidenced. Hysteresis loops reveals the ferromagnetic character of Py films. We have shown that the values of coercive field,  $H_c$ , generally, decrease with increasing thickness. Moreover, the  $H_c$  values are higher for films deposited onto Al2O3 substrate than those on glass one. The nature of substrate and thickness seems to influence the magnetic properties of Py films. A correlation between these physical properties will be established and discussed.

## Preparation of Mn-Zn ferrite nanoparticles and their silica-coated clusters as contrast agents for MRI

O. Kaman<sup>1\*</sup>, J. Kulíčková<sup>1</sup>, V. Herynek<sup>2</sup>, T. Dědourová<sup>1,3</sup>, M. Matyško<sup>1</sup>, J. Kotkan<sup>1,4</sup>, and Z. Jírák<sup>1</sup>

<sup>1</sup> Institute of Physics, AS CR, Cukrovarnická 10, 162 00 Praha 6, Czech Republic

<sup>2</sup> Institute for Clinical and Experimental Medicine, Videnská 1938/9, 140 21 Praha 4, Czech Republic

<sup>3</sup> University of Pardubice, Doubravice 41, 532 10 Pardubice, Czech Republic

<sup>4</sup> University of Chemistry and Technology, Prague, Technická 5, 166 28 Praha 6, Czech Republic

\*E-mail: kaman@seznam.cz

Modern methods in the synthesis of nanoparticles provided MRI with several options how to enhance the effects of negative contrast agents (CAs). Traditional CAs were restricted to iron oxides, but nanoparticles of other metal oxides show higher magnetization, and thus higher transverse relaxivities ( $r_2$ ) might be achieved. Moreover, a careful optimization of their extrinsic properties, i.e., the mean size of crystallites ( $d_{xxd}$ ), clustering, and suitable coating can further increase the relaxivity. The present contribution demonstrates such efforts and shows that in addition to high  $r_2$ , a pronounced temperature variance of the contrast effect can be obtained at physiological temperatures.

Three samples of Mn-Zn ferrite nanoparticles were synthesized by hydrothermal treatment of precursors obtained by alkaline precipitation under inert atmosphere. XRD patterns proved their single-phase spinel structure of the  $Fd\bar{3}m$  symmetry, whereas peak broadening of diffraction lines showed  $d_{xrd} \approx 10$  nm. The chemical composition of particles, determined by XRF analysis, closely reflected the ratio of cations employed for the synthesis. SQUID magnetometry evidenced the ferrimagnetic arrangement and revealed that all samples are in superparamagnetic state at room temperature (see the inset of Fig. 1b).

The composition  $Mn_{0.6}Zn_{0.4}Fe_{1.97}O_4$  was selected for a detailed study, based on its high magnetization ( $M_{796.5A/m} = 107.1$  and  $53.3$  Am<sup>2</sup>/kg at 5 and 300 K, respectively) and  $T_c \approx 380$  K. Silica-coated products with efficient core size of  $\approx 30$  nm (Fig. 1a) were prepared by hydrolysis and polycondensation of tetraethoxysilane, followed by repeated differential centrifugation. The high transverse relaxivities with steep temperature dependence, related to suitably adjusted  $T_c$ , have been observed.

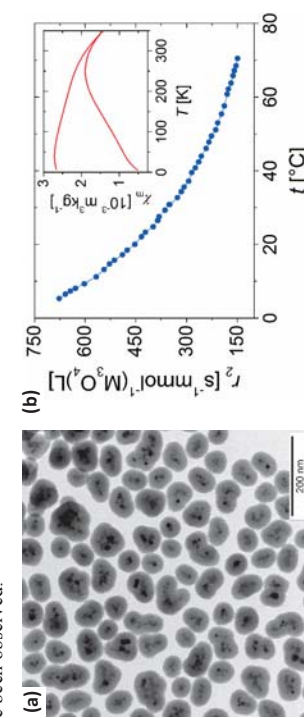


Fig. 1 Silica-coated clusters of  $\approx 10$  nm  $Mn_{0.6}Zn_{0.4}Fe_{1.97}O_4$  nanocrystallites: a) TEM micrograph, b) temperature dependence of  $r_2$  at  $B = 0.5$  T, the ZFC-FC susceptibilities of bare cores at  $H = 1.5$  kA/m are shown in the inset.

## Developing the Massart Method for Obtaining Biocompatible Magnetite Nanoparticles of Given Sizes

L.Kh. Komissarova<sup>1\*</sup>, A.S. Tatikolov<sup>1</sup>, N.A. Marnaufov<sup>1</sup>, V.N. Erohin<sup>1</sup>, V.A. Semenov<sup>1</sup>, N.A. Brusentsov<sup>2</sup>, O.P. Barinova<sup>3</sup>, O.O. Vasilkov<sup>3</sup>, A.B. Elfimov<sup>3</sup>

<sup>1</sup> N.M. Emanuel Institute of Biochemical Physics, Russian Academy of Sciences, Kosygin str., 4, 119334 Moscow, Russia, <sup>2</sup> Blokhin Russian Cancer Research Center, Russian Academy of Sciences, 115478 Moscow, Russia, <sup>3</sup> Moscow State University of Information Technologies, Radio Engineering and Radio Electronics, Vernadsky Avenue 78, 119454 Moscow, Russia, \*E-Mail: komissarova-lkh@mail.ru

The Massart method is one of the main methods for synthesizing magnetite nanoparticles. Still there is not yet a reproducible methodology of obtaining biocompatible magnetite nanoparticles of a given size for biomedical purposes with the use of this method. The aims of the research are: to work out a reproducible procedure of synthesizing biocompatible magnetite nanoparticles of a given size using the Massart method by adjusting the environment and optimizing reaction conditions; to study sizes, structure, and chemical composition of the particles by transmission electron microscopy, electron diffraction studies and other methods; to check the particles for toxicity by intraperitoneally injecting intact mice.

Fig. 1 shows a microphotograph of the nanoparticles synthesized in the argon atmosphere at 12% of the total concentration of  $FeCl_3 \cdot 6H_2O$  and  $FeSO_4 \cdot 7H_2O$  salts. Fig. 2 shows microphotographs of these nanoparticles in a dark field and their electron diffraction.

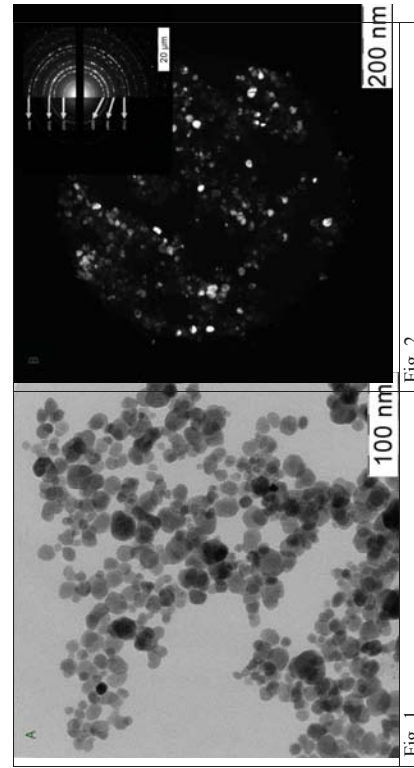


Fig. 2

It has been shown that in order to obtain biocompatible magnetite nanoparticles of  $14 \pm 6$  nm in size by the Massart method it is worthwhile to conduct the reaction in an inert atmosphere (argon). The process conditions have been optimized: concentrations of the salts, temperature, reaction time and stirring speed. By intraperitoneally injecting the preparation to the intact mice we have shown that the obtained nanoparticles are non-toxic and may be used for biomedical purposes, including as drugs carriers for target delivery to a tumor.

## Preparation of Poly-L-Lysine Functionalized Magnetic Nanoparticles and Influence on Cancer Cells Viability

M. Koneracka<sup>1</sup>, M. Kubovčíková<sup>1</sup>, I. Khamra<sup>2</sup>, V. Závišová<sup>1</sup>, S. Matovičová<sup>3</sup>, P. Kopencansky<sup>1</sup>,

<sup>1</sup> Institute of Experimental Physics, Slovak Academy of Sciences, Watsonova 47, Košice, Slovakia

<sup>2</sup>Pavol Jozef Šafárik University, Faculty of Sciences, Watsonova 47, Košice, Slovakia

<sup>3</sup>Institute of Virology, Slovak Academy of Sciences, Dubová cesta 9, Bratislava, Slovakia, E-Mail: konerack@stesk.sk

The aim of this study was developing of biocompatible amino functionalized nanoparticles for their further use as substrates for binding specific antibodies that are able to detect cancer cells. The amino-modified magnetic nanoparticles were prepared by precipitation of Fe (II) and Fe (III) salts in an alkali medium, and this was subsequently followed by the addition of poly-L-lysine (PLL). Biocompatible poly-L-lysine (PLL), which is in fact a synthetic polymer, has wide use in pharmaceutical industry and, its sub-products, monomeric amino acid lysine units, occur naturally in human body. To find the optimal PLL/Fe<sub>3</sub>O<sub>4</sub> weight ratio, several samples were prepared and examined as a function of the initial PLL amount, ranging from 0.12 to 4.8 mg, with the amount of magnetite being kept constant (1.26 mg). The prepared samples (MFPLLS) were tested in terms of particle size and zeta potential measurements, where the optimal value of weight ratio turned out to be 1.5. The optimal value based on zeta potential measurements was in agreement with the outcome of UV/VIS measurements. Measuring magnetic properties of naked and biofunctionalized magnetic nanoparticles using Superconducting Quantum Interference Device (SQUID) showed superparamagnetism. Spherical shape of nanoparticles was confirmed by SEM microscope observation (Fig. 1 left) and hydrodynamic nanoparticle diameter, ranging from 100 to 200 nm in dependence on PLL/Fe<sub>3</sub>O<sub>4</sub> weight ratio, was obtained by means of DLS measurement.

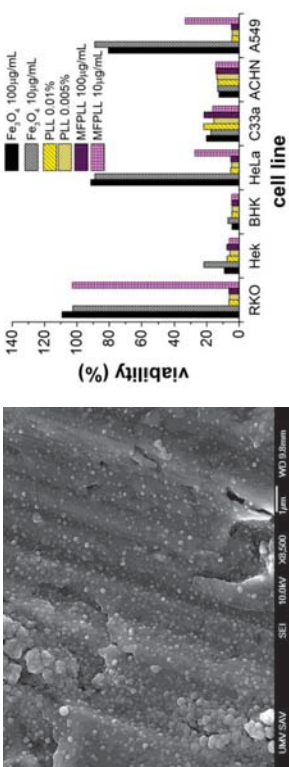


Fig. 1: SEM image of amino modified magnetic nanoparticles (left) and the effect of naked magnetic particles, pure PLL and MFPLL on the cell viability of various cancer cells after incubation 5 days (right).

The cytotoxic effect of different samples at concentrations 10 and 100 µg/mL of nanoparticles on various cells lines was examined by the Cell Titer Blue viability assay. A dose-dependent reduction in colour was observed after 5 days of treatment, and 80–95% of the cells were dead at the highest concentration of MFPLL and PLL tested (100 µg/mL and 0.005% respectively). Lower concentration (10 µg/mL) of MFPLL was not toxic for RKO human colon carcinoma cell line (Fig. 1 right).

**Acknowledgements** This work was supported by Slovak Research and Development Agency under the contracts No. APVV-14-0120 and APVV-14-0932.

## Radiation-enhanced decomposition of protein amyloid fibrils by magnetic nanoparticles

P. Kopencansky<sup>1\*</sup>, K. Siposova<sup>1</sup>, M. Koneracka<sup>1</sup>, V. Závišová<sup>1</sup>, I. Haysak<sup>2</sup>, V. Martishichkin<sup>2</sup>,

<sup>1</sup>Institute of Experimental Physics, SAS, Watsonova 47, Košice, Slovakia

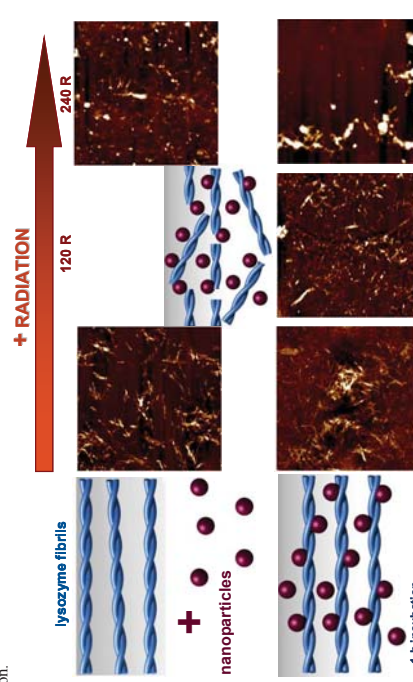
<sup>2</sup>Uzhgorod National University, Narodna str. 4, Uzhgorod, Ukraine

\*Corresponding author e-mail: konerack@saske.sk

A common feature associated with most of neurodegenerative diseases is the formation of extended, β-sheet rich amyloid fibrils. Compelling evidence indicates that amyloid aggregation is critical for neurodegeneration and therefore the preventing of amyloid formation and/or the reduction of amyloid assemblies is potentially the most effective therapeutic approach for the treatment of amyloid-related diseases. Thus, nanoparticles are being explored for their role in diagnosing, preventing, treating or even causing amyloid diseases.

In addition to amyloid pathology, in present work we have investigated effect of radiation on amyloid fibrils and fibrils in presence of nanoparticles (NPs). To preformed lysozyme fibrils, we add NPs and after 1 hour incubation we apply radiation at four different exposure doses: 20.8 R, 77 R, 122 R and 244 R, correspondingly (bremsstrahlung gamma rays of betatron B-25). After irradiation, we used atomic force microscopy to examine effect of radiation. In the absence of NPs and radiation, lysozyme amyloid fibrils shows typical amyloid morphology of aggregates displaying long fibrillar structure and protofibrillar twisting. It should be noted, that in our previous work we demonstrated destruction of fibrils after 24 h incubation [1,2]. However, application of irradiation significantly enhanced the destruction of fibrils in presence of NPs and similar extent of destruction was observed already after 1 h (incubation of fibrils+NPs) and dosing interval 15 min. (122 R) as demonstrated on Scheme. Longer radiation doses lead to total destruction of fibrillar morphology.

Thus, our results may provide better understanding of the general effect of radiation on organisms and the possible interaction between proteins and radiation. Further investigations will help to identify the role of radiation in the etiology of neurodegenerative diseases, because they are considered to be late effects of radiation.



Schematic representation of radiation enhanced decomposition of lysozyme fibrils in presence of nanoparticles.

**Acknowledgment:** This work was supported by grants: VEGA No. 2/0062/14, APVV 14-0120, Macosystem ERA Net Grant and by grant of Ministry of Education and Science of Ukraine No. 01/15/U/001098.

Reference:

[1] Bellova A., et al. Nanotechnology, 2010, 21(6), 065103

## Disparity of Native, Reconstructed Ferritin and Magneto-Ferritin in Low-field and High-field MRI

L. Balejčíková<sup>1,2</sup>, O. Sribák<sup>1</sup>, L. Bacík<sup>3</sup>, M. Masarová<sup>1</sup>, A. Krafčík<sup>1</sup>, P. Kopcanský<sup>2</sup> and I. Frullo<sup>1</sup>

<sup>1</sup>Institute of Measurement Science SAS, Dubravská cesta 9, 841 04 Bratislava, Slovakia

<sup>2</sup>Institute of Experimental Physics SAS, Watsonova 47, 040 01 Košice, Slovakia

<sup>3</sup>Faculty of Chemical and Food Technology STU, Radlinského 9, 812 37 Bratislava, Slovakia

Email: andrea.krafck@stuba.sk

Ferritin is a biological iron storage macromolecule, which consist of protein shell (apoferitin) and ferrhydrite-like mineral core. Due to its biocompatible properties attracts interest in biomedical applications. However, it also plays a crucial role in pathological processes of disrupted iron homeostasis and iron accumulation (magneticite formation), linked with various disorders (e.g. neuroinflammation, neurodegeneration, cirrhosis, etc.). Iron overloaded ferritin, with the help of MRI techniques, has such potential to become a non-invasive biomarker of these processes. However, there is still lacking a method, which enables to distinguish between physiological and pathological ferritin. Therefore, with the help of T<sub>2</sub>-weighted MRI pulse sequences (GE, STIR, TSE), we have tried to find differences in MRI parameters between native (physiological), reconstructed ferritin and magneto-ferritin (pathological). For that reason, reconstructed ferritin and magneto-ferritin with different iron loadings were synthesized to simulate iron-induced pathological model systems. Measurements were performed at low-field ESAOTE 0.2 T, and high-field VARIAN 4.7 T systems, for the possibility of comparison. Relative contrast, T<sub>2</sub> relaxation time, as well as relaxivity r<sub>2</sub> values were evaluated and compared.

Low-field results suggest that we are able to clearly distinguish between physiological (native) and pathological (reconstructed and magneto-) ferritin, even with ferritin trapped in gelatine (Fig. 1). In case of r<sub>2</sub> values in high-field system, the results significantly differ. Reconstructed ferritin is poorly distinguishable from native ferritin, without regard whether it is entrapped in gelatine or not (Fig. 2). On the other hand, magneto-ferritin differentiability from native ferritin is obvious. These results can serve as a starting point in developing of MRI techniques able to distinguish of physiological and pathological ferritin. Such method is necessary in developing of non-invasive diagnostics of iron-based disorders.

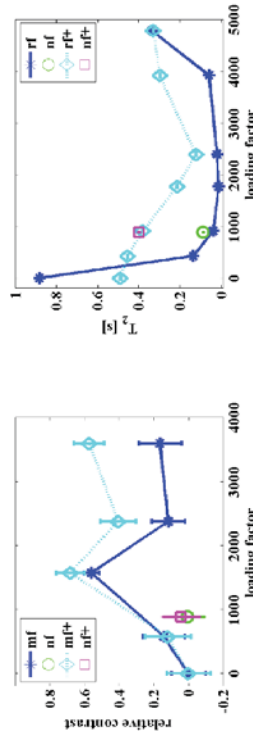


Figure 1: Relative contrast of magneto-ferritin (mf) and native ferritin (nf) in comparison with loading factor. (+) samples are entrapped in gelatine. Measured at 0.2 T ESAOTE system.

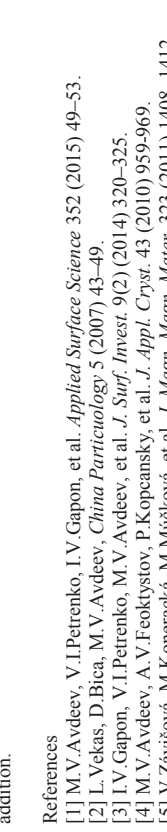


Figure 2: T<sub>2</sub> values of reconstructed ferritin (rf) and native ferritin (nf) in comparison with loading factor. (+) samples are entrapped in gelatine. Measured at 4.7 T VARIAN system.

## STRUCTURE AND STABILITY OF MAGNETIC FLUIDS AT INTERFACE WITH SILICON BY NEUTRON REFLECTOMETRY

M.Kubovčíková<sup>1</sup>, V.Závisová<sup>1</sup>, M.Koneračká<sup>1</sup>, V.I.Petrenko<sup>2,3</sup>, M.V.Avdeev<sup>2</sup>, I.V.Gapon<sup>2,3</sup>, P.Kopcanský<sup>1</sup>

<sup>1</sup>Institute of Experimental Physics, Slovák Academy of Sciences, Košice, 04001, Slovakia;

<sup>2</sup>Frank Laboratory of Neutron Physics, Joint Institute for Nuclear Research, Dubna, 141980, Russia;

<sup>3</sup>Physics Department, Kyiv Taras Shevchenko National University, Kyiv, 03022, Ukraine;

The adsorption of surfactant coated magnetic nanoparticles from highly stable magnetic fluids on crystalline silicon was studied by neutron reflectometry (NR). Two types of magnetic fluids (MFs) based on nanomagnetic (co-precipitation reaction) dispersed and stabilized in a non-polar organic solvent (coating by oleic acid in deuterated benzene) and a strongly polar solvent (coating by sodium oleate in heavy water) were considered. The range of the volume fractions of the dispersed magnetite was restricted by 10% for the organic fluid and 2% for the aqueous fluid. It was obtained that along with the structural stability in bulk the considered MFs are characterized by the interface adsorption layer of colloidal polydisperse particles from MFs, which is insensitive to the effect of the external magnetic field. For the organic MF which is free of any kind of aggregates [2] the concentration of free particles at the interface becomes higher as compared to that in bulk with the particle concentration growth, thus indicating to a wide spatial transition from the adsorption layer to bulk. In the aqueous MF because of lower maximal particle concentration this transition is much sharper, so that the mean scattering density of the interface and bulk are very close. The interpretation of the NR experiment in this case is complicated by the contribution of the diffuse scattering [3] from comparatively large aggregates which were revealed previously by small-angle neutron scattering [4]. Nevertheless, it was shown that individual nanoparticles are preferably adsorbed on the silicon surface. To check this statement aqueous ferrofluids modified by poly(ethylene glycol) (PEG) was considered. Since from bulk structure investigation it was found that comparatively small and compact nanoparticle aggregates (size at level of 40 nm) in the initial samples transfer to large (size above 120 nm) and developed (fractal dimension 2.5) associates after PEG coverage molecular mass MW = 1000 g/mol is added to the system with the ratio above 2:1 with respect to magnetic content [4,5]. And indeed no any adsorption of nanoparticles was detected from reflectometry experiments in the case of large and developed fractal in the ferrofluid with PEG addition.

### References

- [1] M.V.Avdeev, V.I.Petrenko, I.V.Gapon, et al. *Applied Surface Science* 352 (2015) 49-53.
- [2] L.Vekas, D.Bica, M.V.Avdeev, *China Particulology* 5 (2007) 43-49.
- [3] I.V.Gapon, V.I.Petrenko, M.V.Avdeev, et al. *J. Surf. Invest.* 9(2) (2014) 320-325.
- [4] M.V.Avdeev, A.V.Feoktystov, P.Kopcanský, et al. *J. Appl. Cryst.* 43 (2010) 959-969.
- [5] V.Závisová, M.Koneračká, M.Múčková, et al. *J. Magn. Magn. Mater.* 323 (2011) 1408-1412.

## Non-invasive High Resolution Magnetic Field and Temperature Imaging

Julia M. McCoy\*, D.A. Simpson<sup>1</sup>, R. Ryan<sup>2</sup>, and L.C.L. Hollenberg<sup>1</sup>

<sup>1</sup>School of Physics, University of Melbourne, Parkville, 3052, Australia,

<sup>2</sup>School of Chemistry and the Ba21 Institute, University of Melbourne, Parkville, 3052, Australia

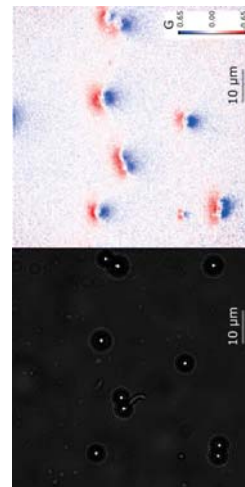
\*Email: [mccoyj@student.unimelb.edu.au](mailto:mccoyj@student.unimelb.edu.au)

Magnetic particles are currently seeing applications in a wide range of biological environments. The ability to non-invasively image the location and field strength of these particles within cells would be highly desirable. Additionally, understanding spatial or temporal variations of temperature in biological systems is an active field of research. We have developed a quantum diamond-based temperature and magnetic imaging device to investigate these and other biological questions.

The diamond-based sensing chip exploits the quantum properties of negatively-charged nitrogen-vacancy (NV) centres. NV centres fluoresce in the red, and the rate of fluorescence indicates the NV centre spin state. By manipulating the NV centres with microwave pulses, and then detecting the change in the spin state, properties such as magnetic field strength and local temperature can be extracted. In order to map such effects in 2D, we engineered a layer of near-surface NV centres into a single-crystal diamond and imaged the NV array with a wide-field microscope coupled to an sCMOS imaging detector. We have demonstrated its application by imaging the temperature response from ohmic heating of a gold wire, the magnetic dipole fields from paramagnetic micro-spheres, and electron paramagnetic resonance spectroscopy of Cu<sup>2+</sup> ions in solution.

Our imaging capabilities comprise a magnetic field spatial resolution of 440 nm, sub-micron temperature imaging resolution, and magnetic and thermal sensitivities of  $\sim 1.5 \text{ }\mu\text{T}/\sqrt{\text{Hz}}$  and  $\sim 1\text{K}/\sqrt{\text{Hz}}$ . Micron-sized magnetic signals are detectable up to  $\sim 4 \text{ }\mu\text{m}$  above the diamond sensor. In electron spin spectroscopy mode, the system can detect paramagnetic ions with a sensitivity of zeptomoles per pixel.

There are many applications we are exploring for our device, and we aim to find more as there are wide-ranging potential applications from cell biology to plasmonics.



Micro-magnetic spheres imaged in bright-field (left), and the corresponding magnetic image of their dipoles (right) on the quantum imaging system.

## The Transduction Mechanism and Applications of Giant Magnetoresistive Biosensors

Jung-Rok Lee<sup>1,3\*</sup>, Noriyuki Sato<sup>2</sup>, Daniel J.B. Bechstein<sup>3</sup>, and Shan X. Wang<sup>1,2</sup>

<sup>1</sup> Department of Materials Science and Engineering, Stanford University, Stanford CA, USA

<sup>2</sup> Department of Electrical Engineering, Stanford University, Stanford CA, USA

<sup>3</sup> Department of Mechanical Engineering, Stanford University, Stanford CA, USA, \*E-mail: jungrok@stanford.edu

Giant magnetoresistive (GMR) biosensors consisting of many rectangular stripes are being developed for high sensitivity medical diagnostics of diseases at early stages, but many aspects of the sensing mechanism remain to be clarified. Using e-beam patterned masks on the sensors, we showed that the magnetic nanoparticles with a diameter of 50 nm located between the stripes predominantly determine the sensor signals over those located on the sensor stripes. Based on computational analysis, it was confirmed that the particles in the trench, particularly those near the edges of the stripes, mainly affect the sensor signals due to additional field from the stripe under an applied field. We also demonstrated that the direction of the average magnetic field from the particles that contributes to the signal is indeed the same as that of the applied field, indicating that the particles in the trench are pivotal to produce sensor signal. Importantly, the same detection principle was validated with a duplex protein assay. Also, 8 different types of sensor stripes were fabricated and design parameters were explored. According to the detection principle uncovered, GMR biosensors can be further optimized to improve their sensitivity, which is highly desirable for early diagnosis of diseases. In addition, the GMR biosensors are a versatile platform, and can be used for fundamental researches and clinical applications.

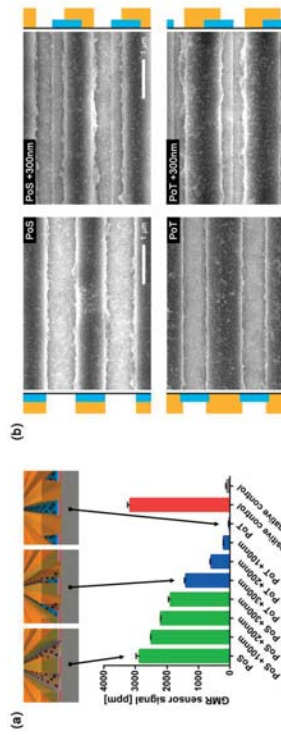


Figure (a) GMR sensor signals from the sensors with different types of masks. The top three images show the relative locations of sensor stripe, photoresist mask, and the particles, approximately (not to scale) for the corresponding signals. The positive control is the sensor without any masks but coated with biotinylated BSA, while the negative control sensors are coated with BSA without any masks. The error bars are the standard deviations of identical sensors on the same chip. (b) SEM images of 4 different types of masks (PoS, PoS + 300 nm, PoT, and Po T + 300 nm) on the sensor stripes after the particles are attached. The blue bars next to the SEM images indicate the sensor stripes, and the orange bars indicate the photoresist masks.

Jung-Rok Lee *et al.* (2016) *Sci. Rep.* 6, 18692

## Magnetophoretic transport system for digital control of single particle and cells

**Byeonghwa Lim, Sri Ramulu Torati, XingHao Hu, CheolGi Kim\***

Department of Emerging Materials Science, DGIST, Daegu, 42988, Republic of Korea,  
Email: [limbh@dgist.ac.kr](mailto:limbh@dgist.ac.kr)

The cell manipulation has important applications for gene sequencing, single cell analysis and cell separation technology. Even though, several single cell techniques are exist, it is still challenge and complex to collect rare cells and their digital manipulation in large-scale operation. In recent years the flexibility of magnetic transport technology using nano/micro scale magnets for the digital magnetophoresis has experienced marvelous advances and has been used for a wide variety of single cells manipulation tasks such as selection, capture, transport, encapsulation, transfection, or lysing of magnetically labeled cells. The magnetic transport technology, which can be integrated within microfluidic channels, relies on both magnetic energy and force tunability and remote control implemented by micro-and nano-patterned magnetic structures. Here, we have demonstrated a class of integrated magnetic track circuits for executing sequential and parallel, timed operations on an ensemble of single particles and cells. The magnetic circuitry tracks are designed by conventional lift-off technology and were used for the passive control of cells/particles similar concept to electrical conductor, diodes and capacitor. When the magnetic tracks are combined into arrays and driven by rotating magnetic field, the single cells are precisely control for multiplexed analysis. In addition, the concentric cell translocation and separation were performed by the assembly of this magnetic track into a novel architecture, resembled with spider web network, where all the cells are concentrated into one position and then transported to apartments array for the single cell analysis.

### References:

- [1] B. Lim, V. Reddy, X. H. Hu, K. W. Kim, M. Jadhav, R. Abedini-Nassab, Y. W. Noh, Y. T. Lim, B. B. Yellen; C. G. Kim, *Nat. Commun.* **2014**, 5, 1
- [2] S. Anandakumar, V. Sudha Rani, S. Oh, B. L. Sinha, M. Takahashi, C. G. Kim, *Biosens Bioelectron.* **2010**, 26, 1755.

## Synthesis of Functional Magnetic Nanoparticles for Microalgal Cell Separation

Chunzhao Liu  
National Key Laboratory of Biochemical Engineering, Institute of Process Engineering,  
Chinese Academy of Sciences, Beijing, China.

Recently, microalgae are considered as good candidates for biofuel production and have gained enormous research interests. In order to reduce initial capital investment, energy and running costs as well as flocculant toxicity, there is still a great interest to develop new economic and efficient approaches for harvesting microalgal cells. A simple and rapid harvesting method by magnetic separation with various functional magnetic nanoparticles has been developed for recovering cells of various microalgal species. After adding the magnetic particles to the microalgal culture broth, the microalgal cells were captured and recovered quickly by an externally magnetic field. The maximal recovery efficiency for various microalgal species reached more than 95% within 3-5 minutes, and the capture mechanism between the magnetic nanoparticles and the microalgal cells was elucidated. The low-cost magnetic nanoparticles can be easily regenerated from the harvested microalgal cells, and the regenerated magnetic nanoparticles maintained the same recovery efficiency for the microalgal cells as the newly synthesized ones after 10 times of reuse. These functional magnetic nanoparticles together with a novel continuous magnetic separator provide a great potential for economic and efficient microalgal cell separation in practice.

## Magnetic Nanoparticles in different biological environments as seen by Magnetic Particle Spectroscopy

Norbert Löwa, Patricia Radon, and Frank Wiekhorst

Physikalisch-Technische Bundesanstalt, Abestr. 2-12, 10587 Berlin

\*E-Mail: norbert.loewa@ptb.de

### Introduction

The quantification of magnetic iron oxide nanoparticles (MNP) in biological systems is of vital importance in the development of novel biomedical applications such as magnetofection, magnetic drug targeting or hyperthermia. Among several techniques established to detect MNPs in tissue or cells, magnetic particle spectroscopy (MPS) [1] provides signals specific for MNP and provides linear calibration curves over three orders of magnitude down to the nanogram range. We recently demonstrated the feasibility of this technique to quantify MNP uptake in living cells [2] and even in a liquid flow [3] using the calibration curve of a reference sample for quantification. Furthermore, MPS signal crucially depends on the magnetic properties of the MNP as well as on the influence of the surrounding biological environment causing viscosity changes and aggregation. Therefore, different physiological parameters (e.g. pH-value, ionic strength, mobility) may have distinct impact on the amplitudes of MPS signal which could increase reference sample based quantification uncertainty. To study this we investigated the MPS signals of different MNP types (size and coating) in various environments.

### Methods

We used 14 different MNP formulations (including commercially available Resovist® and Feraheme® all at the same iron concentration of 50 µmol/L). Different biological environments (media) were then supplied by solutions of demineralized water, bovine serum albumin (BSA), NaCl, HNO<sub>3</sub>, HCl, glycerol, glycocomingolycanes, sodium silicate, and EDTA stabilized human blood. First the MPS signal of 10 µL of the pure MNP solution (28 µg(Fe)) was recorded and after addition of 10 µL of the corresponding medium solution the MPS signals were recorded repeatedly at defined time intervals over 350 h. All MPS spectra were taken at room temperature using a commercial MPS device (MPS-3, Bruker BioSpin) operating at 25 kHz excitation frequency and 25 mJ excitation amplitude. We used the third harmonic amplitude A<sub>3</sub> and the harmonic ratio A<sub>3</sub>/A<sub>1</sub> (representing the shape of the spectrum) to assess changes of the MPS signal due to the influence of different media.

### Results

None of the MNP systems showed any changes in MPS signal amplitude or shape over the investigated time period after addition of BSA-buffer and demineralized water. In all other media the MPS signal amplitude of most MNP types underwent strong alterations. For most MNP types the signal amplitude A<sub>3</sub> was reduced by up to 80% whereas few MPS systems showed a signal increase up to 18%. At the same time, the observed alteration of the amplitude became apparent in changes of the harmonic ratio A<sub>3</sub>/A<sub>1</sub>. Normalizing A<sub>3</sub> and the A<sub>3</sub>/A<sub>1</sub> of the MNP in different media to the corresponding values of MNP in the initial state (in water) resolved a universal relation as shown in the Figure.

### Conclusion

Our results reveal that MPS is a powerful tool to monitor the behavior of MNP in different physiological media. Both parameters, amplitude A<sub>3</sub> and harmonic ratio A<sub>3</sub>/A<sub>1</sub> allow for a sensitive and specific detection of changes caused by the interaction of MNP with surrounding physiological environment. Furthermore, the high linear correlation between MPS amplitude and harmonic ratio alterations enables the reduction of quantification uncertainty for MNP in a biological environment.

### References:

- [1] Biederer S et al., *Appl. Phys. Lett.* 42 (2009).
  - [2] Poller WC et al., *J. Biomed. Nanotechnol.* 12(2) 2016.
  - [3] Radon P et al., *IEEE Trans. Magn.* 51(2), 15.
- Acknowledgements:** This research was supported by German Research Foundation (priority program 1681, grant WI 4230/1-2, and research group FOR917, Nanoguide TR408/7-2).

## Standardization of the analysis of single-core magnetic nanoparticles

Frank Ludwig<sup>(1)\*</sup>, Christoph Balceris<sup>(1)</sup>, Oliver Posth<sup>(2)</sup>, Uwe Steinhoff<sup>(2)</sup>, Rocío Costo<sup>(3)</sup>, María del Puerto Morales<sup>(3)</sup>, and Christer Johansson<sup>(4)</sup>

(1) Institute of Electrical Measurement and Fundamental Electrical Engineering, TU Braunschweig, Hans-Sommer-Str. 66, 38106 Braunschweig, Germany, \*E-Mail: fludwig@tu-bs.de (2) Physikalisch-Technische Bundesanstalt, Abestr. 2-12, 10587 Berlin, Germany (3) Instituto de Ciencia de Materiales de Madrid, ICM-CSIC, Sor Juana Inés de la Cruz 3, 28049 Madrid, Spain (4) ACREO Swedish ICT AB, 40014 Göteborg, Sweden

There is a wide field of applications of iron oxide magnetic nanoparticles (MNPs) with sizes from a few nm up to several micrometers in biomedical diagnosis, therapy and imaging. Central objective of the EU FP7 project NanoMag is the standardization of MNP characterization methods. MNPs can be classified into single- and multi-cores. This contribution deals with the analysis of single-core nanoparticles. Single-core MNPs in biomedical applications consist of a magnetic core, either magnetite, maghemite or a mixture of both, surrounded by mostly an organic shell. There is a variety of analysis methods which can be applied to estimate the core's magnetic moment, its size, anisotropy energy and the hydrodynamic size of the whole particle. In addition, since most methods measure the response of an ensemble of MNPs, the quantification of magnetic interactions between particles is an important issue.

In this work, we summarize the analysis results of single-core iron oxide nanoparticles with nominal core diameters of 14 nm and 19 nm coated with Dimercaptosuccinic acid (DMSA) applying static magnetization  $M_H$ , AC susceptibility (ACS), magnetorelaxometry (MRX), transmission electron microscopy (TEM) and dynamic light scattering (DLS) measurements. As a consequence of the variety of analysis methods, there is some redundancy in parameters which helps one to verify and refine models. For example, the core size can be directly determined from TEM measurements, on the other hand it can also be deduced from  $M_H$ - and ACS measurements on suspensions and MRX measurements on immobilized particles. Fig. 1 depicts the ACS spectra measured at two different particle concentrations of a single-core nanoparticle samples with core diameter of 19 nm (from TEM). Obviously, there are influences of interactions between the particles at both low and high frequencies. The hydrodynamic size is accessible by DLS as well as by ACS and MRX measurements on suspensions. The analysis results and the underlying models will be discussed and compared as well as checked for self-consistency.

### Acknowledgment

This work was supported by the European Commission Framework Programme 7 under the NanoMag project (grant agreement no: 604448).

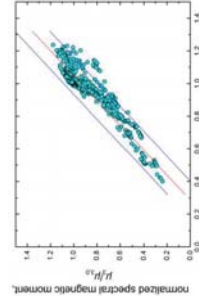
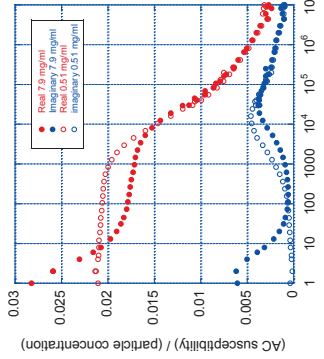


Figure: MPS amplitudes as a function of harmonic ratios of 14 different MNP in 9 different media measured over 350 h. All MPS signals were normalized to the signal of the respective MNP sample in water.

## Biocompatibility of DNA Engineered Cobalt-ferrite Nanoparticles for Cancer Cell Imaging and Hyperthermia Therapy

Madhuri Mandal Goswami<sup>\*1</sup>, Aprita Das<sup>2</sup>, Debarati De<sup>2</sup>, Arghya Adhikari<sup>2</sup>, Ajay Ghosh<sup>2</sup>

<sup>1</sup>Dept. of Condensed Matter Physics and Material Science

S N Bose National Centre for Basic Sciences

Block JD, sector III, Salt lake, Kolkata 700106, India

Phone: +91 (033) 2335 5706-8

Fax: +91 (033) 2335 3477

\*Email id: [madhuri@bose.res.in](mailto:madhuri@bose.res.in)

<sup>2</sup> Centre for Research on Nanoscience and Nanotechnology, Calcutta University,

Block JD, sector III, Salt lake, Kolkata 700106, India

Hyperthermia therapy is heat treatment. Now a days it has been received immense interest for cancer therapy utilizing magnetic nanoparticles as magnetic nanoparticles produce heat under AC magnetic field. Hence by controlling magnetic properties of the particles heating effect can be controlled and using these particles cancer cell can be killed by controlled heating of particles. The cobalt ferrite nanoparticles have suitable property which may provide a new direction in such field. Therefore we have interested on this material and have made some investigations in this direction. For biomedical application and to make proper biocompatible these cobalt ferrite nanoparticles was properly engineered with DNA. Here cobalt ferrite nanoparticles were synthesized on Deoxyribonucleic acid (DNA) scaffold by wet chemical co-precipitation method. Here certain amount of CoCl<sub>2</sub>. 6H<sub>2</sub>O and FeCl<sub>3</sub>. 6H<sub>2</sub>O were added with water in DNA solution and then it was heated & stirred upto 85° C. In that time the certain amount of KOH was added and again heated & stirred. After 1hr the solution was turned to black colour then particles were separated from solution by centrifuging them and then dried under 60 ° C. Different batches of particle were synthesized by varying the amount of DNA.

The cobalt ferrite nanoparticles attached with DNA was analyzed by infrared spectroscopy (IR), scanning electron microscope (SEM), squid, X-ray diffraction (XRD) etc. From XRD data it was confirmed that the above mentioned nanoparticles is cobalt ferrite in pure phase and from IR and SEM analysis it was shown that cobalt ferrite nanoparticles were attached with DNA. From the investigation it was observed that with increasing amount of DNA, cobalt ferrite nanoparticles showed enhanced magnetic

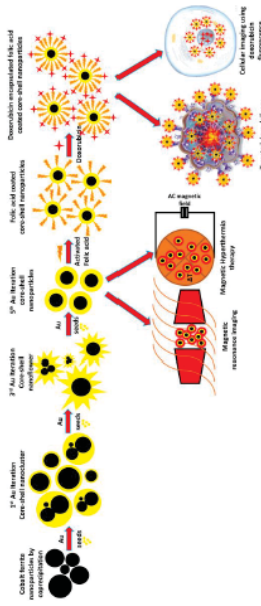
## Au@CoFe<sub>2</sub>O<sub>4</sub> yolk-shell nanoparticles: An efficient MRI contrast agent, Magneto-Hyperthermal and drug-delivery armada for cancer Theranostics

M. Ravichandran,<sup>a</sup> Goldie Ozra,<sup>b</sup> Jose Tapia Ramirez,<sup>c</sup> S. Velumani,<sup>\*b</sup>

<sup>a</sup>Program on Nanoscience and Nanotechnology, <sup>b</sup>Department of Electrical Engineering, Department of Genetics and Molecular Biology, CINVESTAV-IPN, Mexico D.F.

E-mail: [csmmano@gmail.com](mailto:csmmano@gmail.com)

An iterative-seeding based magneto-plasmonic Au@CoFe<sub>2</sub>O<sub>4</sub> yolk-shell nanoparticles using ascorbic acid and cobalt ferrite as reducing nanotemplates has been designed. We have proposed a novel aspect of site-specific targeting of Doxorubicin using iterative Au coated CoFe<sub>2</sub>O<sub>4</sub> yolk-shell nanoparticles as a nanopayload and folic acid as a targeting agent for cancerous cells. The multiple iterations and different shell size and shapes have been well explained using XRD and HRTEM. One single layer of Au on Cobalt ferrite nanoparticles enhances the capability of binding drugs, but multiple coating further augments the physiological stability and tunes surface plasmon resonance as well as dielectrics for proficient loading of drugs as well as pH-dependent release in specific microenvironment. The functionalization of folic acid and Doxorubicin was confirmed by FTIR and TGA. SQUID explained the efficacy of iterative method by confirming that even after 5 Au iterations, Au@CoFe<sub>2</sub>O<sub>4</sub> was highly superparamagnetic. MRI showed that the yolk-shell possess enhanced T<sub>2</sub> contrast for imaging both normal and cancer cells. Magnetic Hyperthermia studies exhibited an overwhelming augmentation in the temperature rise for yolk-shell nanoparticles. Doxorubicin release kinetics profile has been fit based on Zero-order, First Order, Higuchi and Hixson-Crowell model. This nanocarrier as an efficient MRI contrast agent, Magneto-hyperthermal and drug-delivery nanofleet is a step ahead towards the success of cancer theranostics. This drug delivery system can act as an efficient nanocarrier in the cancer micromilieu for synaphic targeting and assassination of the cancer cells, thus rescuing the life of patients.



## Magnetic Nanoparticle-Gel Materials for Development of Magnetic Particle Imaging Phantoms

A. Mattern<sup>1</sup>, R. Sandig<sup>1</sup>, A. Joos<sup>2,3</sup>, D. Baumgarten<sup>1</sup>, O. Kosch<sup>2</sup>, A. Weidner<sup>1</sup>, F. Wiekhorst<sup>2</sup>, S. Dutz<sup>1</sup>

<sup>1</sup> Institute of Biomedical Engineering and Informatics (BMTI), Technische Universität Ilmenau, Ilmenau, Germany

<sup>2</sup> Physikalisch-Technische Bundesanstalt, Berlin, Germany

<sup>3</sup> Zentralinstitut für Medizintechnik, Technische Universität München, Germany

E-mail: silvio.dutz@tu-ilmenau.de

A promising approach to directly determine the spatial distribution of magnetic nanoparticles (MNP) within tissue is Magnetic Particle Imaging (MPI). In the past 10 years, there was a rapid progress in development of MPI scanners and nowadays the very first preclinical devices are commercially available from Bruker BioSpin (Ettlingen, Germany). To evaluate performance of commercial as well as various custom-made scanners in several laboratories, dedicated phantoms with defined MNP distributions are required.

Pre-requirement for the development of such phantoms is the establishment of suitable MNP-matrix combinations. They should enable homogeneous MNP distributions at defined concentrations combined with immobilization of the MNP within the matrix to guarantee long-term stability of magnetic behavior and high mechanical stability of the matrix material. In this study, two different gel types were used as matrix materials, which show similar imaging behavior in MRI and MPI compared to body tissue: (i) water based biopolymers (e.g. agarose or gelatin) and (ii) synthetic polymers (e.g. silicones). Aqueous suspensions of MNP coated with functionalized dextrans were used for embedding particles into the biopolymers, and organic fluids (e.g. docetane or DMF) with oleic acid coated MNP for synthetic polymers, respectively.

The obtained MNP-matrix combinations were tested for their mechanical stability by means of mechanical load tests. The homogeneity of MNP distribution and immobilization within the matrix was determined by optical investigation of the samples with a microscope and by investigation of the magnetic particle properties measured by vibrating sample magnetometry. The most promising MNP-matrix combinations were used to manufacture measurement objects of different shape (spheres, cylinders, and cubes) and different size (5, 10, 20 mm) embedded in a phantom matrix with an overall geometry of a cylinder with D = 50 mm and H = 60 mm. The obtained test phantoms were evaluated for their suitability to simulate MNP loaded areas within a nonmagnetic matrix by means of MRI (Bruker Icon) and MPI (Bruker BioSpin preclinical MPI-scanner).

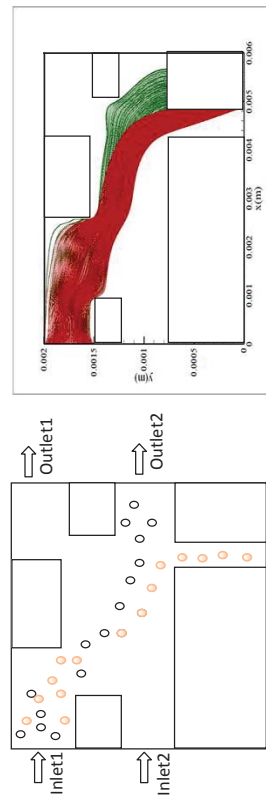
In summary, we found suitable combinations of coated magnetic nanoparticles and matrix materials for the buildup of MPI phantoms, which guarantee a fixation of the MNP within the matrix without agglomeration of the particles. From these materials, MPI phantoms were designed, produced, and tested by means of MRI and MPI. Several strategies for preparation of measurement objects and their embedding in the phantom matrix were tested and will be discussed together with the results of the test measurements in our presentation.

## Separation of magnetic beads in a Hybrid continuous flow microfluidic device

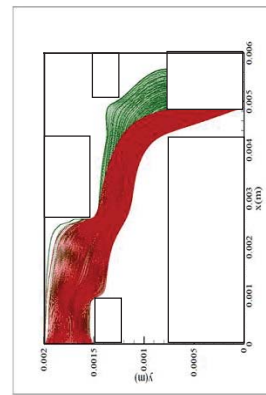
Abhishek Samanta<sup>1</sup>, Ranjan Ganguly<sup>2</sup>, Amitava Datta<sup>2</sup> and Nipu Modak<sup>3,\*</sup>,  
<sup>1</sup> Haldia Institute of Technology, Production Engg. Dept., Haldia, India  
<sup>2</sup> Jadavpur University, Power Engg. Dept., India  
<sup>3</sup> Jadavpur University, Mechanical Engg. Dept., India  
\*E-Mail: nmechju@gmail.com

### Abstract

Magnetic separation of biological entities in microfluidic environment is a key task for a large number of bio-analytical protocols. In magnetophoretic separation biochemically functionalized magnetic beads are separated from a solution using magnetic field. Here we present a numerical study characterizing a magnetophoretic hybrid microfluidic device (as shown in Fig. 1(a)). The hybrid device works on the principle of split-flow thin (SPLITT) fractionation and field-flow fractionation (FFF) mechanism. Under the influence of a magnetic field actual trajectories of the magnetic particles in the microchannel have been predicted (as shown in Fig. 1(b)) by simulation using an indigenous numerical code. An attempt is made to design a two inlet and three outlet micro-channel using the simulation for isolation of two different size species from a continuous flow. Influence of geometrical variation of the channel is carried out to observe the resulting influence on trajectories of magnetic beads and the particle capture and separation indices. Finally, an optimum regime of channel dimension is identified that yields the maximum capture efficiency and separation index.



(a)



(b)

Figure 1: Schematic diagrams of the geometrical configuration in (a) hybrid channel, and (b) trajectories of the particles

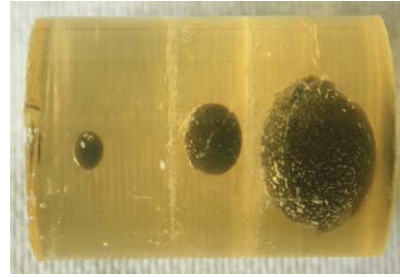


Figure: Photograph of a typical gelatin phantom (D=5 cm, H=6 cm) containing MNP filled spheres of different size.

**Acknowledgements**  
The authors thank M.Sc. Mathias Fritz (TU Ilmenau) for assistance during microscopy. This work was supported by Deutsche Forschungsgemeinschaft (FKZ: DU 1293/6-1 and TR40/8-9-1).

## Permeability of Matrigel to magnetic nanoparticles

I Morales<sup>a</sup>, Y Luengo<sup>b</sup>, P de la Presa<sup>a,c</sup>, A Barbáchano<sup>d</sup>, A Fernández-Barral<sup>d</sup>, A Costales-Carrera<sup>d</sup>, A Hernando<sup>a,c</sup>

<sup>a</sup> Instituto de Magnetismo Aplicado (UCM-ADIF-CSIC), P.O. Box 155, Las Rozas, Madrid 28230, Spain.

<sup>b</sup> Instituto de Ciencia de Materiales de Madrid. ICM-M-CSIC, Sor Juana Inés de la Cruz 3, Madrid 28049, Spain

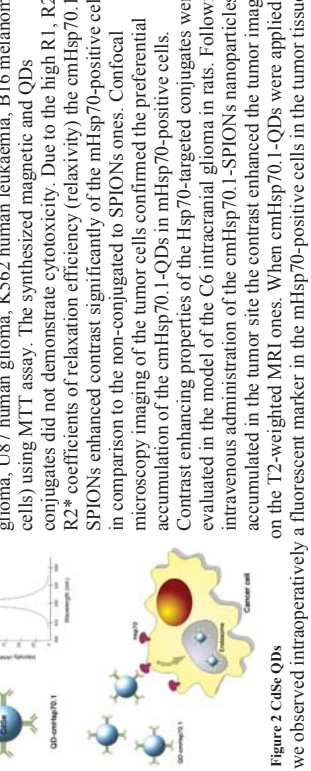
<sup>c</sup> Dto Física de Materiales, Fac. CC Fisicas, Univ. Complutense de Madrid, Madrid 28040, Spain.

<sup>d</sup> Instituto de Investigaciones Biomédicas "Alberto Sols", CSIC-UAM, Arturo Duperier 4, Madrid 28029 (Spain)

Up to day, the study of in-vitro cellular uptake of magnetic nanoparticles is performed in cells growing in two-dimensional (2D) cultures, i.e., cell monolayers on a Petri dish. However, 2D culture conditions do not represent the more intricate environment of the in-vivo cells. At present, 3D cell culture reflects better an environment in which cells grow interacting with their polarized growth and represent the in-vivo situation more accurately.

Matrigel is a gelatinous protein mixture that resembles the complex extracellular matrix found in tissues and is used as a substrate for 3D culture. Then, previous to the investigation of nanoparticles cellular uptake in 3D cells, it is necessary to understand how the nanoparticles interact with the extracellular environment.

In this work, we investigate the permeability of Matrigel to the magnetic nanoparticles. For this purpose, an aliquot of magnetic colloid is deposited on the Matrigel surface and the colloidal diffusion is investigated by Confocal Fluorescence Microscopy for “as-deposited” at 24, 48 and 72 h after colloid deposit. By measuring the temporal evolution of the depth length of the colloid it is possible to analyse the permeability of the Matrigel to the magnetic nanoparticles. The permeability of the Matrigel to the magnetic nanoparticles is investigated also as a function of the nanoparticle size.

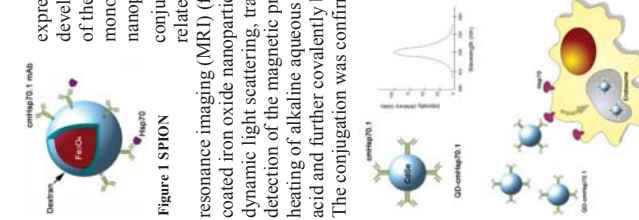


In conclusion, mHsp70-targeted agents could be applied for the visualization of the brain tumors using various imaging modalities. Thus, cmHsp70.1-SPIONs could be efficiently applied as a negative contrast-enhancing agent for the MRI and cmHsp70.1-QDs as a fluorescent probe for microscopy detection of the tumorous tissue *in vivo*. QDs synthesis was supported by Russian Science Foundation, grant № 14-15-00324.

## Magnetic and Fluorescent Nanoparticle Conjugates for Targeting of Hsp70-positive Malignant Brain Tumors

M.A. Shevtsov<sup>1</sup>, O.A. Aleksandrova<sup>2</sup>, L.B. Matyushkin<sup>2</sup>, D.S. Mazing<sup>2</sup>, V.A. Moshnikov<sup>2,3</sup>, S.F. Musikhin<sup>3\*</sup>, B.P. Nikolaev<sup>4</sup>, Ya.Yu. Marchenko<sup>4</sup>, L.Yu. Yakovleva<sup>4</sup>, A.V. Dobrodumov<sup>5</sup>

<sup>1</sup>Institute of Cytology of the Russian Academy of Sciences (RAS), 194064, 4 Tikhoretsky Ave., St. Petersburg Electrotechnical University "EIETI", 5 Professor Popov Str., 3 Palet, the Great St. Petersburg Polytechnic University 195251, 29 Polytechnicheskaya Str., <sup>4</sup>State Research Institute of Highly Pure Biopreparation, Institute of macromolecular compounds of the RAS, St. Petersburg, Russian Federation, E-mail: sergei.musikhin@rphf.spbstu.ru



In conclusion, mHsp70-targeted agents could be applied for the visualization of the brain tumors using various imaging modalities. Thus, cmHsp70.1-SPIONs could be efficiently applied as a negative contrast-enhancing agent for the MRI and cmHsp70.1-QDs as a fluorescent probe for microscopy detection of the tumorous tissue *in vivo*. QDs synthesis was supported by Russian Science Foundation, grant № 14-15-00324.

## Focusing Magnetic Particles to Central Targets between External Electromagnets

<sup>1</sup>Weinberg Medical Physics, LLC. <sup>2</sup>Children's National Medical Center. <sup>3</sup>Fischell Department of Bioengineering and the Institute for Systems Research, University of Maryland at College Park. \*Corresponding author: alek.nacyv@weinbergmedicalphysics.com

Using magnets external to the body to focus therapy to deep tissue targets has remained an open challenge in magnetic drug targeting. Researchers have been able to manipulate magnetic nano-therapeutics *in vivo* with nearby magnets, and have proposed attracting them to deep tissue targets with the aid of implanted magnetic materials (e.g. stents), but have remained unable to focus therapies to deep targets by only using magnets external to the body.

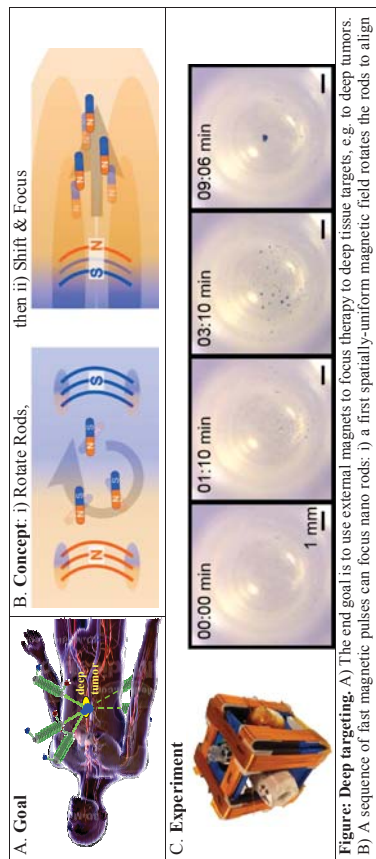


**Figure 1: Deep targeting.** A) The end goal is to use external magnets to focus therapy to deep tissue targets, e.g. to deep tumors. B) A sequence of fast magnetic pulses can focus nano rods: i) a first spatially-uniform magnetic field rotates the rods to align them North to South, then ii) a second non-uniform magnetic field in the opposite (South to North) direction moves them away from an external coil before they can reorient. Rods on the left (closer to the turned-on coil) experience a stronger magnetic field gradient and get moved further than rods on the right (which are further from the coil). The end result is to pack the rods along the horizontal x axis. C) In experiments, external coils produce fast anti-aligned magnetic pulses along two of the cardinal directions (x and y axes) to focus dispersed magnetic rods (optically undetectable at the start time 00:00 min) to the center within a few minutes (by 09:06 min the rods are observed focused at the center).

In experiments we have demonstrated that pulsed magnetic fields applied by external magnets can focus nano rods to a central target between the magnets. The method works by using fast magnetic pulses to exploit the physics of nano rods in order to circumvent the restriction on stable magnetic traps between magnets that follows from Samuel Earnshaw's classic 1842 theorem<sup>1</sup>. The main idea is that unlike spherical ferrimagnetic particles, which under the action of an applied magnetic pulse rotate to align before they move, ferrimagnetic rods can move before they align. Hence it is possible to orient the rods with one pulse (panel B i in the figure) and then move them away from a magnet with a second pulse before they have a chance to realign (panel B ii). The first pulse is uniform in space so that it aligns but does not move the rods (there is no spatial gradient), and this is achieved by turning on two magnets along one axis (as shown by the two turned-on coils in B i). The second pulse is non-uniform in space so that it moves the rods away from the magnet (just one magnetic coil is turned on in panel B ii). Rods closer to this powered coil experience a larger magnetic gradient and move away faster from the coil, which packs them together (rods closer to the coil catch up to rods further away). By repeating this i) rotate and ii) shift sequence along two of the cardinal axes (x and y), the end result is that dispersed rods are focused to the center. Focusing has been shown in experiments for coated and uncoated nickel and cobalt rods, in tap water, saline buffer, and in hexane isopropanol solution (panel C shows focusing results for 200 μm long, 200 nm wide cobalt rods).

The location of the focus can be varied by changing the strength of the coils one against the other. Experiments in live animals are underway, as are efforts to scale up the system to distances needed for human patients. Success would grant clinicians a tool capable of delivering therapy where it is needed, a key goal in magnetic targeting.

[1] Eanshaw, "On the nature of the molecular forces which regulate the constitution of the luminiferous ether", Trans Cambridge Philosophical Society, 1842

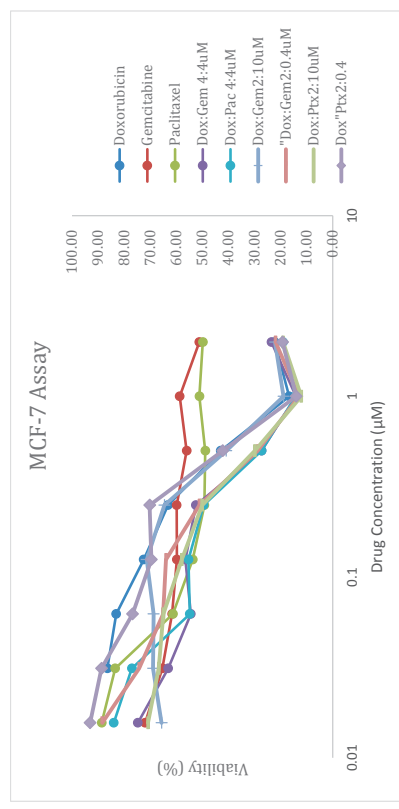
## SYNERGETIC EFFECT OF MULTI-DRUG LOADED MAGNETIC LIPOSOME IN CHEMO-THERMOTHERAPY

Lilin Wang, Kuan Boone Tan, Nguyen T. K. Thanh\*

Biophysics group, Department of Physics & Astronomy, University College London, Gower Street, London WC1E 6BT, UCL Healthcare Biomaterials and Nanomaterials Laboratories, 21 Albemarle Street, London W1S 4BS

<http://www.ntk-thanh.co.uk> Email: ntk.thanh@ucl.ac.uk

Magnetic nanoparticles have been widely investigated as a promising nano-medicine agent since last decade. A number of *in vitro* and *in vivo* results suggest the chemo-thermotherapy via multifunctional magnetic nanoparticle has positive effect in cancer treatment [1]. However, unlike the thermo-radiotherapy, the clinical trials of chemo-thermotherapy could not make a consistent synergism conclusion. [2] Apart from the complicated tumor architecture, it may due to the tumour heterogeneity. Herein, our group constructs a multifunctional magnetic thermo sensitive liposome and optimizes it by introducing both pharmaceuticals and biomolecular concepts. In the first part, we refined the polyol method for synthesis the multi core magnetic nano-flower that has high magnetic property. In order to boost the chemo-thermo effect, the most synergistic chemodrugs combination ratio was carefully chosen among the 3 most prevalent anti breast cancer medicines: gemcitabine, paclitaxel and doxorubicin, by testing on different breast cancer cell lines. Both of them were loaded into the thermosensitive liposomes via thin film hydration methods. The efficiency of the multifunctional magnetic chemosensitive liposome will be verified and compared with the baseline among all cell lines. Based on the outcomes, the second part will be focusing on further optimizing our chemo-thermotherapy strategy via biomolecular analysis.



Ref:

- [1] A. Hervault and N. T. K. Thanh, "Magnetic nanoparticle-based therapeutic agents for thermo-chemotherapy treatment of cancer," *Nanoscale*, vol. 6, no. 20, pp. 11553–11573, 2014.

- [2] B. Hildebrandt, P. Wust, O. Ahlers, A. Dieing, G. Sreenivasa, T. Kerner, R. Felix, and H. Riess, "The cellular and molecular basis of hyperthermia," vol. 43, pp. 33–56, 2002

## Peptide Dendrimer- $\text{Fe}_3\text{O}_4$ Nanoparticles as contrast agents in non-invasive magnetic resonance imaging

Saumya Nigam<sup>1</sup>, D. Bahadur<sup>2\*</sup>

<sup>1</sup>IITB-Monash Research Academy, IIT Bombay, Powai, Mumbai, India  
<sup>2</sup>Department of Metallurgical Engineering and Materials Science, Indian Institute of Technology Bombay, Powai, Mumbai, India

\*Corresponding Author: dhiren@iitb.ac.in

### Abstract

Superparamagnetic iron oxide ( $\text{Fe}_3\text{O}_4$ ) nanoparticles have recently found an appreciable place as  $T_2$  contrast agents in the magnetic resonance (MR) imaging of cancer. Their surface modification by dendritic macromolecules effect their relaxation times and play an important role in their efficacy as MR contrast agents. This work demonstrates the fabrication of a peptide dendrimer used in subsequent engineering of  $\text{Fe}_3\text{O}_4$  nanoparticles as an effective  $T_2$  contrast agent for non-invasive MR imaging *in vitro*. The fabricated system was evaluated for its comparative  $r_1$  and  $r_2$  relaxivity under different environmental parameters using 9.4 Tesla small animal MRI. The effect of temperature, buffer solutions and iron concentration was assessed by investigating the magnetic properties and induced MR signals. The MR measurements indicate a significant increase in the transverse relaxation and relaxation ratios of the dendritic nanosystem. Both  $T_1$ - and  $T_2$ -weighted phantoms showed significant change in signal intensity with an increasing amount of Fe concentration. This indicates that these dendritic  $\text{Fe}_3\text{O}_4$  generate MR contrast on both longitudinal ( $T_1$ ) and transverse ( $T_2$ ) proton relaxations-times weighted sequences due to the dipolar interaction of magnetic moment of the particles and protons of the water. The relaxation ratio ( $r_2/r_1$ ) of was seen to be 100.7 in an aqueous environment as against 62.3 in buffer environment at 25 °C. This difference in the contrast properties and relaxivity was seen to be largely dependent on the temperature and buffer ions in the surrounding microenvironment. These dendritic  $\text{Fe}_3\text{O}_4$  were also employed for the  $T_2$ -weighted MR imaging of human cervical cancer (HeLa) cells *in vitro* after various time intervals over a period of 24 h.

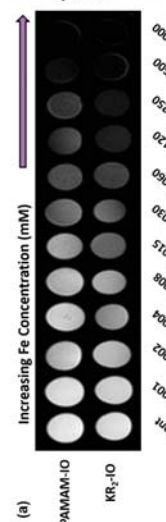
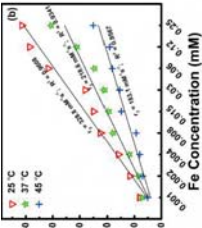


Figure 1. (a)  $T_2$  relaxation of dendritic- $\text{Fe}_3\text{O}_4$  in simulated body fluid (b) dependence of transverse relaxivity ( $r_2$ ) of dendritic- $\text{Fe}_3\text{O}_4$  on iron concentration and temperature



## Production of Magnetic Microspheres by a Micro Co-Flowing Device as a Potential Approach for Magnetic Resonance Navigation Technology

Zeynab Nosrati<sup>1</sup>, Sahan Ranamukhaarachchi<sup>1</sup>, Alexandre Bigot<sup>2</sup>, Ning Li<sup>3</sup>, Sylvain Martel<sup>3</sup>, Gilles Soulez<sup>2</sup>, Karayoun Saatchi<sup>1</sup>, Urs Häfeli<sup>1,\*</sup>

<sup>1</sup>University of British Columbia, Faculty of Pharmaceutical Sciences, Vancouver BC, Canada; <sup>2</sup>Clinical Image Processing Laboratory (LCTI), Centre de Recherche du Centre Hospitalier de l'Université de Montréal (CRCHUM), Montréal QC, Canada; <sup>3</sup>NanoRobotics Laboratory, Department of Computer and Software Engineering and Institute of Biomedical Engineering, Polytechnique Montréal, Montréal QC, Canada; \*Email: urs.hafeli@ubc.ca

Biodegradable polymer microspheres are safe and effective drug delivery systems known to control drug release. For a technique called Magnetic Resonance Navigation (MRN) magnetic nanoparticles are embedded into polymer microspheres to yield magnetic microspheres (MMS). Drug loaded MMS can be navigated through the blood vessels with an external magnetic field for selective delivery to the target tissues. The present study provides a simple and reliable method to prepare MMS with a novel 3-D printed micro-co-flowing device based on an emulsion-solvent evaporation method.

Our simple and high-through-put method produces uniformly sized MMS by pumping poly(lactic-co-glycolic acid) (PLGA) dissolved in dichloromethane containing 50 weight% superparamagnetic iron oxide nanoparticles as the dispersed phase, through a 30G needle seated at the center of the tubing system. The continuous phase consisted of a 2% polyvinyl alcohol (PVA) solution which was pumped at a constant but X times higher flow rate than the disperse phase through the tubing (Figure 1). MMS sized between 150 to 400  $\mu\text{m}$  with narrow quasi-monodispersed size distribution ( $CV < 15\%$ ) were fabricated with this method in continuous mode. Figures 2 and 3 show an example batch with MMS of  $250 \pm 38 \mu\text{m}$ .

Depending on the dimensions of the vascular network and target vessels, different sizes might be required for MRN. We investigated the relationship between geometric and flow parameters of the micro-co-flowing device and the final particle size. The most important parameter for size and uniformity of the MMS was the size of the injection needle. Other important parameters are concentration and viscosity of the dispersed phase, the diameter of the tubing system and the flow rates. Results of these varying parameters on the final size and size distribution of the magnetic microspheres will be presented.

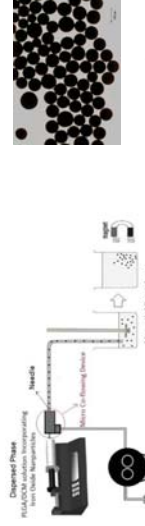


Figure 2. Optical microscopy image of the prepared MMS.

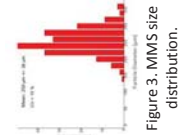


Figure 3. MMS size distribution.

Figure 1. Micro-co-flowing device used for the preparation of magnetic microspheres.

## A capillary viscometer designed to measure the magnetoviscous effect of biocompatible ferrofluids diluted in sheep blood.

J. Nowak<sup>1</sup>, S. Odenbach<sup>1</sup>

<sup>1</sup> Chair of Magnetofluidynamics, Measuring and Automation Technology, Institute of Fluid Mechanics  
Technische Universität Dresden, Germany

Ferrofluids, suspensions of magnetic nanoparticles in suitable carrier liquids, are receiving a growing interest in biomedical applications. New treatment approaches like e.g. magnetic drug targeting (MDT) are of great interest. MDT focuses on binding chemotherapeutic agents to the magnetic particles suspended in the fluid. These ferrofluids are arterially injected and subsequently concentrated in the tumour by the application of external magnetic fields in the diseased region, potentially decreasing side effects and increasing efficacy of chemotherapy.

To guarantee a safe and effective application of the ferrofluids the knowledge of the flow behaviour is rather important. For ferrofluids used in the engineering context the magnetoviscous effect (MVE), a rise in viscosity due to the formation of particle-structures caused by the application of an external magnetic field, is well known and investigated in some detail. This effect has been proven for biocompatible ferrofluids as well. Nevertheless up to now no attempts were made to characterize the flow behaviour of biocompatible ferrofluids in a flow situation close to a potential application and if a dilution in blood occurs.

This experimental study introduces a novel capillary viscometer, designed for the characterization of biocompatible ferrofluids, especially if a dilution in blood occurs.

It was found that an increasing viscosity can still be measured despite the high shear rates applied in potential biomedical applications and despite a dilution of the ferrofluids with sheep blood, showing the potential to influence an actual biomedical application. Furthermore interactions between the structures formed by the magnetic nanoparticles and the blood cells have to be expected due to different MVEs found using the same concentrations of sheep blood or respectively water as diluting agent (Figure 1).

Financial support by the Deutsche Forschungsgemeinschaft under grant no. OD1823-1 is gratefully acknowledged.



This work was partially supported by JSPS grand  
15H05764 and 26289124.

[1] Ota *et al.*, *J. Appl. Phys.*, **117**, 17D713 (2015).

[2] Yoshida *et al.*, *Jpn. J. Appl. Phys.*, **48**, 127002 (2009).

[3] Ota *et al.*, *J. Appl. Phys.*, **117**, 17D713 (2015).

[4] Yoshida *et al.*, *Jpn. J. Appl. Phys.*, **48**, 127002 (2009).

[5] Ota *et al.*, *J. Appl. Phys.*, **117**, 17D713 (2015).

[6] Yoshida *et al.*, *Jpn. J. Appl. Phys.*, **48**, 127002 (2009).

[7] Ota *et al.*, *J. Appl. Phys.*, **117**, 17D713 (2015).

[8] Yoshida *et al.*, *Jpn. J. Appl. Phys.*, **48**, 127002 (2009).

The magnetoviscous effect  $R$  depending on the dilution  $K$  of a biocompatible ferrofluid diluted with water and sheep blood for a shear rate of  $120 \text{ s}^{-1}$ . The magnetic field strength is  $H=40 \text{ kA/m}$ . A higher MVE can be detected if sheep blood is used as diluting agent.

## Magnetization dynamics of magnetic nanoparticle associated with magnetic relaxation characterized by alternating current hysteresis measurement

Satoshi Ota<sup>1</sup>, Ryoji Takeda<sup>1</sup>, Tsutomu Yamada<sup>2</sup> and Yasushi Takemura<sup>2</sup>

<sup>1</sup> Department of Electrical and Electronic Engineering, Shizokuwa University, Hamamatsu, Japan

<sup>2</sup> Department of Electrical and Computer Engineering, Yokohama National University, Yokohama, Japan

\*E-Mail: ota.s@shizuoka.ac.jp

The dynamics of magnetic nanoparticles (MNPs) such as Brownian and Néel rotations associated with magnetic relaxation were assessed by ac hysteresis measurements. We revealed that Brownian rotation was also occurred after Néel rotation despite quit shorter Néel relaxation time than Brownian relaxation time.

A water based  $\gamma\text{-Fe}_2\text{O}_3$  nanoparticle, Ferucarbotran, was supplied from Meito Sangyo Co. Ltd., Japan. The primary and hydrodynamic diameters of this MNP were 5 and 71 nm, respectively. MNPs dispersed in water and fixed with agar were prepared as the liquid and fixed samples, respectively. Applied ac fields were intensity of  $2\text{--}10 \text{ kA/m}$  and frequency of  $0.2\text{--}400 \text{ kHz}$ .

Figure 1 shows the frequency and field dependence of the intrinsic loss power (ILP) estimated from the area of ac hysteresis loops in the liquid and fixed samples. In the liquid sample, the local peaks of ILP were indicated, which were associated with Brownian relaxation because these peaks were not shown in the fixed sample [1]. The theoretical peak frequency of Brownian relaxation is  $1.3 \text{ kHz}$ . In addition, the peak frequency increased with the increase of field intensity. It is indicated that the Brownian relaxation time shorten with the increase of field intensity because of the strong magnetic torque [2]. The theoretical Brownian relaxation time is longer than measured one because zero field intensity is conditioned in theory. ILP increased with the increase of field intensity in the fixed sample and liquid sample in high frequency due to Néel relaxation. The theoretical peak frequency of Néel relaxation is  $150 \text{ MHz}$ .

Figure 2 shows the magnetization signals and the models of the magnetization and particle rotations. The contribution of particle rotation to magnetization reversal is indicated by the signal of particle. In the low frequency, particle rotation followed magnetization with the small phase delay ( $<\pi/2$ ) [Fig. 2 (a)]. In contrast, the large phase delay ( $>\pi/2$ ) of particle rotation was confirmed in the high frequency [Fig. 2 (b)]. Thus, Brownian rotation also slightly occurred with the delay from Néel rotation in high frequency in spite of quit longer Brownian relaxation time than Néel relaxation time.

[1] Ota *et al.*, *J. Appl. Phys.*, **117**, 17D713 (2015).

[2] Yoshida *et al.*, *Jpn. J. Appl. Phys.*, **48**, 127002 (2009).

[3] Ota *et al.*, *J. Appl. Phys.*, **117**, 17D713 (2015).

[4] Yoshida *et al.*, *Jpn. J. Appl. Phys.*, **48**, 127002 (2009).

[5] Ota *et al.*, *J. Appl. Phys.*, **117**, 17D713 (2015).

[6] Yoshida *et al.*, *Jpn. J. Appl. Phys.*, **48**, 127002 (2009).

[7] Ota *et al.*, *J. Appl. Phys.*, **117**, 17D713 (2015).

[8] Yoshida *et al.*, *Jpn. J. Appl. Phys.*, **48**, 127002 (2009).

[9] Ota *et al.*, *J. Appl. Phys.*, **117**, 17D713 (2015).

[10] Yoshida *et al.*, *Jpn. J. Appl. Phys.*, **48**, 127002 (2009).

[11] Ota *et al.*, *J. Appl. Phys.*, **117**, 17D713 (2015).

[12] Yoshida *et al.*, *Jpn. J. Appl. Phys.*, **48**, 127002 (2009).

[13] Ota *et al.*, *J. Appl. Phys.*, **117**, 17D713 (2015).

[14] Yoshida *et al.*, *Jpn. J. Appl. Phys.*, **48**, 127002 (2009).

[15] Ota *et al.*, *J. Appl. Phys.*, **117**, 17D713 (2015).

[16] Yoshida *et al.*, *Jpn. J. Appl. Phys.*, **48**, 127002 (2009).

[17] Ota *et al.*, *J. Appl. Phys.*, **117**, 17D713 (2015).

[18] Yoshida *et al.*, *Jpn. J. Appl. Phys.*, **48**, 127002 (2009).

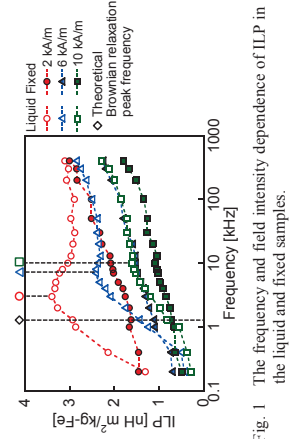


Fig. 1 The frequency and field intensity dependence of ILP in the liquid and fixed samples.

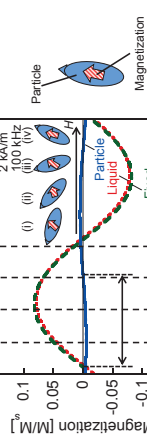


Fig. 2 The models of magnetization and particle rotations at (a) 1 kHz and (b) 2 kHz in  $2 \text{ kA/m}$  of sinusoidal fields.

## Layer-by-layer Assembled Prednisolone Magnetic Microcapsules (PMC) Assisted Controlled and Targeted Drug Release at Rheumatoid Arthritic Joints

Chakrapani Prabu, Subbiah Latha, Palanisamy Selvamani\*

Department of Pharmaceutical Technology & Centre for Excellence in Nanobio Translational Research, Anna University, Bharathidasan Institute of Technology Campus, Tiruchirappalli, Tamil Nadu, India  
E-mail: pselvamani@hotmail.com, lathasuba2010@gmail.com

It is proposed to develop prednisolone loaded magnetic microcapsules (PMC) in order to improve the therapeutic efficacy relatively at a low dose than the conventional formulations through magnetic drug targeting at rheumatoid arthritis joints and bioavailability enhancement. Poly(sodium 4-styrenesulfonate) doped porous calcium carbonate core particles were prepared by biomimetic mineralization method, by mixing equal molar concentrations of 50 ml calcium chloride with sodium carbonate doped with 200 mg of Poly(sodium 4-styrenesulfonate). The developed core particles were found to be spherical with porous surface, in the size range of ~4 microns with a zeta potential of -22.7 mV. Prednisolone was loaded to the core particles using solvent evaporation technique i.e., 50 mg of the prednisolone dissolved in ethanol and added drop wise to the 200 mg of calcium carbonate microparticles in aqueous medium under continuous stirring at 300 rpm in room temp. Thermo-gravimetric analysis showed loss of weight upto 29.5% and 7.4% for the drug loaded and unloaded calcium carbonate microparticles respectively confirmed the drug loading to the calcium carbonate microparticles. Results of the powder XRD analysis confirmed the porosity of the microparticles besides the presence of calcium carbonate in vaterite and calcite phase. Drug encapsulation efficiency and loading capacity was found to be 63% and 18.2% respectively. Either of polyallylamine hydrochloride or polystyrene sulphonate (2 mg/ml) equilibrated at pH 6.5 were added alternatively up to 5 cycles to the drug incorporated calcium carbonate microparticles particles by layer by layer technique. After each addition, unloaded electrolytes was removed by addition of 0.05 M solution of sodium chloride followed by centrifugation. Zeta potential analysis was carried out after each layer assembly to confirm the coating of the electrolyte layer. Previously magnetic ferrofluid prepared by co-precipitation technique was added in between the polyelectrolyte layers during the 3<sup>rd</sup> cycle. Then, the calcium carbonate core was dissolved by etching using 0.2 M ethylene diamine tetra acetic acid leads to the formation of prednisolone loaded magnetic microcapsules. No significant chemical associations or interactions were observed between the drug and excipients as well as the presence of chemically intact prednisolone, ferrofluid and polyelectrolytes was confirmed through the FT-IR spectral analysis. Magnetic susceptibility of the PMC was found to be  $6.8 \times 10^{-5}$  with a DC magnetization value of 55.004 emu/g. Thus, the prepared PMC was found to be suitable and relatively more efficient for the controlled and targeted drug release at the arthritic joints in the adjuvant induced arthritis model in rats than the conventional formulations.

## Optimizing magnetic properties for self-controlled hyperthermia applications

Sudip Pandey<sup>1</sup>, Abdiel Quez<sup>1</sup>, Anil Aryal<sup>1</sup>, Igor Dubenko<sup>1</sup>, Dipanjan Mazumdar<sup>1</sup>,  
Shane Stadler<sup>2</sup>, and Naushad Ali<sup>1</sup>  
Email: sudip@siu.edu

<sup>1</sup>Department of Physics, Southern Illinois University, Carbondale, IL 62901 USA  
<sup>2</sup>Department of Physics & Astronomy, Louisiana State University, LA 70803 USA

The self- controlled hyperthermia is a new non-invasive technique to employ heat treatment to cure cancer cells without overheating the normal cells. We try to study a number of magnetic materials by substituting Ag, Cr, Cu, and Al for Ni. The samples were prepared by arc melting technique, and were annealed at 900 °C for 8 hours in a sealed quartz tubes. Magnetic properties of the samples were investigated, including saturation magnetization, Curie temperature and hysteresis using Superconducting Quantum Interference Device (SQUID). We have synthesized a number of materials that have their Curie temperature in the desired range (310-320 K). Thus by controlling the doping concentration, we are able to tuned the Curie temperature and this alloys might be a good candidates for self-regulating magnetic hyperthermia applications.

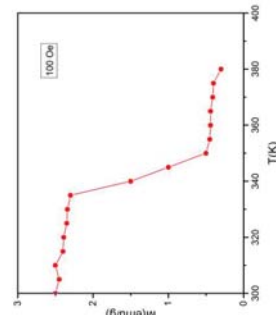
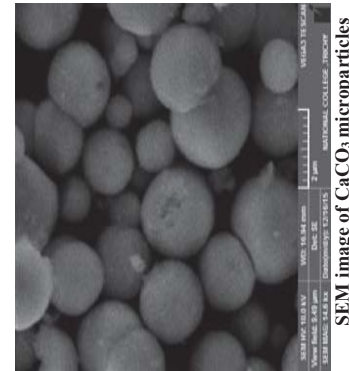
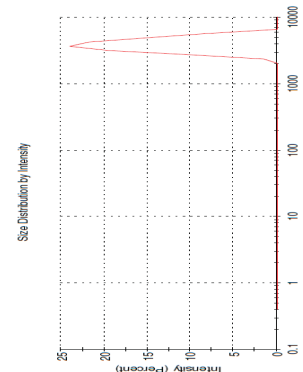


Fig. 1: Estimation of Curie temperature for the Ni based compounds: Magnetization versus Curie temperature data in a magnetic field of 100 Oe.

Acknowledgement: This work was supported by the Office of Basic Energy Sciences, Material Science Division of the U.S. Department of Energy (DOE Grant No. DE-FG02-06ER46291 and DE-FG02-13ER46946).

## Size distribution of CaCO<sub>3</sub> microparticles



SEM image of CaCO<sub>3</sub> microparticles

## In vivo biodistribution of sterically stabilised superparamagnetic iron oxide nanoparticles via intraperitoneum injection

Binh T.T. Pham,<sup>1</sup> Nguyen TH Pham,<sup>1</sup> Byung J. Kim,<sup>1</sup> Nirmesh Jain,<sup>1</sup> Nicole S. Bryce,<sup>1</sup> Emily K. Cobin,<sup>1</sup> Emily S. Fuller,<sup>2</sup> Vivie M. Howell,<sup>2</sup> Elizabeth A. Moon,<sup>2</sup> Samuel Yuen,<sup>2</sup> Stephanie A. Bickley,<sup>3</sup> Marcel Tanudji,<sup>3</sup> Stephen K. Jones,<sup>3</sup> Brian S. Hawkett<sup>1</sup>  
**binh.pham@sydney.edu.au**

### Magnetic-Relaxation and Heat-Dissipation Characteristics of Iron-Oxide Ferrofluids Prepared by Surfactant-Assisted Ball-Milling

P. Burnham<sup>1\*</sup>, C. H. Li<sup>2</sup>, A. J. Vilesas<sup>1</sup> and G. C. Papaefthymiou<sup>1\*\*</sup>  
<sup>1</sup>908. \*\*E-mail: gcp@villanova.edu

*Department of Physics, Department of Mechanical Engineering, Villanova University, Villanova, PA*

When subjected to a magnetic field whose direction alternates rapidly, ferrofluids absorb electromagnetic energy, which is readily dissipated to their environment by Brownian (particle rotation) and Neel (moment reorientation) magnetic relaxation mechanisms. *In vitro* studies indicate that these processes result in heat dissipation and an increase in local temperature. When experiments are replicated *in vivo*, elevated local temperatures of 40 °C to 46 °C can be achieved, adequate to induce cell death or cell ablation in tumor tissue. Iron-oxide based ferrofluids are desirable due to their low toxicity, owed to established biological pathways for iron management *in vivo*. Comparative studies are presented of magnetite ( $\text{Fe}_3\text{O}_4$ ) and maghemite ( $\gamma\text{-Fe}_2\text{O}_3$ ) iron oxide nanoparticles in the 7 - 15 nm average diameter range ball-milled dry and in hexane in the presence of oleic acid. Transmission electron microscopy studies, micro-magnetic characterization via Mössbauer spectroscopy and macro-magnetic investigations via SQUID magnetometry are presented. The specific absorption rates (SAR) of ferrofluids based on these nanoparticle preparations with various surfactant concentrations are also presented in order to test and contrast their efficacies as hyperthermia agents.

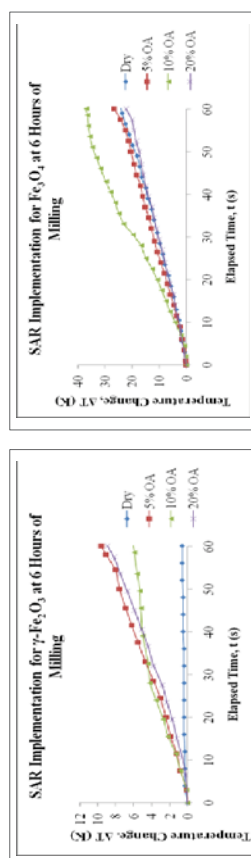


**Figure Caption:** Comparison of SAR characteristics of magnetite vs. maghemite based ferrofluids. The figures indicate change in sample temperature vs. elapsed time of AC field exposure for  $\gamma\text{-Fe}_2\text{O}_3$  (left panel) and  $\text{Fe}_3\text{O}_4$  (right panel) nanoparticle preparations milled for 6 hours dry or in hexane with various concentrations of oleic acid as indicated. (Note the difference in the vertical scales).

\*Present address: Department of Physics, Cornell University, Ithaca, NY 14850  
\*\*Corresponding author.

**Figure 1:** (A) Co-localisation of Fe (left, by Prussian blue staining) and macrophages (right, by F4/80 anti-body staining) in the omentum specimen collected at 4 hours post IP injection; (B) H & E immunohistology of three main organs (liver, spleen and kidney) from the control (top row) and SPIONs treated (bottom row) mice 7 days after the IP injection. No fibrosis was observed in any tissues

### References:

1. B.S. Hawkett, N. Jain, T.T.B. Pham, Y. Wang, G.G. War, *WO 2009/137890 A1*, US 2010/129417 A1.
2. N. Jain, Y. Wang, S.K. Jones, B.S. Hawkett, G.G. War, *Lancet* 5, 2010, 26, 446-447.
3. T.T.B. Pham, N. Bryce, N. Jain, T. Hambley, B.H. Hawkett, N. Jain, T. Pham, Nirmesh Jain, Eh Hau Pan, Renee M. Whan, Trevor W. Science, 2013, 1, 1260-1272.
4. Nicole S. Bryce, Binh T.T. Pham, Nirmesh Jain, Nicole W. S. Fong, Nirmesh Jain, Eh Hau Pan, Trevor W. Hawkett, Brian S. Hawkett, *Biomaterials* 2013; 34: 6645–6655.
5. Binh TT Pham, Nirmesh Jain, Philip W Kachel, Bogdan E Chapman, Stephanie A Bickley, Stephen K Jones, Brian S Hawkett, *International Journal of Nanomedicine* 2015; 10, 6645–6655.
6. Steven S. Famiglio, Michael W. Weible II, Binh T.T. Pham, Brian S. Hawkett, Stuart M. Grieve, Taioi Chan-Ling, *Biomaterials*, 2014, 35, 5549-5564.

## Stable and non-toxic superparamagnetic iron oxide nanoparticles as multimodal (PET/SPECT-MRI) imaging probes

Binh T. T. Pham,<sup>1</sup> Nguyen T. H. Pham,<sup>1\*</sup> Nigel A. Lengkeek,<sup>2</sup> Ivan Gregoric,<sup>2</sup> Paul A. Pellegrini,<sup>2</sup> Byung Kim,<sup>1</sup> Stephanie Bickley,<sup>1</sup> Marcel Tamudi,<sup>1</sup> Steve Jones,<sup>3</sup> and Brian S. Hawlett<sup>1\*</sup>  
<sup>1</sup> Key Centre for Polymers and Colloids, School of Chemistry, University of Sydney, NSW 2006, Australia  
<sup>2</sup> ANSTO LifeSciences, Australian Nuclear Science and Technology Organisation, NSW 2232, Australia  
<sup>3</sup> Sirtex Medical Ltd., North Sydney, NSW 2060, Australia

Several approaches to label superparamagnetic iron oxide nanoparticles (SPIONS) with radionuclides as imaging agents for PET/MRI or SPECT/MRI have been reported via either chelation or chelate-free techniques [1,2]. However, challenges still remain in the simple and robust synthesis of fully dispersed and stable radiolabelled SPIONS with tightly bound radionuclides.

In our present study, sterically stabilized SPIONS of two different core diameters, 10 and 25 nm, are investigated as potential candidates for multimodal imaging PET/SPECT – MRI techniques. These SPIONS have been shown in our previous study as excellent negative contrast agents with very-high  $T_2$  relaxivities of 368 and 958  $\text{s}^{-1}\cdot\text{mM}^{-1}$ , respectively [3]. In addition, these SPIONS have demonstrated non-cytotoxicity and excellent bio-distribution profile *in vivo* [4]. The SPIONS were successfully radio-labelled with both  $^{57}\text{Co}$  or  $^{67}\text{Ga}$  in aqueous acetate buffers. The radio-labelling efficiency was strongly dependent on temperature and time for both raw ferro-fluid (unstabilized iron oxide cores) and sterically stabilized SPIONS. No detectable loss of radionuclides from the particles to the aqueous phase in various physiological media was observed. The radiolabelled sterically stabilized SPIONS were fully re-dispersed and remained stable in a physiological buffer solution such as PBS (see Figure 1), which is crucial property for an injectable formulation in biomedical applications.

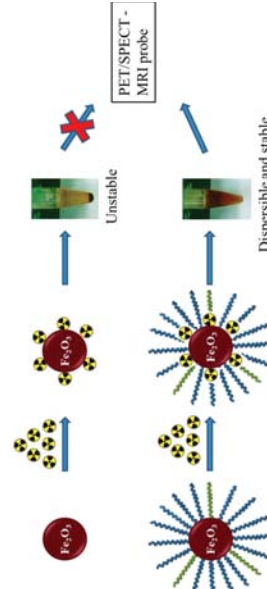


Figure 1. Radio-labelling of SPIONS

## Synthesis, Characterization, Drug Release and Transdental Delivery Studies of Magnetic Nanocubes coated with Biodegradable Poly(2-(dimethyl amino)ethyl methacrylate)

Phranot Alkidkarn,<sup>1</sup> Patcharee Rupprajak,<sup>2</sup> Nunpon Insin,<sup>3\*</sup>

<sup>1</sup>Petrochemistry and Polymer Science program, Faculty of Science, Chulalongkorn University, Bangkok, Thailand

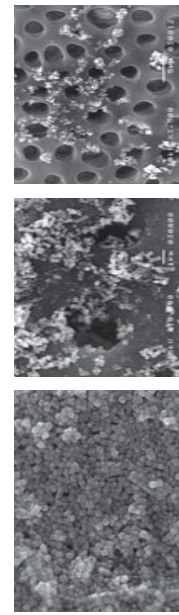
<sup>2</sup>Department of Microbiology, Faculty of Dentistry, Chulalongkorn University, Bangkok, 10330, Thailand

<sup>3</sup>Department of Chemistry, Faculty of Science, Chulalongkorn University, Bangkok, 10330, Thailand

\*E-mail: Nunpon.1@chula.ac.th

Nanotechnology on magnetism and magnetic materials has been developed and studied extensively for the recent decades. Magnetic nanoparticles were applied in magnetic targeting, magnetic drug carriers, and diagnostic materials. In this work, the development of magnetic nanocomposites and their applications as drug carriers for applications in dentistry were investigated.

Well-defined ferromagnetic magnetic nanocubes (FMNCs) with the diameter of around 60 nm were synthesized using a thermal decomposition method at 290°C with iron-oleate complexes as starting materials resulting in nanostructure with high saturation magnetization. The FMNCs were then coated with poly(2-(dimethyl amino)ethyl methacrylate) (PDMAEMA), a water-soluble, biodegradable, and pH-responsive polymer, in order to become good drug carriers with excellent dispersity in biological buffer, low cytotoxicity, and controllable drug release. The polymer coating was performed using atom transfer radical polymerization (ATRP). Furthermore, FMNCs/PDMAEMA were studied for cytotoxicity to fibroblast and raw cells using 3-(4,5-dimethylthiazol-2-yl)-2,5-diphenyl tetrazolium bromide (MTT) assay, and the result showed that FMNCs/PDMAEMA were biocompatible with those cells with cell viability of more than 80% after incubation with the highest nanocomposites concentration of 100  $\mu\text{g}/\text{mL}$  for 24 h in humidified hood at 37°C and 5%  $\text{CO}_2$ . The behavior of model drug alkaline hypochlorite released from the FMNCs/PDMAEMA indicated that the drug release could be controlled by altering pH of the environment. As a result of successfully synthesized FMNCs/PDMAEMA, dentine infiltration of FMNCs/PDMAEMA was performed. It was observed that FMNCs/PDMAEMA could significantly infiltrate the dentine within 30 min under an external magnetic field, indicating the potential of these composites as transdental drug carriers.



FE-SEM images of (A) magnetic nanocubes, (B) front and (C) back of FMNCs/PDMAEMA infiltrated through dentin disc.

- E. Boros; A.M. Bowen; L. Josephson; N. Vasdev; J.P. Holland, *Chem Sci* **2015**, *6*, 225.
- F. Ai; C.A. Ferreira; F. Chen; W. Cai, *Wiley Interdiscip Rev Nanomed and Nanobiotechnol* **2015**.
- B.T. Pham; N. Jain; P.W. Kuchel; B.E. Chapman; S.A. Bickley; S.K. Jones; B.S. Hawlett, *Int J Nanomedicine* **2015**, *10*, 6645.
- Pham et al., to be submitted.

## 3D Imaging of Magnetic Particles Using the 7-Channel Magnetoencephalography Device Without Pre-Magnetization or Displacement of the Sample

M.A.Polkarpov<sup>1</sup>, M.N.Ustinin<sup>2</sup>, S.D.Rybnikov<sup>2</sup>, A.Y.Yurenyan<sup>1,3</sup>, S.P.Naurazakov<sup>1</sup>, A.P.Grebennikov<sup>1</sup>, V.Y.Panchenko<sup>1,3</sup>

<sup>1</sup>National Research Center "Kurchatov Institute"<sup>2</sup>; Moscow, Russia  
<sup>3</sup>Institute of Mathematical Problems of Biology, Russian Academy of Sciences, Pushchino, Russia

E-mail: polkarov.inmp@mail.ru

The transparency of biological tissue to low-frequency magnetic fields permits the magnetic particles imaging (MPI) within the body. Usually the MPI method requires a sample containing the superparamagnetic particles, a static magnetic field, an oscillating field and a magnetic field detector, which can be based on receive coils [1] or superconducting quantum interference devices (SQUID) [2]. The high sensitivity of SQUIDs allows detecting of the magnetic nanoparticles in the samples subjected to the motion instead of the pre-magnetization [3]. The possibility of detection of the magnetic nanoparticles using 151-channel magnetoencephalography (MEG) device without pre-magnetization or mechanical movement of the sample was first demonstrated in [4]. In this study the increase of the magnetic noise in the frequency domain was used for approximate localization of the sample.

The purposes of our work were to clarify the physical mechanism of the magnetic noise generation by the stationary vial of ferrofluid inside the MEG device and to verify the possibility of using the effect for the 3D imaging of ferrofluids. The planar set of sensors included 7 second-order SQUID gradiometers. No magnetic shielding was used. The samples were prepared on the base of Fe<sub>3</sub>O<sub>4</sub> nanoparticles of two sizes. In order to restrict the Brownian movement of the particles they were dispersed in matrixes of various viscosity (water, agar, ice). It was revealed that the ferrofluid in vial generates spontaneous magnetic field sufficient to detect the presence of nanoparticles in the described experimental setup. Quasirandom time series were recorded and then processed with recently developed method [5], based on the precise Fourier transform and coherence analysis. This method decomposes the multichannel signal into the large set of elementary oscillations, which can be localized individually, providing the functional tomogram of the system. It can be concluded, that the detailed 3D imaging of nanoparticles can be performed from their spontaneous movement by SQUID magnetometry.

The work was supported in part by the Russian Science Foundation under Grant 14-15-01096.

### References

- Gleich B., Weizenecker J. Tomographic imaging using the nonlinear response of magnetic particles. *Nature*, 2005, 435, 1214-1217.
- Flynn E.R., Bryant H.C. A biomagnetic system for *in vivo* cancer imaging. *Phys. Med. Biol.* 2005, 50(6): 1273-1293
- Jia W., Xu G., Scibassi R.J., Zhu J.G., Bagic A., Sun M. Detection of magnetic nanoparticles with magnetoencephalography. *Journal of Magnetism and Magnetic Materials* 320, 2008, 1472-1478.
- Cheung T., Kavanagh K., Kirby U. A new technique for magnetic nanoparticle imaging for magnetoencephalography using frequency data. *Front. Neurosci.* Conference Abstract: Biomag 2010 - 17th International Conference on Biomagnetism, doi:10.3389/conf.neuro.2010.06.00387.
- Linas R.R., Ustinin M.N. Precise Frequency-Pattern Analysis to Decompose Complex Systems into Functionally Invariant Entities. U.S. Patent, US20140107979 A1. 2014

## EVALUATING MAGNETIC NANOPARTICLES DISTRIBUTION THROUGH ACB TOMOGRAPHY

R. V. R. Matos<sup>1</sup>, P. R. Fonseca<sup>2</sup>, C. C. Quint<sup>1</sup>, A. G. Próspero<sup>1</sup>, L. A. Pinto<sup>1</sup>, F. P. F. de Mello<sup>1</sup>, N. Zifelato<sup>3</sup>, A. F. Batuzis<sup>3</sup>, J. R. A. Miranda<sup>1</sup>.

<sup>1</sup>Laboratório de Biomagnetismo, Bioscience Institute of Botucatu, Unesp, SP - Brazil

<sup>2</sup>Universidade Federal do Mato Grosso, Campus Barra do Garça, MS - Brazil

<sup>3</sup>Instituto de Física, Universidade Federal de Goiás, Goiânia, GO - Brazil

Biomagnetic systems have become important tools for organs and systems functional evaluation on both animals and human models. Among these, the AC Biomagnetometry (ACB) has been widely applied for mapping ferrromagnetic tracers on meals and solid dosage forms. Recent improvements in the ACB instrumentation allowed us to obtain tomographic *in vitro* images of magnetic nanoparticles. Here, we employed the same technology to acquire tomographic images on small animal models. The AC Biomagnetometer used on this paper consists of 13 channels detection coils, arranged in a first-order gradiometric configuration, coupled to a pair of excitation coils working as magnetic flux transformer. When any high-susceptibility material approximates the sensor probe, its response to the excitation magnetic field alters the magnetic flux on the detection system, generating a signal that can be recorded. The ACB system was attached on a non-magnetic R-O computer controlled system, responsible by the sample rotation and linear displacement to 100 radial and 80 angular different positions for 0.5s, while the ACB signals were recorded by a lock-in amplifiers (Stanford Research Systems), digitalized at 100 Hz (PCL-MIO-16XE-10, NationalInstruments Inc.) and stored for posterior processing (ASCII format). All signal and imaging processing, were performed on Matlab® (Mathworks Inc.) including background signal intensity correction, sinogram calculation, reconstruction (filtered backprojection with cubic interpolation and Hamming windowing) and enhancement. After the system was set up, each animal (*5 male Wistar rats*) received intravenously a Citrate coated, manganese doped Iron Oxide Nanoparticles. After 120 minutes, all animals were sacrificed and *ex-vivo* images acquired. The red line on figure 1A represents the approximate position where the images were acquired and the corresponding images are exhibited on 1B, where it is possible to notice that the maximum concentration of the nanoparticle was concentrated in the liver, followed by lungs (considering its size and position). Also, from the 3D rendering (1C), we could estimate that all the liver lobes absorbed the tracer while the lung had almost half of its volume marked. This study showed that ACB tomography is a viable technique to acquire tomographic images of magnetic nanoparticles distribution.

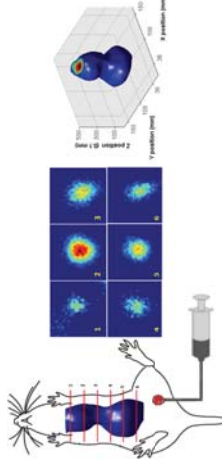


Figure 1: 1A presents the experimental set up for the image acquisitions, highlighting the region in each image, followed by the tomographic images (1B) and the 3D reconstruction (1C).

# Design and Characterization of a device to quantify the Magnetic Drug Targeting Efficiency of Magnetic Nanoparticles in a Tube Flow Phantom

Patricia Radon, Norbert Löwa, Maik Liebl, Dirk Gutkelsch, Frank Wiekhorst  
 Physikalisch-Technische Bundesanstalt, Abbestrasse 2-12, 10587 Berlin  
 \*E-Mail: patricia.radon@ptb.de

The aim of magnetic drug targeting (MDT) is to transfer a therapeutic drug coupled to magnetic nanoparticles (MNP) to desired disease locations (tumor region) with the help of magnetic fields. To transfer the MDT approach into clinical practice a number of important issues remain to be solved. We developed and characterized an *in vitro* flow phantom to provide a defined and reproducible MDT environment. Integrated into this setup is a magnetic particle spectroscopy (MPS) device to determine the targeting efficiency as defined as the ration between magnetically targeted and applied total MNP amount. MPS is based on the detection of the non-linear magnetic susceptibility of MNP in an oscillating excitation field at a frequency of 25 kHz and amplitude of 25 mT offering an excellent temporal resolution of seconds and an outstanding specific sensitivity of some nanograms of iron.

The flow phantom (Fig 1, left) is composed of a peristaltic pump which circulates an MNP suspension through a polymer tube system. At the retention site a strong neodymium targeting magnet (magnetic field gradient of about 83 T/m) is located to concentrate the MNP. Mounted on a sliding device the magnet can be accurately positioned at a defined distance to the tube during a MDT application. The tube system is directed through the detection coil of the MPS device.

The active MNP suspension volume in the detection coil of the MPS is about 29.1  $\mu\text{l}$ . The flow rate of the peristaltic pump used can be adjusted within the range of 27  $\mu\text{l}/\text{min}$  and 2.7  $\mu\text{l}/\text{min}$  and by the inner diameter of the tube. We found considerable magnetic impurities in some tube materials and an adhesion depending on the MNP type on tube materials even without MDT. We determined a reproducibility for the basic flow phantom of less than 5 % by repeated MDT measurements.

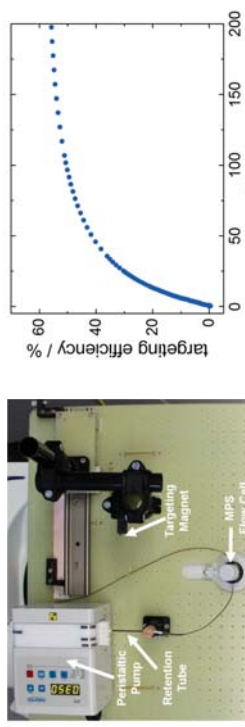


**Fig 1:** Left: Tube flow phantom setup mounted on top of the Magnetic Particle Spectrometer. Right: MDT efficiency of MNP (fluidMAG-D MNP, chemicell GmbH, Germany, with 200 nm hydrodynamic diameter) quantified by MPS in our basic flow phantom setup.

In the flow phantom different MNP types, magnet geometries and tube materials can be employed to vary physical parameters like diameter, flow rate, magnetic targeting gradient, and MNP properties. The combination with MPS allows for quantification of the targeting efficiency as a function of time and these physical parameters, an example is shown in Fig.1. This device might become a valuable tool for assessment of MNP dedicated for MDT application.

Acknowledgements: The research was supported by German Research Foundation (SPP) 681 WI 4230/1-2, NanoGuide TR 408/7-2.

# Investigation of Magnetic Targeting Properties of FluidMAG-D

Patricia Radon, Norbert Löwa, Maik Liebl, Frank Wiekhorst

Physikalisch-Technische Bundesanstalt, Abbestrasse 2-12, 10587 Berlin

\*E-Mail: patricia.radon@ptb.de

Magnetic iron oxide nanoparticles (MNP) are indispensable constituents in promising novel biomedical applications especially magnetically targeted drug delivery. The huge magnetic moment of the MNP administered to the vascular system is exploited to accumulate a therapeutically active drug through the vascular system at the target, e.g. tumor, by a strong magnetic field gradient from outside the body. The success of such an approach is depending on the complex interplay between physiological (geometry, flow conditions of the vessels) and physical parameters (geometry and strength of the magnet, moment and size of the MNP).

We applied the recently developed tube flow phantom device with integrated MNP quantification to investigate the influence of hydrodynamic size and targeting duration on the targeting efficiency. For this purpose, we employed fluidMAG-D nanoparticle system (chemicell GmbH, Berlin), iron oxide MNP with the same cores but available with different hydrodynamic diameters  $d_{\text{hydr}} = 50 \text{ nm}, 100 \text{ nm}, 200 \text{ nm}, 300 \text{ nm}$  and are coated by hydrophilic starch to protect them against aggregation.

For the targeting experiments we used MNP suspension at a fixed iron concentration  $c(\text{Fe}) = 7.5 \text{ mmol/L}$  (preclinical dosage of 300  $\mu\text{l}$  Fe/kg). The suspension was circulated by a pump in the flow phantom (polymer tube, 1.4 mm inner diameter, total volume 1 mL, corresponding total iron amount about 400  $\mu\text{g}$ ) at a flow rate of 350  $\mu\text{l}/\text{min}$  passing the targeting magnet with a magnetic field gradient of about 80 T/m at a distance of 1 mm. After the magnet the tube is directed through the detection coil of a commercial Magnetic Particle Spectrometry (MPS) device (MPS-3, Bruker BioSpin, Ettlingen) where the non-linear dynamic magnetic susceptibility (25 kHz excitation frequency, 25 mT field amplitude) is used to determine the iron (MNP) content every 10 s with sensitivity down to some nanogram. The decrease of iron content measured at the tube volume inside the MPS detection coil (about 29  $\mu\text{l}$ ) was then attributed to the amount of MNP accumulated at the magnet site.

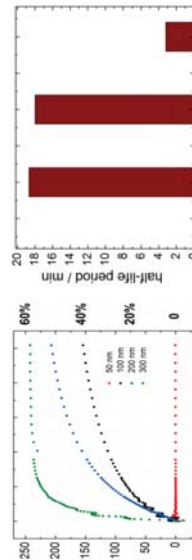


**Fig 1: Left:** Amount of accumulated iron during magnetic drug targeting of the four different fluidMAG-D systems with  $d_{\text{hydr}} = 50, 100, 200, 300 \text{ nm}$  as a function of time determined by MPS in our tube flow phantom. **Right:** Half life period as a function of  $d_{\text{hydr}}$ .

Figure 1, left, shows the targeting efficiency (ratio of accumulated iron amount after time  $t$  and 400  $\mu\text{g}$  total iron amount) is strongly depending on hydrodynamic size and targeting time. Nearly no accumulation is observed for  $d_{\text{hydr}} = 50 \text{ nm}$  whereas the largest particle (300 nm) were most efficiently accumulated to about 60% already after 30 min targeting. From the curves the targeting half life periods were determined; for  $d_{\text{hydr}} = 300 \text{ nm}$  we found the very short duration of about 3 min (Fig 1, right).

The online MPS quantification is a direct and sensitive method to quantify MNP of various sizes even in flowing liquids. Combined with the tube flow phantom setup the MNP targeting efficiency can be quantitatively assessed prior to *in vivo* experiments.

Acknowledgements: This research was supported by German Research Foundation (priority program 1681, grant WI 4230/1-2, and research group FOR917, Nanoguide TR 408/7-2).

## Long-term calibration phantom for MRI, MRX-CT and X-ray-CT imaging of body tissues enriched with magnetic nanocomposites

H. Rahn<sup>1,2</sup>, R. Woodward, M. House<sup>2</sup>, S. Dutz<sup>3</sup>, D. Engincer<sup>4</sup>, M. Liebl<sup>5</sup>, K. Feindel<sup>6</sup>,

S. Odenbach<sup>1</sup>, and T. SPiere<sup>2</sup>

<sup>1</sup>Technische Universität Dresden, Institute of Fluid Mechanics, Chair of Magnetofluidynamics,

Measuring and Automation Technology, 01062 Dresden, Germany

<sup>2</sup>The University of Western Australia, School of Physics, Crawley, Perth WA 6009, Australia

<sup>3</sup>Institute of Biomedical Engineering and Informatics (BMTI), Technische Universität Ilmenau, Ilmenau, Germany

<sup>4</sup>The University of Western Australia, Centre for Microscopy and Characterisation Analysis, Crawley, Perth WA 6009, Australia

<sup>5</sup>PIB – Physikalisch Technische Bundesanstalt Berlin, Abbestraße 2–12 10587 Berlin

A study of a long-term phantom of body tissues enriched with magnetic nanocomposites (MNC) suitable for 3-dimensional and quantitative imaging of biological tissues after, e.g. magnetically assisted cancer treatments was performed. The approach was to develop a suitable phantom for different imaging modalities as well as to perform a cross-calibration of X-ray Computed Tomography (XCT), Magnetic Resonance Imaging (MRI) and Magnetorelaxometry (MRx). The developed phantoms consist of an elastomer PermaGel (PG) [1] with different concentrations of multi-core magnetic nanocomposites (MNC) [2]. We prepared 12 different MNC concentrations in a range of 0 mg/ml to 6.91 mg/ml. These cylinders have been layered to stack of three PG-MNC-cylinders which are separated by blank PG as shown in Figure 1(a)). The phantoms were imaged with X-ray microcomputed tomography (XμCT) and a 9.4 T MRI. Additionally, the MNC concentrations in phantoms were determined with Nuclear magnetic resonance (NMR), Inductively coupled plasma mass spectrometry (ICP-MS), Magnetic Particle Spectroscopy (MPS), and MRx-Tomography (MRx-CT).

The result is the specification of a sensitivity range for standard imaging techniques as XCT and MRI (Figure 1(b)). Furthermore, a quantification of the MNC content in biological tissue samples shall be obtained and validated with MRx-CT.

a)

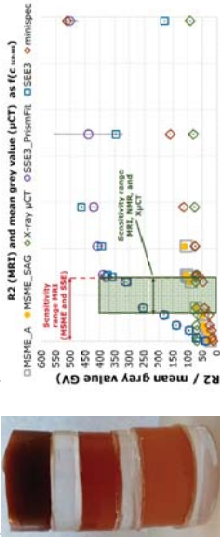


Figure 1(a): one of four stacks of cylinders with three nanoparticle concentrations separated by blank gel cylinders; b): Summary of NMR, XμCT, and MRI results.

### Acknowledgments

These studies are supported by the Deutsche Forschungsgemeinschaft (DFG- RA 2633/1-1).

### References

- [1] Perma Gel Safety Data Sheet, 1907/2006/EC (REACH), 1272/2008/EC (CLP), a. GHS
- [2] Dutz S., et al. J. of Magn. and Magn. Mat. 321 (2009) 1501 – 1504

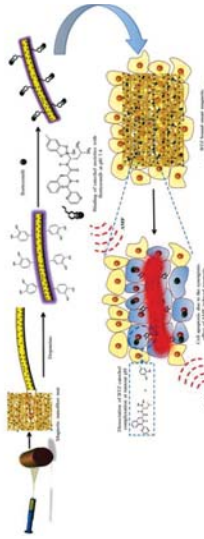
## An Implantable Smart Magnetic Nanofiber Device for Endoscopic Hyperthermia Treatment and Tumor-Triggered Controlled Drug Release

Afieesh Rajan Unnithan<sup>1\*</sup>, Arathiram Ramachandra Kurup Sasikala<sup>1</sup>, Yeo-Heung Yun<sup>2</sup>,

Chan Hee Park<sup>1</sup>, Cheol Sang Kim<sup>1</sup>

<sup>1</sup>Department of Bionanosystem Engineering, Graduate School, Chonbuk National University, Jeonju 561-756, Republic of Korea, <sup>2</sup>Department of Bioengineering, North Carolina Agricultural & Technical State University, Greensboro, North Carolina 27411, United States, \*E-Mail : afieeshnano@gmail.com

The study describes the design and synthesis of an implantable smart magnetic nanofiber device for endoscopic hyperthermia treatment and tumor-triggered controlled drug release. This device is achieved using a two-component smart nanofiber matrix from monodisperse iron oxide nanoparticles (IONPs) as well as boritezomib (BTZ), a chemotherapeutic drug. The IONP-incorporated nanofiber matrix was developed by electrospinning a biocompatible and bioresorbable polymer, poly (d,L-lactide-co-glycolide) (PLGA), and tumor-triggered anticancer drug delivery is realized by exploiting mussel-inspired surface functionalization using 2-(3,4-dihydroxyphenyl)ethylamine (dopamine) to conjugate the borate-containing BTZ anticancer drug through a catechol metal binding in a pH-sensitive manner. Thus, an implantable smart magnetic nanofiber device can be exploited to both apply hyperthermia with an alternating magnetic field (AMF) and to achieve cancer cell-specific drug release to enable synergistic cancer therapy. The results confirm that the BTZ-loaded mussel-inspired magnetic nanofiber matrix (BTZ-MMN) is highly beneficial not only due to the higher therapeutic efficacy and low toxicity towards normal cells but also, as a result of the availability of magnetic nanoparticles for repeated hyperthermia application and tumor-triggered controlled drug release.



<sup>1</sup>Technische Universität Dresden, Institute of Fluid Mechanics, Chair of Magnetofluidynamics, Measuring and Automation Technology, 01062 Dresden, Germany

<sup>2</sup>The University of Western Australia, School of Physics, Crawley, Perth WA 6009, Australia

<sup>3</sup>Institute of Biomedical Engineering and Informatics (BMTI), Technische Universität Ilmenau, Ilmenau, Germany

<sup>4</sup>The University of Western Australia, Centre for Microscopy and Characterisation Analysis, Crawley, Perth WA 6009, Australia

<sup>5</sup>PIB – Physikalisch Technische Bundesanstalt Berlin, Abbestraße 2–12 10587 Berlin

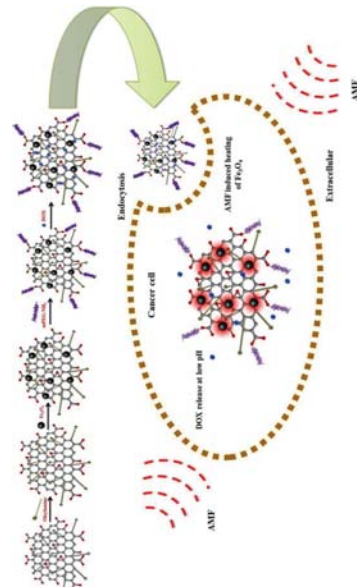
## Multifunctional Nanocarpets for Cancer Theranostics: Remotely Controlled Graphene Nanoheaters for Thermo-Chemosensitisation and Magnetic Resonance Imaging

Arathyram Ranachandra Kurup Sasikala<sup>1\*</sup>, Afeesh Rajan Unnithan<sup>1</sup>, Chan Hee Park<sup>1</sup>,

Cheol Sang Kim<sup>1</sup>

<sup>1</sup>Department of Bionanosystem Engineering, Graduate School, Chonbuk National University, Jeonju 561-756, Republic of Korea, \*Email: arathyramnair@gmail.com

A new paradigm in cancer theranostics is enabled by safe multifunctional nanoplatform that can be applied for therapeutic functions together with imaging capabilities. Herein, we develop a multifunctional nanocomposite consisting of Graphene Oxide–Iron Oxide -Doxorubicin (GO-IO-DOX) as a theranostic cancer platform. The smart magnetic nanoplateform acts both as a hyperthermic agent that delivers heat when an alternating magnetic field is applied and a chemotherapeutic agent in a cancer environment by providing a pH-dependent drug release to administer a synergistic anticancer treatment with an enhanced T2 contrast for MRI. The novel GO-IO-DOX nanocomposites were tested in vitro and were found to exhibit an enhanced tumoricidal effect through both hyperthermia and cancer cell-specific DOX release along with an excellent MRI performance, enabling a versatile theranostic platform for cancer. Moreover the localized antitumor effects of GO-IO-DOX increased substantially as a result of the drug sensitization through repeated application of hyperthermia.



## Magnetic drug delivery to the cochlea to prevent cisplatin induced hearing loss

B.Ramawatny<sup>1</sup>, S.Roy<sup>1</sup>, A.Apolo<sup>2</sup>, D.Depireux<sup>3</sup>, B.Shapiro<sup>1,3</sup>

<sup>1</sup>Dept of Biengineering, <sup>2</sup>Institute for Systems Research, University of Maryland, College Park, MD, USA, <sup>3</sup>Center for Cancer Research, National Cancer Institute, MD, USA, Presenter: [bharath@umd.edu](mailto:bharath@umd.edu)

Cisplatin and other platinum based drugs are the drugs of choice for various genito-urinary cancers, certain types of breast cancers, and as radiosensitizers for most head and neck cancers. However, these drugs are very toxic to the kidneys, the inner ear/cochlear,<sup>1</sup> and sometimes the peripheral nervous system. Nephro-toxicity is mitigated by hyper-hydrating patients but ototoxicity in cisplatin-treated patients remains an unmet medical need. Thirty percent of patients receiving cisplatin get severe to complete hearing loss.<sup>2</sup>

Steroids have been shown to reduce cisplatin-induced hearing loss<sup>2</sup>, presumably by counteracting the effect of the reactive oxygen species induced by cisplatin administration. We have developed a magnetic injection method that can deliver steroid-eluting magnetic nanoparticles into the cochlea.<sup>3</sup> To evaluate the efficacy of our method for protecting hearing from chemotherapy regimens, we tested our methods in a recognized mouse model of cisplatin induced hearing loss<sup>4</sup>. All mice received chemotherapy. Mice in group A received saline to one ear. Mice in group B received the steroid (prednisone) to one ear trans-tympanically, meaning that the steroid was deposited in the middle ear which is adjacent to the cochlea. (Trans-tympanic injection is a current option for local delivery to the ear.) Finally, mice in group C received prednisolone-eluting magnetic nanoparticles (Chemical) and a magnet was applied to transport those particles into the cochlea. For all mice, the other ear remained untreated as a same-animal control. Mice in all groups were then tested for hearing using auditory brainstem response before and after their chemotherapy administrations. The cochleas of the mice in all the groups were then dissected and their cochlear hair cells were assessed for damage using histo-staining and confocal microscopy.

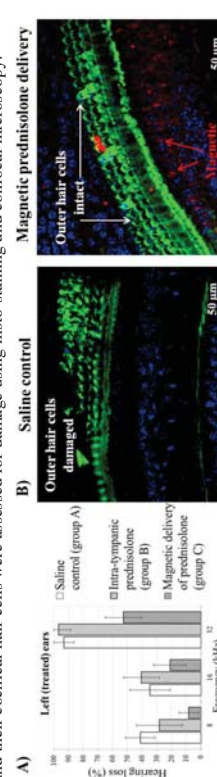


**Figure 1:** A) Comparison of percent cisplatin induced hearing loss between the three groups at different frequencies using auditory brainstem response recordings. B) Outer hair cells of the cochlea in group C (right) after cisplatin injections as compared to the saline control group A (left). The cochlear hair cells are stained using phalloidin for actin (green). The magnetic nanoparticles (red) emit red fluorescence. Magnetic forces transported the nanoparticles all the way to the cochlea hair cells. We found that magnetic delivery protected hearing from the cisplatin regimens. At 32 kHz, the magnetic delivery group C (Fig 1A) ears experienced substantially less hearing loss ( $53\% \pm 12\%$ ) as compared to ears that received saline (group A,  $93\% \pm 7\%$ ) or intra-tympanic prednisolone (group B,  $97\% \pm 3\%$ ). Hair cell preservation was evident in the magnetically treated cochlea (Fig 1B, right) as compared to group A (saline) and group B (intra-tympanic steroid) (Fig 1B, left). Magnetically delivered nanoparticles can be seen among the hair cells in the cochlea (red fluorescence in Fig 1B, right). In summary, magnetic delivery of steroids protected hair cells more effectively and concomitantly reduced the degree of cisplatin-induced hearing loss, compared to no treatment or to intra-tympanic steroid administration.

- [1] Rademaker-Lakha JM et al. "Relationship between cisplatin administration and the development of ototoxicity". *J Clin Oncol Off J Am Soc Clin Oncol*. 2006 Feb; 24(6):918-24. [2] Marashki T et al. "Prevention of Cisplatin-Induced Hearing Loss by Intratympanic Dexamethasone: A Randomized Controlled Study". *Int J Head Neck Surg*. 2014 Mar 1; 15(6):983-90. [3] Shapiro B et al. "Pre-Clinical Development of Magnetic Delivery of Therapy to Middle and Inner Ears". *ENT & Audiology News*. 23rd ed. 2014 Apr-5-6. [4] Roy S et al. "Sound preconditioning therapy inhibits ototoxic hearing loss in mice". *J Clin Invest*. 2013 Nov; 123(11):4645-9.

## On the safety of magnetic nanoparticle (MNP) motion in live brain tissue

B. Ramaswamy<sup>1\*</sup>, S.D.Kulkarni<sup>2</sup>, P.S.Villar<sup>3</sup>, C.Eberly<sup>3</sup>, R.C.Aranda<sup>3</sup>, D.A.Depireux<sup>4</sup>, B.Shapiro<sup>1,4</sup>

<sup>1</sup>Dept. of Bioengineering, <sup>3</sup>Dept. of Biology, Institute for Systems research, Univ of Maryland, USA  
<sup>2</sup>Western Digital Inc., California, USA, \* Presenter: [bharathi@umd.edu](mailto:bharathi@umd.edu)

Magnetic nanoparticles (MNPs) could be more effective in treating various neurological disorders, such as glioblastoma, due to the ability of magnetic forces to circumvent or cross the blood brain barrier<sup>1,2</sup>. Most prior studies focused on the motion of MNPs in blood vessels and then observed their presence or absence in target neurological tissue<sup>1,2</sup>. We focused our investigations on the motion of MNPs in the brain tissue itself, rather than in blood vessels within that tissue. Furthermore, we investigated the impact of this motion on normal neuronal functioning using electrophysiology, imaging and immunohistochemistry.

To do so, we injected 4  $\mu$ L of 300 nm diameter starch coated fluorescent MNPs (Chemilab) in the cortex of freshly dissected rat brain tissue. After injection, cortical slices were extracted from the rat brain and exposed to a uniform magnetic field. The resulting motion of the MNPs was monitored using fluorescent microscopy. To assess the safety of MNP motion in live brain tissue, we extracted brain slices containing the olfactory bulb from transgenic mice expressing green fluorescent protein (GFP). We then performed electro-physiological recordings in the neurons of the olfactory bulb while the MNPs were in motion. Using calcium imaging, we investigated the effect of MNP motion on the overall neural circuit function. Subsequently, the nerve fibers in these slices were visualized using immunostaining to assess any damage caused by MNP movement.

In the presence of a uniform magnetic field, the MNPs moved towards each other to form MNP chains as shown in Fig. 1A. The motion of the MNPs did not alter the dependence of neuron firing frequency for different currents injected into the cells (Fig. 1B) or disrupt the brain nerve fibers in the region of motion. We

also assessed the responsiveness of neurons to activation by the excitatory neurotransmitter glutamate after MNP movement in the region using a calcium sensing fluorescent dye. As shown in Fig. 1C, following the movement of MNPs in the slice, glutamate still produced a robust increase in intracellular calcium in the neurons suggesting a functionally intact neural circuit in the region.

In summary, we showed that MNP motion in the brain did not disturb normal brain function.

[1] Kong et al. "Magnetic targeting of nanoparticles across the intact blood-brain barrier." *Journal of controlled release* 164.1 (2012): 49-57.

[2] I.N.Wanberg et al. "Non-invasive image Guided Brain access with Gradient Population of Magnetic Nanoparticles." *IEEE Medical Imaging Meeting*, Anaheim, CA, Oct 2012.

## Glycoconjugate-Functionalized Magnetic Nanoparticles for Bacteria Specific Targeting and Inactivation via MagMED

Yash Raval<sup>1</sup>, Benjamin Fellows<sup>2</sup>, O. Thompson Mefford<sup>2</sup>, and Tzuen-Rong J. Tzeng<sup>1</sup>

<sup>1</sup> Department of Biological Sciences, Clemson University, Clemson, SC 29634

<sup>2</sup> Department of Materials Science and Engineering, Centre for Optical Materials Science and Engineering Technologies (COMSET), Clemson University, Clemson, SC 29634

Email: [yraval@g.clemson.edu](mailto:yraval@g.clemson.edu); [tzunrt@clemson.edu](mailto:tzunrt@clemson.edu)

Since the discovery of the very first antibiotic (penicillin), mankind has been engaged in a complex battle to overcome drug resistant bacteria. New technologies that do not rely on antibiotics are urgently needed in current clinical settings to treat bacterial infections caused by multi-drug resistant bacteria. In this research work, we explore the feasibility of using MagMED to inactivate enterotoxigenic *Escherichia coli* strain K99 (EC K99) in the presence of multifunctional glycoconjugate-functionalized magnetic nanoparticles. PEO-PAA functionalized magnetic nanoparticles (PEO-MNPs) were synthesized and functionalized with bacteria-specific glycoconjugate Neu5Ac( $\alpha$ 2-3)Gal- $\beta$ (1-4)GlcNAc-sp (GM3-MNPs) for adherence to EC K99. Mixing GM3-MNPs and EC K99 in appropriate ratio resulted in rapid aggregation of EC K99 when visualized through different microscopic techniques<sup>1</sup>. Further, when such mixtures were exposed to alternate current magnetic field (field intensity >34 KA/m, frequency @ 207 KHz, approximately 3-log reduction in colony forming units (CFUs) of EC K99 was achieved in 120 minutes of hyperthermia treatment. Control experiments using non-functionalized PEO-MNPs or alternative strains of EC showed no decrease in CFUs of bacteria. These results suggest that targeted MagMED can be potentially used as a novel non-antibiotic treatment platform to inactivate/kill multi-drug resistant bacterial pathogens, without harming the affected body region/tissue.

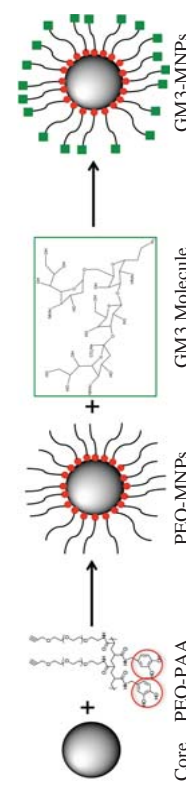


Figure 1: Graphical representation of producing multifunctional glycoconjugate functionalized MNPs

## References:

- Raval, Y., Stone, R., Fellows, B., Qi, B., Huang, G., Mefford, O.T. & Tzeng, T.R. Synthesis and application of glycoconjugate-functionalized magnetic nanoparticles as potent anti-adhesion agents for reducing enterotoxigenic *Escherichia coli* infections. *Nanoscale* 7, 8326-8331 (2015).

## Dynamics of magnetic nanoparticles in viscoelastic media

H. Remmer<sup>1\*</sup>, E. Roeben<sup>2</sup>, A. M. Schmidt<sup>2</sup>, M. Schilling<sup>1</sup>, and F. Ludwig<sup>1</sup>

<sup>1</sup>Institute of Electrical Measurement and Fundamental Electrical Engineering, TU Braunschweig, Hans-Sommer-Str. 66, D-38106 Braunschweig, Germany; \*E-Mail: h.remmert@tu-bs.de

<sup>2</sup>Institute of physical chemistry, Universität zu Köln, Köln, Germany

Whereas the Brownian relaxation of magnetic nanoparticles (MNP) in Newtonian fluids has been successfully utilized to study viscosity changes on the nanoscale, many biomedically relevant media exhibit non-Newtonian behavior. In particular, there are elastic components in addition to the viscous ones. As a consequence, the relationship between characteristic time constants, e.g. determinable from complex ac susceptibility measurements, and material properties of the matrix becomes more complex.

In this work we exemplarily investigate the gelation process of aqueous gelatin solutions mixed with MNP by using complex ac susceptibility measurements [1]. Gelatin solutions can be considered as model system for the Voigt-Kelvin model which includes a viscous and an elastic term in parallel. The CoFe<sub>2</sub>O<sub>4</sub> nanoparticles used in this study are coated with a PAA shell and have a mean hydrodynamic diameter  $d_{\text{hyd}} = 18 \pm 0.4$  nm. The measured data were analyzed with two models which are based on the Voigt-Kelvin model. The expression for the dynamic susceptibility proposed by Raikher et al. [2] is based on the equation of motion  $I\ddot{\theta} + \zeta\dot{\theta} + K\theta = y(t)$ . Here,  $I$  is the moment of inertia of the particle,  $\zeta$  the rotational friction coefficient,  $K$  the linear elastic restoring parameter,  $y(t)$  the stochastic driving torque due to thermal energy and  $\theta$  the angle between magnetic moment and applied magnetic field. The equations are only numerically solvable. As an alternative, we replace – similarly to DiMarzio and Bishop [3] – the viscosity  $\eta$  in the Debye model by a complex and frequency-dependent one:  $\eta(\omega) = \eta_0 - G(i\omega)$  with viscosity  $\eta_0$ , shear modulus  $G$  and angular frequency  $\omega$ .

Figure 1 depicts the results for the shear modulus and the viscosity for both models as a function of gelation time. It is found that the values for the viscosity are quite similar but the shear modulus calculated by the Raikher model is approximately twice the values calculated by the alternative model. Possible reasons for the discrepancy are discussed and the obtained  $\eta$  and  $G$  values are compared with macro rheologically measured ones. Similar measurements applying MNP with larger sizes are in progress.

### Acknowledgment:

This work was supported by the Deutsche Forschungsgemeinschaft, DFG Priority Program 1681 (LU800/4-2, SCHM1747/10-2).

### References:

- [1] H. Remmer et al., Phys. Proc. 75, 1150 (2016).
- [2] Y. L. Raikher et al., Phys. Rev. E 63, 031402 (2001).
- [3] E. A. DiMarzio and M. Bishop, J. Chem. Phys. 60, 3802 (1974).

## Structural and magnetic properties of Mg<sub>1-x</sub>Zn<sub>x</sub>Fe<sub>2</sub>O<sub>4</sub> magnetic nanoparticles prepared sol-gel method

P. Y. Reyes-Rdz<sup>1\*</sup>, D. A. Cortes-Hernández<sup>1</sup>, J. Sánchez<sup>1</sup>, A. Jasso-Terán<sup>1</sup>, L. E. De León-Prado<sup>1</sup>, J. M. Méndez-Nonell<sup>2</sup>, G. F. Hurtado-López<sup>3</sup>

<sup>1</sup>Cinvestav-1 Unidad Saltillo, Av. Industria Metalúrgica #1062, Parque Industrial Saltillo-Ramos Arizpe, CP 25900, México. <sup>2</sup>Centro de Investigación en Materiales Avanzados, Ave. Miguel de Cervantes # 120, Complejo Industrial Chihuahua, CP 31109, Chihuahua, México. <sup>3</sup>Centro de Investigación en Química Aplicada, Blvd. Enrique Reyna Hermosillo #140, CP 25294, Saltillo, Coah. México.

\*pamelala2244\_4@hotmail.com

Magnetic nanoparticles (MNPs), have attracted considerable attention for their structural and magnetic properties. These materials can be used in biomedical applications such as drug delivery, magnetic resonance imaging agents (MRI) and hyperthermia. These applications require that MNPs show high biocompatibility and high saturation magnetization, particle size smaller than 100 nm, a narrow particle size distribution and a biocompatible surface coating to provide stability under physiological conditions.

In this work, the synthesis of Mg<sub>1-x</sub>Zn<sub>x</sub>Fe<sub>2</sub>O<sub>4</sub> magnetic nanoparticles ( $x=0.0-0.9$ ) by sol-gel method, using ethylene-glycol as reaction medium, is reported. The effect of Zn<sup>2+</sup> incorporation into the spinel structure and magnetic properties of the synthesized ferrites was evaluated. The X-ray diffraction patterns exhibit the formation of a crystalline phase with an inverse spinel structure that corresponds to magnesium ferrite (JCPDS 88-1935), crystallite sizes are between 17-22 nm. The magnetic properties of ferrites, such as the saturation magnetization ( $M_s$ ), remanent magnetization ( $M_r$ ) and coercive field ( $H_c$ ) were measured by vibrating sample magnetometry.  $M_s$  values increased as the partial Zn<sup>2+</sup> substitution was increased (27.81-42.85 emu/g), while the  $M_r$  and  $H_c$  values were within the accepted ranges for biomedical applications. Selected nanoparticles were characterized by Fourier transform infrared spectroscopy (FTIR), transmission electron microscopy (TEM) and energy dispersive spectroscopy (EDS). These materials showed an absorption band at 532 cm<sup>-1</sup> corresponding to the Metal-O vibration related to the tetrahedral and octahedral sites of the spinel structure. TEM micrographs showed average particle sizes of 5 to 33 nm with a morphology close to the spherical. The heating ability of nanoparticles was evaluated under a magnetic field (10.2 kA/m and frequency 354 kHz), 8 and 10 µg/ml suspensions showed heating up to 44 °C, obtaining magnetic nanoparticles potentially viable for biomedical applications.

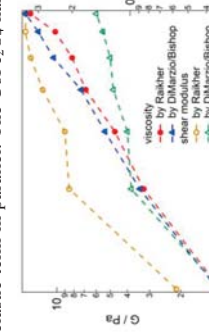


Fig. 1: Viscosity (closed symbols) and shear modulus (open symbols) determined by the models of Raikher and DiMarzio/Bishop for a 2.5 w% aqueous gelatin solution sample.

Figure 1 depicts the results for the shear modulus and the viscosity for both models as a function of gelation time. It is found that the values for the viscosity are quite similar but the shear modulus calculated by the Raikher model is approximately twice the values calculated by the alternative model. Possible reasons for the discrepancy are discussed and the obtained  $\eta$  and  $G$  values are compared with macro rheologically measured ones. Similar measurements applying MNP with larger sizes are in progress.

### Acknowledgment:

This work was supported by the Deutsche Forschungsgemeinschaft, DFG Priority Program 1681 (LU800/4-2, SCHM1747/10-2).

### References:

- [1] H. Remmer et al., Phys. Proc. 75, 1150 (2016).
- [2] Y. L. Raikher et al., Phys. Rev. E 63, 031402 (2001).
- [3] E. A. DiMarzio and M. Bishop, J. Chem. Phys. 60, 3802 (1974).

## Magnetic Alloys and Nanoparticle-based Bio-nanomagnetic Materials and Devices

Conrad Rizal  
E-mail: crizal@ucsd.edu

University of California, San Diego, 9500 Gilman Dr, La Jolla, CA, 92093, USA

The future of magnetic alloys and magnetic nanoparticles (MNPs)-based biomedical structures and devices looks promising in a wide variety of sectors from both fundamental and applied research points of view [1-3]. Several possible integrated functionalities of magnetic materials have been identified for potential future biomagnetic applications, with more forth coming. One is the actively investigated areas in biomagnetics where GMR sensors are combined with the MNPs for early disease detection, prevention, and cure [1]. However, in order for this detection scheme to have practical applications in the medical field, the room temperature field sensitivity of the sensors and the magnetizations of the alloys must be improved. Another area in which magnetic materials will find application is in medical imaging where the MNPs are first modified for bio-compatibility and then guided to targeted locations as contrast agents for either already available MRI or for future MNPs-based imaging. For single molecule studies, on-chip magnetic tweezers are integrated with the MR sensors. These tweezers can detect single molecules in real time. In addition, using alternating magnetic field, MNPs can be used for therapeutics, such as hyperthermia. Likewise, biocompatible MNPs when functionalized, can be used as drugs that can be released in response to the magnetic, optical, thermal, and pH stimuli. The same can be useful for ultra-immunoassay where small samples, e.g., blood, can be used to concentrate the signal. Except for the biochip-based detection system [1], all other biomagnetic techniques for biomedical applications are still at the proof-of-concept stage. Nevertheless, with the continuous improvement in nanofabrication, characterization, and imaging techniques, we should see great advances in biomedical nanomagnetics in the coming years. Another area where ferromagnetic nanoparticles may shine is in *magnetoplasmatics* due to its the flexibility in controlling material properties using optical radiation and magnetic field [4]. I expect this research will lead to new insights and discoveries along the away. These applications can also extend to energy production and even in space exploration. To realize the full potential of bionanomagnetics in new technologies, various physical and chemical principles of the magnetic materials and their impacts, on bio-medical imaging, bio-physics, energy, drug delivery, hypothermia, and immuno-assays, and a wide variety of other applications must be explored.

## References

- [1] D. Hall, R. S. Gaster, K. Makinwa, S. X. Wang and B. Murmann. A 256 pixel magnetoresistive biosensor microarray in 0.18  $\mu\text{m}$  CMOS. *Solid-State Circuits, IEEE Journal of* 48(5), pp. 1290-1301. 2013.
- [2] C. Rizal and B. B. Niraula. Ferronanomaterials: Magnetoresistance, microstructure, magnetism, and beyond (Review). *Journal of Nano-and Electronic Physics* 7(4), pp. 23 pages. 2015.
- [3] C. Rizal, Z. Liu and E. Fullerton. "Magnetic, microstructure, and magneto-optic properties of Ti/Au/Co/Au Nanostructures," Conference proceeding, *MRS meeting*, 2015, SF, USA.
- [4] I. S. Maksymov. Magneto-plasmonic nanoantennas: Basics and applications (Review). *ArXiv Preprint arXiv:1601.03101*. 2016.

## Magnetoplasmonic Nanosensors for Biosensing

Conrad Rizal  
University of California, San Diego, La Jolla, CA, 92093, USA  
E-mail: crizal@ucsd.edu

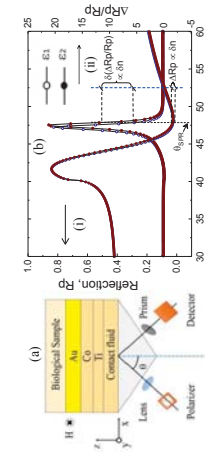


**Figure 1** (a) Schematics of SPR excitation (b-i) SPR and (b-ii) MOSPR effects. (b) Reflectance vs Incident angle,  $\theta$  for (i) SPR and (ii) MOSPR. The plots show the reflectance as a function of the incident angle. The y-axis is Reflectance and the x-axis is Incident angle,  $\theta$ .

Magnetoplasmronics, MPs, is relatively a new field of science that has a great potential application in biosensing and biomedical technologies [1] [2, 3, 4]. It merges the physics of nanophotonics, nano-optics, and nano-plasmonics, where biological samples such as cells, DNA, etc., are made to interact with magnetic moments or applied magnetic fields, optical radiation in visible to telecommunication wavelength ranges, and *surface plasmonic waves*.

Surface plasmonic waves are oscillating charge density waves that are created on the interface of multilayer and dielectric layer when excited by electromagnetic radiation. These waves, are called surface plasmon polaritons (SPPs), decay exponentially in the direction perpendicular to the interface and practically vanish at both sides of the interface.

Surface plasmon resonance (SPR) requires an optical radiation with a wavenumber  $k$  equal to that of SPPs,  $k_{\text{spp}} = \omega/c (\sqrt{\epsilon_d \mu_d \epsilon_m / \epsilon_d \mu_d + \epsilon_m \mu_m}}$ , where,  $\omega$  is the angular frequency,  $c$  is the speed of light, and  $\epsilon_d$ ,  $\mu_d$  and  $\epsilon_m$ ,  $\mu_m$  are the dielectric and magnetic permeability constants of the bio-sample and multilayer, respectively. Using *Kretschmann configuration* shown in Figure 1(a), the SPP are excited at an angle of incidence,  $\theta_{\text{spp}}$ , that generate a sharp decrease in the intensity of reflected optical radiation at  $\theta_{\text{spp}}$ . Given that  $k_{\text{spp}}$  is very sensitive to the change of  $\epsilon_d$ ,  $\mu_d$  and  $\epsilon_m$ ,  $\mu_m$  of the multilayer, the fundamental detection principle of SPR sensors relies on the change of  $\theta_{\text{spp}}$  with respect to the  $\epsilon$  (or  $\mu$ ) of a bio-sample. Assuming that  $\mu_d$ ,  $\epsilon_m$  and  $\mu_m$  are fixed, the reflectivity is a 2-dimension function of  $\theta$  and  $\epsilon_d$ ,  $R_p(\theta, \epsilon_d)$ . As shown in Figure 1 (b-i), at a minimal reflectivity, we have,  $\delta R_p(\theta_{\text{spp}}, \epsilon_d)/\delta \theta = 0$ . This implies that  $\theta_{\text{spp}}$  is a function of  $\epsilon_d$  and the ratio  $|\delta \theta_{\text{spp}}/\delta \epsilon_d|$  is required to be as large as possible for a highly sensitive SPR sensor, which is challenging in practice. Given the shape of the reflectivity curve with respect to  $\theta$ , the ratio that is clearly large is  $|\delta R_p(\theta_{\text{spp}}, \epsilon_d)/\delta \theta|$  near  $\theta_{\text{spp}}$  and this ratio is what MO-SPR sensors exploit to obtain high sensitivity in Figure 1(b-ii). By applying an external H field, parallel to the multilayer, but perpendicular to the incident plane, the MO Kerr effect is induced and this causes a shift in  $k_{\text{spp}}$  and, therefore, a small variation in  $\theta_{\text{spp}}$ . The variation of  $R_p$  with and without H can be expressed as,  $\Delta R_p = R_p(H) - R_p(0) = (\delta R_p/\delta \theta)\Delta \theta_{\text{spp}}$ . By normalizing with respect to  $R_p(0)$ , we get  $\Delta R_p/R_p = (\delta R_p/\delta \theta)/(\Delta \theta_{\text{spp}}/R_p)$ . In addition to eliminating the noise caused by the fluctuation in the incident radiation source, the ratio  $\Delta R_p/R_p$  is more sensitive to the changes of  $\epsilon_d$  than  $\theta_{\text{spp}}$ . This allows MOSPR to have a high resolution and improve the signal to noise ratio over the conventional SPR sensors. In this talk, we will show that due to the tunability of the optical radiation and magnetic fields, this new MOSPR configuration can detect as small as  $10^{-7}$

## Using Injection molding for fabrication of a continuous-flow magnetic cell sorter

David ROYET<sup>1</sup>, Pascal SIMONET<sup>1</sup> and Marie FRENEA-ROBIN<sup>1</sup>,  
<sup>1</sup>*Lyon Lyon, ECL, UCB Lyon I, CNRS, AMPERE, F-6934, ECULLY, France*  
 E-mail : david.royet@doctorant.ec-lyon.fr

Magnetism and microfluidics are two key concepts for the development of inexpensive and reliable tools dedicated to high-throughput biological analysis and providing large panel of applications from fundamental biology to biotechnology.

Cell separation under continuous flow is typically achieved by applying both magnetic and hydrodynamic forces on the target particles to guide them into different paths<sup>1</sup>. A large variety of cell sorting devices exploiting integrated magnetic flux sources are already described in the literature. However, their accessibility to non-specialists remains limited as their fabrication usually relies on highly specific equipment.

Magnetic composite polymers (M-CPs) may offer a viable alternative to conventional microfabrication approaches, bringing numerous advantages such as low cost, bio-compatibility, ease of fabrication and ease of integration with microfluidic components thanks to conservation of polymer mechanical properties, and compatibility with the undoped polymer.

In this work, we introduce a simple protocol, relying on an injection molding manufacturing process, for building a continuous flow magnetic sorter using only standard soft-lithography equipment. Simple Fe-doped PDMS stripes were integrated at the bottom of a whole PDMS chip with two inlets and two outlets. This design enables to deviate magnetic particles or magnetically labeled cells from one flow path to another when placing a magnet under the chip. Early results show the effective deviation of magnetic particles as sample flows through the microchannel, proving the potential of this rapid prototyping approach for easy building of magnetic cell sorters.

**Figure 1: Schematic representation of the magnetic cell sorter.**

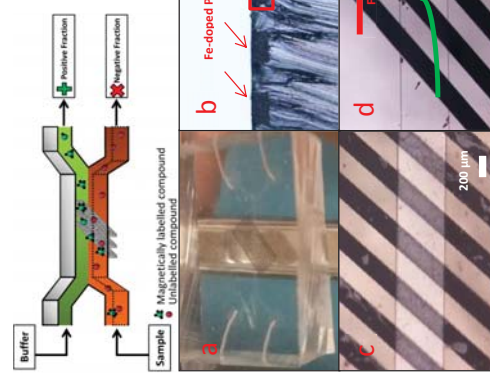


**Figure 2:** a) Picture of the device. b) Cross section of the magnetic stripes that are leveled with the PDMS surface (microchannel floor). c) Top view of the microchannel after PDMS-PDMS assembly. d) Top view of the microchannel 1 showing deviation of 10  $\mu\text{m}$  superparamagnetic particles.

### Reference

1. D.W. Inglis, R. Riehn, R.H. Austin, and J.C. Sturm, *Appl. Phys. Lett.* **85**, 5093 (2004).

## Comparison of Magnetic Nanoparticles with different Functional Groups for the Detection of Molecules using Magnetic Resonance

C. Rümenapp<sup>1,2</sup>, J. Marchiszy<sup>1</sup>, B. Gleich<sup>1,3</sup>

<sup>1</sup>Zentraleinstitut für Medizintechnik (IMETUM), Technische Universität München, Garching, Germany

<sup>2</sup>Email: tuermenapp@tum.de, <sup>3</sup>Email: gleich@tum.de

Magnetic resonance measurements can be applied together with functionalised magnetic nanoparticles (MNP) for the detection of small molecules, proteins or even cells [1, 2]. For this work, the surface of the MNP was functionalised with primary amino or carboxylic acid groups. The performance of the primary amino or the carboxylic acid MNP were compared according to their magnetisation, their relaxivity and their size distribution. Finally, for the proof of principle both particle types were functionalised with biotin, their relaxivities were again determined and avidin was detected using magnetic resonance measurement. For further detection applications the MNP can be functionalised with any specific binding molecule and either functional group can be used for its covalent binding.

The synthesised magnetic nanoparticles were colloidal stable and showed a narrow size distribution as previously shown [3]. After the functionalization procedure they were characterised according to their size, their surface chemistry, their magnetization and their relaxivities. The size distribution was obtained using transmission electron microscopy and dynamic light scattering. The core material was characterised by Moessbauer spectroscopy as previously shown [4]. The magnetization was determined by M(H) measurements and the particle surface chemistry by infrared spectroscopy (Figure 1 c).

The relaxivities of the primary amino and the carboxylic acid MNP before and after functionalization with biotin were determined at 0.5 T ( $\approx$  21.7 MHz) (Figure 1 a), as well as their detection limit for avidin through the change in the  $T_2$  relaxation time. For visualisation the avidin molecules were labelled with FITC (Figure 1 b). The detection limit for FITC-avidin of the primary amino Biotin MNP was determined to be 30.3  $\mu\text{M}$  and 7.5  $\mu\text{M}$  of the carboxylic Biotin MNP.

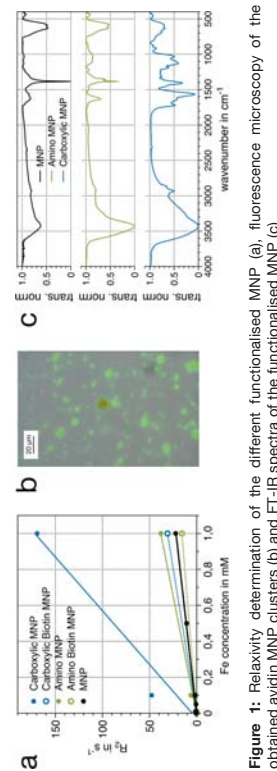


**Figure 1: Relaxivity determination of the different functionalised MNP (a), fluorescence microscopy of the obtained avidin MNP clusters (b) and FT-IR spectra of the functionalised MNP (c)**

1. Haun, J.B., et al., *Magnetic nanoparticle biosensors*, Wiley Interdiscip. Rev Nanobiotechnol, 2010; 2: p. 291-304.
2. Issadore, D., et al., *Miniature magnetic resonance system for point-of-care diagnostics*, Lab Chip, 2011; 11: p. 2282-2287.
3. Rümenapp, C., et al., *Detection of molecules and cells using nuclear magnetic resonance with magnetic nanoparticles*, Journal of Magnetism and Magnetic Materials, 2015; **380**: p. 271-275.
4. Rümenapp, C., F.E. Wagner, and B. Gleich, *Monitoring of the sizing of magnetic nanoparticles using Mössbauer spectroscopy*, Journal of Magnetism and Magnetic Materials, 2015; **380**: p. 241-245.

# Synthesis of Magnetic Nanocomposites for Application in Protein Delivery to Immune Cell

Chalatharn Saengsuengrit<sup>1</sup>, Patcharee Rirajak<sup>2</sup>, Numpon Insin<sup>1\*</sup>

<sup>1</sup>Department of Chemistry, Faculty of Science, Chulalongkorn University, Bangkok, 10330 Thailand

<sup>2</sup>Department of Microbiology, Faculty of Dentistry, Chulalongkorn University, Bangkok, 10330 Thailand

\*E-mail: Numpon.I@Chula.ac.th

Magnetic nanocomposites (MNCs) have received much attention in many applications especially in drug delivery systems. In this study, we interested in the protein (antigen model) delivery using MNCs as they can carry protein and be directed to target cells using an external magnetic field. Magnetic nanoparticles (MNPs) were synthesized by thermal decomposition method and coated with a biocompatible polymer, poly(lactic-co-glycolic acid), PLGA, by double emulsion method.

The particle size, shape, size distribution and surface charge of the nanocomposites were characterized using various techniques including transmission electron microscopy (TEM), field emission scanning electron microscopy (FESEM), Zeta potential analysis, and infrared spectroscopy (IR). The results showed that MNPs with the sizes of about 10 nm in diameter were obtained, while protein -loaded MNCs have diameters of around 300 to 500 nm. Moreover, protein loading content were analyzed using UV-visible spectrometry, and cytotoxic effects of MNCs comparing with PLGA particles were tested with macrophage cell line by MTT assay. A large size of MNCs showed greatly enhanced cellular uptake of macrophages, especially under external magnetic field. Moreover, MNCs promoted bone marrow-derived dendritic cell (BM-DC) maturation by up regulating MHC II, CD80 and CD86 expression.

These results indicated that MNCs carrying proteins can stimulate immune cells with low cytotoxicity and could be a potential platform for magnetically-guided antigen delivery systems in vaccination.

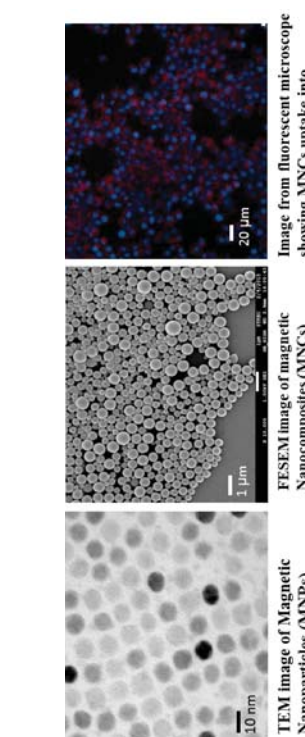
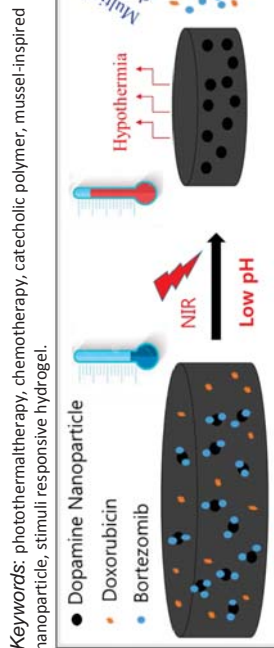


Image from fluorescent microscope showing MNCs uptake into macrophage cells



**Keywords:** photothermal therapy, chemotherapy, catecholic polymer, mussel-inspired nanoparticle, stimuli responsive hydrogel.

## pH/NIR light-Controlled Multi-Drug Release via a Mussel-Inspired Nanocomposite Hydrogel for Chemo-Photothermal Cancer Therapy

Melisa Samarakkulahaj, Amin GhavamiNejad, Chan Hee Park and Cheol Sang Kim

<sup>1</sup>Department of Bionanosystem Engineering Graduate School, Chonbuk National University, Jeonju City, Republic of Korea.

This study reports an intelligent composite hydrogel with both pH-dependent drug release in a cancer environment and heat generation based on the NIR laser exposure for the combined application of hypothermia and chemotherapy. For the first time in the literature, Dopamine nanoparticle (DP) was incorporated as a highly effective photothermal agent as well as anticancer drug (Bortezomib (BTZ)) carrier inside a stimuli responsive pNIPAAm-co-pAAm hydrogel. In order to increase the synergistic effect by dual drug delivery, Doxorubicin (DOXO) loaded pNIPAAm-co-pAAm/DP-BTZ hydrogel were also prepared by equilibrium partitioning technique. As prepared composite hydrogel exhibited an efficient heating ability under NIR laser exposure. The swelling-deswelling of the nanocomposite hydrogel as well as releasing DOXO can be controlled remotely by a NIR laser exposure or non-exposure. Furthermore, a properly sustained release of BTZ can be achieved at pH 5.0 due to the dissociation between catechol groups of DP and boronic acid functionality of BTZ. In vitro studies demonstrated that our mussel inspired nanocomposite with excellent heating property and controllable Multi-Drug release can be considered as a potential material for cancer therapy due to the synergistic effect of hypothermia and chemotherapy.

## Synthesis of $Mn_xGa_{1-x}Fe_2O_4$ magnetic nanoparticles by thermal decomposition method for medical diagnosis applications

J. Sánchez\*, L. E. De-León-Prado, D.A. Cortés-Hernández, J. C. Escobedo-Bocardo, P. Y. Reyes-Rodríguez, R. A. Jasso-Terán, J. M. Almanza-Robles

Cinvestav-Unidad Saltillo, Industria Metalúrgica 1062, Parque Industrial Saltillo-Ramos Arizpe, Ramos Arizpe, Coahuila, México, CP 25900. \*E-Mail: haxiersanchez@hotmail.com

Magnetic nanoparticles (MNPs) with a superparamagnetic behavior are one of the most investigated materials for their potential use in biomedical areas such as thermoseeds for cancer treatment by hyperthermia method and as contrast agents for medical diagnosis by magnetic resonance imaging (MRI) technique. The nanoparticles possess a spinel structure with  $M^{2+}Fe^{3+}_2O_3$  as a general formula ( $M = Fe, Mn, Ni, Co, Zn, Mg$ ) and lower cytotoxicity values in comparison to those of gadolinium-based paramagnetic molecules. These characteristics allow the synthesis of MNPs with high relaxation time which can be safe for obtaining images for medical diagnosis.

In this work, the synthesis of  $Mn_xGa_{1-x}Fe_2O_4$  ( $x = 0-1$ ) nanosized particles by thermal decomposition method, using tetraethylene glycol (TEG) as a reaction medium, has been performed. The crystalline structure of the inverse spinel obtained in all the cases was identified by X-Ray Diffraction (XRD). Vibration Sample Magnetometry (VSM) was used to evaluate saturation magnetization ( $28.4 - 50.5$  emu/g) and to demonstrate the superparamagnetic behavior (coercive field  $< 13$  Oe), which was due to the  $Mn^{2+}$  ions incorporation into the  $Fe_{1.4}Ga_{0.6}O_4$  structure. Transmission electron microscopy, Energy dispersive spectroscopy (TEM-EDS), Fourier transformed-infrared spectroscopy (FT-IR) and X-ray photoelectron spectroscopy (XPS) were used to characterize the obtained MNPs. These particles showed a near spherical morphology, an average particle size of  $5.6 \pm 1.5$  nm and a TEG coating layer on their surface. Both chemical composition and Fe<sup>c</sup>, Ga and Mn oxidation states of the magnetic core for a selected samples were also determined.

In all the cases MNPs showed no response when submitted to an alternating magnetic field (AMF, 10.2 kA/m, 354 kHz) using magnetic induction tests. These results suggest that the synthesized nanoparticles can be potentially used as contrast agents for medical diagnosis applications by MRI.

## Ni nanorods interact with human cells and induce changes in intracellular signalling and gene expression

Ann-Kathrin Schmidt<sup>1</sup>, Christine Gräfe<sup>1</sup>, Florian Krämer<sup>2</sup>, Andreas Tschope<sup>2</sup>, Rainer Birninger<sup>2</sup>, Andreas Hochhaus<sup>1</sup>, Joachim H. Clement<sup>1,3</sup>

<sup>1</sup>Department of Hematology and Oncology, Jena University Hospital, Jena, Germany

<sup>2</sup>Experimentalphysik, Universität des Saarlandes, Saarbrücken, Germany

<sup>3</sup>Jena Center for Soft Matter (JCSM), Friedrich-Schiller-University Jena, Jena, Germany

Magnetic nanomaterials are of great interest for biomedical applications. Spherical iron oxide nanoparticles are most widely used because of their extensively tested biocompatibility. In contrast heavy metals, e.g. nickel (Ni) or cobalt are considered to be toxic. Because of their superior magnetic properties and the perspective to safely shield heavy metal-based materials we investigate the effects of Ni nanorods on human cells. The applied Ni nanorods with (L)  $\approx 250$  nm and (D)  $\approx 22$  nm are ferromagnetic single domain particles and show distinct optical anisotropy. Ni nanorods were synthesized by the AAO-template method and for colloidal stability they were coated with a 4 nm polyvinylpyrrolidone (PVP) layer. A portion of the PVP-covered particles was coated with silica or gelatine. Human brain microvascular endothelial cells (HBMEC) were used for nanorod-cell interaction studies. The cell line is a well-established *in vitro* model of the blood-brain barrier. Short-term biocompatibility was tested with the PrestoBlue-Assay (Invitrogen, Germany) and long-term studies were performed with real-time cell analysis (RTCA, ACEA Biosciences, USA). Nanorod-cell interactions were monitored by laser-scanning microscopy (RTCA, ACEA Biosciences, USA). Nanorod intracellular changes on the protein level were analysed by immunoblotting and on gene expression by quantitative real-time PCR. Endothelial cells interact with Ni nanorods and internalize the particles (Figure 1). Ni nanorod effects on HBMEC are modulated by the particular functionalization. Cell vitality is only moderately affected within the first 24h independent of the coating and the concentration of the Ni nanorods. Up to 96% higher concentrations of Ni nanorods (25  $\mu$ g/cm<sup>2</sup>) cause a clear reduction of cell vitality (vitality silica coated > gelatine coated > PVP-coated). Therefore, we studied the role of PVP-coated Ni nanorods on intracellular processes. The activity of the stress- and inflammation-related Akt and p38-pathway are enhanced up to 2.9-fold upon a 3h-incubation. This causes changes in the expression of target genes. For example, the expression of the immediate early gene *c-fos* (up to 11-fold) and the inflammation-induced gene *pfgs2* (up to 3-fold) is elevated. Ni nanorods affect cell vitality and activate stress- and inflammation associated pathways in a time- and concentration-dependent manner. An adequate coating of Ni nanorods might allow the use of their excellent magnetic and shape-related properties for biomedical applications.

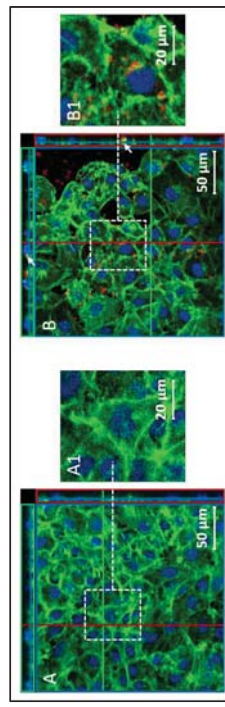


Figure 1: Localisation of internalised silica-rhodamine B-coated Ni nanorods into HBMEC after 24 hours of exposure.

This work was supported by the DFG high priority program 1681 (CL202/3-1, TS62/4-1).

## Nanoparticle Ensembles: a Hybrid Molecular and Spin Dynamics Approach

C. SCHRÖDER and L. TEICH

Bielefeld Institute for Applied Materials Research, Bielefeld University of Applied Sciences, Interaktion 1,  
33619 Bielefeld, Germany

### ABSTRACT

Ensembles of magnetic nanoparticles dispersed in fluids or gels have recently attracted much attention. Such systems allow to study basic collective phenomena [1] but also show promising features for the development of novel magnetoresistive sensor devices [2] or biomedical applications [3]. In order to understand the microscopic magneto-dynamics of such systems we have developed a hybrid molecular and spin dynamics approach which allows us to simulate the trajectories and magnetic moment orientations of the interacting nanoparticles in the fluid [4]. Using this approach we have investigated the self-organizing magneto-dynamics of various nanoparticle ensembles (see fig. 1) and will discuss the results.

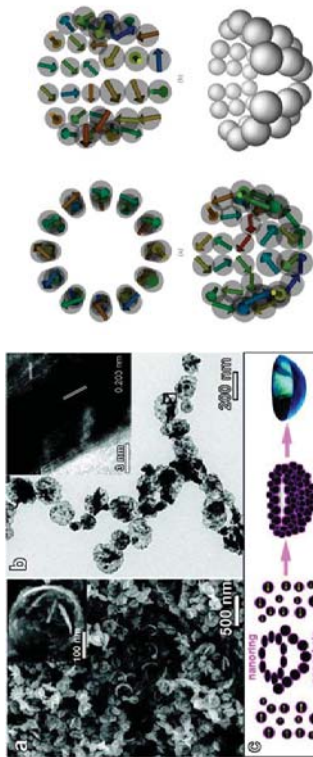


Fig. 1: Left panel: (a) SEM image of Ni bowls. The inset shows a typical bowl. (b) TEM image of Ni bowls with HRTEM image inserted corresponding to the marked frame in (b). (c) Illustration for the growth mechanism of Ni bowls [5]. Right panel: Hybrid molecular and spin dynamics simulation results of a tubular configuration that consists of three rings each containing 12 cobalt particles similar to the configuration of five rings that is shown in left panel: (a) front view of the initial configuration with randomly oriented magnetic moments of the particles; (b) tilted view of the initial configuration; (c) final, bowl-shaped configuration and (d) representation of the final configuration with hidden magnetic moment orientations.

- [1] P. Tierno, *Phys. Rev. Lett.* **116**, 038303 (2016)
- [2] L. Teich, D. Kappe, T. Rempel, J. Meyer, C. Schröder, A. Hüttner, *Sensors* **2015**, 9251
- [3] E. Duguet, S. Vasseur, S. Monnet, J.-M. Devoselle, *Nanomedicine* **1** (2), 157 (2006)
- [4] L. Teich, C. Schröder, *Sensors* **2015**, 28826
- [5] W. Zhou, L. Lin, D. Zhao, L. Guo, *J. Am. Chem. Soc.* **133** 8389 (2011)

Kun-Yau Shih<sup>1\*</sup>, Cheng-Yu Dai<sup>1</sup>, Chun-Rong Lin<sup>2</sup>, Yaw-Teng Tseng<sup>2</sup>

<sup>1</sup> Department of Applied Chemistry, National Pingtung University, Pingtung 90003, Taiwan  
<sup>2</sup> Department of Applied Physics, National Pingtung University, Pingtung 90003, Taiwan

E-mail: hello2sky@gmail.com

In this study, a green and rapid process of silver/magnetite/graphene composites were synthesized by microwave assisted method and were utilized for antibacterial application. The crystal structure and properties of composites were characterized by X-ray diffractions (XRD), Fourier transform infrared spectroscopy (FTIR) and Raman spectroscopy. The antibacterial activity of Fe<sub>3</sub>O<sub>4</sub>/RGO and Ag/Fe<sub>3</sub>O<sub>4</sub>/RGO composites against *E. coli* on nutrient agar plates were also investigated. The XRD results showed that GO was effectively reduced into reduced graphene oxide. The RGO pattern also indicated the formation of Fe<sub>3</sub>O<sub>4</sub> and Ag/Fe<sub>3</sub>O<sub>4</sub> nanoparticles on the RGO matrix. The FT-IR spectra showed the stretching vibration because of the interactions of Fe–O bond. We also found that the increase of Ag in composites, the Raman intensities  $I_0/I_G$  of composites increased obviously may attributed to the forming the smaller sp<sup>2</sup>-domains during the reduction process. The antibacterial activities of commercial nano-Ag, Fe<sub>3</sub>O<sub>4</sub>/RGO and Ag/Fe<sub>3</sub>O<sub>4</sub>/RGO composites against *E. coli* were assessed by colony counting method from the agar plates. The results showed that antibacterial activities follows the order as Ag/Fe<sub>3</sub>O<sub>4</sub>/RGO > commercial nano-Ag > Fe<sub>3</sub>O<sub>4</sub>/RGO under the 1.8 mg/mL dispersion concentration. We also found that antibacterial activities are concentration and time dependent. The cell viability were showed that increasing the concentration of the Ag/Fe<sub>3</sub>O<sub>4</sub>/RGO composites, the higher antibacterial activities. The bacterial inactivation happens in ten mins for Ag/Fe<sub>3</sub>O<sub>4</sub>/RGO composite. The better antibacterial activities of graphene-based composite materials may increase the clinical application.

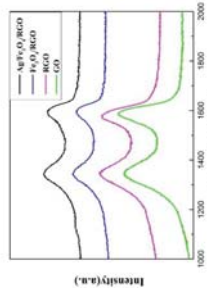


Fig. 2 Raman spectra of GO, RGO, Fe<sub>3</sub>O<sub>4</sub>/RGO, Ag/Fe<sub>3</sub>O<sub>4</sub>/RGO composites.

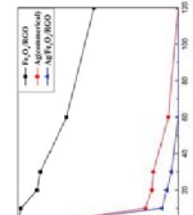


Fig. 3 Photographs of inhibitory effects of blank, Commercial Ag, Fe<sub>3</sub>O<sub>4</sub>/RGO, Ag/Fe<sub>3</sub>O<sub>4</sub>/RGO composites.



Fig. 4 Cell viability of Commercial Ag, Fe<sub>3</sub>O<sub>4</sub>/RGO, Ag/Fe<sub>3</sub>O<sub>4</sub>/RGO composites.

## Synthesis and characterization of Iron oxide/Reduced graphene oxide composites

Kun-Yau Shih<sup>\*</sup>, Zhen-Yuan Han<sup>1</sup>, Arseniy O. Baskakov<sup>2</sup>, Sergey S. Starchikov<sup>2</sup>, Igor S. Lyubutin<sup>2</sup>, Chun-Rong Lin<sup>3</sup>, Yaw-Teng Tseng<sup>3</sup>

<sup>1</sup>Department of Applied Chemistry, National Pingtung University, Pingtung 90003, Taiwan

<sup>2</sup>Shubnikov Institute of Crystallography, Russian Academy of Sciences, Moscow 119333, Russia

<sup>3</sup>Department of Applied Physics, National Pingtung University, Pingtung 90003, Taiwan  
E-mail: hello2sky@gmail.com

Iron oxide nanoparticles (IONPs)/reduced graphene oxide (RGO) composites were prepared via reflux and heat treatment process. The X-ray diffractions (XRD), Raman spectroscopy, Fourier transform infrared spectroscopy (FTIR), and Mössbauer spectroscopy were used for the sample characterization. XRD data shows that the crystal structure of the iron oxide NPs is close to cubic spinel-type (space group  $Fd\bar{3}m$ ). The results showed that the mean crystallite sizes of iron oxide/RGO composites between 16–18 nm and were not tended to aggregate with increasing temperature from 600–800°C, may attribute the RGO avoid the strong magnetic dipole-dipole attractions between iron oxide nanoparticles. The FT-IR spectra showed the stretching vibration because of the interactions of Fe–O bond. We also found that the increase of heat treatment temperature, the Raman intensities  $I_{D}/I_G$  of composites increased obviously may indicate the remove of the oxygen-containing groups in reduced graphene oxide. Mössbauer spectra of all samples were recorded at room temperatures (RT) and 90K. We found that each spectrum can be fit to one paramagnetic doublet and a distribution of magnetic sextets (Table 1). The most important result is the absence (in all samples) of the isomer shift  $\delta$  with the values corresponding to  $\text{Fe}^{2+}$  ( $\delta$  ~0.8–0.9 mm/s) or to  $\text{Fe}^{2.5+}$  ( $\delta$  ~0.6–0.7 mm/s), which are expected for bulk magnetite ( $\text{Fe}_3\text{O}_4$ ). Instead, there are two high-intensive components corresponding to  $\text{Fe}^{3+}$  ( $\delta$  ~0.3–0.4 mm/s) both for RT and 90 K. The parameters of the paramagnetic doublet component also correspond to the  $\text{Fe}^{3+}$  iron state. Moreover, the Raman spectra show a big plateau that can be related to maghemite ( $\gamma\text{-Fe}_2\text{O}_3$ ) NPs. Based on these considerations, we suppose that the  $\gamma\text{-Fe}_2\text{O}_3$  phase is the dominant phase in the composites. The influence of graphene on the valence state of iron oxide should be taken into account.

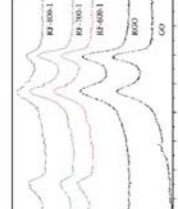


Fig. 1 X-Ray diffraction patterns of GO, RGO, IONPs/RGO.

Fig. 1 Raman spectra of GO/RGO, IONPs/RGO, and IONPs/GO. Table 1 The hyperfine parameters of IONPs/RGO composite powder. H1 – magnetic hyperfine field at Fe nuclei related to the biggest peak in the field distribution graph; G0/G1 – magnetic hyperfine field related to the second biggest peak in the field distribution graph; G2/G3 – magnetic hyperfine field corresponding to H1/2, (G1/G3) = (H1/H2); L1/L2 – quasi-angle that corresponds to H1/2, (L1/L2) = (G1/G3); F1/F2 – line width ratio; S1/S2 – (G1/G3) × 100%.

Sample/component	H1	H2	G1	G2	L1	L2	F1	F2	S1	S2	S1/S2
RF-600, sextet, RT	-0.481	-0.444	0.32	0.32	0	-0.010	0.55	0.55	20%	19%	5/5
RF-600, doublet, RT	-0.517	-0.489	0.44	0.4	0.35	-0.005	-0.03	0.51	0.51	0.51	7%
RF-600, sextet, 90K	-0.480	-0.444	0.44	0.44	-0.015	-0.015	0.51	0.51	0.1%	0.1%	1/1
RF-600, doublet, 90K	-0.485	-0.452	0.44	0.44	-0.02	-0.02	0.51	0.51	0.1%	0.1%	1/1
RF-700, sextet, RT	-0.486	-0.447	0.32	0.31	0.015	-0.027	0.54	0.54	30%	17%	1.775
RF-700, doublet, RT	-0.515	-0.483	0.43	0.4	-0.005	-0.03	0.53	0.53	0.1%	0.1%	1/1
RF-700, sextet, 90K	-0.485	-0.452	0.43	0.43	-0.02	-0.02	0.54	0.54	0.1%	0.1%	1/1
RF-700, doublet, 90K	-0.486	-0.452	0.43	0.43	-0.02	-0.02	0.54	0.54	0.1%	0.1%	1/1
RF-800, sextet, RT	-0.520	-0.497	0.41	0.41	-0.02	-0.037	0.52	0.52	0.0%	0.0%	1/1
RF-800, doublet, 90K	-0.520	-0.497	0.41	0.41	-0.02	-0.037	0.52	0.52	0.0%	0.0%	1/1

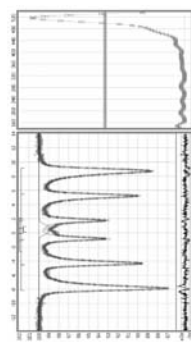


Fig. 3 Selected 90K Mössbauer spectra of IONPs/RGO composite powder synthesized at 700°C.

## Protein Corona Nanoparticles Increase Cancer Cell Proliferation

**Soukup, D.<sup>1</sup>**, Dobson, J.<sup>2</sup> and Telling, N. D.<sup>1</sup>

<sup>1</sup>Institute for Science and Technology in Medicine, Keele University, Stoke-on-Trent, Staffs ST4 7QB, UK  
<sup>2</sup>J.C. Crayton Pruitt Family Department of Biomedical Engineering, University of Florida, Gainesville, FL, USA

e-mail: d.soukup@keele.ac.uk

### Abstract

Protein corona on nanoparticles has been widely studied. However, little is known about its effect on cellular functions. In this study, we investigated two types of nanoparticles with protein corona (360 nm and 112 nm hydrodynamic size) with respect to proliferation and metabolic activity. This difference allows us to tune the amount of nanoparticles and therefore protein that goes into cells. Our results indicate that both nanoparticle formulations (560 nm and 112 nm) significantly increase cancer cell proliferation and metabolic activity. *In vitro* 560 nm clusters showed much higher uptake of nanoparticles with protein corona which lead to a higher proliferation rate in comparison with 112 nm clusters that showed lower uptake. In addition, we cultured cells in media with no source of amino acids or proteins. After 24 h, the number of cells slightly decreased in control, the number of cells exposed to nanoparticles with protein corona slightly increased while nanoparticles without it showed a strong cytotoxic effect. Therefore, our results indicate that protein corona is removed from the surface of nanoparticles inside cells [1] and proteolytic degradation occurs. Subsequently, amino acids are metabolised to support cancer cell proliferation.

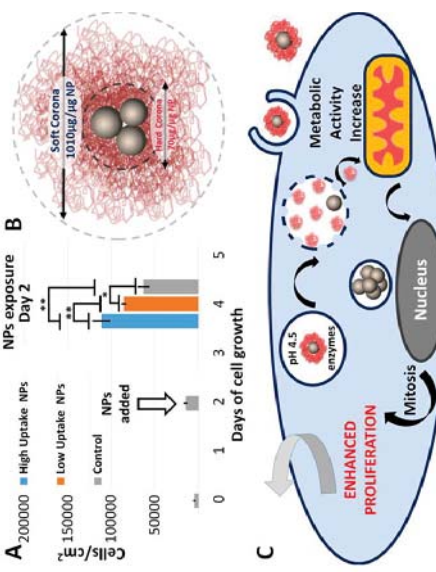


Fig. 1. (A) Cell population density of human osteoblast-like MG-63 cells on day 2. (B) Protein quantification in soft & hard corona. (C) Schematic of proposed mechanism of action.

**[II] In Situ Measurement of Magnetization Relaxation of Internalized Nanoparticles in Live Cells.**  
Daihur Soukup, Sandhya Moise, Eva Cespedes, Jon Dobson, and Neil D. Telling. *ACS Nano* 2015 **9** (1), 23–240

## The Effect of Inter-Particle Interactions on SAR values and Magnetic Response of Biogenic Zn-doped Nanoparticles

D. Soukup<sup>1</sup>, S. Moise<sup>1</sup>, E. Céspedes<sup>1,2</sup>, J. Dobson<sup>3</sup> and N. D. Telling<sup>1</sup>

<sup>1</sup>Institute for Science and Technology in Medicine, Keele University, Stoke-on-Trent, ST4 7QB, UK

<sup>2</sup>IMDEA NANOCiENCIA, C/ Fuenlabrada, 9 Ciudad Universitaria de Cantoblanco, 28049 Madrid, SPAIN

<sup>3</sup>J. Crayton Pruitt Family Department of Biomedical Engineering, University of Florida, Gainesville, Florida 32611, USA

e-mail: d.soukup@keele.ac.uk

### Abstract

The potential use of nanoparticles in medicine is an example of how research at the interface between material and biological sciences can bring benefits and more complete understanding to both fields of endeavour. For successful cell-based applications of magnetic nanoparticles (MNP), it is important to be aware of any change in MNP properties throughout their whole life cycle. It may occur at each step due to the development of the protein corona, clustering, changes in magnetic response or degradation of MNP. We address all of the above using a novel application of AC-susceptometry to monitor the stability and follow the *in situ* magnetic response of magnetic nanoparticles, from water-based suspensions to cell culture media, following their cellular internalisation and subsequent release by freeze-thaw lysis [1]. The results demonstrate that cellular internalisation can alter magnetisation relaxation, which has significant implications for designing suitable nanoparticles for intracellular hyperthermia applications. However, MNP inside cells are typically stored as large clusters in endosomes therefore the effect of inter-particle interactions cannot be neglected. Thus, we also investigated the effect of inter-particle interactions on heating efficacy of MNP. Two formulations of three types of Zn doped magnetic (Zn10%, Zn5%, Zn10%) were tested. Small clusters MNP ( $d_h = 44$  nm) and large clusters ( $d_h = 560$  nm). The results indicate that aggregation of MNP can significantly reduce the heating efficacy of MNPs – implication for intracellular heating. In addition, we also observed changes in the magnetic response using AC-susceptometry.

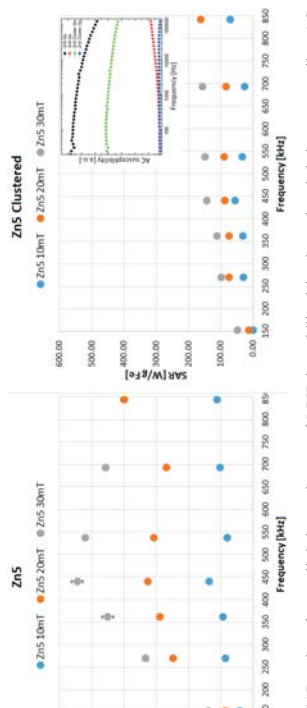


Fig. 1. SAR values for small & large clusters of MNP immobilized in glycerol and their corresponding AC-susceptibility curves

## The Effect of Protein Coated *In-Situ* Formed Aggregates of Iron Oxide Nanoparticles on Cell-Nanoparticle Interactions

D. Soukup<sup>1</sup>, J. Dobson<sup>1,2</sup> and N. D. Telling<sup>1</sup>

<sup>1</sup>Institute for Science and Technology in Medicine, Keele University, Stoke-on-Trent, ST4 7QB, UK

<sup>2</sup>J. Crayton Pruitt Family Department of Biomedical Engineering, University of Florida, Gainesville, Florida 32611, USA

e-mail: d.soukup@keele.ac.uk

Aggregation of nanoparticles in physiological solutions seems inevitable for all nanoparticle types, however, very little is known about how this can affect cellular response. Aggregated Large Clusters (560 nm) prepared by naturally occurring precipitation of citric acid coated magnetic nanoparticles (MNPs) in cell media and un-aggregated Small Clusters (112 nm), both with protein corona. We used the AC-susceptometry to non-invasively monitor and quantify the uptake of MNPs *in vitro* in live cells. The uptake of Large Clusters was three times higher compared to Small Clusters. The difference can be attributed to either sedimentation or different mechanism of endocytosis – difficult to separate. Two cell culture configurations were tested to identify the dominant factor. Inverted cells at the top of the well and conventionally cultured cells at the bottom. For the top orientation, contrary to bottom orientation, Small Clusters showed a much higher uptake compared to Large Clusters. Therefore, our results indicate that the uptake strongly depends on nanoparticle-cell interactions which can be altered by aggregation and subsequent sedimentation – implications on *in vitro* uptake and cytotoxicity studies.

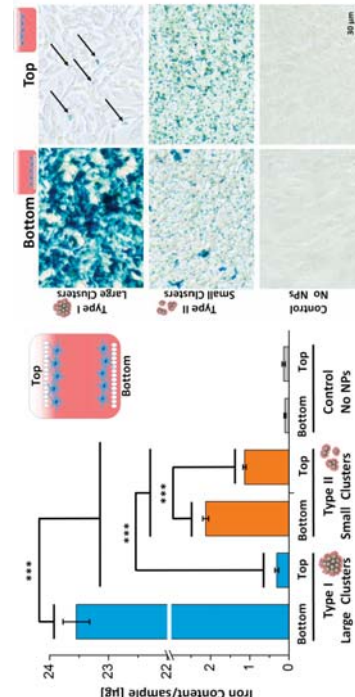


Fig. 1. (Left) Uptake quantification comparison between Large Clusters and Small Clusters in cells cultured at two different configurations for 2 days (conventionally at the Bottom and inverted at the Top). Data presented as mean  $\pm$  S.E.M.  $n = 4$  independent samples (\*\* $p < 0.001$ ). (Right) Bright field images of cells with internalized nanoparticles cultured at two different configurations (Bottom and Top), iron oxide nanoparticles stained with Prussian blue for iron.

# Temperature and AC Field Dependence of Magnetic Susceptibility and its use in Magnetic Hyperthermia

P. Southern<sup>1,2</sup>, F.-Y. Lin<sup>2</sup>, S. Hattersley<sup>1</sup>, Q. A. Parkhurst<sup>2</sup>

<sup>1</sup>Resonant Circuits Limited, 21 Albemarle Street, London W1S 4BS, United Kingdom  
<sup>2</sup>UCL Healthcare Biomagnetics Laboratory, 21 Albemarle Street, London W1S 4BS, United Kingdom  
E-mail: psouther@resonantcircuits.com

Over the past few decades, magnetic nanoparticles (MNPs) have been applied in a variety of medical research activities, such as magnetic hyperthermia and drug delivery. This study examines the magnetic susceptibility of MNPs, and its potential use as a metric to determine, non-invasively, the temperature of magnetic particles during hyperthermia by tracking the change of susceptibility (inductance) as a function of the resonant frequency of a magnetic hyperthermia system. For multi-domain ferrromagnets, the correlation between the temperature and susceptibility is described by Hopkinson phenomenon. This effect indicates an increase in susceptibility is associated with an increase in temperature, because the heating facilitates the rotation of the domain wall, which leads to a higher susceptibility. The susceptibility finally peaks at the Curie temperature, and rapidly becomes zero as the material transitions to a paramagnetic state. However, for superparamagnetic materials even though they are widely applied in clinical applications, the relationship between susceptibility and temperature is less known.

Here we present how the susceptibility of MNPs vary at different temperatures and magnetic field strengths. Furthermore, we present how these measurements can be used to determine the temperature of the nanoparticles during a magnetic hyperthermia measurement. At low fields for AC hyperthermia and DC SQUID susceptibility measurements, the change in susceptibility over 280–400K increases by approximately 25% (figure 1 – red open circles) and can be highlighted by a noticeable change in resonant frequency of the hyperthermia system –  $5^\circ\text{C}$  temperature rise per 1 Hz change in resonance (figure 2). At higher field strengths (125 Oe), the susceptibility change is small (figure 1 – purple open diamonds) with a 4x higher temperature change to see the same 1 Hz change in resonance (figure 2). In both cases we demonstrate the ability to determine the temperature of the MNPs by using a measurement of the change in resonant frequency of a hyperthermia system.

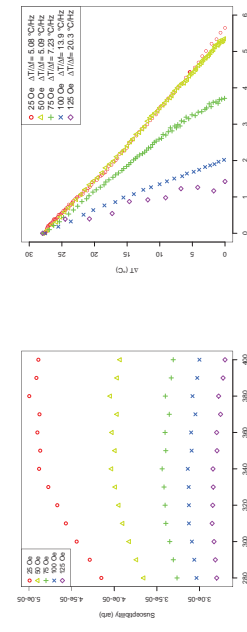


Fig 1 (left): The correlation between susceptibility and temperature as a function of DC field.  
Fig 2 (right): The change in resonant frequency and temperature as a function of AC field.

# Acceleration of superparamagnetic particles due to an optimized magnetic field to improve Biomagnetic Separation

R. Stange<sup>1</sup>, F. Lenk<sup>2</sup>, T. Bley<sup>1</sup>, K. Eckert<sup>2</sup>, E. Boschke<sup>1</sup>

<sup>1</sup>Institute of Food Technology and Bioprocess Engineering, TU Dresden, Dresden, Germany

<sup>2</sup>Institute of Fluid Mechanics, TU Dresden, Dresden, Germany

In context of Biomagnetic Separation (BMS) using superparamagnetic particles (beads) high capture efficiency requires an efficient mixing of beads and cells. Due to the laminar flow with low Reynolds number and the very low characteristic diffusion time, effective convective mixing concepts are required.

To improve the BMS we developed a process using variable magnetic fields to accelerate the beads in a sample container [1]. Therefore, an experimental setup has been equipped with three electromagnets. We intended to induce a double circular stream and a high relative velocity of the beads to the cells in a defined process of charging the magnets [2]. Based on the simulations of the magnetic field in our setup these effects could be shown and a model was developed. It includes the force field acting on the beads. To evaluate this model beads were observed in a microchamber under microscope equipped with a long working distance objective. Thereby the movement of the beads in the field gradient force given by the magnetic field of the experimental setup was confirmed (Fig. 1).

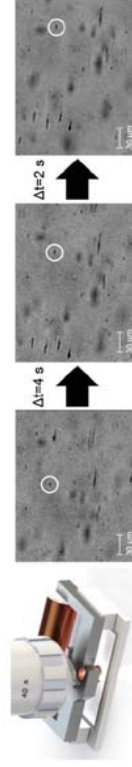


Figure 1: Motion of beads (1  $\mu\text{m}$  in diameter) observed in a microchamber under microscope equipped with a long working distance objective during the ON-phase of one of the magnet planes  
In addition CFD simulations were performed in order to characterize the influence of the bead movement on the fluid dynamics and to show the double circular bead stream.

[1] Stange, R. et al. (2013) Vorrichtung sowie Verfahren zur Steigerung der Anbindungsseffizienz von zur Bindung befähigten Zielstrukturen, DE 10 2013 009 773.8.

[2] Stange, R. et al. (2015) A new method for mixing of suspended superparamagnetic beads using variable magnetic fields, Engineering in Life Sciences, vol. 15, 727-732.

## Interpreting static and dynamic magnetization behavior of magnetic nanoparticles in terms of magnetic moment and energies

Uwe Steinhoff, Oliver Posth, Frank Wiekhorst

Fysikalisch-Technische Bundesanstalt, Abbestrasse 2-12, 10587 Berlin, Germany. ([uwe.steinhoff@ptb.de](mailto:uwe.steinhoff@ptb.de))

The measurement of the effective magnetization  $M(H)$  of a sample of magnetic nanoparticles (MNP) in dependence of an external magnetic field  $H$  provides important characteristics of magnetic nanoparticulate material. In many cases, data are interpreted using a model of spherical MNPs with a lognormal (or otherwise shaped) size distribution and sometimes including the anisotropy of the individual particles [1]. In addition, assumptions on the structure of the iron oxide core (magnetite, maghemite, hematite, wustite, etc.) and on the homogeneity of magnetic ordering in the magnetic core (single core, multi core MNP) are made and quantitative model parameters are then extracted from  $M(H)$  measurements.

Additionally, magnetic interaction between individual crystallites inside a multi-core MNP or between different MNPs in the model may be included as well, but more *a priori* assumptions are needed to achieve reasonable quantitative estimates for unknown model parameters such as MNP size distribution. Thus, discrepancies between MNP size estimates are found if extracting values especially from different measurement techniques like quasistatic  $M(H)$  measurements, dynamic magnetic measurement techniques like magnetorelaxometry and AC susceptibility, or from structural imaging or scattering techniques like TEM or SAXS [2]. These discrepancies are then resolved by introducing a ‘‘magnetic size distribution’’ which differs from the geometrical size distribution.

However, it is important to keep in mind that this magnetic particle size is a projection of an effective magnetic behavior often on a oversimplified and inadequate model assuming spherical particles. It has no structural geometrical correlate, but is completely defined by energy barriers and magnetic dynamics of the system.

With our contribution we want to put into more perspective the modeling of magnetic data merely using magnetic moment and magnetic energies (anisotropy, interaction, rotational in liquids). We show, it is not necessary to introduce model parameters that are not susceptible to observation and often leading to misinterpretation.

This work is supported by EU FP7 project NanoMag (grant no. 604448).

Model parameter	Symbol	Geometry based formulation
Anisotropy energy per particle	$E_a$	$KV$
Magnetic moment per particle	$\mu_p$	$M_V$
Field dependent moment of an ensemble	$\mu_p(H) = \sum_i \mu_{i_0} \left( \coth \left( \frac{\mu_i \mu_{i_0}}{k_b T} \frac{H}{\mu_i \mu_{i_0}} \right) - \frac{k_b T}{\mu_i \mu_{i_0}} \frac{1}{H} \right)$	
Néel relaxation time	$\tau_N = \tau_0 \exp \left( \frac{E_a}{k_b T} \right)$	
In liquid suspension		
Angular momentum per particle	$L$	$\eta V_h$
Rotational energy per particle	$E_n = L\omega$	$\omega = \text{angular velocity}$
Brownian relaxation time	$\tau_B = \frac{3L}{k_b T}$	

[1] Chantrell, R. W., Popplewell, J. and Charles, S. W. (1978). Measurements of particle size distribution parameters in ferrofluids. *Magnetics, IEEE Transactions on*, 14(5), 975-977.

[2] Eberbeck, D., Wiekhorst, F., Wagner, S., and Trahms, L. (2011). How the size distribution of magnetic nanoparticles determines their magnetic particle imaging performance. *Applied physics letters*, 98(18), 182502.

## Magnetoliposomes nanocarriers for drug delivery applications: synthesis and characterization

Rares Stiufluc<sup>1,2</sup>, Cristian Iacovita<sup>1</sup>, Stefan Nitica<sup>1</sup>, Gabriela Stiufluc<sup>2,3</sup> and Constantin Mihai Lucaciu<sup>1,2</sup>

1) “Iuliu Hatieganu” University of Medicine and Pharmacy, Cluj-Napoca, Romania

2) “Octavian Fodor” Regional Institute of Gastroenterology-Hepatology, Cluj-Napoca, Romania

3) “Babeș-Bolyai” University, Faculty of Physics, Cluj-Napoca, Romania

The design of hybrid multifunctional nanoobjects having a liposomal core and possessing magnetic properties emerged as a very hot research topic for drug delivery and controlled drug release applications. The main idea of this concept is to combine the drug delivery properties of the liposomes with the magnetic properties of SPION nanoparticles for the creation of multifunctional nanoobjects capable of delivering and releasing therapeutic agents in a very controllable manner.

The here reported magnetoliposomes have been synthesized using the dry film hydration method. Briefly, neutral phospholipids have been mixed with hydrophobic superparamagnetic  $\text{Fe}_3\text{O}_4$  nanoparticles (SPIONs) produced by thermal decomposition of magnetic precursors. The organic solvent of the lipid-SPIONs mixture has been removed using a rotary evaporator. The as obtained lipid film has been hydrated with Tris-buffered saline solution (TBS) containing hydrophilic chemotherapeutic agents. The multilamellar magnetoliposomes have been tested. The drug release capacity upon interaction with an external alternating magnetic field of different amplitudes and frequencies has also been evaluated.

The magnetoliposomes have been characterized by UV-VIS absorption spectroscopy,

Dynamic Light Scattering (DLS), Zeta Potential Measurements and Transmission Electron

Microscopy (TEM). Their magnetic induced hyperthermia properties have been assessed in external magnetic fields with intensities ranging between 5 and 60 kA/m and frequencies between 100-400 kHz. The TEM images confirmed the intercalation of hydrophobic SPIONs with an average diameter of 7 nanometers into liposomal lipid bilayer membrane. The toxicity of the nanohybrids have been assessed in-vitro on different cell lines using the standard MTT assay.

This research was supported by CNCSIS-UEFISCDI, projects no. PN-II-ID-PCE-2011-3-0954 and PN-II-RU-TE-2014-4-1770

## Gemcitabine Loaded Magnetic Nanoparticles for Magnetically Triggered Thermo-Chemo Therapy

S. Latha<sup>1</sup>, C. Prabu<sup>1</sup>, P. Selvamani<sup>1</sup>, A. Weidner<sup>2</sup>, S. Dutz<sup>2</sup>

<sup>1</sup> Department of Pharmaceutical Technology & Centre for Excellence in Nanobio Translational Research, Anna University, Bharathidasan Institute of Technology Campus, Thiruchirappalli, Tamil Nadu, India  
<sup>2</sup> Institute of Biomedical Engineering and Informatics (BMTI), Technische Universität Ilmenau, Germany

E-mail: silvio.dutz@tu-ilmenau.de, lathasuba2010@gmail.com

We present the results of a series of experiments performed with an objective to develop drug loaded iron oxide magnetic nanoparticles (MNP) for possible use as magnetically triggered drug release system for efficient cancer targeting therapy. MNP were prepared by means of alkaline co-precipitation. A 1 M NaHCO<sub>3</sub> solution was slowly added under permanent stirring to a 0.625 M FeCl<sub>2</sub>/FeCl<sub>3</sub> solution with different drop times to obtain different particle sizes. For the production of anchor layers for drug loading of the MNP, the particles were coated with biocompatible coating materials carboxymethyl dextran, dextran, and amino dextran. Obtained particles were characterized by means of TEM and X-ray diffraction (size), vibrating sample magnetometry (magnetic properties and concentration), and magnetic field calorimetry (heating performance). MNP with the best heating performance (with the 3 different coatings) under our field conditions of 210 kHz and 20 A/m were used for further drug loading/release experiments.

For this, Gemcitabine (an antimetabolite anti-cancer drug) was used in this study. Drug loading was done by using 100 mg of drug dissolved in water added to 1 g of either surface coated MNP under permanent stirring at 37°C for 8 hours leading to an adhesive binding of the drug to the particles surface. The loading efficiency was investigated by means of UV/VIS and maximum amount of drug loading was observed with amino dextran magnetic particles (26% of applied Gemcitabine). Only negligible amounts of drug loading were observed for other coatings. FT-IR spectral analysis confirmed, no significant drug excipient interactions exist in the formulation as all the characteristics peaks were observed i.e., amine bands at 1652 cm<sup>-1</sup>; ureido group at 1710 cm<sup>-1</sup> with NH<sub>2</sub> stretching vibrations at 3356 cm<sup>-1</sup>. Drug release studies were carried out under water bath maintained at 42°C for 10 minutes and in AC magnetic field at 42°C for 10 minutes and gemcitabine release of up to 6% was found by means of UV/VIS more or less similar and equivalent for both heating methods. By this way we prepared a magnetic nanoparticles system, which is loaded with drugs and can release the loaded drug thermally by an external magnetic trigger. Thus, the prepared formulation may be utilized to target the cancer site by using the external magnetic field for dual modes (i.e., chemo and thermo) of therapy.

## The Force Analysis for Superparamagnetic Nanoparticles-based Gene Delivery in an Oscillating Magnetic Field

Jiajia Sun<sup>1,\*</sup>, Zongqian Shi<sup>1</sup>, Shenli Jia<sup>1</sup>, Pengbo Zhang<sup>2</sup>

<sup>1</sup> State Key Laboratory of Electrical Insulation and Power Equipment, Xi'an Jiaotong University, No. 28 Xianming West Road, Xi'an, Shaanxi Province 710049, China,

<sup>2</sup> Department of Anesthesiology, Second Affiliated Hospital of Xi'an Jiaotong University School of Medicine, No.157 West 5 Read, Xi'an, Shaanxi Province 710004, China,  
\* E-Mail: sunjiajia1981@qq.com

### Abstract

Due to the peculiar magnetic properties and the ability to function in cell-level biological interaction, superparamagnetic nanoparticles have been being the attractive carrier for gene delivery. The superparamagnetic nanoparticles with surface-bound gene vector can be attracted to the surface of cells for uptake by the Kelvin force provided by external magnetic field. In this article, the influence of the oscillating magnetic field on the characteristics of magnetofection is studied in terms of the Kelvin force. The magnetic field of a cylindrical permanent magnet is calculated by equivalent current source (ECS) method, and the Kelvin force is derived by using effective moment method. The results show that the static magnetic field accelerates the sedimentation of the particles, and drives the particles inward towards the axis of the magnet. Based on the investigation of the Kelvin force under horizontal oscillating magnetic field, we observed an oscillating magnetic force within the amplitude of the magnet oscillation. Furthermore, the influence of the amplitude and frequency of the oscillating magnet on the Kelvin force indicates that the oscillating amplitude plays an important role in regulating the active region of the oscillating force, and the oscillating frequency affects the action time of the positive/negative force. The analysis of the Kelvin force gives us an insight into the physical mechanism of the magnetofection. It's also helpful to the optimal design of the magnetofection system.

**Keywords:** Superparamagnetic nanoparticles, oscillating magnetic field, Kelvin force, cell, magnetofection, gene delivery;

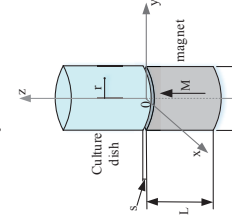


Fig.1. The schematic diagram of cylindrical permanent magnet

Acknowledgements  
This work was supported by The German Academic Exchange Service (DAAD) in frame of "India-Germany Joint Research Collaboration" [FKZ 57129737] and by Department of Science and Technology, Ministry of Science and Technology, Government of India [Sanction No. INT/FRG/DAAD/P-255/2015].

## The effect of polycarboxylate shell of magnetic nanoparticles on protein corona formation in blood plasma

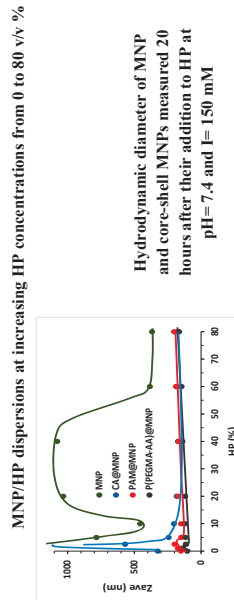
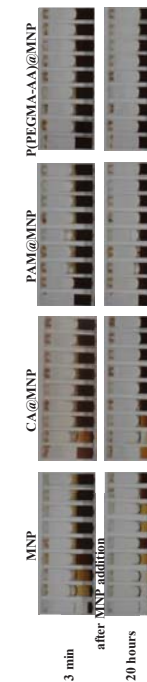
Márta Szekeres\*, Ildikó Y. Tóth and Etelka Tombácz

Department of Physical Chemistry and Materials Sciences, University of Szeged, Hungary  
1. Áradai vt, 6720 Szeged, Hungary, \*szekeres@chem.u-szeged.hu

The development of a protein corona around nanoparticles upon administration to human body is responsible in large part for their biodistribution, cell-intercalation and toxicity patterns. The chemical/physico-chemical characteristics of the outer surface of nanoparticles greatly affect the protein composition, density and thickness of the corona as well as its ability to stabilize the nanoparticles in the biological environment.

In the present work, we studied the effect of the chemical composition of magnetic nanoparticles' (MNP) surface on the formation of protein corona for naked citric acid (CA), poly(acrylic-co-maleic acid) (PAM) and poly(PEG-methacrylate-*cis*-acrylic acid) (P(PEGMA-AA)) coated nanoparticles in blood plasma. In TRIS buffer saline ( $\text{pH}=7.4$  and  $I=150 \text{ mM}$ ), the MNP surface has positive charge ( $+15 \text{ mV}$ ) and all carboxylated particles (CA@MNP, PAM@MNP and P(PEGMA-AA)@MNP) are negatively charged ( $-35$ ,  $-37$  and  $-32 \text{ mV}$ , respectively) as revealed by electrophoretic potential measurements. We measured the changes in the aggregation state (hydrodynamic diameter by dynamic light scattering method) and zeta potential with changing the human plasma (HP) concentration from 1 to 80 (v/v) %. Naked MNPs could not obtain an efficient stabilizing protein corona regardless of HP concentration, but all carboxylated MNPs got stabilized at higher plasma concentrations. The important difference in the effect of carboxylate coatings was observed at relatively low plasma concentrations (i.e., high local MNP content upon administration to blood). CA@MNPs aggregated instantly with an order of magnitude increase in size while both PAM@MNP and P(PEGMA-AA)@MNP experienced much weaker aggregation. The differences in average charge distance and absence/presence of hydrophilic PEG moieties.

Our results emphasize the critical role of detailed chemical composition of the shell of MNPs on biocompatibility beyond their non-specific physico-chemical characteristics such as charge sign and charge density.



**Acknowledgements:** This research was supported by the OTKA (NK 84014) grant.

## Néel relaxation and its anisotropic behavior in superparamagnetic nanoparticle evaluated by dynamic hysteresis measurement

Ryiji Takeda<sup>1</sup>, Satoshi Ota<sup>2</sup>, Yiliang Wang<sup>1</sup>, Tsutomu Yamada<sup>1</sup> and Yasushi Takekura<sup>1\*</sup>

<sup>1</sup> Department of Electrical and Computer Engineering, Yokohama National University, Yokohama, Japan

<sup>2</sup> Department of Electrical and Electronic Engineering, Shizuoka University, Hamamatsu, Japan

\*E-Mail: takekura@ynu.ac.jp

We have observed clearly anisotropic properties of Néel relaxation of superparamagnetic nanoparticles in dynamic hysteresis measurement. This is important to understand magnetization response of magnetic nanoparticles (MNPs) for their hyperthermia and magnetic particle imaging (MPI) applications.

$\gamma\text{-Fe}_2\text{O}_3$  nanoparticles (Meito Sangyo Co. Ltd., Japan) were used. Their primary and hydrodynamic diameters were 4 nm and 38 nm, respectively. They exhibited superparamagnetic behavior. One of the **solid samples** dispersed in water and two solid samples (MNPs were fixed in epoxy bond) were prepared. One of the **solid samples** contained the MNPs with **random orientation**. During the preparation, a static magnetic field of 575 kA/m was applied to the other solid sample. As this field intensity gives magnetization of 85% of saturation magnetization, the **easy-axis of MNPs was oriented**.

Figure 1 shows dc and ac hysteresis loops of the solid sample with oriented MNPs. Along its easy-axis, delay of the magnetic moment was observed above 10 kHz. But, dynamic magnetization process along the hard-axis did not indicate phase delay up to 100 kHz, resulting in no hysteresis.

Figure 2 shows ac hysteresis loops of the liquid sample, solid with random and oriented MNPs samples. The solid sample with oriented MNPs indicates the highest magnetization along its easy axis because of the lowest anisotropic energy barrier. It is notable that this magnetization is still higher than that of the liquid sample even at 10 kHz. The liquid sample normally exhibits higher magnetization by Brownian relaxation than fixed MNPs [1]. By contrast, magnetization along hard-axis indicates the lowest magnetization. Details including quantitative analysis of orientation and results from other ferromagnetic MNPs are also discussed in the presentation.

[1] Ota et al., JAP 117, 17D13 (2015). This work was partially supported by JSPS grand 15H05764 and 26289124.

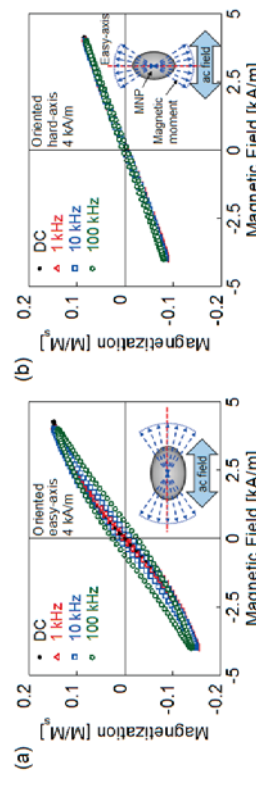


Fig. 1 Hysteresis loops of the solid sample with oriented MNPs along (a) easy-axis (b) hard-axis.

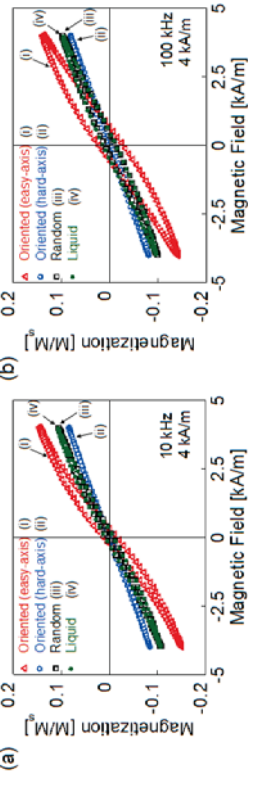


Fig. 2 Hysteresis loops of two solid and one liquid samples at (a) 10 kHz and (b) 100 kHz.

## Three-Dimensional Magnetic Nanoparticle Imaging Using a Small Gradient Field and Multiple Pickup Coils

T. Sasayama\*, Y. Tsujiya, M. Morishita, M. Muta, and K. Enpaku  
 Department of Electrical and Electronic Engineering, Kyushu University, Fukuoka, Japan  
 \*E-Mail: sasayama@sc.kyushu-u.ac.jp

Magnetic particle imaging (MPI) is a new imaging method that detects the position and amount of magnetic nanoparticles (MNPs) accumulated in a human (or animal) body for in vivo medical diagnosis. In MPI, a DC gradient field is usually used to improve the spatial resolution for MNP detection. However, we have to develop a gradient coil that can generate a strong field gradient (typically 1–2 T/m). As a result, the detection system becomes increasingly large as the size of the object to be measured increases.

In this study, we propose a detection method that combines a small gradient field with multiple pickup coils. The information on the spatial distribution of the MNPs can be added by using multiple pickup coils; therefore, we can expect to improve the spatial resolution even when a small gradient field is used. Figure 1 schematically depicts the detection system. An excitation coil generates an AC excitation field of 1.6 mT at a frequency of 3 kHz. A planar gradient coil generates a DC gradient field with a typical value of 0.2 T/m. The so-called field-free line (FFL) is produced at the center of the gradient coil. The third harmonic signal generated from the MNPs is detected using two pickup coils.

In the experiment, two MNP samples were set at different positions with a spacing of 15 mm, as shown in Fig. 1. The two samples were set on a single sample holder, and the sample holder was mechanically scanned in the  $x-y$  plane to obtain a field map of the MNP samples. Then, the field maps, measured using the two pickup coils, were analyzed using the non-negative least square method to obtain three-dimensional positions of the MNP samples. Figure 2 shows the three-dimensional imaging of the MNP samples obtained in this manner. As shown, we could clearly distinguish between the two MNP samples. As listed in Table 1, we could estimate the position of the MNP samples with good accuracy despite using a small gradient field of 0.2 T/m. This result confirmed the usefulness of the proposed method. The accuracy of the position estimation was significantly improved by increasing the number of pickup coils.

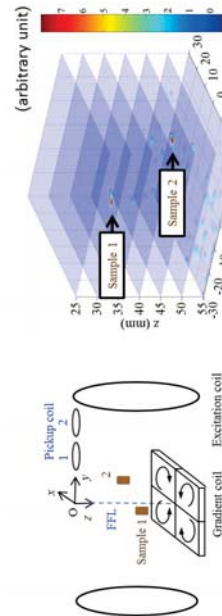


Fig. 1. Measurement system.

	Real position			Estimated position		
	$x$ (mm)	$y$ (mm)	$z$ (mm)	$x$ (mm)	$y$ (mm)	$z$ (mm)
Sample 1	-7.5	-7.5	35	-8	-6	35
Sample 2	7.5	7.5	50	8	8	50

Fig. 2. Three-dimensional imaging of two MNP samples.

## Protein A conjugated iron oxide nanoparticles for separation of *Vibrio cholerae* from water samples

Tran Q. Huy<sup>a</sup>, Pham V. Chung<sup>a</sup>, Nguyen T. Thuy<sup>a</sup>, Cristina Blanco-Andujar<sup>b</sup>,  
 \*Nguyễn T. K. Thành<sup>\*b</sup>

<sup>a</sup> National Institute of Hygiene and Epidemiology, 1 Yersin Street, Hai Ba Trung District,

Hanoi, Vietnam.  
 b Biophysics Group, Department of Physics and Astronomy, University College London, London, WC1E 6BT and UCL Healthcare Biomagnetic and Nanomaterials Laboratories, 21 Albermarle Street, London W1S 4BS.  
 E-mail: [ntk-thanh@ucl.ac.uk](http://www.ntk-thanh.co.uk); <http://www.ntk-thanh.co.uk>

Pathogen separation is of great significance for precise detection and prevention of outbreaks. For the first time, protein A conjugated with chitosan-coated iron oxide nanoparticles was prepared for pathogen separation at low concentrations from liquid samples. *Vibrio cholerae* O1 (VO1) bacteria were used for testing the effectiveness of this conjugate. Transmission electron microscopy (TEM) was used to confirm the presence of captured VO1. The results showed that after binding with a specific antibody, the conjugate allows separating VO1 bacteria from water samples at a concentration as low as 10 cfu/mL. Moreover, the conjugate can be used in parallel with conventional or modern diagnostic tests for quick and accurate detection of pathogens.

IONP@CHI@GA@PrA@Ab

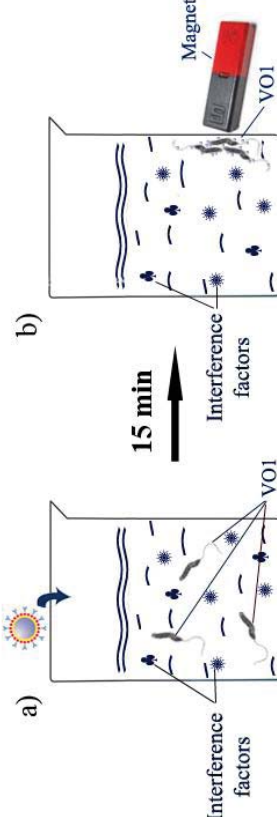


Fig. 1. Separation of VO1 bacterial cells from water samples with interference factors: (a) adding the complex of IONP@CHI@GA@PrA@Ab to the sample, and (b) attracting bacterial cells with a bar magnet

Ref. T. Q. Huy, P. V. Chung, N. T. Thuy, C. Blanco-Andujar, N. T. K. Thành (2014)  
 Protein A conjugated iron oxide nanoparticles for separation of *Vibrio cholerae* from water samples. *Faraday Discussion*. [175: 73–82](https://doi.org/10.1039/C4FD00022B)

**Synthesis of magnetic cobalt ferrite nanoparticles with controlled morphology, monodispersity and composition: the influence of solvent, surfactant, reductant and synthetic condition**

Le T. Lu<sup>a</sup>, Ngo T. Dung<sup>a</sup>, Le D. Tung<sup>b</sup>, Cao T. Thanh<sup>c</sup>, Ong K. Quy<sup>d</sup>, Nguyen V. Chuc<sup>e</sup>, Shinya Maenosono<sup>e</sup> and Nguyen T. K. Thanh<sup>f\*</sup>

<sup>a</sup>Institute for Tropical Technology-Vietnam Academy of Science and Technology, 18 Hoang Quoc Viet, Cau Giay, Hanoi, Vietnam; <sup>b</sup>Department of Physics and Astronomy, University College London, Gower Street, London WC1E 6BT, UK; <sup>c</sup>Institute of Materials Science, Vietnam Academy of Science and Technology, 18 Hoang Quoc Viet, Cau Giay, Hanoi, Vietnam; <sup>d</sup>Institute of Materials, Ecole Polytechnique Federale de Lausanne, Lausanne, Switzerland; <sup>e</sup>School of Materials Science, Japan Advanced Institute of Science and Technology, 1-1 Asahidai, Nomi, Japan.

[ntk\\_thanh@ucl.ac.uk](http://www.ntk-thanh.co.uk) <http://www.ntk-thanh.co.uk>

In our present work, magnetic cobalt ferrite ( $\text{CoFe}_2\text{O}_4$ ) nanoparticles have been successfully synthesised by thermal decomposition of Fe (III) and Co (II) acetylacetone compounds in organic solvent in the presence of oleic acid (OA) oleylamine (OLA) as surfactants and 1,2-hexadecanediol (HDD) or octadecanol (OCD-oil) as accelerating agent. As a result,  $\text{CoFe}_2\text{O}_4$  nanoparticles of different shapes were tightly controlled in size (range of 4-30 nm) and monodispersity (standard deviation only at ca. 5 %). Experimental parameters, such as reaction time, temperature, surfactant concentration, solvent, precursor ratio, accelerating agent, in particular, the role of HDD, OCD-oil, OA/OLA have been intensively investigated in detail to discover the best condition for the synthesis of the above magnetic nanoparticles. The obtained nanoparticles have been successfully applied for producing oriented carbon nanotubes (CNTs), and they have potential to be used in biomedical applications.

Multimodal graphene@ $\text{Fe}_3\text{O}_4$  superparamagnetic nanoparticles with unusually enhanced specific absorption rate for synergistic cancer therapeutics and magnetic resonance imaging

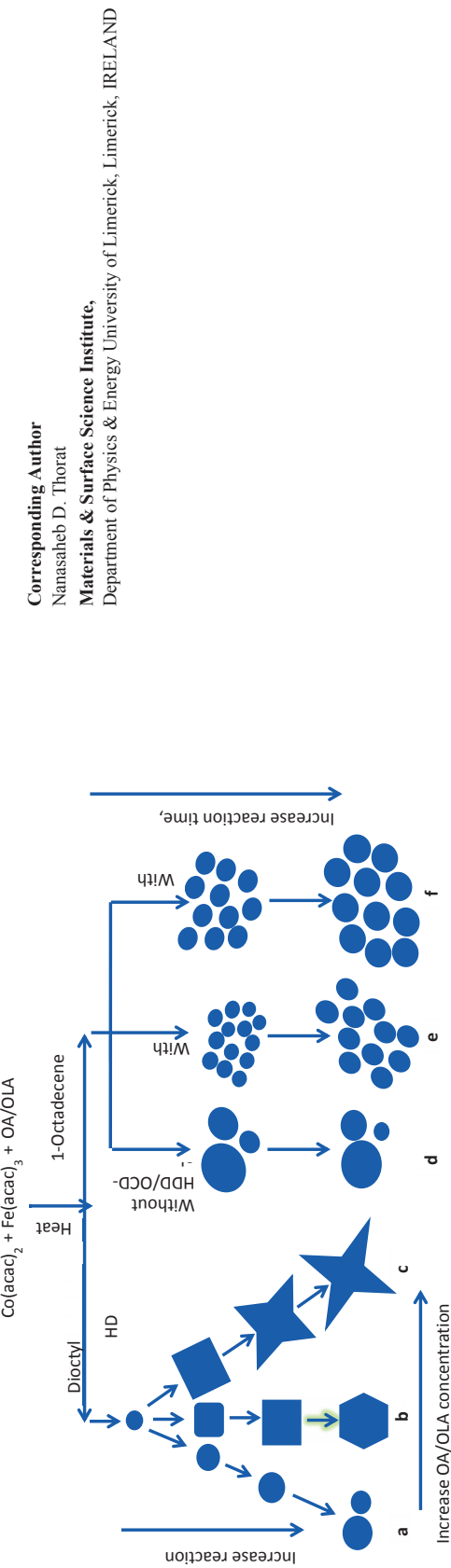
Nanasaheb D. Thorat<sup>1,2\*</sup>, Kevin C.-W. Wu<sup>3</sup>, Yususke Yamuchi<sup>4</sup> and Tofail Syed<sup>1,2</sup>

<sup>1</sup>Department of Physics & Energy, University of Limerick, Limerick, Ireland

<sup>2</sup>Materials & Surface Science Institute, University of Limerick, Limerick, Ireland

<sup>3</sup>Department of Chemical Engineering, National Taiwan University, No. 1, Sec. 4, Roosevelt Road, Taipei, Taiwan

<sup>4</sup>World Premier International (WPI) Research Center for Materials Nanoarchitectonics (MANA), National Institute for Materials Science (NIMS), 1-1 Namiki, Tsukuba, Ibaraki 305-0044, Japan.



Ref. L. T. Lu, N. T. Dung, L. D. Tung, C. T. Thanh, O. K. Quy, N. V. Chuc and N. T. K. Thanh\* (2015). *Nanoscale*, **7**, 19596-19610.

## Aqueous droplets with a superparamagnetic and -hydrophobic particle shell for lab-in-a-drop bioprocesses

K. Kuthan, H. Al-Kaidy, R. Ulber, N. Tippkötter

Institute of Bioprocess Engineering, University of Kaiserslautern, Germany

Integrated bioprocesses may take great advantage in the directed control a magnetic carriers for the immobilization of microorganisms, enzymes or fermentation products. In the past, our group has developed different magnetic carrier-based bioreaction systems for catalyst retention and mixing or selective separation in high magnetic field gradients. Recently, a new magnetic particle based lab-in-a-drop system has been developed. In comparison to lab-on-a-chip platforms, a significant improvement is offered by the possibility to randomly move the liquid phase as a drop on the surface of a reaction platform. The new system is based on the actuation of small liquid volumes (1-30 µl) with the new feature that one or several droplets can be simultaneously positioned by means of overlapping electromagnetic field gradients [1]. Droplet movement is possible as their outer shells are made of a thin layer of superhydrophobic magnetizable microparticles synthesized in our lab.

The reaction platform consists of a matrix of stacked electrical coils that accommodate either neodymium permanent magnets or iron cores. By automated sequencing, magnets can be moved perpendicular to the plane of the platform so that droplets follow the respective field gradients. The optimal magnetic gradients were simulated by a finite element method (FEM) and experimentally verified. Reactions with the droplets have been performed by merging them or positioning one on top of surface immobilized enzymes. This allows the implementation of complex enzyme cascades and can even result in future developments of cell-free bio-chemical reaction systems. Currently, automation of the reaction platform is advanced by the integration of a x-y-z picoliter dispenser system. With it, the micro droplet generation, liquid application and even surface alterations can be performed contactless. As outlook, the combination of freely movable droplets and automatized surface activations can be used to design and execute complete experimental reaction designs *in silico*.



## Possibilities and limitations of carboxylated/PEGylated SPIONs for theranostics

Etelka Tombácz\*, Erzsébet Illés, Ildikó Y. Tóth, Tamás Szabó, Márta Székeres  
Department of Physical Chemistry and Materials Science, University of Szeged, Aradi vt 1,  
6720 Szeged, Hungary \*tombacz@chem.u-szeged.hu

Superparamagnetic iron oxide nanoparticles (SPIONs) seem to have great potential for use in therapeutic applications due to their biocompatibility and unique magnetic properties. In biomedical applications, SPIONs require an optimized coating via which IONS interact with any biological entities (e.g., proteins, cell membranes).

We have worked out the spontaneous one-step process to form carboxylated/PEGylated shell on SPIONs by post-coating of naked surface of purified synthesis products, in which optimized magnetic cores were combined with different commercial polyelectrolytes (e.g. poly(acrylic acid) [1-3] and designed polymer molecules [4]. The magnetic cores were mostly the same in each product and the carboxylated shells were also similar regarding their hydrophobicity, size and surface charge [5]; and so a very similar behavior should be expected according to the interactions at the nanobio interface [6]. In a novel recently synthesized polymer, poly(ethylene glycol) methyl ether methacrylate (PEGMA) and acrylic acid (AA) were chemically coupled in a comb-like copolymer, P(PEGMA-co-AA) with PEG chains and pendant carboxylates in a single coating molecule. The multiple bindings of polycarboxylated macromolecules on SPIONs via surface complexation of  $\equiv\text{Fe-OH}$  sites by carboxylates are spontaneous. The formed polyelectrolyte layer hinders SPIONs' dissolution, provides combined electrostatic and steric (electrosteric) stabilization, and high protein repellency due to super-hydrophilicity of PEG moieties. In addition, free carboxylates still exist in the shell for anchoring bioactive molecules via both covalent and non-covalent strategies, where peptide bonds form through carbodiimide activation and ionic coupling of positively charged bio-entities, respectively, if pH- and ionic strength dependent dissociation of carboxylated shell and isolectric point (IEP) of complex molecules such as antibodies or proteins are considered.

In the lecture, we allow to get an insight into the synthesis and post-coating of naked SPIONs and their physicochemical and colloidal characterization. The possibilities and limitations of different products will be explained by comparing their performance in hemocompatibility (blood sedimentation rate, blood smear and blood cell viability) and *in vitro* cell tests (MTT cell proliferation assay, Prussian blue staining), in MRI contrast and hyperthermia efficiency. The financial support of OTKA (NK 84014) grant is acknowledged.

## References

1. Hajdú A, et al., Colloids and Surfaces B: Biointerfaces 94 (2012) 242-249
2. Tombácz E, et al., Colloids and Surfaces A: Physicochem. Eng. Asp. 435(2013) 91-96
3. Tóth YI, et al., Langmuir 30 (2014) 15451-15461
4. Illés E, et al., Journal of Magnetism and Magnetic Materials, 380(2015) 132-139
5. Székeres M, et al., Int. J. Mol. Sci., 14(2013), 14550-14574
6. Nel AE, et al., Nature Materials, 7(2009) 543-557

## Clustering of carboxylated magnetite nanoparticles with polyethylenimine via electrostatic or chemical interactions

I.Y. Tóth<sup>1\*</sup>, D. Nesztor<sup>1</sup>, L. Novák<sup>2</sup>, E. Illés<sup>1</sup>, M. Szekeres<sup>1</sup>, T. Szabó<sup>1</sup>, E. Tombácz<sup>1</sup>

<sup>1</sup> Department of Physical Chemistry and Materials Science, University of Szeged,  
Aradi ut. tere 1, Szeged, Hungary, \* E-Mail : [Ildiko.Toth@chem.u-szeged.hu](mailto:Ildiko.Toth@chem.u-szeged.hu)

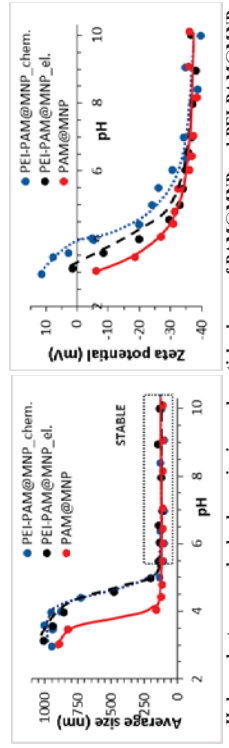
<sup>2</sup> Department of Colloid and Environmental Chemistry, University of Debrecen,  
Egyetem tér 1, Debrecen, Hungary

The application of magnetite nanoparticles (MNP) in medicine has been in the focus over the past few decades. The most advanced approach is to combine the diagnostic (magnetic resonance imaging) and therapy (magnetic hyperthermia), but for greater potential in therapeutic application, modified MNP particles with enhanced properties are required. The recently synthesized, poly(acrylic acid-co-maleic acid) coated magnetite nanoparticles (PAM@MNP) clusped by polyethylenimine (PEI-PAM@MNP) are promising candidate for theranostics<sup>1</sup>. Our goal was to synthesize and characterise comprehensively the PEI-PAM@MNP clusters attached by electrostatic interaction and chemical way, respectively.

Naked MNPs prepared by co-precipitation were coated with PAM followed by the removing of excess PAM. To synthesize the clusters, two different methods were used: 1) the  $-COO^-$  surface groups of PAM@MNP and the  $-NH_3^+$  functional groups of PEI were adhered by electrostatic interaction (PEI-PAM@MNP\_el.), 2) peptide bonds were performed by controlled chemical reaction (PEI-PAM@MNP\_chem.).

pH-dependent particle size and zeta potential of clusters were measured using dynamic light scattering and electrophoretic mobility measurements. The prepared clusters are colloidally stable at pH > 5. SAXS measurements suggest that the formation of PEI-cluster has no significant effect on the scattering behaviour of MNP cores. The analysis of ATR-FTIR spectra proves that different bonds form between MNP and PEI in the two ways of synthesis. The values of specific absorption rate (SAR) measured in various AC magnetic fields are about two times higher in case of the PEI-PAM@MNP chem.. The  $\tau_2$  values determined by MRI measurement are ~390, ~450 and ~690 mM<sup>-1</sup>s<sup>-1</sup> for PAM@MNP, PEI-PAM@MNP\_el. and PEI-PAM@MNP\_chem., respectively.

Based on these results, the chemically clustered PEI-PAM@MNP product shows greater potential for feasible theranostic applications.



pH-dependent average hydrodynamic size and particle charge of PAM@MNP and PEI-PAM@MNP clusters linked via electrostatic interaction or chemical bond (10 mM NaCl).

### Literature:

1. D. Nesztor et al. Journal of Magnetism and Magnetic Materials. 380 (2015) 144-149.

Acknowledgements: This research was supported by the OTKA (NK 84014) grant.

## Tuning the magnetic properties of ferrhydrite by dextran coating

Lucía Gutiérrez<sup>a,b</sup>, Francisco J. Lázaro<sup>c</sup>, M. Puerto Morales<sup>a</sup>, Sabinio Veintemillas- Verdiguier<sup>a</sup>

<sup>a</sup> Instituto de Ciencia de Materiales de Madrid (ICMM)/CSIC, 28049 Madrid, Spain.  
<sup>b</sup> Instituto de Nanociencia de Aragón/Departamento de Química Analítica, Universidad de Zaragoza, Zaragoza, Spain.  
<sup>c</sup> Departamento de Ciencia y Tecnología de Materiales y Fluidos, Universidad de Zaragoza, Zaragoza, Spain.

Recent studies on the magnetic properties of ferrhydrite during the aging process to hematite have revealed an intermediate phase with pronounced ferrimagnetism [Michel et al., PNAS, 2010, 107, 2787]. This finding has encouraged the study of the magnetic properties of this new phase as it could be a promising alternative material for biomedical applications.

We have prepared a series of samples following the same procedure as to obtain ferrimagnetic (aged) ferrhydrite. In this case, though, a varying amount of dextran was added in the synthesis in order to determine the variations of the relaxometric properties in a context of conceiving this material as an MRI contrast agent. A detailed characterization of the series has been performed by X-ray diffraction, Transmission Electron Microscopy (TEM), AC and DC magnetic measurements and in-solution <sup>1</sup>H Nuclear Magnetic Resonance measurements.

As suspected, the amount of dextran used during the ferrhydrite nanoparticle synthesis results in a departure of the magnetic properties from those of ferrimagnetic ferrhydrite. The ratios between the transverse and longitudinal relaxivities ( $r_2/r_1 \approx 25$ ) indicate the possible use of dextran coated ferrhydrite as a negative contrast agent but not as a positive one. The detailed magnetic characterization of the series provides more insights on the effect of the dextran amount on the mechanisms of particle growth.

Our results explore the particle formation during the synthesis of ferrhydrite in the presence of different amounts of coating and its influence on modifying its magnetic properties.

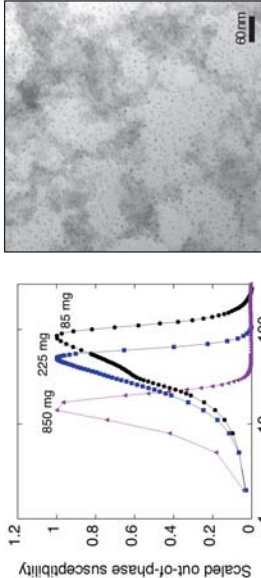


Figure. (Left) Temperature dependence of the out-of-phase susceptibility scaled to its maximum of ferrhydrite samples prepared with different amounts of dextran (mg indicated in the figure). (Right) TEM image showing the presence of ferrhydrite nanoparticles prepared using 225 mg of dextran. All synthesis were prepared in a 80 ml volume.

### Literature:

1. D. Nesztor et al. Journal of Magnetism and Magnetic Materials. 380 (2015) 144-149.

## Simulation of essential probe characteristics for intra-operative handheld detection of magnetic tracers

M. Visscher, J.J. Poutw, S. Waanders, D.M.C. Bastiaan, B. ten Haken\*

MIRA Institute for Biomedical Engineering and Technical Medicine, NIM - Magnetic Detection, University of Twente, P.O. Box 217, 7500 AE, Enschede, The Netherlands, E-mail: b.tenhaken@utwente.nl

To overcome problems associated with the use of radioactivity, intra-operative detectors of magnetic tracer were recently introduced as alternative for sentinel lymph node biopsy (SLNB) with a handheld gamma probe and radioisotopes. The optimal surgical probe should enable transcutaneous identification of lymph nodes deep inside the body (~5 cm) [1] as well as, intra-operative detection after incision, the latter of which requires a small probe diameter. However, unlike the gamma probe, the performance of currently used magnetometers is limited by their sensitivity to the diamagnetic human body and a low depth sensitivity. This complicates the clinical introduction of the new magnetic technique for SLNB. The main design parameters that influence clinical performance and surgical applicability are the diameter of the probe, which is strongly related to the depth sensitivity, and the tracer specificity. In the present study these aspects are investigated for four different probe designs in a finite element method analysis, using COMSOL Multiphysics.

The model is based on a probe in a water environment that simulates tissue with diamagnetic properties. In the water volume a small disk-shaped volume with the magnetic properties of superparamagnetic iron oxide (SPIO) tracer (Sienna+) simulates a magnetically labeled lymph node. Depth sensitivity of the probes is characterized using different probe-lymph node distances. The influence of the presence of diamagnetic tissue on lymph node identification is investigated by modeling probe insertion into the water volume and by comparison with an air environment. A commercial linear AC-probe (d=24 mm), a larger version of the linear AC-probe (d=40 mm), a handheld DiffMag probe (d=22 mm) and large diameter DiffMag probe (d=50 mm) are characterized in a simulation using different amounts of magnetic tracer at different node-probe distances. The DiffMag principle is designed to eliminate the effect of diamagnetic tissue in standard AC susceptometry, exploiting the nonlinear magnetic properties of the SPIO tracer [3]. The detection distance of the commercial probe is limited to 1.4 cm for a lymph node containing 50 µg iron, which does not meet the requirement of at least 5 cm for transcutaneous hotspot detection of deeply located lymph nodes. In addition, its sensitivity to diamagnetic tissue significantly reduces the detection distance for lymph nodes located deeply into the tissue. Similar results were obtained for the large linear probe [Fig. 1]. The small diameter DiffMag probe effectively eliminates the effect of tissue, but shows a reduced detection distance compared to the commercial probe. The large diameter DiffMag probe shows an increased detection distance in combination with a high tracer specificity by elimination of the diamagnetic response providing transcutaneous detection of deep nodes. The combined use of a large diameter DiffMag probe for transcutaneous localization, and a small diameter DiffMag probe for post-incision identification overcomes problems of the current generation magnetometers, and provides the means for successful clinical introduction of the magnetic technique for SLNB.

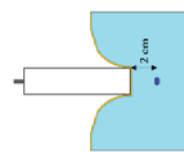
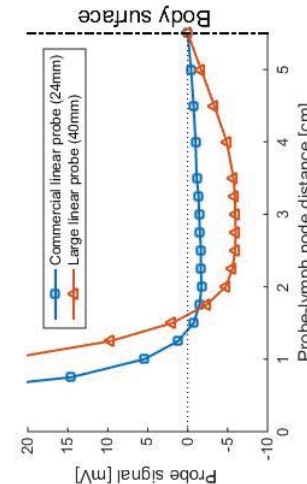


Fig. 1. Simulations of the detection signal of the commercial and an enlarged probe for a node containing 50 µg iron placed in a tissue-like environment at 5.5 cm depth. The figure on the right shows a 3.5 cm approach from the body surface



[1] Gammie, F., et al., European Journal of Nuclear Medicine and Molecular Imaging, 2013, 40(12), p.1932-1947.

[2] Douek, M., et al., Annals of Surgical Oncology, 2014, 21(4), p. 1237-1245.

[3] Visscher, M., et al., Journal of Magnetism and Magnetic Materials, 2014, 365, p. 31-39.

## Magnetism engineered nanoparticles towards innovative biocolloids combining MRI and magnetic hyperthermia properties

Geoffrey Cotin<sup>†</sup>, Christine Affolter-Zbaraszczuk<sup>‡</sup>, Catalina Bordeianu<sup>†</sup>, Damien Mertz<sup>†</sup>, Beatrice Uring-Lambert<sup>†</sup>, D. Felder-Flesch<sup>†</sup>, Florent Meyer<sup>†</sup> and Sylvie Beguin-Colin<sup>†,\*</sup>

<sup>†</sup>Institut de Physique et Chimie des Matériaux, UMR CNRS-Uds 7504

University of Strasbourg, 23 Rue du Loess, BP 43, 67034 Strasbourg, France

<sup>‡</sup>INSERM, UMR 1121, 11 rue Hurmann, 67085 Strasbourg, France

<sup>\*</sup>Nouvel Hôpital Civil, laboratoire d'Immunologie, 1 Place de l'hôpital, 67091 Strasbourg, France

In the field of the synthesis and functionalization of inorganic nanoparticles (NPs) for biomedical applications, most researches aim at developing multifunctional therapeutic NPs which can both identify disease states and deliver therapy and allow thus following the effect of therapy by imaging. The current challenge is the design of NPs able to combine in one nano-objects both magnetic hyperthermia (MH) and MRI with the best efficiency in order to reduce the dose injected in the patient. To be used as T2 contrast agents for MRI, iron oxide based NPs should exhibit high saturation magnetisation and be functionalised with ligands ensuring optimal diffusion of water molecules around the magnetic core. For therapy by magnetic hyperthermia, the amount of heat generated by magnetic NPs strongly depends on the NPs magnetic properties which have to display high saturation magnetization and in particular high anisotropy energy which depend strongly on the NPs size, composition and shape...The particle size distribution is also important as size distribution or energy barriers can cause overheating and undesired magnetic thermal ablation. The tuning of the shape will allow the magnetisation to be easier in specific direction as the tuning of the composition will induce magnetic exchange interaction in core-shell NPs consisting of a core with a high magnetic anisotropy and a shell with a small magnetic anisotropy (or the inverse). Mixed ferrites (Mn, Co) are considered as good candidates for this study as they present enhanced magnetic anisotropy and/or saturation magnetization than iron oxide NPs. Despite their potential, the development of doped ferrites was thus limited because of the complexity of their synthesis, which commonly leads to core-shell NPs or chemical heterogeneities

By mastering the synthesis of our metal reactants, we were able to synthesize, by the thermal decomposition technique, NPs with different shapes and sizes : nanoplates, nanocubes, octopods with different compositions : doped ferrites with Mn and Co and core-shell NPs. Their structural and magnetic properties have been finely characterized as well as their MRI and MH properties. They have been then coated with dendron molecules suitable for biomedical applications. The colloidal stability of these dendronized NPs have been investigated in different physiological media and their MRI and MH properties have been assessed performing respectively relaxivity and SAR measurements. Some designed NPs were shown to combine very high heating values and MRI properties very promising for biomedical applications.

## The interaction of bacterial magnetosomes and human liver cancer cells *in vitro*

Pingping Wang<sup>1\*</sup>, Chuanfang Chen<sup>1</sup>, Changyu Chen<sup>1</sup>, Yue Li<sup>1</sup>, Weidong Pan<sup>1</sup>, Tao Song<sup>1</sup>

<sup>1</sup> Beijing Key Laboratory of Bioelectromagnetism, Institute of Electrical Engineering, Chinese Academy of Sciences, Beijing, P. R. China, <sup>2</sup> Graduate University of Chinese Academy of Sciences, Beijing, P. R. China, \*E-mail: wangpp@mail.iee.ac.cn.

As the biological synthesized magnetic nanomaterial, bacterial magnetic nanoparticles (namely magnetosomes) have many advantages, such as high homogeneity, strong magnetic power, biocompatibility and convenient decoration, which enable them great potentials in numerous biomedical applications, such as tumor hyperthermia, drug delivery, magnetic resonance imaging and bioseparation. Several kinds of nanoparticles can accumulate in liver tissue, making them the promising drug carrier targeting to liver tumors. However, whether the bacterial magnetosomes interact with liver cancer cells has not been well researched until now.

In the present study, we examined the interaction between the bacterial magnetosomes with human liver cancer HepG2 cells. Firstly, after 24 h incubation, prussian blue staining showed numerous blue stained particles in the cells, indicating that the magnetosomes could bind with the cultured HepG2 cells. In order to distinguish whether the magnetosomes entered inside the cell bodies or merely attached/conjugated to the cell surfaces, we performed transmission electron microscopy (TEM) to observe the cellular ultrastructures. The results showed that the magnetosomes could be internalized into the cells, some of which were encapsulated in membrane vesicles (endosomes/lysosomes), while some others were located in the cytoplasm freely. Moreover, we also found that some magnetosomes on the cell surfaces were encapsulated by the cell membrane invagination, indicating that the magnetosomes could be internalized into HepG2 cells via cell endocytosis. Real-time PCR is ongoing to validate the specific endocytosis pathway(s) of magnetosomes. Furthermore, we applied inductively coupled plasma atomic emission spectroscopy (ICP-AES) to detect the intracellular iron concentrations of HepG2 cells that were treated with different amounts of magnetosomes, and the results indicated that the intracellular iron concentrations increased as the magnetosomes amounts increasing.

In summary, the present study demonstrates that the bacterial magnetosomes can interact with liver cancer cells, and should be considered as potential target drug carriers, imaging contrast agents and promising hyperthermal materials for the diagnosis and therapy of liver tumors.

Keywords: Bacterial magnetosome, Liver cancer cell, Interaction, Cell internalization

## Intentional Formation of a Protein Corona on Magnetic Nanoparticles

A. Weidner<sup>1</sup>, C. Gräfe<sup>2</sup>, M. von der Lühe<sup>3</sup>, H. Remmer<sup>4</sup>, J.H. Clement<sup>2</sup>, D. Eberbeck<sup>5</sup>, F. Ludwig<sup>4</sup>, R. Müller<sup>6</sup>, F.H. Schacher<sup>3</sup>, S. Dutz<sup>1</sup>

<sup>1</sup> Institut für Biomédizinische Technik und Informatik (BMT), Technische Universität Ilmenau, Ilmenau, Germany

<sup>2</sup> Klinik für Innere Medizin II, Abteilung Hämatologie und Internistische Onkologie, Universitätsklinikum Jena, Jena, Germany

<sup>3</sup> Institut für Organische und Makromolekulare Chemie (IOMC) und Jena Center for Soft Matter (JCSM), Friedrich Schiller Universität Jena, Jena, Germany

<sup>4</sup> Institut für Elektrische Messtechnik und Grundlagen der Elektrotechnik, Technische Universität Braunschweig, Braunschweig, Germany

<sup>5</sup> Physikalisch-Technische Bundesanstalt, Berlin, Germany

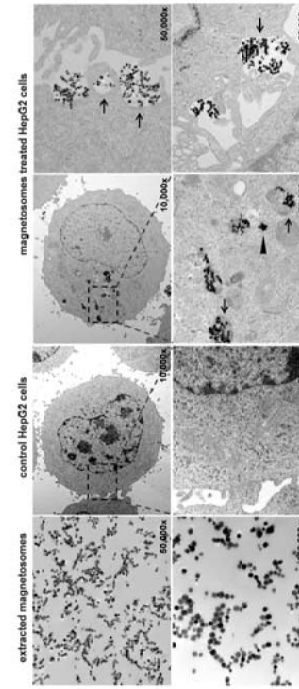
<sup>6</sup> Abteilung Nanobiophotonik, Leibniz-Institut für Photonische Technologien (IPHT), Jena, Germany

E-mail: silvio.dutz@tu-ilmenau.de

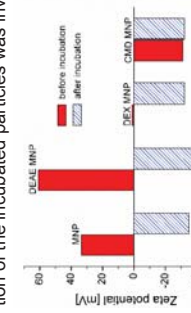
When magnetic nanoparticles (MNP) are exposed to the blood circulation, a protein corona consisting of various components is formed immediately. The composition of the formed protein corona might be of major importance for cellular uptake of magnetic nanoparticles. The aim of our study is to analyze the formation of the protein corona during *in vitro* serum incubation in dependence of incubation time, temperature, and the protein concentration of the incubation medium. MNPs were prepared by alkaline precipitation and coated with different shells (amino-dextran, dextran, and carboxymethyl-dextran). The obtained core/shell nanoparticles were incubated in fetal calf serum (FCS) at different temperatures (20 to 70 °C) by magnetic heating (hyperthermia) of the MNP in the serum and by adding the MNP to FCS with the desired temperature (water bath). The incubation was performed for different durations up to 20 minutes. To control the amount of proteins binding on the MNP surface, the FCS concentration of incubation medium (FCS + cell medium) was varied. Before and after the incubation, the physical properties of the particles were determined by a variety of methods (Zeta-potential, vibrating sample magnetometry, thermogravimetric analysis, and transmission electron microscopy). The incubated nanoparticles were applied to sodium dodecyl sulfate polyacrylamide gel electrophoresis (SDS-PAGE) and the protein bands were visualized by silver staining. The corona formation as well as a possible agglomeration of the incubated particles was investigated by means of magnetorelaxometry (MRX).

The results clearly demonstrate that the particle shell, incubation temperature, incubation time and composition of incubation media have an influence on the composition of the corona. MRX shows, that the corona is formed within the first seconds of incubation. MNP which were treated with hyperthermia contain more protein than nanoparticles exposed to external heating. By changing the composition of the incubation media the amount of proteins bound to the MNP can be controlled. An increasing FCS concentration in incubation media leads to a higher protein amount on the particles. In ongoing studies, the impact of controlled corona formation on interaction of these particles with human cells is investigated. In our contribution we present a novel type of core-shell MNP for application in medicine.

Acknowledgements  
This work was supported by Deutsche Forschungsgemeinschaft (DFG) in frame of priority programme 1681 (FKZ: CL202/3-1, DU 1283/4-1, LU80/4-1, MU2382/4-1, SCHAT 6407/1, and TR 4088-1) and by Interdisziplinäres Zentrum für Klinische Forschung Jena.



Representative TEM images of magnetosomes, magnetosomes treated and untreated cells



Zeta potential of different MNP before and after FCS incubation

## Particle size- and concentration-dependent separation of magnetic nanoparticles

K. Witte<sup>1,2\*</sup>, K. Müller<sup>2</sup>, C. Grüttner<sup>2</sup>, F. Westphal<sup>2</sup>, C. Johansson<sup>3</sup>

<sup>1</sup> University of Rostock, Institute of Physics, Albert-Einstein-Str. 23, D-18059 Rostock, Germany,  
<sup>2</sup> micromod Partikeltechnologie GmbH, Friedrich-Baumwitz-Str. 4, D-18119 Rostock, Germany  
<sup>3</sup> Acreo Swedish ICT AB, 40014 Göteborg, Sweden, e-mail: witte@micromod.de

On the one hand, magnetic separation of proteins, nucleic acids and other biomolecules from complex reaction mixtures is becoming a suitable approach for large scale production in industrial purification and extraction processes. On the other hand, obtaining magnetic nanoparticles of homogenous composition, in particular with a defined mean particle size and narrow size distribution is challenging and can have a significant effect on the overall physical behavior of the particle suspension. Therefore, in the present study the magnetic mobility of Bionized NanoFerrite (BNF) nanoparticles was investigated for different particle sizes and over a broad range of particle concentrations to demonstrate the analytical and preparative potential of the Sepmag system [1]. The BNF nanoparticles are thermally blocked multi-core particles consisting of individual non-stoichiometric magnetite nanocrystals with cubic or rhombohedral shape with a characteristic individual core size of 10–20 nm covered with a stabilizing starch shell [2]. Aqueous suspensions containing BNF particles of 80 nm, 100 nm, 290 nm and 350 nm in particle diameter were placed inside the cavity of Sepmag Q100ml. Over time the clearance of the opaque suspension was observed. Furthermore, the iron content and the particle size distribution of the initial colloid, the sediment and the supernatant were monitored.

For smaller nanoparticles a significant increase in the separation time of the particles by orders of magnitude was observed, which is demonstrated in Fig. 1. Increasing the particle concentration of the suspension leads to a reduction of the separation time for large nanoparticles as expected for cooperative magnetophoresis [3]. For higher iron concentrations the separation time was constant. Nevertheless, the smaller BNF 80 nm particles show exactly the opposite behavior with rising iron content, as indicated in Fig. 1. These findings are promising for further usage of the magnetic separation for the preparative fractionation of magnetic nanoparticles.

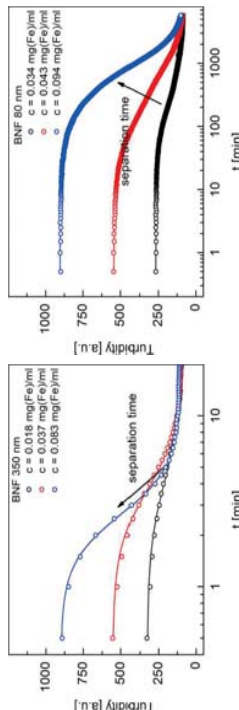


Figure 1: Exemplary separation processes for BNF 350 nm and BNF 80 nm particles for different initial iron concentrations of the suspension. The figures show the turbidity vs time measured with the Sepmag.

### Acknowledgement

Financial support by European Commission Framework Programme 7 under NANOMAG Project (grant agreement no. 604448) is acknowledged.

### References

- [1] <http://www.sepmag.eu>
- [2] F. Ludwig, et al., IEEE Transactions on Magnetics 50 (2014) 1.
- [3] J. S. Andree, et al., Physical Review E 84 (2011) 021402.
- [4] V. Schaller, et al. J. Appl. Phys. 104 (2008) 093018.

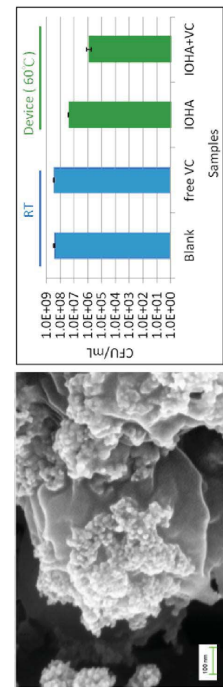
## Hyperthermia enhancement of iron oxide nanoparticle in bacterial biofilms

Ming Da Yang<sup>1,2\*</sup>, Yu Ting Huang<sup>1</sup>, Chia Ni Chang<sup>1</sup>, Ming Chun Lin<sup>1</sup>, Mean Jue Tung<sup>1</sup>,  
Chih Huang Lai<sup>2</sup>

1 Industrial Technology Research Institute, Hsinchu, Taiwan, R.O.C \*E-Mail : ir960331@irit.org.tw  
2 National Tsing Hua University, Hsinchu, Taiwan, R.O.C E-Mail : ir960331@nith.org.tw

Biofilm formation is an important medical problems associated with use of artificial implants. These infections tend to be chronic as they resist innate and adaptive immune defense mechanisms as well as antibiotics, and the treatment of biofilm infections presents a considerable unmet clinical need. To overcome infection-related problems linked to the use of artificial implants, we proposed a novel magnetic guided therapeutic system, which combine the drug conjugated nanoparticles and designed magnetic device, to eradicate biofilm form prosthetic joint infection.

For magnetic hyperthermia applications, an AC magnetic field of 370 kHz at 8.3 kA/m. was applied for 30 sec. An upper limit for the product of frequency and amplitude should not exceed a threshold which was experimentally estimated to equal  $4.8 \times 10^8$  Am<sup>-1</sup>s<sup>-1</sup>. We also test the sterilizing effect of hyaluronic acid coated iron oxide (IOHA) on an extremely heat resistant strain of staphylococcus aureus (S. aureus). The specific absorption rate of IOHA can be enhanced due to the magnetic configuration. The vancomycin conjugated IOHA behave as magnetic guided thermal agent; can be localized intra articular and magnetic drive to destroy the biofilm in the artificial joint surface. The number of  $2.7 \times 10^8$  CFU/ml was obtained from the overnight incubation of bacterial cultures with Gram staining of S. aureus. Using the hyperthermia treatment of IOHA, we can raise the temperature to 60~70 °C and the number of S. aureus is reduced to below  $2 \times 10^6$  CFU/ml. Also, the animal model of prosthetic joint infection show the positive correlations with the hyperthermia treatment for biofilm infections.



Schematic representation of IOHA for the hyperthermia treatment in bacterial biofilms

## Special magnetic structure for cell sorting by novel 3D printing

Ming Da Yang<sup>1,2\*</sup>, Yu Ting Huang<sup>1</sup>, Mean Jue Tung<sup>1</sup>

1 Industrial Technology Research Institute, Hsinchu, Taiwan, R.O.C  
2 National Tsing Hua University, Hsinchu, Taiwan, R.O.C \*E-Mail : ir960331@irit.org.tw

One of the current challenging developments in biomedical science is transplantation therapy and regenerative medicine. To separate the useful stem cells is key issue. Magnetic - activated cell sorting is a method for separation of various cell populations depending on their surface antigens (CD molecules) invented by Miltenyi Biotec, which uses superparamagnetic nanoparticles and columns.. In this research we focus on the design of a magnetic sorting device for cell separation and purification. Main tasks include the high gradient magnetic fluid channel, magnetic field design and the automatic cell sorting procedure. The magnetic column can be designed by novel 3D magnetic printing. The spiral magnetic structure can be printed by combining sintered magnetic powder with biodegradation and biocompatibility of PLA. The simulation of magnetic gradient for period spiral magnetic wire (diameter : 0.5mm) attend to 3800T/m. From the overnight incubation of KG1a (non-adherence) cells cultures, desired cells are targeted with antibody complexes recognizing the superparamagnetic nanoparticles and their surface antigens (CD34). With a multi-channel magnetic chamber, the high magnetic gradient can be extended to the interior of the chamber, and therefore the sorting efficiency can be increased. The experimental results show 90% sorting efficiency. An automatic cell separation device has been developed and verified.



Schematic representation of the specific magnetic column for high cell sorting efficiency

	wash	elution
Fe(μg)	13.8	134.0
%	9.3%	90.7%

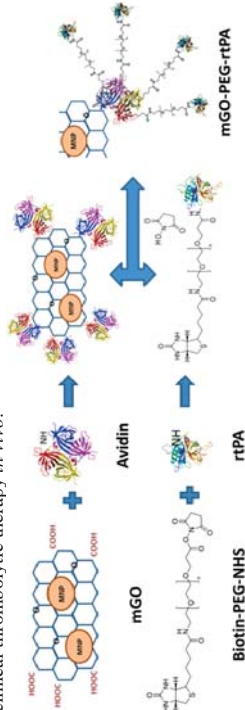
## Immobilization of Recombinant Tissue Plasminogen Activator on Magnetic Graphene Oxide for Targeted Delivery of Thrombolytic Agents

Pei-Ching Yang and Jyh-Ping Chen\*

Department of Chemical and Materials Engineering, Chang Gung University,  
Kwei-San Taoyuan 333, Taiwan, ROC, \*E-mail: jpchen@mail.cgu.edu.tw

A drug delivery approach to deliver tissue plasminogen (PA) under magnetic guidance for targeted thrombolysis will allow rPA to act only at the site of the target. This would potentially reduce the total administered dose of the drug necessary for the treatment, and hence its hemorrhagic side effects. In this study, avidin functionalized magnetic nanoparticle (MNP)-graphene oxide nanocomposite (mGO) was first synthesized by a facile method. The structure and surface properties of mGO nanocomposites were characterized by dynamic light scattering (DLS), Fourier transform infrared (FTIR) spectroscopy, atomic force microscope (AFM), transmission electron microscopy (TEM), thermogravimetric analysis (TGA), X-ray diffraction (XRD), inductively coupled plasma atomic emission spectroscopy (ICP-AES), superconducting quantum interference device (SQUID) and zeta potential measurements. To immobilize a thrombolytic agent recombinant tissue plasminogen activator (rPA), the N-hydroxysuccinimide (NHS) moieties in biotin-PEG-NHS was reacted covalently with the amino groups of rPA, followed by the high affinity of the biotin-avidin binding. This strategy not only introduced polyethylene glycol (PEG) as a spacer to eliminate the steric hindrance effect on rPA enzyme activity but also increased the amount of immobilized rPA with the 4/1 binding ratio of biotin-avidin. The nanodrug efficacy could be further improved by using biotin-PEG-maleimide, a sulfhydryl-reactive biotinylation reagent as the spacer. Since only one cystein group exists in rPA, single point attachment of rPA to mGO further increased the activity loading rPA on mGO (U/mg mGO) up to five times.

From fibrin clot lysis assays in blood, mGO-PEG-rPA showed improved activity compared to free rPA with incubation time, indicating immobilized rPA is more stable than its free form. *Ex vivo* thrombolysis model indicated, under magnetic guidance, mGO-PEG-rPA can reduce the blood clot lysis time by 54% compared with runs without magnetic targeting or with free rPA using the same drug dosage. Since mGO does not elicit cytotoxicity and hemolysis *in vitro*, mGO-PEG-rPA developed in this study will be useful as a magnetic drug delivery system to improve clinical thrombolytic therapy *in vivo*.



## Magnetic Graphene Oxide as a Carrier for Dual Targeted Delivery of Chemotherapy Drugs in Cancer Therapy

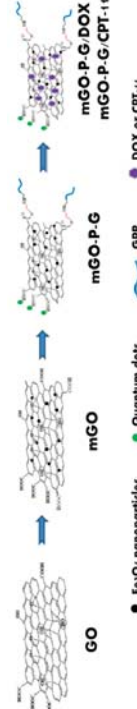
Pei-Ching Yang<sup>1</sup>, Ya-Shu Hwang<sup>1</sup>, Yu-Jen Lu<sup>2</sup>, Jyh-Ping Chen<sup>1,\*</sup>

<sup>1</sup>Department of Chemical and Materials Engineering, Chang Gung University,

<sup>2</sup>Department of Neurosurgery, Chang Gung Memorial Hospital, Kwei-San Taoyuan 333, Taiwan, ROC, \*E-mail: jpchen@mail.cgu.edu.tw

Functionalized nanographene sheets are biocompatible without obvious toxicity and can be loaded with aromatic anticancer drug with high efficiency. In this study, a dual targeted functionalized graphene oxide (GO) complex is constituted as a nanocarrier for targeted delivery and pH-responsive controlled release of chemotherapy drugs into cancer cells. Magnetic graphene oxide (mGO) was prepared by chemical co-precipitation of Fe<sub>3</sub>O<sub>4</sub> magnetic nanoparticles on GO nano-platelets. The mGO was successfully modified by chitosan and NHS-PEG-maleimide through covalent bindings to synthesize mGO-P. The polyethylene glycol (PEG) moiety is expected to prolong the circulation time of mGO by reducing the reticuloendothelial system clearance. Since gastrin-releasing peptide (GRP) receptor is highly expressed on the surface of human glioblastoma cells, mGO-P was further conjugated with GRP to synthesize mGO-P-G. Irinotecan (CPT-11) or doxorubicin (DOX) was loaded to mGO-P-G through π-π stacking interactions with GO for dual (magnetic and ligand-mediated) targeted delivery of the cancer chemotherapy drug. The dual active/magnetic targeting mechanism will enhance the endocytosis of the drug-loaded nanocarrier by the cancer cells, which release its drug cargo in the acidic (pH < 6) endosomal environment and increase the cytotoxicity and decrease the IC<sub>50</sub> of the chemotherapy drug.

The physicochemical properties of mGO-P-G were characterized via dynamic light scattering (DLS), transmission electron microscope (TEM), Fourier transform infrared spectroscope (FTIR) and zeta potential measurements. The measured values of loading efficiency and loading content of CPT-11 were 1.9% and 7% respectively; whereas for DOX, they were 58% and 461.9%. The pH dependent drug release profile was further experimented at different pHs, in which ~60% of DOX was released at pH 5.4 and ~10% was released at pH 7.4. In contrast, ~90 % CPT-11 was released at pH 5.4 and ~70% at pH 7.4. Based on the drug loading and release characteristics, mGO-P-G/DOX was further chosen for *in vitro* cytotoxicity tests against U87 human glioblastoma cell line. The IC<sub>50</sub> value of mGO-P-G/DOX was found to be lower than that of free DOX and further reduced when subject to magnetic targeting. It is concluded that with the high drug loading and pH-dependent drug release properties, mGO-P-G will be a promising drug carrier for targeted delivery of chemotherapy drugs in cancer therapy.



## Poly(lactide-co-glycolide) Magnetic Nanoparticles for Delivery of Plasminogen Activators

Pei-Ching Yang, Yi-Ging Yu, Jyh-Ping Chen\*

Department of Chemical and Materials Engineering, Chang Gung University,  
Kwei-San Taoyuan 333, Taiwan, ROC, \*E-mail: jpcchen@mail.cgu.edu.tw

Lysis of the fibrin clot by plasminogen activators is currently the only approved therapy for treatment of acute ischemic stroke. Delivery of plasminogen activators by binding the thrombolytic drug to a magnetic nanoparticle (MNP) as a drug carrier will ensure the drug to be delivered under magnetic guidance and retained in a local area in circulation, which is potentially useful for targeting fibrin clot *in vivo*. MNP as a drug carrier is usually composed of a magnetic core with superparamagnetic characteristics, and a polymer coating layer providing functional groups for drug binding, inhibiting aggregation, and increasing colloidal stability. In this study, we examine the preparation of poly(lactide-co-glycolide) (PLGA)-coated MNP (PLGA-MNP) and the feasibility of using urokinase-type plasminogen activator (uPA) or recombinant tissue plasminogen activator (rtPA) covalently bound to PLGA-MNP surface for magnetic targeted delivery of the thrombolytic drug. PLGA-MNP prepared with different weight ratios of PLGA and MNP were analyzed by dynamic light scattering (DLS), transmission electron microscopy (TEM), Fourier transform infrared spectroscopy (FT-IR), superconducting quantum interference device (SQUID), thermogravimetric analysis (TGA), atomic force microscopy (AFM), inductively coupled plasma (ICP), zeta potential and X-ray diffraction (XRD).

The best nanodrug preparation was 1 mg PLGA-MNP prepared with a 1:1 weight ratio of PLGA to MNP, to react with 0.5 mg rtPA or 0.75 mg uPA. Magnetic guidance significantly enhanced the thrombolytic effects of PLGA-MNP-uPA and PLGA-MNP-rtPA in an *ex vivo* thrombolysis model. Under magnetic targeting, the thrombolysis test indicated the immobilized drug can reduce the blood clot dissolving time by half compared with free drug at the same dosage. Effective thrombolysis in response to PLGA-MNP-uPA under magnetic guidance is also demonstrated in a rat embolic model where administration of a dosage of PLGA-MNP-uPA with activity equivalent to 10000 IU/kg of free uPA plus magnetic guidance increased tissue perfusion from 37% to 85% of the basal levels before clot introduction.

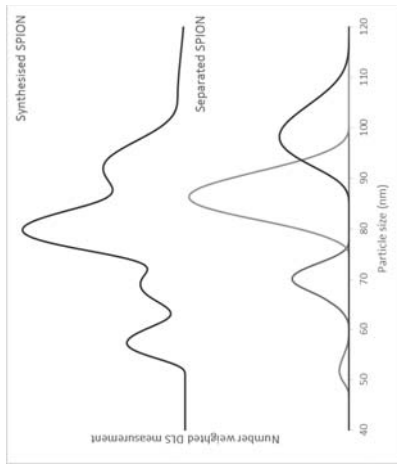
MagCarriersAbstract

## Superparamagnetic nanoparticle homogeneity: particle size separation by magnetic and hydrodynamic properties

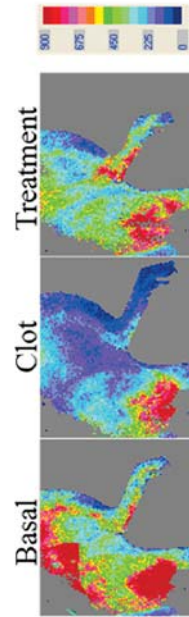
B. J. Yeh, A. E. David<sup>1</sup>

<sup>1</sup>Department of Chemical Engineering, 220 Ross Hall, Auburn University, Auburn, AL 36849, USA, Superparamagnetic iron oxide nanoparticles (SPIONs) have foreseeable potential in biomedical applications, because of its low toxicity and magnetic property. This creates a great interest in pharmaceutical and engineering researches, including drug delivery, hyperthermia, and other *in vivo* applications. SPIONs larger than its critical sizes can only be synthesized with multi-core structures which are multiple smaller SPIONs held together by an external matrix. This creates a very broad size distribution with a dynamic light scattering index (Pdl) about 0.14 from controlled synthesis processes. Furthermore, any additional surface modification will broaden the distribution to Pdl 0.18-0.25.

Poly-disperse PE Gylded superparamagnetic iron oxide nanoparticles with a Pdl of 0.145 are separated into multiple fractions of monodisperse particles. Each fraction has a Pdl of 0.1 or lower which is generally the range for monodisperse particles. The separation process is based on the magnetic and hydrodynamic property of magnetic particles. A periodic external magnetic source immobilizes particles and to form layers of different size particles. The overall field strength controls which layer to be released from the system. The system is design to be a scalable and reusable system to improve size homogeneity of magnetic nanomaterials, which enables us to study the effect of MRI relaxometry, cell cytotoxicity, *in vivo* bio-distribution and more in the future.



Schematic representation of a separation of polydisperse SPIONs into multiple fractions of monodisperse particles.



The effect of PLGA-MNP-uPA on tissue perfusion in a rat iliac embolic model

## Abstract

### A highly Efficient and Cost Effective Bioactivated Superpara-Magnetic beads and its Immuno-diagnostic (Clinical Diagnosis) applications

Calbiotech, Inc., Yonas D. Yohannes, 10461 Austin Drive, Spring Valley, CA 91978, E-mail:[yonas.yohannes@calbiotech.com](mailto:yonas.yohannes@calbiotech.com)

#### Objective:

- To offer clinicians an alternative platform, in the aid of patients' diagnosis, with a fully automated and affordable test method, for all sized reference laboratory settings.
- To study the cost effectiveness and efficacy of streptavidin coated paramagnetic beads, in the application of immunoassay biomarker tests, in a high throughout random access fully automated platform.

**Introduction:** Paramagnetic beads are made of nanometric-sized iron oxide particles encapsulated or glued together with polymers. Superparamagnetic particles are surface modified, optimized and validated for use with high-throughput magnetic platforms, in the application of immune-diagnostics, preparing single stranded DNA templates, immobilization of large DNA fragments, purifying sequencing products, immunoprecipitation, cell isolation, nucleic acid isolation, purification of DNA/RNA binding proteins, protein purification and are more suited for automated processes. Calbiotech has developed one of the most efficient streptavidin coated superparamagnetic bead particles (CalMagBeads™ Streptavidin) that possess unprecedented biotin-ligand binding capacity, in the market. This highest binding feature would enable clinicians to utilize the minimum possible beads per application, which in turn would save tremendous amount of money.

**Experiment:** The data depicted on **Table 1**, exhibits the comparison between 5 different manufacturers/competitors of paramagnetic bead particles, coated with streptavidin (SAV-Beads). The SAV-Beads were used as a solid support during the liquid phase Immuno-Chemiluminescence assays. Except for the Calbiotech SAV-Beads, all other beads were used at 150 $\mu$ g/ml. Calbiotech SAV-Beads were used at one-tenth of the competitors' concentration (15 $\mu$ g/ml), to produce equivalent or better immunophotoreponse.

STD./#ml Calbiotech, Inc.	Competitor's Streptavidin Coated Beads					RLU
	Invitrogen	Ocean Nanotech	Solink	Mardi		
0	10	40	20	110		
5	200	190	180	60		
10	420	420	340	70		
25	1040	1070	860	590		
50	1800	1900	1550	940		
100	2600	2630	2220	1630		

**Table 1.** CalMagBeads™ Streptavidin was compared to 4-commercial streptavidin coated magnetic beads for the liquid phase immunoassay application (ProLectin sandwich principle assay).

The data depicted on **Table 2**, shows the comparison between 4 different batches of CalMagBeads™ Streptavidin. Extreme inter-lot reproducibility was registered. A Thyroxine (T4) Chemiluminescence (MagCL™) assay was used for this study. T4 follows a competitive assay principle, where the signal and concentration of a given sample show inverse relationship.

STD./#ml	CalMagBeads™ Streptavidin					RLU
	Batch Y1	Batch Y2	Batch Y3	Batch Y4		
0	28300	28600	16300	28300		
2	15100	14500	14700	14700		
5	7400	7600	8000	7300		
10	3900	3600	4100	4500		
15	2200	2400	2500	2700		
25	800	800	900	800		

**Table 2.** Inter-batch reproducibility of 4-preparations of CalMagBeads™ Streptavidin, using a competitive functional assay (Thyroxine assay).

**Conclusion:** To our knowledge, CalMagBeads™ Streptavidin, with its proprietary and state-of-the-art coupling technology, is the most efficient (with a 10-fold higher biotin-ligand binding capacity) and the cheapest/cost effective paramagnetic streptavidin coated beads available in the market.

### Effect of Alignment of Easy Axes on Dynamic Magnetization of Immobilized Magnetic Nanoparticles

T. Yoshida, Y. Matsugi, N. Tsujimura, T. Sasayama, and K. Enpuku  
Department of Electrical Engineering, Kyushu University, Motoooka 744, Nishi-ku, Fukuoka 819-0385, Japan.  
E-mail: t\_yoshida@ees.kyushu-u.ac.jp

Magnetic nanoparticles (MNPs) have been widely studied for bio-medical applications such as hyperthermia and magnetic particle imaging (MPI). In these applications, dynamic magnetization of MNPs under AC excitation field is used. When MNPs are internalized in cells, they are physically immobilized, and their dynamic magnetization is dominated by the Néel rotational mechanism, as reported in refs. [1] and [2].

It is well known that Néel relaxation strongly depends on the relative angle between the AC excitation field and easy axes of MNPs. Therefore, it is important to clarify how the alignment of the easy axes affects the dynamic magnetization of immobilized MNPs. To this end, we prepared two immobilized MNPs (Resovist, FUJIFILM RI Pharma) samples, i.e., Sample 1 is the MNPs whose easy axes are aligned along the direction of the AC excitation field, while Sample 2 is the MNPs whose easy axes are randomly oriented. These two samples were immobilized with epoxy resin. In order to obtain the aligned MNPs sample, Sample 1 was exposed to a DC field of 16 mT during the immobilization process. On the other hand, sample 2 was immobilized without DC field. The amount of the MNPs and volume of each sample are 100  $\mu$ g(Fe) and 150  $\mu$ l, respectively. We investigated the dynamic magnetization of these two samples when an AC excitation field with amplitude of  $\mu_0 H_{ac} = 20$  mT and frequency  $f = 20$  kHz was applied.

In Fig. 1, dynamic  $M$ - $H$  curves at  $f = 20$  kHz are shown. As shown, the remanence magnetization and the coercivity of Sample 1 become large compared to those of Sample 2. Consequently, the area of the hysteresis loop of Sample 1, which corresponds to the heat dissipation by MNPs in hyperthermia, becomes approximately 1.7 times larger than that of sample 2. In Fig. 2, the amplitudes of the harmonic magnetizations  $M_i$ , which were obtained by performing a Fourier series expansion of the  $M$ - $H$  curve, are shown. As shown, the harmonics magnetization spectrum of Sample 1, which is used in MPI, becomes larger than that of Sample 2. These results indicate that the dynamic magnetization of immobilized MNPs is strongly affected by the alignment of easy axes.

- [1] S. Ota, T. Yamada, and Y. Takekuma, J. Nanomater., Vol. 2015, 836761 (2015).  
[2] D. Soukup, S. Moise, E. Céspedes, J. Dobson, and N. D. Telling, ACS Nano, Vol. 9, No. 1, pp. 231-240 (2015).

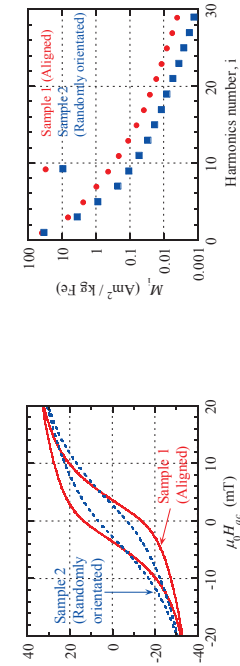


Fig. 1 AC  $M$ - $H$  curve measured at  $f = 20$  kHz.

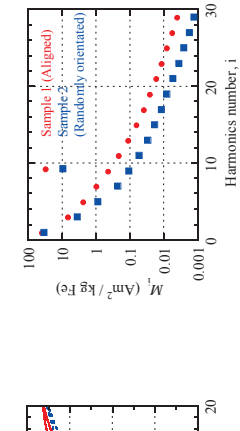


Fig. 2 Amplitude of the harmonic magnetization spectra.

## Effect of Magnetic Field on the Ability of Magnetite Nanoparticles to Penetrate into Live Cells.

A.Y. Yurenova<sup>1,2</sup>, M.A. Polikarpov<sup>1</sup>, E.Y. Moskaleva<sup>1</sup>, A.S. Zhirkov<sup>1</sup>, A.N. Taldenkov<sup>1</sup>, V.Y. Panchenko<sup>1,2</sup>.  
E-mail: anton.yurenova@gmail.com

<sup>1</sup>National Research Center "Kurchatov Institute", Moscow, Russia

<sup>2</sup>Faculty of Physics, Lomonosov Moscow State University, Moscow, Russia

The applications of magnetic nanoparticles have been expanding to biological and medical fields such as medical drug delivery, magnetic resonance imaging, magnetofection, and hyperthermia among others. Penetration of a cell membrane by these nanoparticles (either solely or in combination with a drug) is essential for many of these applications. Earlier we proposed a new radiotherapy enhancement method that entails administration of magnetic nanoparticles into the cells with further irradiation by a gamma-ray beam[1]. Within this framework we were prompted to investigate the capability of these nanoparticles to penetrate into cells and to discover how this process depends on the properties of the nanoparticles.

We used a magnetometer based technique for nanoparticle detection in the cell culture[2]. It was discovered that the presence of the magnetic nanoparticles in the cell culture after its incubation in nutrient solution with ferrofluid can be detected using a SQUID-magnetometer. We

used this technique to estimate the capability of our nanoparticles to reach inside the cells.

To distinguish the particles non-specifically attached to the cell surface from the particles inside the

cells, a set of experiments with low-temperature incubation was carried out (low temperature blocks phagocytosis and endocytosis processes).

In order to study the possibility of the nanoparticle uptake enhancement, some cell

incubations with magnetic particles were carried out in the presence of a magnetic field – the procedure borrowed from magnetofection[3].

Magnetic nanoparticles with different size and stabilization method were used. The amount of nanoparticles (the case of pH stabilization, 10μm diameter) in cell culture (about 3 million cells) was evaluated as 6.8μg

1. R. Gabbaev, M. Polikarpov et. al. Monte Carlo simulation of dose distribution in water around  $^{57}\text{Fe}304$  magnetite nanoparticle in the nuclear gamma resonance condition, *Hyperfine Interact.* 237, 34, (2016).  
2. Hashimoto, S., Oda et. al. The measurement of small magnetic signals from magnetic nanoparticles attached to the cell surface and surrounding living cells using a general-purpose SQUID magnetometer. *Physics in medicine and biology*, 54(8), 2571, (2009).  
3. Plank, C., Schilling et. al. The magnetofection method: using magnetic force to enhance gene delivery. *Biological chemistry*, 384(5), 737-747, (2003).

*The work was supported in part by the Russian Science Foundation under Grant 14-15-01096. The magnetic measurements were done at the resource center of electrophysical methods, NRCKI.*

### References

1. R. Gabbaev, M. Polikarpov et. al. Monte Carlo simulation of dose distribution in water around  $^{57}\text{Fe}304$  magnetite nanoparticle in the nuclear gamma resonance condition, *Hyperfine Interact.* 237, 34, (2016).  
2. Hashimoto, S., Oda et. al. The measurement of small magnetic signals from magnetic nanoparticles attached to the cell surface and surrounding living cells using a general-purpose SQUID magnetometer. *Physics in medicine and biology*, 54(8), 2571, (2009).  
3. Plank, C., Schilling et. al. The magnetofection method: using magnetic force to enhance gene delivery. *Biological chemistry*, 384(5), 737-747, (2003).

## Influence of magnetic fluid with betulinic acid on cancer cells viability

Vlasta Zavislova<sup>1</sup>, Iryna Khmarra<sup>2</sup>, Martina Konaracka<sup>1</sup>, Martina Kubovcikova<sup>1</sup>, Monika Bednarikova<sup>3</sup>, Marta Muckova<sup>3</sup>, Peter Kopansky<sup>1</sup>

<sup>1</sup>Institute of Experimental Physics SAS, Watsonova 47, 040 01 Kosice, Slovakia  
<sup>2</sup>Pavol Jozef Safarik University, Faculty of Science, Park Angelium 9, 041 54 Kosice, Slovakia  
<sup>3</sup>hameir a.s., Horna 36, 900 01 Mora, Slovakia

One of the most important magnetic nanoparticles use in the field of medical applications is cancer treatment. Magnetic particles can be used as a vehicle for magnetic drug targeting. Lot of naturally occurred compounds have potent antitumor activity. One of them is betulinic acid which anticancer property is linked to its ability to induce apoptotic cell death in cancer cells, however normal cells and tissue are relatively resistant.

In the work we focused on preparation stable magnetic fluid with low toxicity to normal cells and with ability to destroy cancer cells. Magnetic nanoparticles ( $\text{Fe}_3\text{O}_4$ ) were prepared by co-precipitation method, being subsequently coated with oleic acid to avoid their aggregation. To improve the biocompatibility of coated magnetic particles, their surface was modified by bovine serum albumin. Core diameter of magnetite nanoparticles determined by magnetic measurements and by transmission electron microscopy was in the range from 4 to 11 nm. Hydrodynamic diameter mean value of modified magnetic nanoparticles measured by dynamic light scattering method was cca 95 nm. Morphology of the studied magnetic particles was observed by scanning electron microscopy (Fig. 1). The cytotoxicity of pure betulinic acid and prepared magnetic particles with betulinic acid was assessed on two normal cell lines (Chinese hamster lung fibroblast cells V79 and mouse fibroblast cells L929) and two cancer cell lines (human cervical cells HeLa and melanoma cells B16) by MTT test *in vitro*. MTT<sub>50</sub> parameter for every tested sample is expressed as represents the betulinic acid concentration (μg/ml) that reduces absorbance of MTT salt in tested cells by 50 % compared to control untreated cells (Fig. 2).

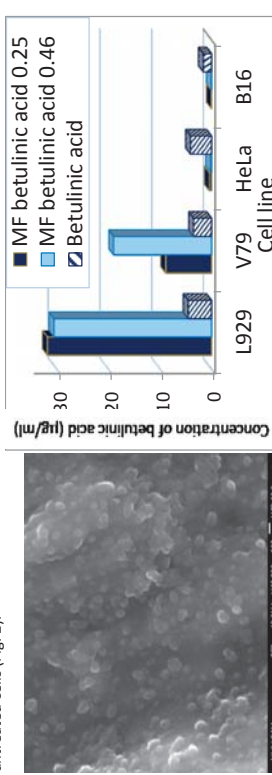


**Figure 1.** Magnetic nanoparticles of magnetic fluid (MF) observed by scanning electron microscopy.

The most important result of testing is the fact that magnetic particles with betulinic acid have not significant influence on the normal cell viability, on the other side tumour cells viability was considerably reduced after the treatment. In addition betulinic acid in magnetic fluids was effective at cca 100-fold lower concentration in comparison to the pure betulinic acid.

### Acknowledgments

The authors thank to the European COST action TD1402 (RADIOMAG). This work has been partially supported by the Slovak Research and Development Agency under Contract nos. APVV-14-0120 and APVV-14-0332.

## Tessellated permanent magnets for flow-through, open gradient separations of weakly magnetic materials

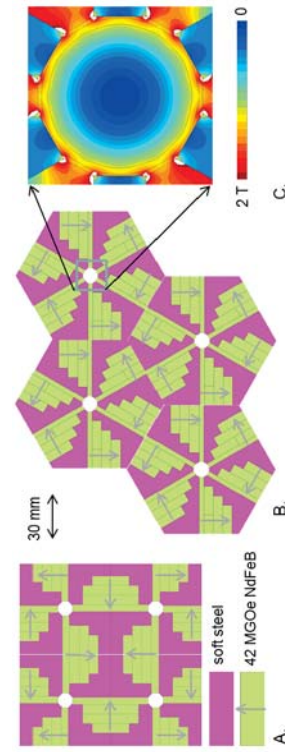
Maciej Zborowski<sup>a\*</sup>, Lee R. Moore<sup>a</sup>, Jeffrey J. Chalmers<sup>b</sup>

<sup>a</sup>Department of Biomedical Engineering, Cleveland Clinic, 9500 Euclid Ave., Cleveland, OH 44195

<sup>b</sup>William G. Lowrie Department of Chemical and Biomedical Engineering, 151 W. Woodruff Avenue, The Ohio State University, Columbus, OH 43210, U.S.A.; \* corresponding author: [zborowm@ccf.org](mailto:zborowm@ccf.org)

Emerging microfluidic-based assays favor a label-free, magnetic red blood cell (RBC) separation. Such separation is possible because of paramagnetism of deoxygenated hemoglobin but the process is slow for open-gradient field configurations [1,2]. In order to increase the throughput, periodic arrangements of the unit magnets were considered consisting of commercially available Nd-Fe-B permanent magnets and soft steel flux return pieces. The magnet design is uniquely suitable for multiplexing by magnet tessellation as shown in examples below (four quadrupole field channels in Fig. A and four hexapole field channels in Fig. B). The periodic pattern of magnet magnetizations allows a reduction of the magnetic material per channel without compromising the field cylindrical symmetry inside the magnet apertures (Fig. C). A number of such magnet patterns are investigated for separator performance, size and economy with the goal of reducing the RBC number concentration at least hundred-fold in 5 mL whole blood per hour.

1. Moore LR, Williams PS, Nehl F, Abe K Chalmers JJ and Zborowski M. (2014) Feasibility study of red blood cell debulking by magnetic field-flow fractionation with step-programmed flow. Analytical and Bioanalytical Chemistry 406, 1651-1670
2. Moore LR, Nehl F, Dorn J, Chalmers JJ and Zborowski M. (2013) Open Gradient Magnetic Red Blood Cell Sorter Evaluation on Model Cell Mixtures. IEEE Transactions on Magnetics 49, 309-315



Examples of tessellated magnet patterns for quadrupole (A) and hexapole (B) field geometries inside multiplexed, circular cross-section flow channels (C). Arrows indicate magnetization directions.

## Pharmaceutical Formulation of HSA hybrid coated Iron Oxide Nanoparticles for Magnetic Drug Targeting

Jan Zaloga<sup>1</sup>, Johannes Nowak<sup>2</sup>, Rainer Tietze<sup>1</sup>, Ralf P Friedrich<sup>1</sup>, Stefan Lyer<sup>1</sup>, Geoffrey Lee<sup>3</sup>, Christoph Alexiou<sup>1</sup>

<sup>1</sup> Department of Otorhinolaryngology, Head and Neck Surgery, Section for Experimental Oncology and Nanomedicine (SEON), Else Kröner Fresenius-Stiftung Professorship, University Hospital Erlangen, Germany

<sup>2</sup> Chair of Magnetofluidynamics, Measuring and Automation Technology, Technische Universität Dresden, Germany.

<sup>3</sup> Division of Pharmaceutics, Friedrich-Alexander Universität Erlangen, Germany

Magnetic Drug Targeting (MDT) is a promising method for accumulation of drugs in selected tissues using superparamagnetic iron oxide nanoparticles (SPIONS). Using magnetic field gradients, the bioavailability of drugs can be increased over 56-fold compared to intravenous injection[1]. Recently, we have reported about synthesis[2] and purification of a very promising fatty acid/albumin hybrid coated particle system.

Method transfer of nanoparticle synthesis to a good manufacturing practice (GMP) compliant environment is a very challenging stepstone, which has significantly hindered clinical translation of nanoparticle formulations[3]. In this present study we describe how we established a pharmaceutical SPION formulation procedure following GMP regulations[4]. Following aforementioned lab-scale developments we established a reproducible production process using GMP-grade materials and methods. We also conclusively demonstrated the core-shell structure of these particles using cryo – transmission electron microscopy (TEM), pH-dependent electrokinetic mobility measurements and fourier transform infrared (FTIR) spectroscopy. Studies on long-term stability of the formulation, an aspect which is often overlooked, showed that the particles remain colloidally stable over longer periods of time even at higher temperatures up to 45 °C. The corresponding oxidation of the iron oxide cores and the reduction in the saturation magnetization  $M_s$  was shown using complimentary vibrating sample Magnetometry (VSM), TEM and x-ray diffraction (XRD) methods. We showed excellent biocompatibility and concentration-dependent cellular uptake of the synthesized SEON<sup>LA-HSA</sup> particles using flow cytometry and microwave-assisted atomic emission spectroscopy (MP-AES). We investigated binding and the slow pseudo-zero-order release of the

# MALDI-TOF MS Combined With Magnetic Beads For Quantification of Serum Protein Biomarkers

Jie Gao<sup>1\*</sup>, Klaus Meyer<sup>2</sup>, Per Magne Ueland<sup>1</sup>

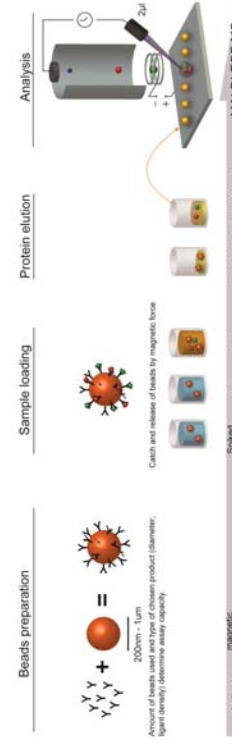
<sup>1</sup>Department of Clinical Science, University of Bergen, Bergen, Norway  
<sup>2</sup>Bevital AS, Bergen, Norway, \*E-Mail: Jie.Gao@uib.no

We have established a multiplex immuno-MALDI assay for targeted enrichment and direct quantification of four disease related serum markers (inflammation: i.e. C-reactive protein (CRP), serum amyloid A (SAA), calprotectin (S100A8/9); kidney function: Cystatin C). The assay combines sample purification by magnetic beads followed by MALDI-TOF MS readout.

The general workflow consists of antibodies immobilization, sample incubation, washing, analyte elution and MALDI analysis. Antibodies are covalently immobilized on the beads surface by different types of linkers. For each sample, 20 µl human serum is spiked with 20 µl internal standard (recombinant histidine-tagged target proteins).

Several types of magnetic beads (0.2-1 µm) from different companies have been tested in CRP and Cystatin C duplex assays. Strong non-specific binding has been observed for nearly all beads, which show 1) dominant peaks at lower mass range (7.5 to 10 kDa) suppressing the analyte signals, 2) interference of analyte peaks with contaminants (11 to 15 kDa) from either blood samples or linking products. In order to decrease the non-specific binding, several commonly used blocking reagent as BSA, Tween 80 and poly (ethylene oxide) have been tested, but without any success. Only one product demonstrated very low non-specific binding and has been applied in the assay. For quantification we prepared standard curves from dilution series, which demonstrated good linearity ( $R^2 > 0.99$ ) for all four markers of CRP, Cystatin C, SAA and S100A8. The method performed well in terms of intra-assay CVs (< 10%) and throughput (192/day).

Due to the fast differentiation of isoforms, the ability to multiplex several biomarkers and the low sample consumption, our assay has great potential for biobank studies investigating the diversity of established protein biomarkers related to inflammation and kidney function. Future work will compare this assay with established reference methods.



## AC BIOSUSCEPTOMETRY TO ASSESS COLONIC CONTRACTILITY IN RATS WITH AC ULCERATIVE COLITIS

Marcos F.F. Calabresi<sup>1\*</sup>, Caio C. Quini<sup>1</sup>, Fabio P.F. Mello<sup>1</sup>, Alexandre Tamimoto<sup>1</sup>, Luis C. Di Stasi<sup>1</sup>, José R. A. Miranda<sup>1</sup>

<sup>1</sup> Bioscience Institute of Bauru, Unesp, SP – Brazil, \*e-mail: micalabresi@bb.unesp.br

The motor activity of the colon plays an important role in the progression and evacuation process of the fecal mass. Related to various types of diseases such as constipation, diarrhea, and inflammatory diseases in this activity is difficult to access by traditional instrumentation. Ulcerative colitis is an inflammatory bowel disease of poorly understood pathogenesis, which is associated with alterations in bowel motility. Due to the inaccessibility of the organ, evaluation methods of the colon motor function are scarce and not practical. The AC Biosusceptometry (ACB) system is an efficient research tool, to access and analyze gastrointestinal parameters and their motor functions. As a detection probe, when compared to other techniques, the method presents considerably higher temporal resolution, mainly due to its physical working principle. Our technique is based upon a magnetic flux transformer, which allow us to detect and quantify magnetic materials based on the variation in magnetic inductance from an excitation pickup coil to a detection one. Using markers attached to the organs walls, ACB allows the investigation of mechanical properties resulting from specific organ / tissue contraction activity.

This study aims to investigate and characterize the mechanical behavior of colonic motility in normal and ulcerative colitis rats, by employing the ACB system to monitor magnetic materials. We used male Wistar rats with a magnetic marker (ferrite nucleus, 0.15 g - MnFe<sub>2</sub>O<sub>4</sub>) fixed in colon serous. Colitis was induced by the rectal administration of 2.4% Trinitrobenzenesulfonic acid (TNBS). The measurements were performed in each animal before induction (control), 48 and 120 hours after induction. Our results showed an intense and speculated activity with periodic contractions before colitis induction (Figure 1). We found two dominant frequencies contractions (10 and 100 mHz) in normal colons. The colitis induction caused a significant pattern modification, shifting to 25 and 50 mHz, respectively.

Summarizing, our study presents an application of magnetic markers, associated with a simple and non-invasive technique, that allows physiological investigation with a unique temporal resolution, resulting in a valuable contribution on regards to perform a methodology standardization for colonic motility evaluation, presenting a reliable and reproducible method.

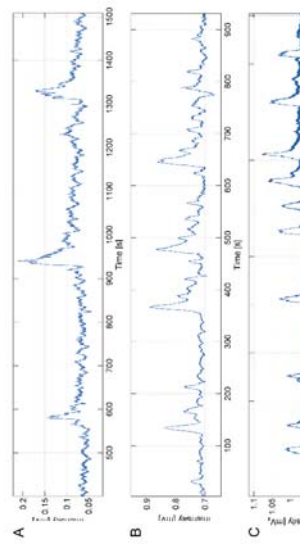


Figure 1: Examples of signals obtained from colon by monitoring magnetic markers with the ACB system: A) Before Colitis induction (control); B) after 48 hours; and C) after 120 hours.

# Exhibitors and Sponsors

We are particularly thankful to all of our main sponsors this year. They allowed us to again hand out many travel grants.



## **Stemcell Technologies**

<http://www.stemcell.com/>

StemCell Technologies – "The Cell Experts" - offers a spectrum of immunomagnetic cell separation products for the isolation of virtually any cell type from any species. These separations can be automated using RoboSep® - the only fully automated immunomagnetic separator. StemCell Technologies also provides specialized media, sera, antibodies and support products for life scientists.



## **Micromod Partikeltechnology GmbH**

<http://www.micromod.de/>

For more than 20 years Micromod has been well known as a reliable source of magnetic and other functional nano and micro particles. Micromod's customers, who come from life sciences industries and research institutions, appreciate the high level of product quality and services.



## **Chemicell**

<http://www.chemicell.com>

Chemicell develops and produces innovative bioseparation- and detection systems based on magnetic, fluorescent and color nano- and microparticles. The focus of our product development are customer-oriented „ready-to use“ kits with special orientation towards the compatibility for labor automation. It is chemicell's policy to be open for cooperations with other companies or scientific institutes to maximize the chances and opportunities that evolve from the rapid development of biotechnological procedures and to distribute innovative new products.



## **American Elements**

<https://www.americanelements.com/>

Global manufacturer of high purity rare earth metals, ferrous & shape memory alloys, superconductors, garnet crystals, advanced magnetic materials, semiconductors, nanomaterials, sputtering targets & MEMS devices



### SEPMAG tecnologies

<http://www.sepmag.eu/>

SEPMAG tecnologies is engaged in developing and providing Large Volume Magnetic Separation systems to the Biotech industry. Taking advantage of their experience with permanent magnet devices, SEPMAG scientists and engineers are fulfilling the needs of the more demanding customers simplifying the magnetic separation processes, reducing the separation time, minimizing the magnetic bead losses and avoiding re-suspension problems. All this features with a completely safe operation, which allows the device to operate just few centimetres away from computers and magnetic recording media. Since the start of the activities, in 2004, we supply Large Volume SEPMAG (up to tens of litres) systems to the production lines of leading IVD companies, in both the European Union and US markets.



### **instituto iMdea Nanociencia** - instituto madrileño de estudios avanzado en Nanociencia

[www.nanociencia.imdea.org/](http://www.nanociencia.imdea.org/)

iMdea Nanociencia is a young research institute focused on research, technological development and innovation in the field of Nanoscience, Nanotechnology and Molecular Design. In the last 5 years, advanced instrumentation has been developed for characterizing magnetic nanoparticles.



### Ferrotec (USA) Corp

[www.ferrotec.com](http://www.ferrotec.com)

Ferrotec, the global leader in ferrofluid technology and production for audio loudspeaker applications, proudly announces their partnership with Liquids Research Limited for advancing the bio-medical nanoparticles market with their EndoMAG®, LiquidMAG®, FluoreMAG® and HyperMAG® suspensions. Please come by our booth for a discussion of how we can improve your performance with these products and/or a customized solution.



### The Cleveland Clinic

<http://www.clevelandclinic.org/>

The mission of The Cleveland Clinic is to provide compassionate health care of the highest quality in a setting of education and research. The Lerner Research Institute is the research part of the Cleveland Clinic and employs more than 1,050 scientists and support personnel.

**Beckman Coulter Life Sciences**

<http://www.beckmancoulter.com/>

Beckman Coulter develops, manufactures and markets products that simplify, automate and innovate complex biomedical testing. Our products are making a difference in people's lives by improving the productivity of medical professionals and scientists, supplying critical information for improving patient health and delivering trusted solutions for research and discovery.



Quantum Design

**Quantum Design GmbH**

<http://qdusa.com/>

Quantum Design's Physical Property Measurement Systems (PPMS®, DynaCool, and VersaLab) provide a range of magnetic measurements, including VSM, Torque, and DC & AC Susceptibility. The SQUID-based Magnetic Property Measurement System (MPMS®3) is the industry standard for ultra-sensitive magnetic measurements and AC Susceptibility measurements. Quantum Design International distributes instrumentation for magnetic hyperthermia made by Nanoscale Biomagnetics. Their DM100 series provides automated solutions for all Magnetic Hyperthermia and Induction Heating instrumentation from magnetic characterization to clinical application. The system allows 8 user-selectable frequencies from 10 KHz to 850 KHz up to 350 Oe (27825 A/m) field. The modular approach allows separate modules for calorimetry (to determine the SAR of a colloid sample), in vitro and tissue experiments, and in vivo small animal experimentation with drug delivery applications.

**Diagnostic Biosensors**

<http://diagnosticbiosensors.com>

Diagnostic Biosensors' magnetic sensor technology enables micro-miniaturized bioassay detection systems because their detectors are tiny integrated circuit chips. The sensors detect and quantify micromagnetic labels that are biochemically bound to analytes of interest, including DNA, proteins, cells, bacteria, and antibodies. SINGLE BEAD DETECTION is possible.



**CDRD**  
<http://www.cdrd.ca/>

Headquartered in Vancouver, British Columbia, The Centre for Drug Research and Development (CDRD) is Canada's national drug development and commercialization engine. The CDRD works in partnership with academia, industry, government and foundations, to provide the specialized expertise and infrastructure to identify and de-risk promising discoveries generated by health-related research, and transform them into commercially viable investment opportunities for the private sector – and ultimately into innovative new therapies for patients.



**Perkin Elmer**  
<http://www.perkinelmer.com/>

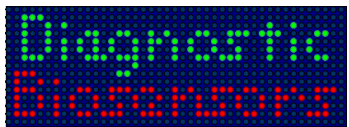
PerkinElmer is a global leader focused on improving the health and safety of people and the environment. Our dedicated team of 8,000 employees worldwide are passionate about providing customers with an unmatched experience as they help solve critical issues in human and environmental health. Our innovative detection, imaging, informatics and service capabilities, combined with deep market knowledge and expertise, help customers gain greater insights into their science to better protect our environment, our food supply and the health of our families.



**nanoTherics Ltd.**  
<http://www.nanotherics.com/>

nanoTherics Ltd. has developed novel, magnetic gene transfection devices based on oscillating magnet arrays (patents pending). In vitro pilot studies in four cell types showed that the nanoTherics magneffect nano systems outperform not only cationic lipid-based reagents but also standard, static-field magnetofection technology, providing a new "gold standard" for non-viral transfection.

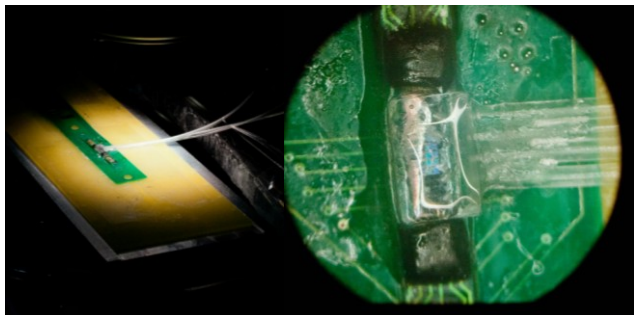
The company has also developed the magneTherm AC system for magnetic nanoparticle hyperthermia testing. Please visit our website for more details on these and other nanoTherics technologies.



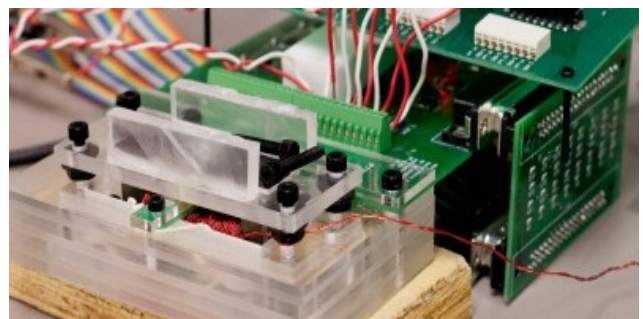
# Diagnostic Biosensors

Diagnostic Biosensors (DBS) designs and produces miniaturized biosensors and actuators integrated with diagnostic sensing systems for life science and analytical applications.

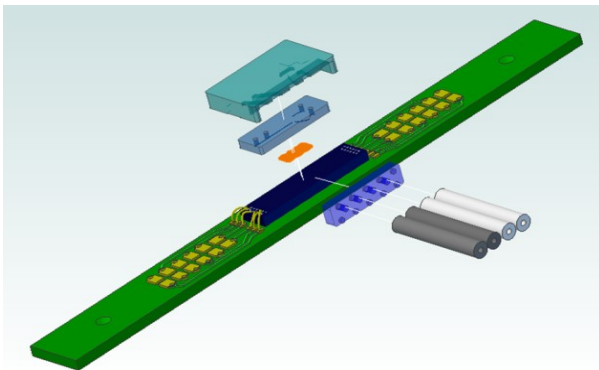
Electronics – Microfluidics integration



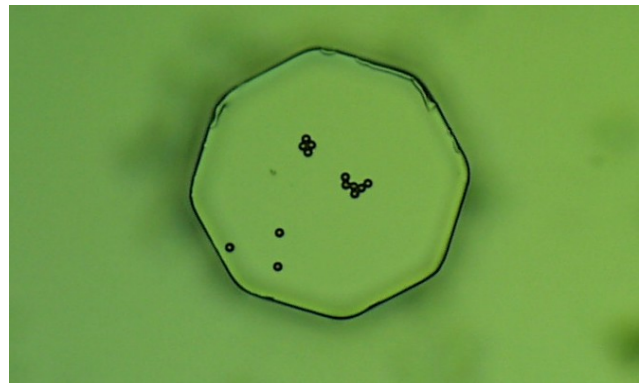
Magnetic – Fluidic Test System



Multilevel Micro-Miniature  
Fluidics + Biosensing Film



Custom nano-structures designed  
and fabricated



## Recent Successful Projects:

- Flow control unit design and build
- Nanomagnetic bead flow detection
- Microelectronic live- cell based toxicity monitor
- Custom fluidic and magnetic test system designed and fabricated

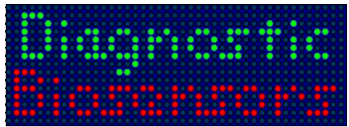
MT DBS SN#2015-07-22-rev04

**Diagnostic Biosensors, LLC**

1712 Brook Ave. SE; Minneapolis, Minnesota 55414-2422 USA

Contact: [Info@DiagnosticBiosensors.com](mailto:Info@DiagnosticBiosensors.com); +011 612 331-3584

[www.DiagnosticBiosensors.com](http://www.DiagnosticBiosensors.com)



# Miniaturized Fluidics Integration: Design and Consulting

## Capabilities:

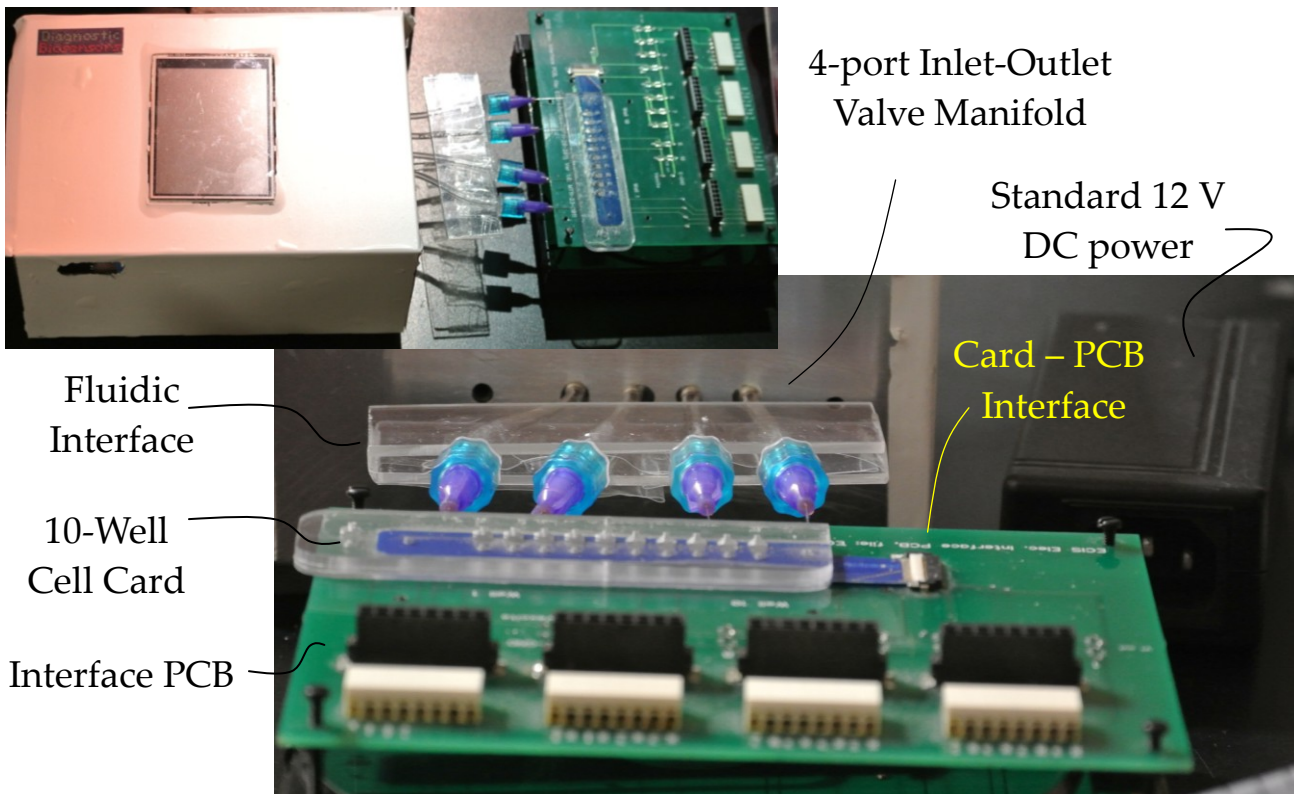
- Microfluidic – MEMS molding
- Electronic – microfluidic assembly
- Magnetic detection and actuation
- Sensor and circuit design
- Custom nanofabrication
- Micro cell culture and monitor

## Equipment and Software:

- Micro mold design, CAD, and embossing and thinning, uMill, lathe, press
- System control software and electronics
- Microelectronics schematic, PCB, assembly, and test
- Micro-assembly alignment tool
- Wet lab, microscopy, access to: SEM, particle size analyzer, full analytical lab



## Microfluidic Flow Controller and Biosensor Test System



MT DBS SN#2015-07-22-rev04

**Diagnostic Biosensors, LLC**

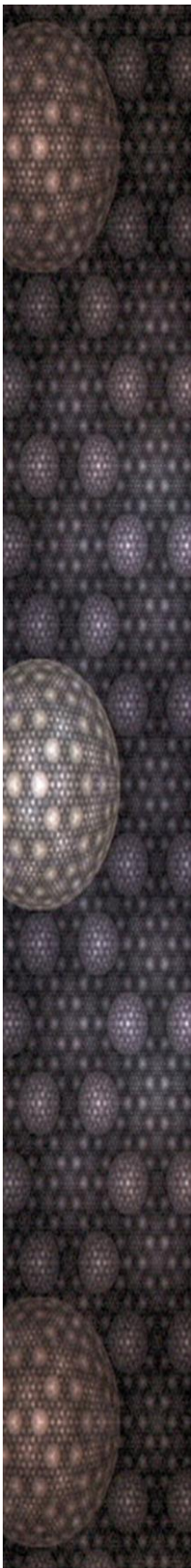
1712 Brook Ave. SE; Minneapolis, Minnesota 55414-2422 USA

Contact: [Info@DiagnosticBiosensors.com](mailto:Info@DiagnosticBiosensors.com); +011 612 331-3584

[www.DiagnosticBiosensors.com](http://www.DiagnosticBiosensors.com)

# Advanced instrumentation Unit

Servicio de Instrumentación (*ServIns*)



*Giving support to scientists for characterising or exploiting the dynamical magnetic response of magnetic nanoparticles*

## Prototypes portfolio

### AC magnetic field generators

AC magnetic field generators are developed at *ServIns* since 2011 for different purposes: calorimetry, in vitro/in vivo magnetic hyperthermia studies,..

### Calorimeters for SAR determination

Non-adiabatic calorimeter to accurately determine SAR values from colloidal dispersions of magnetic nanoparticles subjected to alternating magnetic fields and/or laser irradiation.

### Magnetometers

Probing magnetization cycles of magnetic nanoparticles dispersed in any liquid under alternating magnetic fields.

### Measurement service

*ServIns* offers the opportunity to perform customized measurements of different AC magnetic responses (hysteresis loops and heat dissipation) upon request.

### Contact :

Dr. Francisco J. Teran

Servicio de Instrumentación

iMdea Nanociencia

Calle Faraday,9

Campus Universitario de Cantoblanco

28049 Madrid

Spain

Phone : + 34 91 299 88 64

[servins@imdea.org](mailto:servins@imdea.org)



In Partnership with



### **Ferrofluids and SPION materials for bio-medical applications:**

- Separation of sub-cellular organelles with EndoMAG® Fluids
- Study of endocytotic pathways with FluoreMAG® Fluids
- Study of adjuvant vaccines, transfection techniques, viral infectivity, and stabilization of proteins with LiquidMAG® Fluids
- Magnetic Hyperthermia therapies with HyperMAG® Fluids

**Find out more today by visiting our booth at the:**

**11th International Conference on the Scientific and Clinical  
Applications of Magnetic Carriers**

**Univ. of British Columbia, Vancouver / May 31 - June 4, 2016**



**Key CDRD Benefits:**

Access to infrastructure and expertise required for preclinical drug development

Project-specific funding opportunities and leveraging of grant funding

Pre-existing Intellectual Property (IP) remains with the Investigators and their affiliated institutions

**CDRD helps overcome scientific and project management roadblocks by:**

Identifying critical issues required to establish commercialization potential

Designing and conducting pivotal experiments

Identifying and facilitating collaborations

Providing project management for multi-investigator programs

The Centre for Drug Research and Development (CDRD) is Canada's fully-integrated national drug development and commercialization centre, providing expertise and infrastructure to enable researchers from leading health research institutions to advance promising early-stage drug candidates. Its mandate is to de-risk discoveries stemming from publicly-funded health research and transform them into viable investment opportunities for the private sector — thus successfully bridging the commercialization gap between academia and industry, and translating research discoveries into new therapies for patients. Canada's Networks of Centres of Excellence Program has recognized CDRD as a Centre of Excellence for Commercialization and Research (CECR).

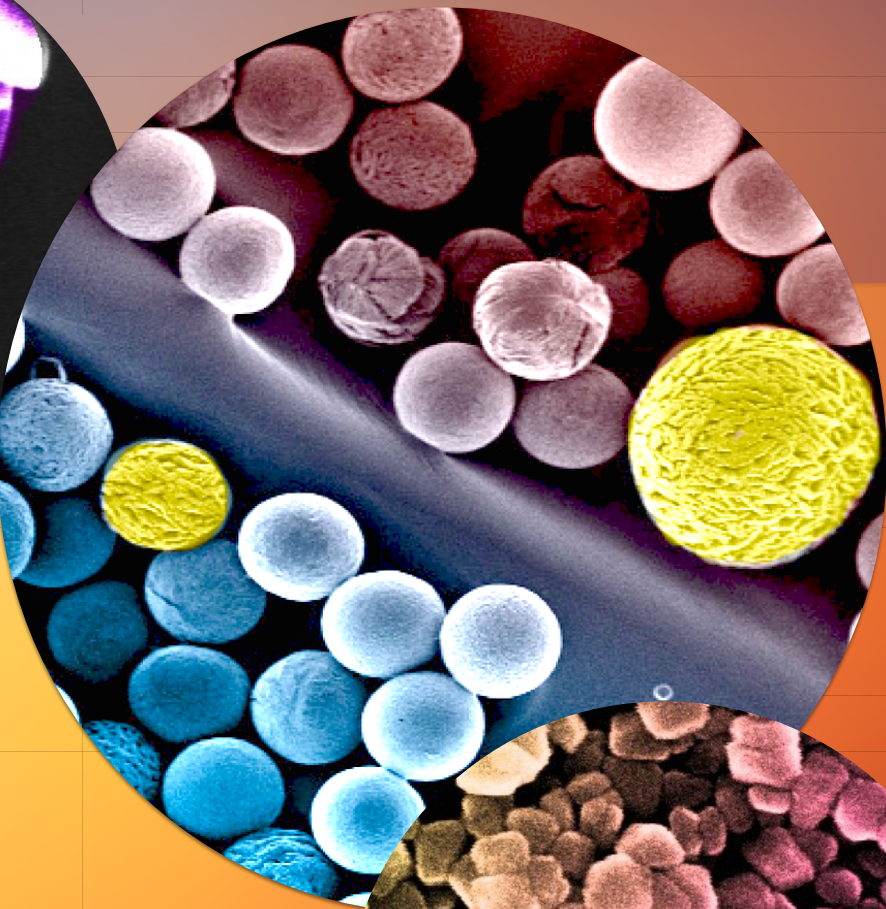
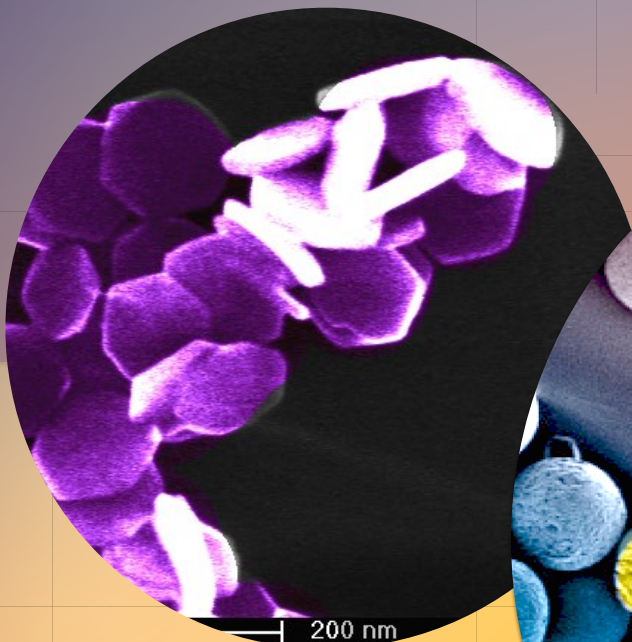
CDRD's commercialization vehicle, CDRD Ventures Inc. (CVI) licenses select promising technologies with the goal to further advance them to a stage where they can attract licensing partners, form the foundation for a new spin-off company, or secure the investment needed for clinical development.



# 12th

# International Conference on the SCIENTIFIC AND CLINICAL APPLICATIONS OF MAGNETIC CARRIERS

COPENHAGEN, DENMARK  
MAY 22-26 2018



FH KREMS  
UNIVERSITY OF APPLIED  
SCIENCES / AUSTRIA

WOLFGANG SCHÜTT  
KREMS, AUSTRIA



Cleveland Clinic

MACIEJ ZBOROWSKI  
CLEVELAND, OHIO, U.S.A



a place of mind

URS HAFELI

VANCOUVER, CANADA  
COPENHAGEN, DENMARK

